Title

An anatomical and developmental analysis of neural lineages, the fundamental units of circuitry in the central brain of Drosophila melanogaster

Author

Lovick, Jennifer Kelly

Publication Date

2015

Peer reviewed|Thesis/dissertation

UNIVERSITY OF CALIFORNIA

Los Angeles

An anatomical and developmental analysis of neural lineages, the fundamental units of circuitry in the central brain of *Drosophila melanogaster*

A dissertation submitted in partial satisfaction of the requirements for the degree Doctor of Philosophy in Molecular, Cell, and Developmental Biology

by

Jennifer Kelly Lovick

2015

ABSTRACT OF THE DISSERTATION

An anatomical and developmental analysis of neural lineages, the fundamental units of circuitry in the central brain of *Drosophila melanogaster*

by

Jennifer Kelly Lovick

Doctor of Philosophy in Molecular, Cell, and Developmental Biology

University of California, Los Angeles, 2015

Professor Volker Hartenstein, Chair

This work examines a variety of fundamental biological questions regarding the central brain of *D. melanogaster.* These questions focus on topics relating to neurons which form the neural circuits of the larval and adult brain. We focused specifically on the neurons which form the central brain and are organized into developmental-

structural units termed lineages. Through a combination of genetics and immunohistochemical assays we were able to create a detailed atlas of lineages in the early larval brain (made by embryonic-born primary neurons) and the adult brain (made mostly by larval-born secondary neurons; Chapters 2 and 6); show that secondary lineages are born in a strict temporal manner and how they develop during larval and pupal stages (Chapters 3-5). By observing secondary lineages in both wild-type and various mutant conditions we were able to show the following: pattern and timing of secondary lineage axon tract extension in the larva; movement of cell body clusters due to the growing central brain and optic lobe neuropils during metamorphosis; which secondary lineages retain their entire cohort of neurons (many lose a hemilineage in the pupa); and proper differentiation of secondary lineages relies on the presence of both synaptic partners. Taken together, these studies make a significant contribution to our understanding of *Drosophila* brain circuitry and development. They support the overall goal of mapping all central brain lineages (primary and secondary components), from their inception in the early embryo (when neuroblasts first appear) to their final mature form in the adult.

The dissertation of Jennifer Kelly Lovick is approved.

Mark Frye

Alvaro Sagasti

Volker Hartenstein, Committee Chair

University of California, Los Angeles

2015

DEDICATION

I would like to dedicate this dissertation to my friends, family, and most of all my parents. They have always been a constant source of guidance, support, and wisdom.

TABLE OF CONTENTS

LIST OF FIGURES AND TABLES

ACKNOWLEDGEMENTS

I would like thank my thesis advisor, Volker Hartenstein, for making my graduate school experience at UCLA such a positive one. He has been an amazing mentor and I truly appreciate all that he has enabled me to learn and experience during my time in his lab. I've not only grown as a scientist, but I've developed so much as a person, gaining skills that I will be able to utilize in the future.

I also would like to acknowledge past and present members of the Hartenstein lab including Shana Spindler, Shigeo Takashima, Lolitika Mandal, Amelia Younossi-Hartenstein, Kathy Ngo, Darren Wong, Jaison Omoto, Melina Grigorian, Patrick Aghajanian, Manash Paul, Siaumin Fung, Albert Cardona, Maria (Coca) del Mar de Miguel, Manuel Hakimi, Paola Ortiz, Angel Kong, Wichanee Borisuthirattana, Joseph Duy Nguyen, and Tanu Shenoy. I would like to say a special thank you to those which have been not only wonderful lab-mates, but friends as well, thank you for making my graduate school experience so wonderful.

Thank you also to my committee members Jau-Nian Chen, Mark Frye, and Alvaro Sagasti. I would like to acknowledge them for guiding and shaping the aims of my thesis, their suggestions have been invaluable.

I would also like to thank my family and friends who have supported me throughout my graduate school experience. I especially want to thank my parents, David and Jeanne, who have gone above and beyond to help me and encourage me to follow my heart. I also would like to acknowledge my extended family that has been so kind and encouraging. Finally, thank you to all my close friends for your unwavering

support and inspiration, especially Elizabeth, Greg, Amber, Darren, Kathy, Steve, Anna, Sky, Sue, Chad, Brittany, Matt, Jeanine, Beth, Lindsay, Linda, and Jason. These extraordinary people have kept me motivated to always be at my best.

Chapter 2 is a copy of the manuscript entitled “Lineage-associated tracts defining the anatomy of the *Drosophila* first instar larval brain” by Volker Hartenstein, Amelia Younossi-Hartenstein, Jennifer Lovick, Angel Kong, Jaison Omoto, Kathy Ngo, and Gudrun Viktorin and was accepted to Developmental Biology in 2015 (406:14-39; doi: 10.1016/j.ydbio.2015.06.021). This manuscript is reproduced with permission from the Journal Developmental Biology (License # 3701110069869). Experiments were conducted by Amelia, Jennifer, Angel, Jaison, and Kathy; data analysis and publication preparation by Volker, Jennifer, and Jaison. We thank Dr. J. Truman for generous help in the screen for Gal-4 lines with expression in larval brain lineages.

Chapter 3 is a copy of the manuscript titled “Hydroxyurea-mediated neuroblast ablation establishes birth dates of secondary lineages and addresses neuronal interactions in the developing *Drosophila* brain” by Jennifer Lovick and Volker Hartenstein and was accepted to Developmental Biology in 2015 (402:32-47; doi: 10.1016/j.ydbio.2015.03.005). This manuscript is reproduced with permission from Elsevier (License # 3698930573709). Experiments were conducted by Jennifer; data analysis and publication preparation by Jennifer and Volker. We thank the members of the Hartenstein laboratory for critical discussions during the preparation of this manuscript. We thank K.T. Ngo, J.J. Omoto, and T. Shenoy for their assistance in several hydroxyurea ablation experiments. We are grateful to the Bloomington Stock

Center and R.F. Stocker for fly strains and the Developmental Studies Hybridoma Bank for antibodies.

Chapter 4 is a copy of the manuscript “Patterns of growth and tract formation during the early development of secondary lineages in the *Drosophila* larval brain” by Jennifer Lovick, Angel Kong, Jaison Omoto, Kathy Ngo, Amelia Younossi-Hartenstein, and Volker Hartenstein and was accepted to Developmental Neurobiology in 2015 (doi: 10.1002/dneu.22325). This manuscript is reproduced with permission from John Wiley and Sons (License # 3693960839846). Experiments were conducted by Jennifer, Angel, Jaison, Kathy, and Amelia; data analysis and publication preparation by Jennifer, Jaison, Kathy, and Volker. We would like to thank the members of the Hartenstein laboratory for critical discussions during the preparation of this manuscript and are grateful to the Bloomington Stock Center and the Developmental Studies Hybridoma Bank for fly strains and antibodies.

Chapter 5 is a copy of the manuscript “Postembryonic lineages of the *Drosophila* brain: I. Development of the lineage-associated fiber tracts” by Jennifer Lovick, Kathy Ngo, Jaison Omoto, Darren Wong, Joseph Nguyen, and Volker Hartenstein and was accepted to Developmental Biology in 2013 (384:228-257; doi: 10.1016/j.ydbio.2013.07.008). This manuscript is reproduced with permission from Elsevier (License # 3701101458509). Experiments were conducted by Jennifer, Kathy, Jaison, Darren, and Joseph; data analysis and publication preparation by Jennifer, Kathy, Jaison, Darren, and Volker. We thank the members of the Hartenstein laboratory for critical discussions during the preparation of this manuscript. We would like to thank

the Bloomington Stock Center and the Developmental Studies Hybridoma Bank for fly strains and antibodies.

Chapter 6 is a copy of the manuscript entitled “Postembryonic lineages of the *Drosophila* brain: II. Identification of lineage projection patterns based on MARCM clones” by Darren Wong, Jennifer Lovick, Kathy Ngo, Wichanee Borisuthirattana, Jaison Omoto, and Volker Hartenstein and was accepted to Developmental Biology in 2013 (384:258-289; doi: 10.1016/j.ydbio.2013.07.009). This manuscript is reproduced with permission from Elsevier (License # 3701110132046). Experiments were conducted by Darren, Jennifer, Kathy, Wichanee, and Jaison; data analysis and publication preparation by Darren, Jennifer, Kathy, and Volker. We thank the members of the Hartenstein laboratory for critical discussions during the preparation of this manuscript. We thank S. Fung, F. Wang, J.D. Nguyen, and K. Wang for their involvement in generating larval and adult MARCM clones. We are grateful to the Bloomington Stock Center and the Developmental Studies Hybridoma Bank for fly strains and antibodies.

This research was supported by the USPHS National Research Service Award GM07104 (NIH predoctoral training grant in Genetic Mechanisms) to Jennifer Lovick, the Ruth L. Kirschstein National Research Service Award GM007185 to Jaison Omoto (NIH predoctoral training grant in Cellular and Molecular Biology), the NSF Graduate Research Fellowship Program DGE-0707424 to Kathy Ngo, the NIH Grant R01 NS054814 to Volker Hartenstein, and the NIH Grant R01 NS29357-15 to Volker Hartenstein.

VITA

2007	California Lutheran University, Thousand Oaks, California B.S., Biological Sciences, summa cum laude, University Honors
2003 – 2007	University Academic Scholarship, California Lutheran University
2003 – 2007	SBC Foundation Scholarship, SBC Communications (now AT&T)
2005 – 2006	Barry Goldwater Scholarship, Barry Goldwater Scholarship & Excellence in Education Program
2006	Swensen Summer Science Fellowship, California Lutheran University
2007	SCA Recognition Excellence in Science, Swedish Council of America
2008 – 2011	NIH Predoctoral Training Grant in Genetic Mechanisms, University of California, Los Angeles
2013	Travel to 2013 GSA Conference, University of California, Los Angeles
2013	UCLA University Fellowship, University of California, Los Angeles
2006 – 2007	Departmental Assistant, Department of Biological Sciences, California Lutheran University
2009	Teaching Assistant, Department of Molecular, Cell and Developmental Biology, University of California, Los Angeles
2010	Teaching Assistant Teaching Assistant, Department of Life Sciences Core Education, University of California, Los Angeles
2015	Teaching Assistant, Department of Molecular, Cell and Developmental Biology, University of California, Los Angeles

PUBLICATIONS AND PRESENTATIONS

Lovick J.K., Omoto J.J., Hartenstein V. (2015) Flies do the locomotion. Elife. 4. doi: 10.7554/eLife.10317.

Lovick J.K., Kong A., Omoto J.J., Ngo K.T., Younossi-Hartenstein A., Hartenstein V. (2015) Patterns of growth and tract formation during the early development of secondary lineages in the Drosophila larval brain. Dev Neurobiol. doi: 10.1002/dneu.22325.

Hartenstein V., Younossi-Hartenstein A., Lovick J.K., Kong A., Ngo K.T., Omoto J.J., Yao X. (2015) Lineage-associated tracts defining the anatomy of the Drosophila first instar larval brain. Dev Biol. pii: S0012-11606(15)30027-0. doi: 10.1016/j.ydbio.2015.06.021.

Lovick J.K., Hartenstein V. (2015) Hydroxyurea-mediated neuroblast ablation establishes birthdates of secondary lineages and addresses neuronal interactions in the developing Drosophila brain. Dev Biol. 402:32-47.

Kuert P.A., Hartenstein V., Bello B.C., Lovick J.K., Reichert H. (2014). Neuroblast lineage identification and lineage-specific Hox gene action during postembryonic development of the subesophageal ganglion in the Drosophila central brain. Dev Biol. 390, 102-115.

Lovick J.K., Ngo K.T., Omoto J.J., Wong D.C., Nguyen J.D., Hartenstein V. (2013) Postembryonic lineages of the Drosophila brain: I. Development of the lineage-associated fiber tracts. Dev Biol. 384, 228-257.

Wong D.C., Lovick J.K., Ngo K.T., Boristhirattana W., Omoto J.J., Hartenstein V. (2013) Postembryonic lineages of the Drosophila brain: II. Identification of lineage projection patterns based on MARCM clones. Dev Biol. 384, 258-289.

Das A., Gupta T., Davla S., Prieto Godino L.L., Diegelmann S., Reddy O.V., Raghavan K.V., Reichert H., Lovick J., Hartenstein V. (2012) Neuroblast lineage-specific origin of the neurons of the Drosophila larval olfactory system. Dev. Biol. 373, 322-337.

Pereanu W., Younossi-Hartenstein A., Lovick J., Spindler S., Hartenstein V. (2011) Lineage-based analysis of the development of the central complex of the Drosophila brain. J. Comp. Neurol. 519, 661-689. Retraction in: J. Comp. Neurol. 2013 521, 266.

Marcey D., Lovick J., Ward M. (2007) E. coli Catabolite Activator Protein. A Web-based Jmol Marcromolecular Tutorial to Accompany Molecular Biology of the Gene (Watson, et al.) 6e. Benjamin Cummings, San Francisco.

Marcey D., Lovick J. (2007) The Bacteriophage T7 DNA Polymerase. A Web-based Jmol Marcromolecular Tutorial to Accompany Molecular Biology of the Gene (Watson, et al.) 6e. Benjamin Cummings, San Francisco.

Lovick J.K., Omoto J.J., Hartenstein V. (2015). Using a lineage-based approach to study neural circuitry in the fly brain. Research talk for Honors Program Seminar Series. California Lutheran University, Thousand Oaks, California.

Lovick J.K., Omoto J.J., Hartenstein V. (2015). Lineage-based analysis of Drosophila brain development and circuitry: the anterior visual pathway to the central complex. 2015 Neurobiology of Drosophila Conference, Cold Spring Harbor, New York.

Hartenstein V., Lovick J.K., Saafeld S., Tomancak P., Cardona A. (2014). Lineage-related neuronal wiring properties of the Drosophila brain. Poster presented at 2014 GSA Annual Drosophila Research Conference, San Diego, California.

Lovick J., Hartenstein V. (2013) Adult brain compartment formation requires proper scaffolding by secondary lineages. Poster presented at 2013 GSA Annual Drosophila Research Conference, Washington D.C.

Lovick J., Hartenstein V. (2008) Are lineages the link between genes and behavior in Drosophila? Poster presented at UCLA MCDB Departmental Retreat, Lake Arrowhead, California.

Chapter 1

Comparative review of neural lineages in *Drosophila melanogaster* central brain and vertebrate neocortex

What it takes to build a brain

The intricate architecture of the brain is constructed by a vast array of neurons generated in a highly regulated spatiotemporal manner. Timing and location of neuron birth and connectivity to other neurons are critically important for assembly into the neuronal circuits which underlie all brain function. The complex nature of the brain, the repertoire of tasks it is responsible for producing and mediating, makes understanding how circuits are built a daunting task.

The more complex the animal, the more complex the brain. This complexity correlates to an increase in brain size; a feature attributed to an increase in number and variety of neurons and glial cells (reviewed in Arai and Pierani, 2014; Boyan and Williams, 2011; Florio and Huttner, 2014; Reichert, 2009), which manifests itself in increasingly complex neural circuitry and behavioral routines. Neurons organize into structural modules which serve as the building blocks for circuitry and neurons with similar phenotypes likely derive from a common progenitor or pool of progenitor cells. Thus, a more complex brain tends to have a larger and more varied complement of progenitors (reviewed in Jiang and Nardelli, 2015; Taverna et al., 2014). As such, understanding how a complex system like the human brain works (with over one hundred billion neurons), studying the mechanisms underlying circuit building by assemblies of neurons is an overwhelming venture. To get at how neurons of diverse origins organize into neural circuits it is much more feasible to address in a simpler system such as the central brain of *Drosophila melanogaster,* which consists of approximately 100,000 neurons.

Over the last half century, *Drosophila* has been developed into an easily accessible, genetically tractable model system for studying fundamental as well as disease-based neurobiological questions. Inroads have been made into many issues regarding neurogenesis in the *Drosophila* brain including origin and specification of neural progenitors; molecular mechanisms underlying generation, diversification, and differentiation of neurons; neuron morphology and organization into circuits; and the relationship between individual or classes of neurons and function (reviewed in Boyan and Reichert, 2011; Brochtrup and Hummel, 2011; Ito and Awasaki, 2008; Kang and Reichert, 2015; Lin and Lee, 2012; Spindler and Hartenstein, 2010; Urbach and Technau, 2004). Despite the progress that has been made, it is still unclear how developmental programs initiated in neural progenitors translate into neuronal phenotypes (type of connectivity, physical features) and ultimately function (behaviors they elicit). To get at this idea, we and others have postulated that the building blocks of *Drosophila* central brain circuitry are developmental-structural units termed lineages, which also serve as fundamental functional units for higher order processing.

The vertebrate brain also exhibits a modular structure, though it has not been clearly demonstrated that these modules all have a developmental origin. However, a number of anatomical studies suggest that the neocortex of many vertebrate species (cat, monkey, mouse, rat) contain structural units that do have a developmental origin and may underlie cortical function (reviewed in da Costa and Martin, 2010; Rockland, 2010). Here, we aim to provide a comparative analysis of the fundamental architecture of the *Drosophila* brain and neocortex from the perspective of these developmental-structural units.

Constructing a brain requires building blocks

Neurogenesis: variations on a theme

The nervous system develops from a heterogeneous mix of progenitors, multipotent stem cell-like cells which give rise to both neurons and glia. In this chapter, we will be focusing on neural progenitors which only generate neurons. Neurogenesis varies and proceeds via different types of neural progenitors (Fig.1.1) to form neural lineages (reviewed in Hartenstein and Stollewerk, 2015). We present here three general scenarios; in all cases a neuroectodermal cell (NE) directly transforms into a neural progenitor cell (NP). In scenario 'A', the NP divides asymmetrically to self-renew and form an intermediate progenitor (IP), which divides symmetrically to produce two neurons. The NP generates a specific set of neurons in a distinct order; this is called a "fixed" lineage and is found in insects (e.g. *Drosophila melanogaster*) as well as crustaceans (Gerberding, 1997; Goodman and Doe, 1993; Harzsch, 2001; Scholtz, 1992; Ungerer and Scholtz, 2008; Ungerer et al., 2011, 2012; Wheeler and Skeath, 2005). In the second scenario ('B'), the NP divides asymmetrically and makes neurons via a symmetrically dividing IP as in 'A'. However, unlike in a "fixed" lineage, neurons are generated stochastically. Neural lineages which are not "fixed" can be found in the optic lobe medulla of *Drosophila*, arthropods such as sea spiders (pycnogonids) or millipedes (myriapods), and the vertebrate neural tube and neocortex (Brenneis et al., 2013; reviewed in Hartenstein and Stollewerk, 2015; Shitamukai and Matsuzaki, 2012; Stollewerk and Chipman AD, 2006; Suzuki and Sato, 2014). The third scenario ('C') is the most unclear. In this case, a NP symmetrically divides to produce neurons, though

whether or not it does this directly is not known in many animals (e.g. spiders [chelicerates]; Dooeffinger et al., 2010; Mittmann, 2002; Stollewerk, 2004; Stollewerk et al., 2001).

The lineage concept

A set of neuronal progeny descended from a common neural progenitor cell is called a lineage. As straightforward as this may seem, the term lineage is used in varying contexts to mean different things. On the one hand, it simply refers to a single progenitor cell and all of its progeny. It has also been used to describe all of the progeny made by a pool of progenitor cells. In *Drosophila,* for example, one can distinguish between these two scenarios in the following way: progeny of Type I versus Type II neuroblasts form separate lineages of neurons because they arise from two different kinds of progenitor cells; a single neuroblast makes a lineage of neurons that is different from another neuroblast (e.g. lNB makes a different type of antennal lobe projection neurons than the adNB; Das et al., 2008; Lovick and Hartenstein, 2015; Stocker et al., 1997; Wong et al., 2013). In the vertebrate brain, and most clearly described in the neocortex, the term lineage is used to describe sets of neurons that are made by pools of neural progenitors (e.g. Tbr2+ neural progenitors make glutamatergic neurons of all laminar layers of the neocortex, with a bias towards more superficial layers, but make no GABAergic or astrocytic cells; Vasistha et al., 2014). Though studies suggest individual cortical progenitors can form clonal units (discussed later), the term lineage has not been applied to single neural progenitors as it has in *Drosophila*.

Despite this disparity, the lineage concept implies several things: one, all cells within a lineage are developmentally related and likely share some common features; two, a progenitor cell or cells have characteristics which are inherited by their descendants and are important for determining neuronal phenotypes; three, cells derived from different progenitors form separate lineages and are likely to be more dissimilar functionally and morphologically.

In the nervous system, a lineage refers to groups of cells (neurons, glia, or neurons and glia) which derive from a common neural progenitor. A number of factors define the type of lineage a neural progenitor will make: duration of neurogenesis and rate of proliferation determine neuron number; genes expressed in the progenitor dictate the genetic program of its descendants, which translates to the type of neuron a cell will become; migration of neurons away from the progenitor cell(s) and its effect on the overall anatomy of the brain. The means through which all of this is achieved varies substantially between invertebrates and vertebrates.

Another major difference is the manner in which invertebrate and vertebrate neural progenitors are “programmed” to generate neurons. In *Drosophila*, each neuroblast undergoes a set number of asymmetric divisions to sequentially produce neurons of varying phenotypes (based on gene expression patterns, morphology, and function). Thus, the neuronal lineage made by a neuroblast is considered “fixed” because the number, order, and type in which neurons are generated is highly stereotyped and regulated by intrinsic genetic mechanisms (Boyan and Williams, 2011; Ito and Awasaki, 2008; reviewed in Hartenstein et al., 2008; Lin and Lee, 2012; Sousa-Nunes et al., 2010; Spindler and Hartenstein, 2010). In vertebrates, the “fixed” lineage

concept has yet to be conclusively demonstrated. Though genetically-defined pools of progenitors are known to make specific types of neurons, it is not know whether or not this a stochastic process. Furthermore, studies into intrinsic regulatory mechanisms of single neural progenitors have not been thoroughly addressed (Gao et al., 2013; Marín and Müller, 2014).

Common ancestry: it all begins with the neural progenitor

The neuroblast code: position and timing are everything

In *Drosophila* and other insects, neurons derive from a neural progenitor called a neuroblast, which form as a subset of neuroectodermal cells that delaminate during embryogenesis to form the neural primordium (reviewed in Hartenstein and Wodarz, 2013). First defined by Whitman (1878, 1887) and described in detail by Wheeler (1891, 1893) using histological techniques with a nuclear dye in embryos of grasshoppers, neuroblasts, appeared as large pale cells which “budded” off smaller more strongly labeled cells, the neurons of the embryonic nervous system. Panov (1963, 1966) documented the origin and fate of neuroblasts in a variety of insect species, but the idea that a neuroblast produces a readily identifiable cluster of neurons through a series of asymmetric divisions was observed by others, both *in vitro* and *in vivo* (Bate, 1976; Poulson, 1950; Seecof et al., 1972, 1973). However, the fixed nature of insect neural lineages, the concept that neuroblasts organize into arrays and undergo a set number of mitotic divisions, producing neurons in a sequential manner, was not clearly demonstrated until later (Booker and Truman, 1987; Doe and Goodman, 1985; Goodman and Spitzer, 1979; Goodman, 1982; Goodman et al., 1982; Raper et al.,

1983a, b; Taghert and Goodman, 1984; Zacharias et al., 1993). Stereotypic arrangement of neuroblasts in *Drosophila* (Hartenstein and Campos-Ortega, 1984; Hartenstein et al., 1987; Urbach et al., 2003) and differential expression of a host of transcription factors (e.g. gap genes such as *ems* and *otd*; Urbach and Technau, 2003a, b) was shown to provide each neuroblast with a unique spatial and genetic code (Doe, 1992; Skeath and Thor, 2003; Younossi-Hartenstein et al., 1996).

Neuroblasts have two proliferative phases: the first, in the embryo, produces 15-20 neurons per lineage; the second, in the larva, occurs after a period of mitotic quiescence and yields approximately 100 neurons per lineage (Bello et al., 2008; Larsen et al., 2009). Within a lineage, the axons of both primary (embryonic born) and secondary (larval born) neurons fasiculate together forming characteristic axon tracts for each lineage. Central brain neuroblasts exhibit two modes of cell division. Type I neuroblasts divide asymmetrically to self-renew and produce an intermediate cell, the ganglion mother cell, which divides symmetrically to form two daughter neurons. Type II neuroblasts divide asymmetrically, but yield an intermediate progenitor cell which undergoes several rounds of asymmetric divisions before generating neurons (Kang and Reichert, 2015). The timing of primary and secondary neurogenesis is highly regulated by a number of signaling molecules, transcription factors, and extra cellular matrix molecules (Barrett et al., 2008; Chell and Brand, 2010; Dumstrei et al., 2003; Ebens et al., 1993; Park et al., 2003; Sousa-Nunes et al., 2011; Voigt et al., 2002). Only five neuroblasts exhibit an uninterrupted neurogenic phase, they do not enter a period of quiescence (the four mushroom body neuroblasts and one antennal lobe neuroblast; Ito and Hotta, 1992; Ito et al., 1997; Stocker et al., 1997). Utilizing a chemical ablation

technique with the drug hydroxyurea (HU) we and others have shown that central brain neuroblasts initiate secondary neurogenesis during the larval period in a very specific order (de Belle and Heisenberg, 1994; Ito and Hotta, 1992; Lovick and Hartenstein, 2015; Prokop and Technau, 1994); systematic application of HU has allowed us to establish a “birth date” for each secondary lineage in the larva (Lovick and Hartenstein, 2015). The number and type of neurons which a neuroblast generates is a function of the time window (duration as well as stage of development) during which it proliferates. Thus, longer periods of neurogenesis yield larger lineages (compare size of primary versus secondary lineages, primary neurogenesis lasts approximately 6-8 hours whereas secondary neurogenesis lasts approximately 120 hours; Hartenstein et al., 1987; Ito and Hotta, 1992). Secondary lineages exclusively form adult neural circuits (born in the larva), primary lineages the functional larval brain (born in the embryo). Though there is great variation in terms of projection and branching patterns amongst central brain lineages, it is crucial to note that lineages are highly invariant. The rigidity of neural lineages is a direct result of a neuroblast’s genetic programming, intrinsic cues dictate precisely how an individual neuroblast generates its complement of neurons, and this is what is meant by a “fixed” lineage.

Vertebrate neural progenitors: variations on a theme

The cerebral cortex varies greatly in volume and neuron number across species (e.g. compare approximately 2 X 10^7 in mouse to 16 X 10^7 in humans; Azevedo et al., 2009; Herculano-Houzel, 2009). The neocortex forms the majority of the volume of the cerebral cortex (reviewed in Florio and Huttner, 2014; Taverna et al., 2014). A detailed quantitative analysis of the number of neurons produced by a single progenitor cell in

the neocortex has yet to be done, though it is very clear that the expansion of the neocortex in higher mammals (primates and humans) is likely due to a large increase in progenitor cell number (Fietz et al., 2010; Hansen et al., 2010). In mouse, beginning before embryonic day nine (E9), the neural tube consists of symmetrically dividing neuroepithelial cells (NECs). NECs are polarized with processes extending towards the apical (ventrical) and basal (pial) surfaces; NECs give rise to all parts of the central nervous system (e.g. the neocortex derives from NECs in the dorsolateral telencephalon, the most anterior/rostral part of the neural tube; Gilbert, 2000). Utilizing histological and autoradiographic techniques, NECs were shown in a variety of species to have proliferative potential, essentially the first neural stem cells to appear during development (His, 1889, Sauer and Chittenden, 1959; Sauer and Walker, 1959; Sidman et al., 1959; reviewed in Sidman and Rakic, 1973). As development proceeds, stem cells become restricted to zones throughout the brain (e.g. the ventricular and subventricular zones of the neocortex; reviewed in Jiang and Nardelli, 2015; Sun and Hevner, 2014). In the neocortex, NECs form a pseudostratified epithelial layer which lines the cerebral ventricles and divide to produce neurons and more fate-restricted neural progenitor cells, the so-called apical radial glial cells (aRGCs; Götz and Huttner, 2005; Kriegstein et al., 2006; for history of radial glial cells see Bentivoglio and Mazzarello, 1999). aRGCs maintain an apical-basal polarity, extending long processes towards the basal surface (form the ventricular zone, VZ). It is estimated that each aRGC produces approximately six neurons, though the number aRGCs has not been quantitatively assessed (He et al., 2015; Yu et al., 2009). The VZ also contains apical intermediate progenitor cells (aIPCs; Gal et al., 2006; Mizutani et al., 2007; Stancik et

al., 2010; Tyler and Haydar, 2013). aRGCs asymmetrically divide to self-renew and produce a neuron (direct neurogenesis) or basal intermediate progenitor cell (bIPC) which can undergo multiple rounds of division to produce neurons (indirect neurogenesis; form the subventricular zone, SVZ; Hartfuss et al., 2001; Campbell and Götz, 2002; Noctor et al., 2004; Kriegstein et al., 2006). Single-cell clonal analysis in mouse has shown that a bIPC (Tbr2+) can produce up to 32 neurons, though exact numbers or whether the proliferative potential of a given bIPC varies or not has not been examined (Vasistha et al., 2014). In primates and humans the SVZ is subdivided such that the inner SVZ contains bIPCs, while the outer SVZ contains basal RGCs (bRGCs), which have apical or basal processes similar to aRGCs of the VZ (Betizeau et al., 2013; LaMonica et al., 2013). Each neural stem cell subtype is distinguishable based on their expression of different genes: aRGCs express Pax6 and glial markers GLAST and BLBP, bIPCs Tbr2, aIPCs Pax6, and bRGCs Pax6 and Sox 2 (Asami et al., 2011, Englund et al., 2005; Noctor et al., 2004; Sessa et al., 2010; Wang et al., 2011).

Within the VZ and SVZ, the pools of progenitor cells (aRGCs, aIPCs, bRGCs, bIPCs) are not homogenous as evidenced by the expression of a host of different genes (reviewed in Okano and Temple, 2009). Morphogen gradients (e.g. BMP, EGF, FGF, and Wnt) followed by regional expression of various transcription factors (e.g. COUP-TF1, Emx2) pattern the aRGCs. As corticogenesis proceeds, the boundaries between patterning genes becomes progressively more well-defined (Liu et al., 2000; Rubenstein et al., 1999). Furthermore, genes specific to distinct pools of aRGCs in the VZ have been linked to the types of neurons these progenitors give rise to (Chen et al., 2005a, b; Cubelos et al., 2008; Molyneaux et al., 2005; Shen et al., 2006; reviewed in Molyneaux

et al., 2007). More recently, lineage-tracing and clonal analyses of single or small sets of neural stem cells has revealed that in the neocortex, a stem cell can give rise to excitatory glutamatergic neurons of all cortical layers. Furthermore, these neurons primarily migrate radially so that they appear as vertical columns and have a preference for making connections with neurons within the same column (He et al., 2015; Li et al., 2012; Ohtsuki et al., 2012; Vasistha et al., 2014; Yu et al., 2009). A similar phenomenon has been observed with inhibitory interneurons which organize either vertically or horizontally within the neocortex (Brown et al., 2011). What has not been demonstrated is the plasticity of a given neural progenitor cell. It remains to be seen how the behavior of a single neural progenitor compares to the rigid nature of the *Drosophila* neuroblast and the "fixed" lineages they generate.

Lineages as fundamental units for understanding brain circuitry

Neural lineages form the 'macro-circuitry" of the Drosophila brain

Neurons are responsible for coordinating complex behavioral responses. To do this, one might expect that neurons are organized in a manner which reflects the upstream processing required to elicit such complex behaviors. Traditional methods of labeling neural tissue (Golgi, silver staining) show that this is indeed the case (Chen and Chen, 1969; Power, 1943; Strausfeld, 1976). What is immediately apparent is the intricate web of fibers which extend throughout, forming unique shapes and subdividing neural tissue into distinct regions. In the brain and ventral nervous system of *Drosophila,* more refined techniques which allow one to visualize individual or small populations of neurons (antibody markers, genetic labeling techniques) reveal additional details. Axon fibers

bundle together in tracts which vary in thickness and interconnect different regions; these tracts associate with specific fascicle systems (Ito et al., 2014; Lovick et al., 2013; Strausfeld, 1976; Truman et al., 2004, 2015; Wong et al., 2013; reviewed in Spindler and Hartenstein, 2010). Clonal and developmental analyses utilizing Gal4 drivers or MARCM, which allow one to label and visualize a neuroblast and its neuronal progeny with a fluorescent marker, illustrate that neural lineages are organized into highly stereotyped anatomical units, such that neurons which derive from a single neuroblast appear in close proximity (cell somas cluster together and axon fibers remain bundled together; Ito et al., 2013; Pereanu and Hartenstein, 2006; Truman et al., 2004; Wong et al., 2013; Yu et al., 2013). The close interaction of neurons within a lineage is maintained by intrinsic and extrinsic molecules of both the neurons and surrounding glial cells (Dumstrei et al., 2003; Fung et al., 2009; Spindler et al., 2009). Lineages are characterized as having morphologically distinct axon tracts which innervate and branch in one or several compartments; the *Drosophila* central brain consists of approximately 100 (Hartenstein et al., 2015; Ito et al., 2013; Kumar et al., 2009; Pereanu et al., 2010; Wong et al., 2013; Yu et al., 2013). Lineages can be further subdivided based on morphology and gene expression patterns; several well-studied examples in the central brain include those which form the mushroom body, antennal lobe, and ellipsoid body compartments (Lai et al., 2008; Lin et al., 2012; Omoto et al., in preparation; Yang et al., 2013; Yu et al., 2010; Zhu et al., 2006). Within a lineage, differential expression of Notch in daughter neurons (hemilineages) as well as time of birth (sublineages) is critical for determining the phenotype and survival of a neuron (Das et al., 2010; Kumar et al., 2009; Lai et al., 2008; Lin et al., 2010, 2012; Lovick et al., 2015; Omoto et al., in

preparation; Truman et al., 2010; Udolph, 2012; Wang et al., 2014; Yu et al., 2009, 2010). Collectively, lineages form structural units which interconnect to form the neural "macro-circuitry" of the brain.

Interestingly, the unique gene expression patterns observed in neuroblasts, in many cases, is reflected in the neuronal lineages they produce. This suggests that, at a very early stage in development, there are intrinsic programs which establish the type of neurons a given neuroblast will generate (Sen et al., 2014; reviewed in Sousa-Nunes and Somers, 2013). Lineage-specific combinatorial codes in concert with the sequential expression of a series of transcription factors ensure each neuroblast produces a distinct population of neurons, many of which are comprised of anatomically unique subsets (Berger et al., 2001; Blanco et al., 2011; Das et al., 2008, 2013; Grosskortenhaus et al., 2005; Isshiki et al., 2001; Kuert et al., 2014; Kunz et al., 2012; Lovick et al., 2015; Omoto et al., in preparation; Pearson and Doe, 2003; Urbach et al., 2003). The phenotype of a neuronal lineage manifests itself in the morphology of its axonal projection pattern and branching pattern; within a lineage, neurons can vary in terms of their branching pattern and presumably function (Lai et al., 2008; Lee et al., 1999; Wang et al., 2014). For example, the antennal lobe-associated lNB/BAlc lineage, which consists of both local interneurons that exclusively innervate the antennal lobe glomeruli and projection neurons that have dendrites in the antennal lobe and terminal arbors in the calyx and lateral horn (Lai et al., 2008). Each of the 100 secondary lineages of the *Drosophila* larval brain is readily identifiable based on these criteria (Pereanu and Hartenstein, 2006). Importantly, as the brain grows, lineage projection patterns remain relatively unchanged and can be followed from their time of birth in the

larva, through metamorphosis when they differentiate, and into the adult (Lovick et al., 2013, 2015; Omoto et al., in preparation; Pereanu et al., 2010; Wong et al., 2013). As an example, the secondary neurons of the lineage DALv2, which forms the ellipsoid body in the adult brain, has a characteristic tract which projects medially towards the midline between the two brain hemispheres. This tract, using global and lineage-specific markers, can be followed from its inception during the early larval phase, through larval and pupal development, and into the adult (Lovick et al., 2013, 2015; Omoto et al., in preparation). Primary lineages (those born during embryogenesis), though they are approximately a tenth of the size of secondary lineages, exhibit similar projection and branching patterns to their corresponding secondary lineages (e.g. compare the primary and secondary neurons of the adNB/BAmv3 lineage, both project to and form dendrites in the larval/adult antennal lobe, calyx, and lateral horn; Das et al., 2013; Hartenstein et al., 2015).

"Macro-circuits" of the vertebrate brain: ontogenetic columns and the radial unit hypothesis

Histological studies of the vertebrate brain show that different regions of the brain exhibit very distinct anatomical features; for example, the neocortex which contains six laminar layers subdivided by radially-oriented columns (reviewed in Molyneaux et al., 2007; Rakic, 2009; Voogd and Glickstein, 1998). The neocortex is an important center for higher order processing (sensory processing, control motor functions, centers for language, spatial orientation, facial recognition, etc.) and may be the best studied example of neuroanatomical organization in the vertebrate brain. Structurally, the neocortex is divided into six layers, each layer consisting of neurons with different

projection patterns interconnecting the neocortex with other regions of the brain (reviewed in Molyneaux et al, 2007). The six layers are subdivided into cytoarchitectonic areas, functional regions defined by unique biochemical and physiological characteristics (Brodman, 1909; reviewed in Kaas, 1987). The six layers of the neocortex are made up of smaller units, vertical columns which are oriented perpendicularly to the layers. Each column consists of the cell bodies of cortical neurons (glutamatergic pyramidal neurons and GABAergic interneurons; we will be focusing exclusively on glutamatergic neurons). Thus, a single column appears as a vertical array of neuronal cell bodies spanning the six layers of the neocortex. Histological analyses have shown that the boundaries of columns are defined not only by the cell bodies themselves, but also by the processes of radial glial cells, which neurons use to migrate out of the proliferative zones (reviewed in Rakic et al., 2009; Fig.2). More recent studies show that in the developing neocortex, sister excitatory neurons (those which derive from the same progenitor cell in the ventricular zone) preferentially connect with each other and exhibit functional similarities (e.g. similar orientation preferences in the visual cortex; He et al., 2015; Li et al., 2012). However, it has also been observed that neurons of a given column do make connections with neurons of other columns highlighting the fact that a column does not function as a standalone unit (reviewed in Rockland, 2010). This columnar organization was first observed by Lorente de Nó (1938), but it wasn't until Rakic in the 1970s used [^{3}H]thymidine to label dividing neural progenitors and their offspring (neurons) in developing tissue that the origin of these vertical columns was demonstrated. Rakic observed in midgestation fetal monkey neocortex (75-97 days) that cortical progenitors (radial glial cells; aRGCs), which are

located basally in a region adjacent to the ventricle (the ventricular zone, VZ), asymmetrically divide to self-renew and “bud” off cells which migrate apically or vertically along long processes made by the radial glial cells to their final destination where they differentiate, forming the six cortical layers (Rakic 1971, 1972). Neurons organize in a radial manner, extending out from the VZ. Interestingly, this migration pattern is largely conserved throughout development such that all neurons which derive from a single neural progenitor appear as vertical columns which are retained even into the adult (termed ontogenetic columns; Rakic, 1974). This concept is referred to as the radial unit hypothesis and it posits that a radial glial cell (neural progenitor) not only sequentially generates neurons, but it also serves to guide neurons out of the VZ along long processes; neurons migrate radially and minimally, if at all, laterally forming vertical (ontogenetic) columns extending the depth of the cortex and its six layers; neurons organize in cortical layers in an inside-out fashion (neurons born first form deeper layers, neurons born later form more superficial layers; reviewed in McConnell, 1988; Rakic, 1978, 1988). Each radial glial cell, then, would presumably produce a population of neurons that organize into a single ontogenetic column in the neocortex (Gray et al., 1988; Luskin et al., 1988; Price et al., 1987; Turner and Cepko, 1987; Wetts and Fraser, 1988), though this does not take into account neurons formed by other progenitor cell types. An ontogenetic column, then, would contain excitatory glutamatergic neurons found in all six layers of the neocortex (as demonstrated by single aRGC clones in mouse; He et al., 2015; Li et al., 2012). The developing column is visible based on the organization of excitatory neuron cell bodies as well as radial glial cell processes which extend apically from the ventricle wall to the outer pial surface of the neocortex. In the

adult, only orientation of cell bodies (based on clonal analysis) define the ontogenetic columns, radial glial cells are no longer present (differentiate into astrocytes; Schechel et al., 1979; Voigt, 1989). Thus, proliferative units serve as a proto-map for the neurons making up the ontogenetic columns; tangential coordinates are determined by the location of the progenitor cell in the VZ and radial position by the time of birth. The laminar (layered) and columnar organization of the neocortex is a common feature amongst vertebrates (Haug, 1987; Meynert, 1868) and the column (or similar anatomical modular feature) appears to be a common structural theme in other regions of the brain as well (reviewed in Rockland, 2010).

If columns of functionally related neurons do correspond to the ontogenetic columns as described by Rakic (1988), then this suggests that not only are the columns laid out in a mosaic pattern, then so are the progenitor cells from which they derive. Molecular evidence (as reviewed in Rakic et al., 2009) supports this notion that neural progenitors (neuroepithelial cells and radial glial cells) are not homogenous (reviewed above). Regionalization of cortical progenitors occurs in a step-wise manner: early, rostro-caudal (e.g. FGFs) and medio-lateral (e.g. EGFs) morphogen gradients are established; these in turn progressively refine domains of progenitors by regulating expression of various transcription factors (e.g. FGF8 suppresses empty spiracles homeobox 2 (EMX2) anteriorly so it is expressed in a posterior-to-anterior gradient; Fukuchi-Shimogori and Grove, 2003). It is not clear however, how these gradients are translated into more sharply defined boundaries (e.g. those of the visual cortex) made by the combinatorial expression of guidance molecules in developing and mature cortical neurons (reviewed in Homman-Ludiye and Bourne, 2014). Moreover, there is

mounting evidence to suggest that cortical neurons are generated in a sequential manner under the control of transcription factors regulated by intrinsic programs initiated in neural progenitors (Arlotta et al., 2008; Britanova et al., 2008; Chen et al., 2008; Hanashima et al., 2004; Jacob et al., 2007; Lai et al., 2008; Molyneaux et al., 2005; reviewed in Greig et al., 2013). The patterning of cortical progenitors and sequential generation of neurons is reminiscent of the mechanisms underlying lineage development seen in *Drosophila*, though the "fixed" nature in which a lineage is generated has not been documented in the neocortex.

In the vertebrate brain, a common theme in forming brain compartments is that neurons migrate from their places of origin in proliferative centers located throughout the brain. In the neocortex, excitatory glutamatergic neurons migrate radially from the ventricular and subventricular zones to more superficial positions, inhibitory GABAergic neurons migrate tangentially from proliferative regions in the basal ganglia (the medial and lateral ganglionic eminences), and Cajal-Retzius cells from the cortical hem. As the major cortical constituents, these three populations of neurons organize into the characteristic six-layered laminar structure of the neocortex (Anderson et al., 2002; Angevine and Sidman, 1961; Berry and Rogers, 1965; Hicks and D'Amato, 1968; Meyer et al., 1999; Rakic, 1972; Shimada and Langman, 1970; Tan et al., 1998; Wonders et al., 2006; reviewed in Molyneaux et al., 2007). Neurons of the *Drosophila* central brain, in contrast, do not migrate away from their parental neuroblasts or from their sibling neurons. In either case, clonal analyses have shown that sibling neurons remain in close proximity to one another and also preferentially make connections with one another (e.g. in *Drosophila,* larval mushroom body Kenyon cells form many reciprocal

connections in the medial lobe: Hartenstein lab, unpublished observations; in mouse, electrophysiology has shown that sister excitatory neurons of the neocortex are electrically coupled: He et al., 2015).

Tying structure to function: are developmentally/structurally-defined lineages endowed with common functional properties?

Relating origin to function, lineages form the basis for functional units

The complex circuitry of the *Drosophila* central brain is made by neuronal lineages. Lineages have unique projection patterns and interconnect in highly stereotyped ways which may confer on them distinct processing functions. A number of studies in brain compartments of both the larval and adult brain indicate that is likely the case. Specific behaviors (e.g. odorant processing) have been linked to specific regions in the brain (antennal lobe and calyx of the mushroom body). These regions have been shown to be made by discrete sets of neurons which are made by a small number of lineages (Ito et al., 2007, 2013; Jefferis et al., 2001; Marin et al., 2002; Wong et al, 2013; Yu et al., 2013).

The way in which lineages form connections underlies how a circuit functions. Thus, it is important to know then whether connectivity occurs primarily between neurons of a lineage or between neurons of different lineages. In the few cases where this has been studied in the *Drosophila* brain, it appears that neurons of different lineages preferentially make connections forming functional circuits. The circuit which processes olfactory information is one such example. Neurons of the lNB lineage (BAlc) or adNB lineage (BAmv3), which form post-synaptic connections with olfactory receptor

neurons in the primary olfactory center (antennal lobe) and pre-synaptic connections with Kenyon cells in the calyx of the mushroom body (secondary olfactory center), produce groups of neurons that innervate antennal and calyx glomeruli in a non-overlapping pattern. Generally, groups of three projection neurons connect a single glomerulus in the antennal lobe to a set of small glomeruli or boutons in the calyx (Jefferis et al., 2001; Marin et al., 2002; Wong et al., 2002). Whether or not these projection neurons directly synapse with each other is not known, though one study does suggest that BAmv3/projection neurons, which innervate the DM6 antennal lobe glomerulus, make reciprocal electrical connections within the antennal lobe (Kazama and Wilson, 2009). It is important to note that anatomical and electrophysiological studies show that mushroom body Kenyon cells make reciprocal connections with input neurons (antennal lobe projection neurons) in the calyx as well as between individual Kenyon cells (Hartenstein lab, unpublished observations; Christiansen et al., 2011; Leiss et al., 2009). In this case, connections made by projection neurons are important for consolidating and conveying odorant input from the antennal lobe to the higher order processing center, the mushroom body where olfactory learning and memory take place. Reciprocal connections are thought to be more important for modulating signals both in the antennal lobe and mushroom body.

The ontogenetic column: to be or not to be a functional unit

The notion that the cerebral cortex is subdivided into functional regions (cytoarchitectonic areas) is a long standing one. In an effort to understand how these regions (e.g. the somatosensory cortex) actually process information, researchers have taken a two-pronged approach. On the one hand, the cortex is made up of repeating

units, ontogenetic columns of clonally related neurons which suggest that each column or set of columns may respond to a specific set of stimuli and therefore be required for a specific function. Thus, a field of neuronal columns which are sensitized to certain stimuli may explain how the cortex is subdivided into cytoarchitectonic areas. On the other hand, electrophysiologists have demonstrated that regions such as the somatosensory cortex are constructed of functional columns which are much larger than a single anatomical vertical column (Code and Winer, 1986; Goldman and Nauta, 1977; Goldman-Rakic and Schwartz, 1982; Hubel and Wiesel, 1977; Jones et al., 1975; Mountcastle, 1957). Physiological analyses have shown that a single type of stimulus can elicit activity in cortical neurons arrayed over a physical area much larger than the area occupied by a single ontogenetic column, a calculation determined based on the size of ontogenetic columns visualized in histological sections. Efforts to demonstrate that ontogenetic columns represent the smallest units of function in the cerebral cortex have been largely unsuccessful (reviewed in Horton and Adams, 2005). However, recent studies have suggested that based on physical size and common properties of adjacent sets of ontogenetic columns, a functional “column” may actually be comprised of multiple ontogenetic columns (Li et al., 2012).

Present study

In this study we are interested in analyzing the development and anatomy of neural lineages and how they organize to form the circuitry of the central brain of *Drosophila melanogaster*.

We focus on the neural circuitry that forms the functional larval brain (primary lineages) as well as the adult brain (made mostly of secondary lineages). By tracking the development of secondary lineages using a variety of methods we are able to address a number of fundamental biological questions related to brain morphogenesis.

The first portion of this study (Chapter 2) looks at the neurons of the functional larval brain made by primary lineages. Neurons of a given lineage share common structural features and a common origin. Lineages of the adult brain are born during the larval phase and were previously classified based on cell body cluster location and axon tract morphology at the late third instar larval stage (Pereanu and Hartenstein, 2006). Here, we are able to identify a developmental stage at which axon tracts of larval-born neurons and neurons of embryonic origin can be simultaneously labeled with global markers. We are able to assign embryonic-born “primary” lineages to larval-born “secondary” lineages based on the aforementioned criteria. We have generated a detailed map of primary lineages at the late first instar larval stage.

In the second study (Chapter 3) we use a chemical ablation technique with the drug Hydroxyurea to address a number of basic developmental questions regarding the contribution and effect of secondary lineages on other lineages during adult brain morphogenesis. By systematically ablating neuroblasts in short time windows spanning the initial stages of secondary neurogenesis we are able to construct a birth date calendar of when each secondary lineage is born. This correlates well with our observations with global markers of when secondary neurons first appear (third study, Chapter 4). By looking at late larval and adult brains with global and lineage-specific markers we are able to see that the development and differentiation of primary and

secondary lineages is largely unaffected when other secondary lineages are ablated. We also document how adult neuropil compartments are affected by ablation; notably, we are able to completely or nearly completely ablate adult-specific compartments which form *de novo* during metamorphosis. Lastly, we show that the development of collateral axons does not take place in a situation when its partner neurons are chemically ablated.

In the third study (Chapter 4) we follow the development of secondary lineages from their time of birth in the late first instar larval brain to the end of the larval stage. Each lineage has a distinct axon tract which is readily identifiable using global markers. We find that secondary lineages first appear in a highly stereotyped sequence, which matches with data documenting the onset of proliferation by neuroblasts in early larval stages (second study, Chapter 3). Secondary lineages can be subdivided into morphologically unique hemilineages; by inhibiting apoptosis within these lineages we show which retain both hemilineages and which lose a hemilineage during development. We also show that large-scale rearrangements of laterally located lineages are due to the expansion of the optic lobe during larval development. When the optic lobe primordium is genetically ablated using a dominant negative form of EGFR, lineages which typically move dorsally or ventrally, show little to no movement at all.

In the fourth portion (Chapter 5) we continue to follow the development of secondary lineages from the late larval stage, through metamorphosis, and into the adult using global markers. We address a number of developmental changes which take place. While secondary lineage axon tracts change little during metamorphosis (a key phenomenon which allows us to follow them through development), the cell body

clusters located at the brain periphery move and flatten out. Also, hemilineage clusters move apart from one another as neuropil compartments grow and expand. In the adult brain, we assign the secondary lineages to their developmental counterparts classified at the late third larval instar stage, establishing a map of adult brain circuitry.

In the fifth study (Chapter 6) we analyze secondary lineages in the adult brain at a higher resolution, building upon the study conducted in Chapter 5. We created a library of neuroblast (lineage) clones using the MARCM technique and induced at the larval stage during the time when neuroblasts first begin dividing to produce secondary lineages. Each clone is labeled with a membrane-bound fluorescent reporter which allows us to visualize the entire structure of a neuron. We characterize each clone based on our lineage map from Chapter 5 and provide a detailed description of the projection and branching patterns. Lineages are invariant and innervate one or several neuropil compartments; hemilineages of the same lineage have similar, but distinct branching patterns.

Collectively, these studies add to our understanding of how neurons, grouped into lineages, form the macrocircuitry of the *Drosophila* brain. Importantly, they form a significant part of a much larger goal, determining how a lineage develops from a single neural progenitor cell beginning in the embryo.

Figure 1.1

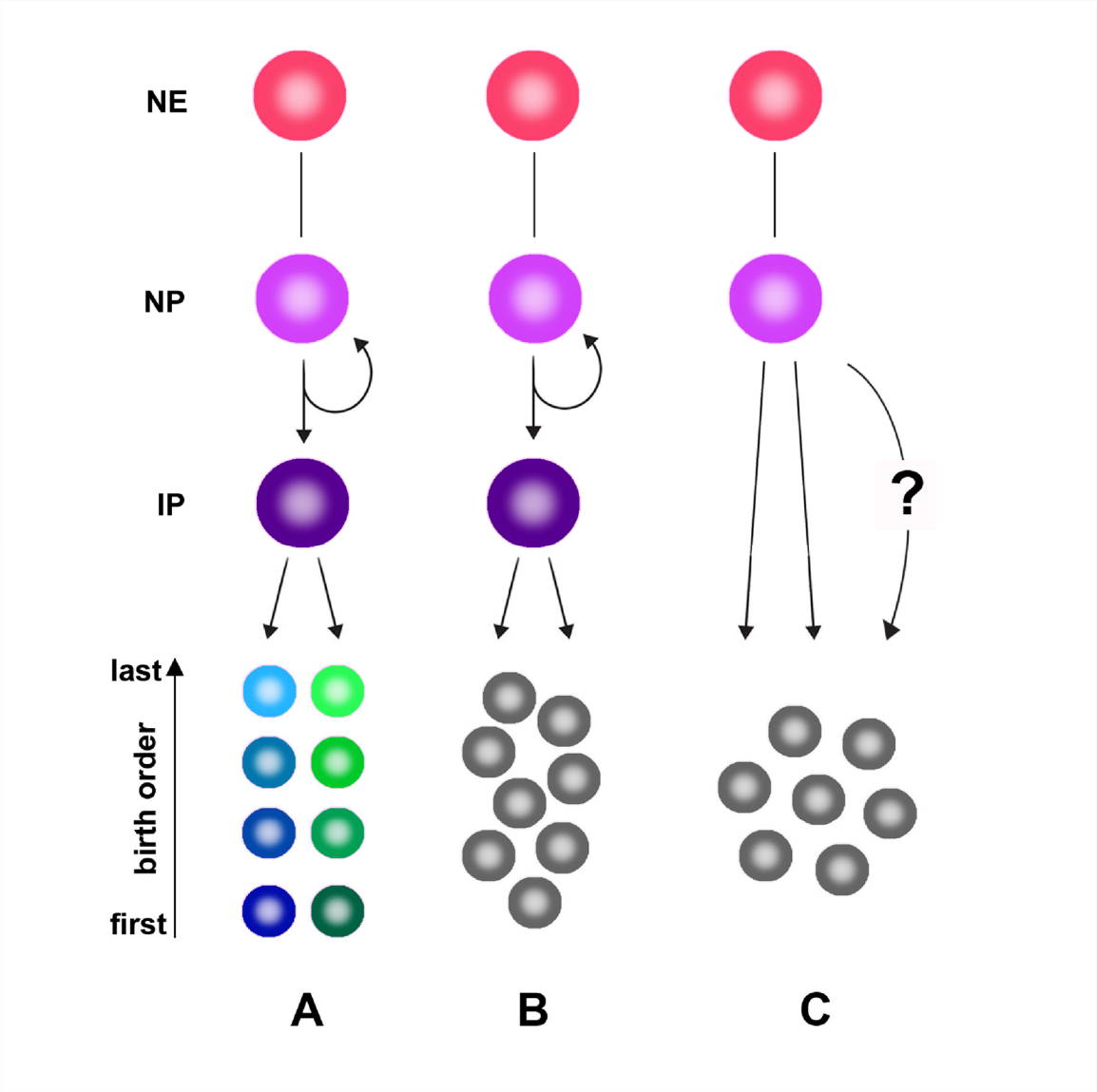

Figure 1.1

Generation of neurons through different modes of proliferation. Neuroectodermal cells (NE; pink spheres) directly become neural progenitor cells (NP; light purple spheres). In a fixed lineage (scenario 'A'), NPs asymmetrically divide a set number of times to self-renew and produce an intermediate progenitor cell (IP; purple sphere) called a ganglion mother cell which divides symmetrically divide to produce two post-mitotic neurons.

Birth order (light blue/green cells to dark blue/green cells) and segregation into hemilineages (blue cells versus green cells) determine the phenotype of each neuron within a lineage. In a lineage which is not fixed (scenario ‘B’), the NP divides asymmetrically to produce neurons via an IP (left). Neurons are generated stochastically (grey spheres), unlike in scenario ‘A’. In scenario ‘C’, NPs divide symmetrically to produce neurons stochastically. In some organisms, it is not clear whether or not NPs divide asymmetrically or symmetrically (denoted by curved arrow with question mark).

References

Arai Y, Pierani A. 2014. Development and evolution of cortical fields. Neurosci Res. 86:66-76. doi: 10.1016/j.neures.2014.06.005.

Asami M, Pilz GA, Ninkovic J, Godinho L, Schroeder T, Huttner WB, Götz M. 2011. The role of Pax6 in regulating the orientation and mode of cell division of progenitors in the mouse cerebral cortex. Development. 138:5067-5078. doi: 10.1242/dev.074591.

Azevedo FA, Carvalho LR, Grinberg LT, Farfel JM, Ferretti RE, Leite RE, Jacob Filho W, Lent R, Herculano-Houzel S. 2009. Equal numbers of neuronal and nonneuronal cells make the human brain an isometrically scaled-up primate brain. J Comp Neurol. 513:532-541. doi: 10.1002/cne.21974.

Barrett AL, Krueger S, Datta S. 2008. Branchless and Hedgehog operate in a positive feedback loop to regulate the initiation of neuroblast division in the Drosophila larval brain. Dev Biol. 317:234-245. doi: 10.1016/j.ydbio.2008.02.025.

Bate CM. 1976. Embryogenesis of an insect nervous system. I. A map of the thoracic and abdominal neuroblasts in Locusta migratoria. J Embryol Exp Morphol. 35:107-123.

Bello BC, Izergina N, Caussinus E, Reichert H. 2008. Amplification of neural stem cell proliferation by intermediate progenitor cells in Drosophila brain development. Neural Dev. 3:5. doi: 10.1186/1749-8104-3-5.

Betizeau M, Cortay V, Patti D, Pfister S, Gautier E, Bellemin-Ménard A, Afanassieff M, Huissoud C, Douglas RJ, Kennedy H, Dehay C. 2013. Precursor diversity and complexity of lineage relationships in the outer subventricular zone of the primate. Neuron. 80:442-457. doi: 10.1016/j.neuron.2013.09.032.

Booker R, Truman JW. 1987. Postembryonic neurogenesis in the CNS of the tobacco hornworm, Manduca sexta. I. Neuroblast arrays and the fate of their progeny during metamorphosis. J Comp Neurol. 255:548-559. doi: 10.1002/cne.902550407.

Boyan G, Williams L. 2011. Embryonic development of the insect central complex: insights from lineages in the grasshopper and Drosophila. Arthropod Struct Dev. 40:334.348. doi: 10.1016/j.asd.2011.02.005.

Brochtrup A, Hummel T. 2011. Olfactory map formation in the Drosophila brain: genetic specificity and neuronal variability. Curr Opin Neurobiol. 21:85-92. doi: 10.1016/j.conb.2010.11.001.

Brown KN, Chen S, Han Z, Lu CH, Tan X, Zhang XJ, Ding L, Lopze-Cruz A, Saur D, Anderson SA, Huang K, Shi SH. 2011. Clonal production and organization of inhibitory interneurons in the neocortex. Science. 334:480-486. doi: 10.1126/science.1208884.

Campbell K, Götz M. 2002. Radial glia: multi-purpose cells for vertebrate brain development. Trends Neurosci. 25:235-238. doi: 10.1016/S0166-2236(02)02156-2.

Chell JM, Brand AH. 2010. Nutrition-responsive glia control exit of neural stem cells from quiescence. Cell. 143:1161-1173. doi: 10.1016/j.cell.2010.12.007.

Chen, J.S., Chen, M.G., 1969. Modification of the Bodian technique applied to insect nerves. Stain Technol. 44, 50-51.

Chen B, Schaevitz LR, McConnell SK. 2005a. FezI regulates the differentiation and axon targeting of layer 5 subcortical projection neurons in cerebral cortex. Proc Natl Acad Sci U S A. 102:17184-17189. doi: 10.1073/pnas.05087332102.

Chen JG, Rasin MR, Kwan KY, Sestan N. 2005b. Zfp312 is required for subcortical axonal projections and dendritic morphology of deep-layer pyramidal neurons of the cerebral cortex. Proc Natl Acad Sci U S A. 102:17792-17797. doi: 10.1073/pnas.0509032102.

Cubelos B, Sebastián-Serrano A, Kim S, Moreno-Ortiz C, Redondo JM, Walsh CA, Nieto M. 2008. Cux-2 controls the proliferation of neuronal intermediate precursors of the cortical subventricular zone. Cereb Cortex. 18:1758-1770. doi: 10.1093/cercor/bhm199.

da Costa NM, Martin KA. 2010. Whose cortical column would that be? Front Neuroanat. 4:16. doi: 10.3389/fnana.2010.00016.

Das A, Sen S, Lichtneckert R, Okada R, Ito K, Rodrigues V, Reichert H. 2008. Drosophila olfactory local interneurons and projection neurons derive from a common neuroblast lineage specified by the empty spiracles gene. Neural Dev. 3:33. doi: 10.1186/1749-8104-3-33.

Das A, Reichert H, Rodrigues V. 2010. Notch regulates the generation of diverse cell types from the lateral lineage of Drosophila antennal lobe. J Neurogenet. 24:42-53. doi: 10.3109/01677060903582202.

de Belle JS, Heisenberg M. 1994. Associative odor learning in Drosophila abolished by chemical ablation of mushroom bodies. Science. 1994. 263:692-695.

Doe CQ. 1992. Molecular markers for identified neuroblasts and ganglion mother cells in the Drosophila central nervous system. Development. 116:855-863.

Doe CQ, Goodman CS. 1985. Early events in insect neurogenesis. I. Development and segmental differences in the pattern of neuronal precursor cells. Dev Biol. 111:193-205. doi:10.1016/0012-1606(85)90445-2.

Doeffinger C, Hartenstein V, Stollewerk A. 2010. Compartmentalization of the precheliceral neuroectoderm in the spider Cupiennius salei: development of the arcuate body, optic ganglia, and mushroom body. J Comp Neurol. 518:2612-2632. doi: 10.1002/cne.22355.

Dumstrei K., Wang F., Hartenstein V., 2003. Role of DE-cadherin in neuroblast proliferation, neural morphogenesis, and axon tract formation in Drosophila larval brain development. J. Neurosci. 23, 3325-3335.

Ebens AJ, Garren H, Cheyette BN, Zipursky SL. 1993. The Drosophila anachronism locus: a glycoprotein secreted by glia inhibits neuroblast proliferation. Cell. 74:15-27. doi: 10.1016/0092-8674(93)90291-W.

Englund C, Fink A, Lau C, Pham D, Daza RA, Bulfone A, Kowalczyk T, Hevner RF. 2005. Pax6, Tbr2, and Tbr1 are expressed sequentially by radial glia, intermediate progenitor cells, and postmitotic neurons in developing neocortex. J Neurosci. 25:247-251. doi: 10.1523/JNEUROSCI.2899-04.2005.

Fietz SA, Kelava I, Vogt J, Wilsch-Bräuninger M, Stenzel D, Fish JL, Corbeil D, Riehn A, Distler W, Nitsch R, Huttner WB. 2010. OSVZ progenitors of human and ferret neocortex are epithelial-like and expand by integrin signaling. Nat Neurosci. 13:690-699. doi: 10.1038/nn.2553.

Florio M, Huttner WB. 2014. Neural progenitors, neurogenesis and the evolution of the neocortex. Development. 141:2182-2194. doi: 10.1242/dev.090571.

Fukuchi-Shimogori T, Grove EA. 2003. Emx2 patterns the neocortex by regulating FGF positional signaling. Nat Neurosci. 6:825-831. doi: 10.1038/nn1093.

Fung S, Wang F, Spindler SR, Hartenstein V. 2009. Drosophila E-cadherin and its binding partner Armadillo/beta-catenin are required for axonal pathway choices in the developing larval brain. Dev Biol. 332:371-382. doi: 10.1016/j.ydbio.2009.06.005.

Gal JS, Morozov YM, Ayoub AE, Chatterjee M, Rakic P, Haydar TF. 2006. Molecular and morphological heterogeneity of neural precursors in the mouse neocortical proliferative zones. J Neurosci. 26:1045-1056. doi: 10.1523/JNEUROSCI.4499-05.2006.

Gao P, Sultan KT, Zhang XJ, Shi SH. 2013. Lineage-dependent circuit assembly in the neocortex. Development. 140:2645-2655. doi: 10.1242/dev.087668.

Gerberding M. 1997. Germ band formation and early neurogenesis of Leptodora kindti (Cladocera): first evidence for neuroblasts in the entomostracan crustaceans. Invertebr Reprod Dev. 32:63-73. doi: 10.1080/07924259.1997.9672605.

Gilbert SF. Developmental Biology. 6th edition. Sunderland (MA): Sinauer Associates; 2000. Differentiation of the Neural Tube. Available from: http://www.ncbi.nlm.nih.gov/books/NBK10034/

Goodman CS. 1982. Embryonic development of identified neurons in the grasshopper. Neuronal Development. Plenum, New York. 171-212.

Goodman CS, Doe CQ. 1993. Embryonic development of the Drosophila central nervous system. In the development of Drosophila melanogaster, M. Bate and A. Martinez-Arias, eds. (New York: Cold Spring Harbor Laboratory Press), pp. 1131-1206.

Goodman CS, Spitzer NC. 1979. Embryonic development of identified neurones: differentiation from neuroblast to neurone. Nature. 280:208-214. doi: 10.1038/280208a0.

Goodman CS, Raper JA, Ho RK, Chang S. 1982. Pathfinding of neuronal growth cones in grasshopper embryos. Development Order: Its Origin and Regulation. Alan R. Liss, New York. 275-316.

Götz M, Huttner WB. 2005. The cell biology of neurogenesis. Nat Rev Mol Cell Biol. 6:777-788. doi: 10.1038/nrm1739.

Hansen DV, Lui JH, Parker PR, Kriegstein AR. 2010. Neurogenic radial glia in the outer subventricular zone of human neocortex. Nature. 464:554-561. doi: 10.1038/nature08845.

Harris RM, Pfeiffer BD, Rubin GM, Truman JW. 2015. Neuron hemilineages provide the functional ground plan for the Drosophila ventral nervous system. Elife. 4. doi: 10.7554/eLife.04493.

Hartenstein V, Campos-Ortega JA. 1984. Early neurogenesis in wild-type Drosophila melanogaster. Roux's Arch Dev Biol. 193:308-325.

Hartenstein V, Stollewerk A. 2015. The evolution of early neurogenesis. Dev Cell. 32:390-407. doi: 10.1016/j.devcel.2015.02.004.

Hartenstein V, Wodarz A. 2013. Initial neurogenesis in Drosophila. Wiley Interdiscip Rev Dev Biol. 2:701-721. doi: 10.1002/wdev.111.

Hartenstein V, Rudloff E, Campos-Ortega JA. 1987. The pattern of proliferation of the neuroblasts in the wild-type embryo of Drosophila melanogaster. Roux's Arch Dev Biol. 196:473-485.

Hartenstein V, Spindler S, Pereanu W, Fung S. 2008. The development of the Drosophila larval brain. Adv Exp Med Biol. 628:1-31. doi: 10.1007/978-0-387-78261-4-1.

Hartenstein V, Younossi-Hartenstein A, Lovick JK, Kong A, Omoto JJ, Ngo KT, Viktorin G. 2015. Lineage-associated tracts defining the anatomy of the Drosophila first instar larval brain. Dev Biol. pii: S0012-1606(15)30027-0. doi: 10.1016/j.ydbio.2015.06.021.

Hartfuss E, Galli R, Heins N, Götz M. 2001. Characterization of CNS precursor subtypes and radial glia. Dev Biol. 229:15-30. doi: 10.1006/dbio.2000.9962.

Harzsch S. 2001. Neurogenesis in the crustacean ventral nerve cord: homology of neuronal stem cells in Malacostraca and Branchiopoda? Evol Dev. 3:154-169. doi: 10.1046/j.1525-142x.2001.003003154.x.

He S, Li Z, Ge S, Yu YC, Shi SH. 2015. Inside-out radial migration facilitates lineage-dependent neocortical microcircuit assembly. Neuron. 86:1159-1166. doi: 10.1016/j.neuron.2015.05.002.

Herculano-Houzel S. 2009. The human brain in numbers: a linearly scaled-up primate brain. Front Hum Neurosci. 3:31. doi: 10.3389/neuro.09.031.2009.

His W. 1889. Die Neuroblasten und deren Entstehung im embryonal Marke. Abh Math Phys Cl Kgl Sach Ges Wiss. 15:313-372.

Homman-Ludiye J, Bourne JA. 2014. Mapping arealisation of the visual cortex of non-primate species: lessons for development and evolution. Front Neural Circuits. 8:79. doi: 10.3389/fnc.ir.2014.00079.

Ito K, Hotta Y. 1992. Proliferation pattern of postembryonic neuroblasts in the brain of Drosophila melanogaster. Dev Biol. 149:134-148. doi: 10.1016/0012-1606(92)90270-Q.

Ito K, Awasaki T. 2008. Clonal unit architecture of the adult fly brain. Adv Exp Med Biol. 628:137-158. doi: 10.1007/978-0-387-78261-4_9.

Ito K, Awano W, Suzuki K, Hiromi Y, Yamamoto D. 1997. The Drosophila mushroom body is a quadruple structure of clonal units each of which contains a virtually identical set of neurones and glial cells. Development. 124:761-771.

Ito M, Masuda N, Shinomiya K, Endo K, Ito K. 2013. Systematic analysis of neural projections reveals clonal composition of the Drosophila brain. Curr Biol. 23:644-655. doi: 10.1016/j.cub.2013.03.015.

Ito K, Shinomiya K, Ito M, Armstrong JD, Boyan G, Hartenstein V, Harzsch S, Heisenberg M, Homberg U, Jenett A, Keshishian H, Restifo LL, Rössler W, Simpson JH, Strausfeld NJ, Strauss R, Vosshall LB; Insect Brain Name Working Group. 2014. A systematic nomenclature for the insect brain. Neuron. 81:755-765. doi: 10.1016/j.neuron.2013.12.017.

Jiang X, Nardelli J. 2015. Cellular and molecular introduction to brain development. Neurobiol Dis. pii: S0969-9961(15)30009-7. doi: 10.1016/j.nbd.2015.07.007.

Kang KH, Reichert H. 2015. Control of neural stem cell self-renewal and differentiation in Drosophila. Cell Tissue Res. 359:33-45. doi: 10.1007/s00441-014-1914-9.

Kriegstein A, Noctor S, Martínez-Cerdeňo V. 2006. Patterns of neural stem and progenitor cell division may underlie evolutionary cortical expansion. Nat Rev Neurosci. 7:883-890. doi: 10.1038/nrn2008.

Kumar A, Fung S, Lichtneckert R, Reichert H, Hartenstein V. 2009a. Arborization pattern of engrailed-positive neural lineages reveal neuromere boundaries in the Drosophila brain neuropil. J Comp Neurol. 517:87-104. doi: 10.1002/cne.22112.

Kumar A, Bello B, Reichert H. 2009b. Lineage-specific cell death in postembryonic brain development of Drosophila. Development. 136:3433-3442. doi: 10.1242/dev.037226.

Lai SL, Awasaki T, Ito K, Lee T. 2008. Clonal analysis of Drosophila antennal lobe neurons: diverse neuronal architectures in the lateral neuroblast lineage. Development. 135:2883-2893. doi: 10.1242/dev.024380.

LaMonica BE, Lui JH, Hansen DV, Kriegstein AR. 2013. Mitotic spindle orientation predicts outer radial glial cell generation in human neocortex. Nat Commun. 4:1665. doi: 10.1038/ncomms2647.

Larsen C, Shy D, Spindler SR, Fung S, Pereanu W, Younossi-Hartenstein A, Hartenstein V. 2009. Patterns of growth, axonal extension and axonal arborization of neuronal lineages in the developing Drosophila brain. Dev Biol. 335:289-304. doi: 10.1016/j.ydbio.2009.06.015.

Li Y, Lu H, Cheng PL, Ge S, Xu H, Shi SH, Dan Y. 2012. Clonally related visual cortical neurons show similar stimulus feature selectivity. Nature. 486:118-121. doi: 10.1038/nature11110.

Lin S, Lee T. 2012. Generating neuronal diversity in the Drosophila central nervous system. Dev Dyn. 241:57-68. doi: 10.1002/dvdy.22739.

Lin S, Lai SL, Yu HH, Chihara T, Luo L, Lee T. 2010. Lineage-specific effects of Notch/Numb signaling in post-embryonic development of the Drosophila brain. Development. 137:43-51. doi: 10.1242/dev.041699.

Lin S, Kao CF, Yu HH, Huang Y, Lee T. 2012. Lineage analysis of Drosophila lateral antennal lobe neurons reveals notch-dependent binary temporal fate decisions. PLoS Biol. 10:e1001425. doi: 10.1371/journal.pbio.1001425.

Liu Q, Dwyer ND, O'Leary DD. 2000. Differential expression of COUP-TF1, CHL1, and two novel genes in developing neocortex identified by differential display PCR. J Neurosci. 20:7682-7690.

Lovick JK, Hartenstein V. 2015. Hydroxyurea-mediated neuroblast ablation establishes birth dates of secondary lineages and addresses neuronal interactions in the developing Drosophila brain. Dev Biol. 402:32-47. doi: 10.1016/j.ydbio.2015.03.005.

Lovick JK, Ngo KT, Omoto JJ, Wong DC, Nguyen JD, Hartenstein V. 2013. Postembryonic lineages of the Drosophila brain: I. Development of the lineage-associated fiber tracts. Dev Biol. 384:228-257. doi: 10.1016/j.ydbio.2013.07.008.

Marín O, Müller U. 2014. Lineage origins of GABAergic versus glutamatergic neurons in the neocortex. Curr Opin Neurobiol. 26:132-141. doi: 10.1016/j.conb.2014.01.015.

Mittmann B. 2002. Early neurogenesis in the horseshoe crab Limulus polyphemus and its implication for arthropod relationships. Bio Bull. 203:221-222.

Mizutani K, Yoon K, Dang L, Tokunaga A, Gaiano N. 2007. Differential Notch signalling distinguishes neural stem cells from intermediate progenitors. Nature. 449:351-355. doi: 10.1038/nature06090.

Molyneaux BJ, Arlotta P, Hirata T, Hibi M, Macklis JD. 2005. Fezl is required for the birth and specification of corticospinal motor neurons. Neuron. 47:817-831. doi: 10.1016/j.neuron.2005.08.030.

Molyneaux BJ, Arlotta P, Menezes JR, Macklis JD. 2007. Neuronal subtype specification in the cerebral cortex. Nat Rev Neurosci. 8:427-437. doi: 10.1038/nrn2151.

Noctor SC, Martínez-Cerdeňo V, Ivic L, Kriegstein AR. 2004. Cortical neurons arise in symmetric and asymmetric division zones and migrate through specific phases. Nat Neurosci. 7:136-144. doi: 10.1038/nn1172.

Ohtsuki G, Nishiyama M, Yoshida T, Murakami T, Histed M, Lois C, Ohki K. 2012. Similarity of visual selectivity among clonally related neurons in visual cortex. Neuron. 75:65-72. doi: 10.1016/j.neuron.2012.05.023.

Panov AA. 1963. The origin and fate of neuroblasts, neurons and neuroglial cells in the central nervous system of the China oak silkworm, Antheraea pernyi (Lepidoptera, Attacidae). Entomological Rev. 42:337-350.

Panov AA. 1966. Correlations in the ontogenetic development of the central nervous system in the house cricket, Gryllus domesticus L. and the mole cricket, Gryllotalpa gryllotalpa L. (Orthooptera: Grylloidae). Entomological Rev. 45:179-185.

Park Y, Rangel C, Reynolds MM, Caldwell MC, Johns M, Nayak M, Welsh CJ, McDermott S, Datta S. 2003. Drosophila perlecan modulates FGF and hedgehog signals to activate neural stem cell division. Dev Biol. 253:247-257. doi: 10.1016/S0012-1606(02)00019-2.

Pereanu W, Kumar A, Jennett A, Reichert H, Hartenstein V. 2010. Developmen t-based compartmentalization of the Drosophila central brain. J Comp Neurol. 518:2996-3023. doi: 10.1002/cne.22376.

Power ME. 1943. The brain of Drosophila melanogaster. J Morphol. 72:517-559. doi: 10.1002/jmor.1050720306.

Poulson DF. 1950. Histogenesis, organogenesis and differentiation in the embryo of Drosophila melanogaster Meigen. Biology of Drosophila. Wiley New York, 168-274.

Prokop A, Technau GM. 1994. Normal function of the mushroom body defect gene of Drosophila is required for the regulation of the number and proliferation of neuroblasts. Dev Biol. 161:321-337. doi: 10.1006/dbio.1994.1034.

Raper JA, Bastiani M, Goodman CS. 1983a. Pathfinding by neuronal growth cones in grasshopper embryos. I. Divergent choices made by the growth cones of sibling neurons. J Neurosci. 3:20-30.

Raper JA, Bastiani M, Goodman CS. 1983b. Pathfinding by neuronal growth cones in grasshopper embryos. II. Selective fasciculation onto specific axonal pathways. J Neurosci. 3:31-41.

Reichert H. 2009. Evolutionary conservation of mechanisms for neural regionalization, proliferation and interconnection in brain development. Biol Lett. 5:112-116. doi: 10.1098/rsbl.2008.0337.

Rockland KS. 2010. Five points on columns. Front Neuroanat. 4:22. doi: 10.3389/fnana.2010.00022.

Rubenstein JL, Anderson S, Shi L, Miyashita-Lin E, Bulfone A, Hevner R. 1999. Genetic control of cortical regionalization and connectivity. Cereb Cortex. 9:524-532. doi: 10.1093/cercor/9.6.524.

Sauer ME, Chittenden AC. 1959. Deoxyribonucleic acid content of cell nuclei in the neural tube of the chick embryo: evidence for intermitotic migration of nuclei. Exp Cell Res. 16:1-6. doi: 10.1016/0014-4827(59)90189-2.

Schmechel DE, Rakic P. 1979. A Golgi study of radial glial cells in developing monkey telencephalon: morphogenesis and transformation into astrocytes. Anat Embryol (Berl). 156:115-152. doi: 10.1007/BF00300010.

Scholtz G. 1992. Cell lineage studies in the crayfish Cherax destructor (Crustacea, Decapoda): germ band formation, segmentation and early neurogenesis. Rouxs Arch. Dev. 202:36-48. doi: 10.1007/BF00364595.

Seecof RL, Teplitz RL, Gerson I, Ikeda K, Donady J. 1972. Differentiation of neuromuscular junctions in cultures of embryonic Drosophila cells. Proc Natl Acad Sci U S A. 69:566-570.

Seecof RL, Donady JJ, Teplitz RL. 1973. Differentiation of Drosophila neuroblasts to form ganglion-like clusters of neurons in vitro. Cell Differ. 2:143-149.

Sessa A, Mao CA, Colasante G, Nini A, Klein WH, Broccoli V. 2010. Tbr2-positive intermediate (basal) neuronal progenitors safeguard cerebral cortex expansion by controlling amplification of pallial glutamatergic neurons and attraction of subpallial GABAergic interneurons. Genes Dev. 24:1816-1826. doi: 10.1101/gad.575410.

Shen Q, Wang Y, Dimos JT, Fasano CA, Phoenix TN, Lemischka IR, Ivanova NB, Stifani S, Morrisey EE, Temple S. 2006. The timing of cortical neurogenesis is encoded within lineages of individual progenitor cells. Nat Neurosci. 9:743-751. doi: 10.1038/nn1694.

Sidman RL, Rakic P. 1973. Neuronal migration, with special reference to developing human brain: a review. Brain Res. 62:1-35. doi: 10.1016/0006-8993(73)90617-3.

Sidman RL, Miale IL, Feder N. 1959. Cell proliferation and migration in the primitive ependymal zone; an autoradiographic study of histogenesis in the nervous system. Exp Neurol. 1:322-333.

Skeath JB, Thor S. 2003. Genetic control of Drosophila nerve cord development. Curr Opin Neurobiol. 13:8-15. doi: 10.1016/S0959-4388(03)00007-2.

Sousa-Nunes R, Cheng LY, Gould AP. 2010. Regulating neural proliferation in the Drosophila CNS. Curr Opin Neurobiol. 20:50-57. doi: 10.1016/j.conb.2009.12.005.

Sousa-Nunes R, Yee LL, Gould AP. 2011. Fat cells reactivate quiescent neuroblasts via TOR and glial insulin relays in Drosophila. Nature. 471:508-512. doi: 10.1038/nature09867.

Spindler SR, Hartenstein V. 2010. The Drosophila neural lineages: a model system to study brain development and circuitry. Dev Genes Evol. 220:1-10. doi: 10.1007/s00427-010-0323-7.

Spindler SR, Ortiz I, Fung S, Takashima S, Hartenstein V. 2009. Drosophila cortex and neuropile glia influence secondary axon tract growth, pathfinding, and fasciculation in the developing larval brain. Dev Biol. 334:355-368. doi: 10.1016/j.ydbio.2009.07.035.

Stancik EK, Navarro-Quiroga I, Sellke R, Haydar TF. 2010. Heterogeneity in ventricular zone neural precursors contributes to neuronal fate diversity in the postnatal neocortex. J Neurosci. 30:7028-7036. doi: 10.1523/JNEUROSCI.6131-09.2010.

Stocker RF, Heimbeck G, Gendre N, de Belle JS. 1997. Neuroblast ablation in Drosophila P[GAL4] lines reveals origins of olfactory interneurons. J Neurobiol. 32:443-456. 10.1002/(SICI)1097-4695(199705)32:5<443::AID-NEU1>3.0.CO;2-5.

Stollewerk A. 2004. Secondary neurons are arrested in an immature state by formation of epithelial vesicles during neurogenesis of the spider Cupiennius salei. Front Zool. 1:3. doi: 10.1186/1742-9994-1-3.

Stollewerk A, Weller M, Tautz D. 2001. Neurogenesis in the spider Cupiennius salei. Development. 128:2673-2688.

Strausfeld, N.J., 1976. Atlas of an insect brain. Berlin: Springer-Verlag. 1-214.

Sun T, Hevner RF. 2014. Growth and folding of the mammalian cerebral cortex: from molecules to malformations. Nat Rev Neurosci. 15:217-232. doi: 10.1038/nrn3707.

Taghert PH, Goodman CS. 1984. Cell determination and differentiation of identified serotonin-immunoreactive neurons in the grasshopper embryo. J Neurosci. 4:989-1000.

Taverna E, Götz M, Huttner WB. 2014. The cell biology of neurogenesis: toward an understanding of the development and evolution of the neocortex. Annu Rev Cell Dev Biol. 30:465-502. doi: 10.1146/annurev-cellbio-101011-155801.

Truman JW, Schuppe H, Shepherd D, Williams DW. 2004. Developmental architecture of adult-specific lineages in the ventral CNS of Drosophila. Development. 131:5167-5184. doi: 10.1242/dev.01371.

Truman JW, Moats W, Altman J, Marin EC, Williams DW. 2010. Role of Notch signaling in establishing the hemilineages of secondary neurons in Drosophila melanogaster. Development. 137:53-61. doi: 10.1242/dev.041749.

Tyler WA, Haydar TF. 2013. Multiplex genetic fate mapping reveals a novel route of neocortical neurogenesis, which is altered in the Ts65Dn mouse model of Down syndrome. J Neurosci. 33:5106-5119. doi: 10.1523/JNEUROSCI.5380-12.2013.

Ungerer P, Scholtz G. 2008. Filling the gap between identified neuroblasts and neurons in crustaceans adds new support for Tetraconata. Proc Biol Sci. 275:369-376. doi: 10.1098/rspb.2007.1391.

Ungerer P, Eriksson BJ, Stollewerk A. 2011. Neurogenesis in the water flea Daphnia magna (Crustacea, Branchiopoda) suggests different mechanisms of neuroblast formation in insects and crustaceans. Dev Biol. 357:42-52. doi: 10.1016/j.ydbio.2011.05.662.

Ungerer P, Eriksson BJ, Stollewerk A. 2012. Unraveling the evolution of neural stem cells in arthropods: notch signalling in neural stem cell development in the crustacean Daphnia magna. Dev Biol. 371:302-311. doi: 10.1016/j.ydbio.2012.08.025.

Urbach R, Technau GM. 2003a. Segment polarity and DV patterning gene expression reveals segmental organization of the Drosophila brain. Development. 130:3607-3620. doi: 10.1242/dev.00532.

Urbach R, Technau GM. 2003b. Molecular markers for identified neuroblasts in the developing brain of Drosophila. Development. 130:3621-3637. doi: 10.1242/dev.00533.

Urbach R, Technau GM. 2004. Neuroblast formation and patterning during early brain development in Drosophila. Bioessays. 26:739-751. doi: 10.1002/bies.20062.

Urbach R, Schnabel R, Technau GM. 2003. The pattern of neuroblast formation, mitotic domains and proneural gene expression during early brain development in Drosophila. Development. 130:3589-3606. doi: 10.1242/dev.00528.

Vasistha NA, García-Moreno F, Arora S, Cheung AF, Arnold SJ, Robertson EJ, Molnár Z. 2014. Cortical and clonal contribution of Tbr2 expressing progenitors in the developing mouse brain. Cereb Cortex. pii: bhu125. doi: 10.1093/cercor/bhu125.

Voight T. 1989. Development of glial cells in the cerebral wall of ferrets: direct tracing of their transformation from radial glia into astrocytes. J Comp Neurol. 289:74-88. doi: 10.1002/cne.902890106.

Voigt A, Pflanz R, Schäfer U, Jäckle H. 2002. Perlecan participates in proliferation activation of quiescent Drosophila neuroblasts. Dev Dyn. 224:403-412. doi: 10.1002/dvdy.10120.

Wang X, Tsai JW, LaMonica B, Kriegstein AR. 2011. A new subtype of progenitor cell in the mouse embryonic neocortex. Nat Neurosci. 14:555-561. doi: 10.1038/nn.2807.

Wheeler WM. 1891. Neuroblasts in the arthropod embryo. J Morphol. 4:337-343. doi: 10.1002/jmor.1050040305.

Wheeler WM. 1893. A contribution to insect embryology. J Morphol. 8:1-161. doi: 10.1002/jmor.1050080102.

Wheeler SR, Skeath JB. 2005. The identification and expression of achaete-scute genes in the branchiopod crustacean Triops longicaudatus. Gene Expr Patterns. 5:695-700. doi: 10.1016/j.modgep.2005.02.005.

Whitman CO. 1878. Memoirs: the embryology of Clepsine. Quarterly Journal of Microscopical Science. 2:215-315.

Whitman CO. 1887. A contribution to the history of the germlayers in Clepsine. J Morphol. 1:105-182. doi: 10.1002/jmor.1050010107.

Wong DC, Lovick JK, Ngo KT, Borisuthirattana W, Omoto JJ, Hartenstein V. 2013. Postembryonic lineages of the Drosophila brain: II. Identification of lineage projection patterns based on MARCM clones. Dev Biol. 384:258-289. doi: 10.1016/j.ydbio.2013.07.009.

Yang JS, Awasaki T, Yu HH, He Y, Ding P, Kao JC, Lee T. 2013. Diverse neuronal lineages make stereotyped contributions to the Drosophila locomotor control center, the central complex. J Comp Neurol. 521:2645-2662. doi: 10.1002/cne.23339.

Younossi-Hartenstein A, Nassif C, Green P, Hartenstein V. 1996. Early neurogenesis of the Drosophila brain. J Comp Neurol. 370:313-329. doi: 10.1002/(SICI)1096-9861(19960701)370:3<313::AID-CNE3>3.0.CO;2-7.

Yu YC, Bultje RS, Wang X, Shi SH. 2009. Specific synapses develop preferentially among sister excitatory neurons in the neocortex. Nature. 458:501-504. doi: 10.1038/nature07722.

Yu HH, Kao CF, He Y, Ding P, Kao JC, Lee T. 2010. A complete developmental sequence of a Drosophila neuronal lineage as revealed by twin-spot MARCM. PLoS Biol. 8. pii: e1000461. doi: 10.1371/journal.pbio.1000461.

Yu HH, Awasaki T, Schroeder MD, Long F, Yang JS, He Y, Ding P, Kao JC, Wu GY, Peng H, Myers G, Lee T. 2013. Clonal development and organization of the adult Drosophila central brain. Curr Biol. 23:633-643. doi: 10.1016/j.cub.2013.02.057.

Zacharias D. Leslie J, Williams D. Meier T, Reichert H. 1993. Neurogenesis in the insect brain : cellular identification and molecular characterization of brain neuroblasts in the grasshopper embryo. Development. 118:941-955.

Zhu S, Lin S, Kao CF, Awasaki T, Chiang AS, Lee T. 2006. Gradients of the Drosophila Chinmo BTB-zinc finger protein govern neuronal temporal identity. Cell. 127:409-422. doi: 10.1016/j.cell.2006.08.045.

Chapter 2

Lineage-associated tracts defining the anatomy of the *Drosophila first* instar larval brain

Lineage-associated tracts defining the anatomy of the *Drosophila* first instar larval brain

Volker Hartenstein [a,n], Amelia Younossi-Hartenstein [a], Jennifer K. Lovick [a], Angel Kong [a], Jaison J. Omoto [a], Kathy T. Ngo [a], Gudrun Viktorin [b]

article info

Article history:
Received 21 April 2015
Received in revised form
25 June 2015
Accepted 27 June 2015

Keywords:
Brain
Development
Drosophila
Larval
Lineage

abstract

Fixed lineages derived from unique, genetically specified neuroblasts form the anatomical building blocks of the *Drosophila* brain. Neurons belonging to the same lineage project their axons in a common tract, which is labeled by neuronal markers. In this paper, we present a detailed atlas of the lineage-associated tracts forming the brain of the early *Drosophila* larva, based on the use of global markers (anti-Neuroglian, anti-Neurotactin, *inscuteable*-Gal4.4-UAS-chRFP-Tub) and lineage-specific reporters. We describe 68 discrete fiber bundles that contain axons of one lineage or pairs/small sets of adjacent lineages. Bundles enter the neuropil at invariant locations, the lineage tract entry portals. Within the neuropil, these fiber bundles form larger fascicles that can be classified, by their main orientation, into longitudinal, transverse, and vertical (ascending/descending) fascicles. We present 3D digital models of lineage tract entry portals and neuropil fascicles, set into relationship to commonly used, easily recognizable reference structures such as the mushroom body, the antennal lobe, the optic lobe, and the Fasciclin II-positive fiber bundles that connect the brain and ventral nerve cord. Correspondences and differences between early larval tract anatomy and the previously described late larval and adult lineage patterns are highlighted. Our L1 neuro-anatomical atlas of lineages constitutes an essential step towards following morphologically defined lineages to the neuroblasts of the early embryo, which will ultimately make it possible to link the structure and connectivity of a lineage to the expression of genes in the particular neuroblast that gives rise to that lineage. Furthermore, the L1 atlas will be important for a host of ongoing work that attempts to reconstruct neuronal connectivity at the level of resolution of single neurons and their synapses.

1. Introduction

As a member of the holometabolan insects, *Drosophila* fashions two different bodies during its life cycle. Living on or inside its food source, the larval body is designed for rapid ingestion of food and growth. The larva lacks segmental appendages for locomotion, and complicated sensory systems, like compound eyes or the (auditory) Johnston's organ, which, in the adult, are required for detecting food sources, mates and enemies. Corresponding to the lesser demands on controlling such complex behaviors, the early larval central nervous system is more than 1 order of magnitude smaller in size and neuronal number than its adult counterpart. However, in part because of its lower complexity, the larval brain has become a promising model system to address problems of neural structure and development, neural function, and behavior. Most of the individual larval sensory organs (sensilla), muscles, and motor neurons have been reconstructed at single cell resolution (Ghysen et al., 1993; Hartenstein, 1988; Kim et al., 2009; Landgraf et al., 2003a; Liu et al., 2003; Johansen et al., 1989; Kwon et al., 2011; Ramaekers et al., 2005; Schrader and Merritt, 2000; Sink and Whitington, 1991; Sprecher et al., 2011; Vactor et al., 1993) and their role in locomotory circuits is being established (Caldwell et al., 2003; Choi et al., 2004; Kohsaka et al., 2012). For some interneurons, including the projection neurons of the antennal lobe, the olfactory input and higher brain targets have also been mapped, and sophisticated learning paradigms are well established (Colomb et al., 2007; Gerber and Stocker, 2007; Masuda-Nakagawa et al., 2005, 2009; Python and Stocker, 2002; Schleyer et al., 2011; Selcho et al., 2009).

http://dx.doi.org/10.1016/j.ydbio.2015.06.021
0012-1606/

The *Drosophila* nervous system develops form a population of asymmetrically dividing stem cells (neuroblasts) that are born in the neurectodermal layer of the early embryo. Each of the segments of the ventral nervous system develops from 30 pairs of neuroblasts; the brain comprises approximately 100 pairs (Urbach and Technau, 2003; Younossi-Hartenstein et al., 1996). Each neuroblast is characterized by the expression of a unique combination of transcriptional regulators, and produces a structurally/functionally distinct lineage of neurons by an invariant sequence of asymmetric divisions (reviewed in Brody and Odenwald, 2005; Pearson and Doe, 2004; Urbach and Technau, 2004). A small number of 5–8 embryonic divisions generate the primary neurons that make up the larval brain (first wave of neurogenesis; Larsen et al., 2009). After a period of quiescence, these aforementioned neuroblasts reactivate in the larva and generate the much larger number of post-embryonic secondary neurons that differentiate during metamorphosis to form the adult brain (second wave of neurogenesis; Ito and Hotta, 1992; Truman and Bate, 1988; reviewed in Hartenstein et al., 2008). Neural lineages constitute developmental-genetic as well as neuro-anatomical "modules" of the developing brain. This has been studied in most detail for the secondary lineages, that were mapped at the late larval stage (Cardona et al., 2010a; Kuert et al., 2012, 2014; Pereanu and Hartenstein, 2006; Truman et al., 2004) and followed throughout metamorphosis into the adult stage (Lovick et al., 2013). The close ties between lineages and neuroanatomy can be easily appreciated at the late larval stage, where global neuronal markers, such as antibodies against the adhesion molecules Neurotactin (BP106; de la Escalera et al., 1990; Hortsch et al., 1990), Neuroglian (BP104; Bieber et al., 1989), or DE-cadherin (Dumstrei et al., 2003) show secondary lineages as cohesive clusters of immature neurons, located in the periphery of the brain (the rind or cortex; Fig. 1A–C). Neurons emit a single nerve fiber towards the brain center (the neuropil). Fibers of the same lineage form one or two tight bundles that follow an invariant trajectory by which the corresponding lineage can be recognized. These lineage-associated tracts (secondary axon tracts or SATs, for the secondary lineages) develop into the fiber bundles that connect the different neuropil compartments of the adult brain. For example, four lineages form the projection neurons connecting the antennal lobe with higher protocerebral centers, including the calyx and lateral horn (Das et al., 2013; Lai et al., 2008). In the late larva, SATs of these four lineages have extended all the way from the antennal lobe towards the target domains, bundling together into a thick tract (antennal lobe tract; ALT). During metamorphosis, dendritic and axonal branches sprout from the SATs proximally and distally, establishing the synaptic circuits within the antennal lobe and the target neuropils, respectively. Similar to the ALT, the remainder of the fiber bundles of the adult brain is formed by other lineages during the larval stage (Lovick et al., 2013; Pereanu et al., 2010).

In contrast to the now existing map of the late larval and adult brain neuropil (Pereanu and Hartenstein, 2006; Wong et al., 2013), the pattern of axon tracts formed by differentiated primary neurons in the early larva has remained relatively obscure. The structure and development of larval neuropil compartments, as well as specific "pioneer tracts" that remain visible from embryonic to larval stages, has been documented in previous works (Nassif et al., 1998, 2003; Younossi-Hartenstein et al., 2003, 2006); however, the overall projection pattern of primary lineages is not known. Primary axon tracts (PATs) of all lineages emerge during the embryonic period; like SATs, they express Neurotactin and Neuroglian, and can be visualized by antibodies against these epitopes. In the present work, we use another global neuronal marker, *insc*-Gal4, expressed neuroblasts and their neuronal progeny, visualized by membrane-localized fluorescent reporters (Betschinger et al., 2006), to follow the scaffold of secondary axon tracts backward from late to early larval stages, where it is utilized to identify the primary axon tracts. Previously, it had been shown for a few lineages (using enhancer- or promoter-Gal4 driver lines), targeted by specific molecular markers, that the SATs forming in the larva follow pre-established pathways of primary axons (Larsen et al., 2009). The findings presented here confirm this notion for lineages in general, which allowed us to generate an atlas of primary axon tracts for the L1 larval brain. A number of Gal4 driver lines expressed in subsets of lineages from early to late larval stages augmented the resolution of the atlas. We here present the pertinent features of the atlas with the help of confocal sections and digital 3D models. Our work serves the following two main purposes.

First, the L1 atlas of lineages constitutes another step towards the goal to follow lineages backward in time towards the neuroblasts of the early embryo, with the underlying objective to link each lineage (with its specific structure and connectivity) to the gene expression pattern defining the parental neuroblast. This has been recently achieved for the lineages of the ventral nerve cord (Birkholz et al., 2015), and a few select lineages of the brain, including the mushroom body (Kunz et al., 2012). In Birkholz et al. (2015), the prior use of labeled embryonic clones was instrumental to identify larval lineages with specific neuroblasts, and we anticipate the same to be true for brain lineages. Our L1 lineage atlas, translated into the late embryonic brain, will provide an anatomical scaffold with discrete landmarks to which embryonic neuroblast clones, as well as lineage-specific markers expressed from the neuroblast stage towards the late embryo, can be related.

Secondly, the atlas will significantly aid ongoing work that attempts to reconstruct neuronal connectivity at single-cell and single-synapse resolution using electron microscopy. Along this line, projects are currently under way where complete series of contiguous ultrathin sections of early larval brains are recorded by transmission electron microscopy (TEM), assembled and registered using specialized software, and digitally reconstructed (Cardona et al., 2010b, 2012). This reconstruction will be greatly aided by the anatomical landmarks provided by the lineage-associated tracts (PATs) charted in the present work. PATs represent easily identifiable elements of the TEM images (Cardona et al., 2010b), making it possible to identify the specific lineages they belong to by comparing the TEM dataset with appropriately oriented confocal stacks. Once identified in the TEM stack, the PATs define a dense grid of fixed "coordinates" to which ultrastructural details (e.g., specific types of synapses; sites of contact between particular neurons) can be related. More importantly, all primary neurons can be assigned to PATs, and thereby classified into groups with developmental significance. It will be possible to ask whether neurons that belong to a given lineage, or sublineage, share certain anatomical properties, such as axonal geometry, placement of synapses, and specific interacting neurons. These properties can then be correlated with the parental neuroblast gene expression patterns. This will serve as a foundation for understanding whether and how specific transcriptional regulators define the various anatomic properties within a lineage or sublineage.

2. Materials and methods

2.1. Fly lines

Flies were grown at 25 °C using standard fly media unless otherwise noted.

en-Gal4 (Tabata et al., 1995; #30564, Bloomington *Drosophila* Stock Center (BDSC), University of Indiana, IN, USA), FasII-Gal4 (Siebert et al., 2009), FasIII-Gal4 (Hayashi et al., 2002; #103948, BDSC), GH146-Gal4 (a gift from R.F. Stocker, University of Fribourg,

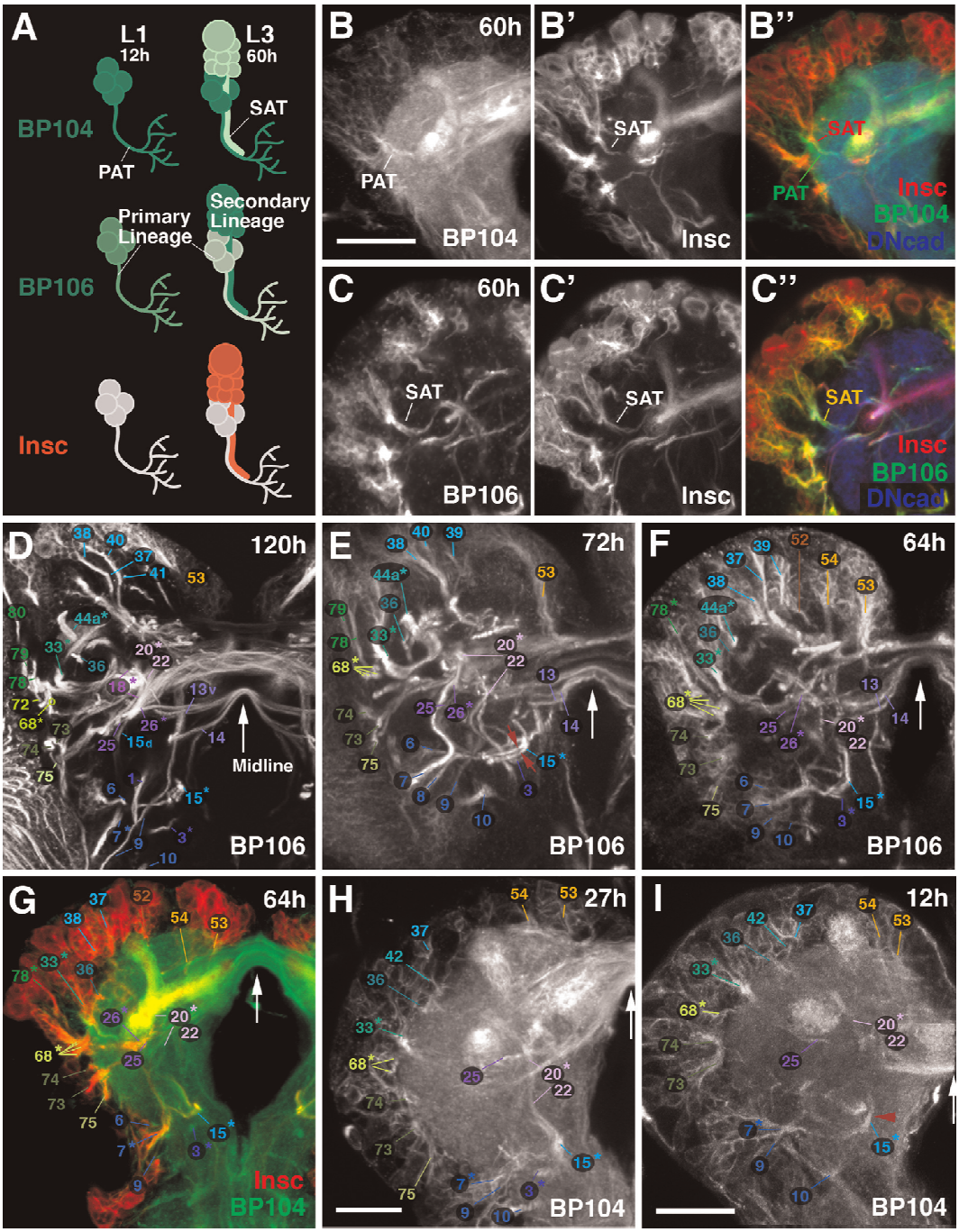
A
L1
12h
L3
60h
BP104
PAT
SAT
Primary
Lineage
Secondary
Lineage
BP106
Insc
B
60h
PAT
BP104
B'
SAT
Insc
B''
SAT
PAT
Insc
BP104
DNcad
C
60h
SAT
BP106
C'
SAT
Insc
C''
SAT
Insc
BP106
DNcad
D
120h
Midline
BP106
E
72h
BP106
F
64h
BP106
G
64h
Insc
BP104
H
27h
BP104
I
12h
BP104

Switzerland; Stocker et al., 1997), *insc*-Gal4 (Mz1407; Betschinger et al., 2006; #8751, BDSC), *per*-Gal4 (Kaneko and Hall, 2000; #7127, BDSC), *ple*-Gal4 (TH-Gal4; Friggi-Grelin et al., 2003; #8848, BDSC), *poxn*-Gal4 (Boll and Noll, 2002), R46C11-Gal4, R82E10-Gal4, R13A10-Gal4, R76A11-Gal4, R67A11-Gal4 (Janelia Farm GAL4 Stock Collection, Jenett et al. (2012); #50262 #48625 #48540 #46957 #39400, BDSC), UAS-chRFP-Tub (Rusan and Peifer, 2007; #25774, BDSC), UAS-mcd8::GFP (Lee et al., 1999; #5137, BDSC).

2.2. Immunohistochemistry

Samples were fixed in 4% formaldehyde or 4% methanol-free formaldehyde in phosphate buffer saline (PBS, Fisher-Scientific, pH¼7.4; Cat no. #BP399-4). Tissues were permeabilized in PBT (PBS with 0.1–0.3% Triton X-100, pH¼7.4) and immunohistochemistry was performed using standard procedures (Ashburner, 1989). The following antibodies were provided by the Developmental Studies Hybridoma Bank (Iowa City, IA): mouse anti-bruchpilot (nc82, 1:20), rat anti-DN-Cadherin (DN-EX #8, 1:20), mouse anti-Fasciclin II (1D4, 1:20), mouse anti-Neuroglian (BP104, 1:30), and mouse anti-Neurotactin (BP106, 1:10). Secondary antibodies, IgG_1 (Jackson ImmunoResearch; Molecular Probes) were used at the following dilutions: Cy5-conjugated anti-rat Ig (1:100), Cy3-conjugated anti-mouse Ig (1:200), Cy5-conjugated anti-mouse Ig (1:250); Alexa 546-conjugated anti-mouse (1:500), DynaLight 649-conjugated anti-rat (1:400), Alexa 568-conjugated anti-mouse (1:500).

2.3. Confocal microscopy

Staged *Drosophila* larval and adult brains labeled with suitable markers were viewed as whole-mounts by confocal microscopy [LSM 700 Imager M2 using Zen 2009 (Carl Zeiss Inc.); lenses: 40 •• oil (numerical aperture 1.3)]. Complete series of optical sections were taken at 2-µm intervals. Captured images were processed by ImageJ or FIJI (National Institutes of Health, http://rsbweb.nih.gov/ij/ and http://fiji.sc/) and Adobe Photoshop.

2.4. Morphologically defined stages in larval brain development

Animals were staged by placing larvae hatched from the egg within a 1 h period on food plates under non crowded conditions at 25 °C. Since even when larvae are reared at low density to guarantee optimal food supply, there is a considerable variability (in the order of 10%) in brain growth of larvae of the same age. We therefore defined specific morphogenetic parameters of the rapidly expanding optic lobe as structural hallmarks of the larval brain. These parameters include the ratio of optic lobe diameter (OOA) to neuropile diameter (OOA/NP), the ratio of neuroblasts versus epithelium within the outer optic anlage (NB/NBÞE), and the thickness of the layer of medulla neurons (MN; Supplementary Fig. S1A). Based on these parameters, presented in Supplementary Fig. 1B, larval brain development can be divided into 9 stages (L1A–L3E) of approximately 12 h length.

2.5. Generation of three-dimensional models

Digitized images of confocal sections were imported into FIJI (Schindelin et al., 2012; http://fiji.sc/). Complete series of optical sections were taken at 2-mm intervals. Since sections were taken from focal planes of one and the same preparation, there was no need for alignment of different sections. Models were generated using the 3-dimensional viewer as part of the FIJI software package. Digitized images of confocal sections were imported using TrakEM2 plugin in FIJI software (Cardona et al., 2012). Surface renderings of larval brains stained with anti-Bruchpilot were generated as volumes in the 3-dimensional viewer in FIJI. Cell body clusters were indicated on surface renderings using TrakEM2. Digital atlas models of cell body clusters and SATs were created by manually labeling each lineage and its approximate cell body cluster location in TrakEM2.

3. Results

3.1. Dynamic expression of adhesion proteins Neuroglian and Neurotactin in developing lineages

The adhesion proteins Neuroglian and Neurotactin serve as markers for the axon tracts of developing brain lineages (Lovick et al., 2013; Pereanu and Hartenstein, 2006; Truman et al., 2004). Both are expressed on neuronal somata and outgrowing neurites from mid-embryonic stages onward (Bieber et al., 1989; Hortsch et al., 1990; not shown). In the early larva, Neuroglian remains strongly expressed in primary neurons and their primary tracts (PATs; Fig. 1A, B), whereas Neurotactin is downregulated (Fig. 1A, C). Neurotactin appears again strongly in secondary neurons, which start to form at the second larval instar and produce secondary axon tracts (SATs; Fig. 1A, C). By contrast, Neuroglian expression reappears in secondary neurons at a later stage than that of Neurotactin (not shown). Similar to Neurotactin, we find that the *inscuteable*- (*insc*)-Gal4 reporter (Betschinger et al., 2006) is preferentially upregulated in secondary lineages and SATs as soon as neuroblasts enter mitosis (Fig. 1A, C′–C″). Double labelings of early larval brains, using Neuroglian (primary lineages) and *insc*-Gal4◄UAS-chRFP-Tubulin (secondary lineages), allowed us to correlate the trajectory of PATs and SATs (Fig. 1B″). For several lineages it had already been previously established that SATs follow PATs, formed by earlier born primary neurons of the same lineages, into the neuropil (Das et al., 2013; Larsen et al., 2009). Our present data demonstrate that the close association between PATs and SATs is true for almost all lineages (Fig. 1G; Supplementary Figs. S2 and S3).

Fig. 1. Reconstruction of lineage-associated axon tracts in the developing larval brain. (A–C″) Developing lineages labeled by three global neuronal markers: anti-Neuroglian (BP104), anti-Neurotactin (BP106), and *insc*-Gal4, UAS-chRFP-Tub. (B–B″) and (C–C″) are *z*-projections of confocal sections of a 60 h larval brain hemisphere. BP104 strongly labels primary neurons and primary axon tracts (PATs; green) in the early larva (L1 in A); it remains strongly expressed in PATs at mid larval stages (early L3; 60 h in A; B, B″). BP106 is expressed only faintly in primary neurons (A), and strongly in secondary neurons and axon tracts (SATs; green in A, right; C, C″). *insc*-Gal4 is not expressed in primary neurons of the larval brain; it only labels secondary neurons and SATs (red in A; B″; C″). Note co-labeling of PATs with BP104 and SATs with *insc*-Gal4 in panel B″. Neuropil is labeled by anti-DN-cadherin (DNcad; blue) in B″ and C″. (D–I) *z*-Projections of frontal confocal sections of larval brain hemispheres labeled with BP106 (D–F), *insc*-Gal4/BP104 (G) and BP104 (H–I). The antibodies/Gal4 drivers mark SATs (D–G) and PATs (G–I) of specific lineages, identified by numbers (see Table 2 for correspondence of lineage name and number). In panel G, similar to B″ above, PATs and SATs are co-labeled by *insc*-Gal4/BP104. All *z*-projections cover a brain slice of 12–15 mm thickness, located at the same antero-posterior level. SATs/PATs can be identified on the basis of their characteristic points of entry and trajectory; note, for example, the crescent-shaped tract formed by the DPLal1-3 lineages (#33n in D–I), the entry of DPLam (#36) medially adjacent to DPLal, the convergence of BLAd (#68n) latero-ventral of DPLal, the convergence of BLAv (#73–75) ventral of BLAd, the convergence of BAlp1-3 (#6–8) ventro-medially of BLAv, the long descending tract, passing over peduncle, formed by DALcm1-2 (#20n) and DALd (#22), or the ventral longitudinal tract formed by BAmv1-2 (#15n). Red arrows in (E) point at the two separable SATs of BAmv1 and BAmv2 in 72 h brain; the corresponding primary tracts form a single bundle in 12 h brain (red arrowhead in I). White arrows in panels D–I indicate brain midline. Bars: 50 µm (B–G); 20 µm (H, I).

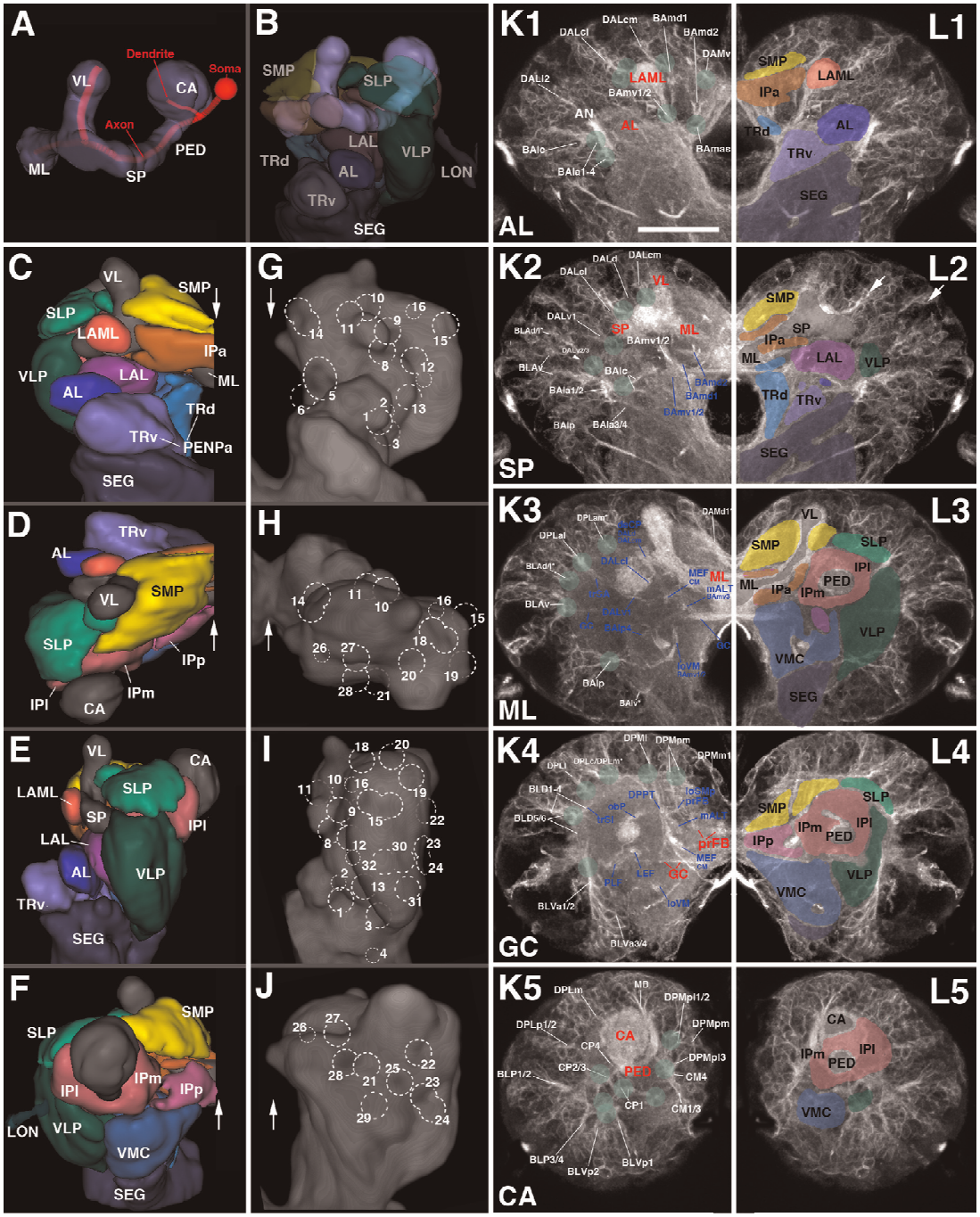
A
Dendrite
Soma
VL
CA
Axon
PED
ML
SP
B
SMP
SLP
LAL
VLP
TRd
AL
LON
TRv
SEG
K1
DALcm
BAmd1
DALcl
BAmd2
DAMv
DALl2
LAML
BAmv1/2
AN
AL
BAlc
BAmab
BAla1-4
L1
SMP
LAML
IPa
AL
TRd
TRv
SEG
AL
C
VL
SMP
SLP
LAML
IPa
VLP
LAL
ML
AL
TRd
TRv
PENPa
SEG
G
10
16
14
11
9
15
8
12
5
6
2
13
1
3
K2
DALcm
DALcl
VL
DALv1
SP
ML
BAmv1/2
BLAd/l*
BLAv
BAlc
BAla1/2
BAmd1
BAmv1/2
BAlp
BAla3/4
L2
SMP
SP
IPa
ML
LAL
VLP
TRd
TRv
SEG
SP
D
TRv
AL
SMP
VL
SLP
IPp
IPl
CA
IPm
H
14
11
10
16
15
18
26
27
20
19
28
21
K3
DPLam*
DAMd1
DPLal
BLAd/l*
DALcl
MEF
ML
CM
mALT
BAmv3
BLAv
GC
BAlp
BAlv*
L3
VL
SMP
SLP
IPl
ML
IPa
PED
IPm
VLP
VMC
SEG
ML
E
VL
CA
LAML
SLP
SP
IPl
LAL
AL
VLP
TRv
SEG
I
18
20
11
10
16
19
9
15
22
8
12
30
23
2
32
24
13
31
1
3
4
K4
DPMl
DPMpm
DPMm1
DPL
DPLc/DPLm*
BLD1-4
DPPT
BLD5/6
oCP
lCl
mALT
pIPB
MEF
CM
GC
PLP
LEF
BLVa1/2
loVM
BLVa3/4
L4
SMP
SLP
IPm
IPl
IPp
PED
VLP
VMC
GC
F
SMP
SLP
IPl
IPm
IPp
LON
VLP
VMC
SEG
J
26
27
28
25
22
21
23
29
24
K5
DPLm
MB
DPMpl1/2
DPLp1/2
DPMpm
CA
CP4
DPMpl3
CP2/3
BLP1/2
PED
CM4
CP1
CM1/3
BLP3/4
BLVp2
BLVp1
CA
L5
CA
IPm
IPl
PED
VMC

3.2. Reconstruction of primary axon tracts in the L1 larval brain

Drosophila brain lineages were initially identified and mapped for the late larval stage (L3), when each lineage forms a distinct SAT that can be visualized using global markers such as BP106 (Cardona et al., 2010a; Pereanu and Hartenstein, 2006). With only two exceptions all of these lineages were validated by MARCM clones in the adult brain (Kuert et al., 2014; Wong et al., 2013). Using the above described markers for SATs and PATs, we traced lineages backward in time from the late larval stage into the late first/early second instar, when secondary lineages are born (Fig. 1D–I; Supplementary Figs. S2 and S3; see also Lovick et al., 2015). Given that SATs project along the tracts formed earlier by the corresponding primary neurons, we could establish a map of primary axon tracts for the L1 larval brain ("L1 PAT map"). In the absence of specific markers, the map is of less resolution than the map of lineages and tracts in the late larva, because fiber bundles formed by pairs or small groups (3–4) of lineages have collapsed into one tract. Thus, as previously described, most lineages are arranged in pairs (e.g., BAmv1/2) or small groups of 3–4 (e.g., DPLal1-3; BLAd1-4) whose SATs enter and then extend through the neuropil in close apposition. In the late larva, when secondary neurons with their SATs have been added to each lineage, the SATs of these pairs or small groups can be separately followed from the cortex into the neuropil (see, for example, the two tracts formed by BAmv1/2, 15n shown by red arrows in Fig. 1E). In the L1 brain, at the level of primary lineages, the tracts have collapsed into one bundle (e.g., BAmv1/2 bundle indicated by red arrowhead in Fig. 1I). This decline in resolution aside, the primary axon tract map of the L1 brain reconstructed in this paper still represents a rich three-dimensional scaffold of structural landmarks around which neuroblasts and their progeny are grouped.

3.3. Neuropil compartments and long axon fascicles form a neuroanatomical framework for the lineage map

The brain neuropil has been described in terms of distinct compartments, domains of high synaptic density surrounded by bundles of long axons and glial processes that form visible boundaries (Pereanu et al., 2010). Compartments and selected fiber bundles forming compartment boundaries constitute a framework of landmarks of the developing *Drosphila* brain. The points of entry of lineage tracts, defined as the "entry portals" of the corresponding lineages (Lovick et al., 2013; Wong et al., 2013), as well as the fiber trajectories within the neuropil, can be described with respect to their invariant spatial relationship to compartment boundaries. We will therefore provide a brief review of the compartmental composition of the larval brain (for detail see legend of Fig. 2).

The most conspicuous compartment is the mushroom body (MB), which is formed by four lineages located at the posterior surface of the brain (Fig. 2A and B), and comprises the peduncle (PED), calyx (CA), spur (SP), vertical lobe (VL), and medial lobe (ML; Fig. 2A). Four compartments, the antennal lobe (AL), anterior peri-esophageal neuropil (PENPa), lateral appendix of the medial lobe (LAML), and anterior inferior protocerebrum (IPa), flank the MB lobes anteriorly (Fig. 2B, C, L1, and L2). [Note that we will in the following use the nomenclature that reflects the correspondence between larval and adult compartments; see Ito et al. (2014) and Pereanu et al. (2010). For correspondences between these terms and the nomenclature originally introduced for the larval brain in Younossi-Hartenstein et al. (2003) see Table 1.] The lateral

Fig. 2. Architecture of the first instar (L1) larval brain. (A and B) Digital 3D model of mushroom body, antero-lateral view. Mushroom body is rendered in blue gray (A and B; CA calyx; ML medial lobe; PED peduncle; SP spur; VL vertical lobe). In (A), an individual mushroom body neuron (Kenyon cell) is shown in red. In (B), neuropil compartments surrounding the mushroom body are shown in a semitransparent manner and in the same colors used in the following panels. (C–F) Digital 3D models of L1 brain hemispheres shown in different views (C: anterior; D: dorsal; E: lateral; F: posterior). Midline indicated by white arrow. Mushroom body rendered in gray, compartments in different colors. (G–J) Volume renderings of L1 brain neuropil labeled with anti-DN-cadherin, visualizing relief of neuropil surface. Except for I, each panel shows the contralateral brain hemisphere in the same view as 3D model to the left (G: anterior; H: dorsal; I: lateral; J: posterior). Numbered hatched circles indicate entry portals of lineage associated tracts. (K1–5, L1–5) z-Projections of frontal confocal sections of a L1 brain hemisphere labeled with anti-Neuroglian (BP104), illustrating lineages and lineage-associated fiber bundles (K1–5) in the context of larval brain neuropil compartments (L1–L5). Each z-projection represents a brain slice of approximately 8–10 mm thickness. z-Projections are presented in anterior (K1/L1) to posterior (K5/L5) order. Details of the anatomy of the mushroom body and surrounding structures present distinct "hallmarks" for a z-projection taken at a specific antero-posterior level (appear in red in K1–K5). These hallmarks are used in this and all following figures to define and name the antero-posterior level represented in the corresponding z-projection. The anterior level ("AL"; K1, L1) includes the neuropil anterior of the MB lobes, notably the antennal lobe (AL) and lateral appendix of the medial lobe (LAML); the second level ("SP"; K2, L2) is defined by the mushroom body spur (SP) and junction between vertical lobe (VL) and medial lobe (ML); the third slice ("ML"; K3, L3) contains the distal tips of the ML. The fourth level ("GC"; K4, L4) is defined by the posterior commissures, notably the great commissure (GC) and the primordium of the fan-shaped body (prFB). The posterior level ("CA"; K5, L5) shows the junction between the peduncle (PED) and calyx (CA). In panels K1–K5, lineages and neuropil fiber tracts are annotated with white lettering and blue lettering, respectively. White arrows in (L2) point at two examples of clusters of primary neurons that express higher levels of BP104 than surrounding cells. For additional information on lineages and fiber tracts they associate with, see Table 2. In panels L1–L5, which show the opposite hemisphere, compartments are rendered in different colors, following the color scheme used in panels B–F. For abbreviations of fiber tracts and compartments, see Table 1. Bar: 20 μm (for all panels).

Quick guide to neuropil compartments:

Anterior compartments: The PENPa represents the neuropil domain flanking the esophagus. It is subdivided into a ventral domain (TRv), which appears as the anteriorly directed tip of the subesophageal ganglion (SEG; C), and a dorsal domain (TRd). Both of these subdivisions receive input from the mouth cavity and foregut via the pharyngeal nerve (Rajashekhar and Singh, 1994); in view of its sensory input and internal lineage composition (discussed in detail in Kuert et al., in preparation), the PENPa domain corresponds to the tritocerebrum defined in adult flies (Rajashekhar and Singh, 1994) and other insects. The antennal nerve, carrying olfactory stimuli, defines the AL compartment, located laterally of the PENPa (panels C, L1). The LAML (Selcho et al., 2009), which has no counterpart in the adult brain, is a hemispherical structure capping the spur of the mushroom body (panels C, L1). Further medially, the IPa forms a cuff-shaped compartment that surrounds the medial lobe of the mushroom body (panels C, L1, and L2).

Ventral compartments: The LAL is located ventrally of the MB medial lobe and spur, and dorso-posteriorly of the antennal lobe and periesophageal neuropil (panels B, C, E, L2). A vertically-oriented gap in the ventral brain neuropil defines the boundary between the LAL and laterally adjacent VLP (panels C, G) and, further posteriorly, between the VLP and VMC (see Supplementary Fig. S4B and C).

Inferior protocerebrum: formed by compartments surrounding the lobes and peduncle of the mushroom body. Posterior to the anteriorly located IPa (flanking the medial lobe; see above) is the medial inferior protocerebrum (IPm). The IPm is separated from the postero-medially adjacent posterior inferior protocerebrum (IPp) by a robust mass of fibers/glia formed by the antennal lobe tract (ALT) and medial equatorial fascicle (MEF; panels K4, L4). A virtual vertical plane through the peduncle separates the IPm from the lateral inferior protocerebrum (IPl; L3–L5). Borders between IPm/l and ventrally adjacent VMC and VLP, respectively, are defined by several primary axon tracts (e.g., PLF; panels K4, L4; see also Supplementary Fig. S4H).

Superior protocerebrum: The superior medial protocerebrum (SMP) lies dorsal of the IPa and is bounded medially by the vertical lobe of the mushroom body (VL; panels C, D, F, L2, L3). Posterior of the vertical lobe, axon bundles of the DPLc lineages (see below) separate the SMP from the laterally adjacent superior lateral protocerebrum (SLP; panels K4, L4). Several longitudinally and transversally oriented fiber bundles (longitudinal superior medial and superior lateral fascicles (loSM, loSL); transverse superior fascicles (trSA/l/P); see below) delineate the border between the superior and inferior protocerebral compartments (panels K3-K4, L3, L4; and Supplementary Fig. S4G and H).

accessory lobe (LAL), ventromedial cerebrum (VMC), and ventrolateral protocerebrum (VLP) represent the ventral compartments of the L1 brain (Figs. 2B–G and S4A–C). The neuropil domains surrounding the peduncle and medial lobe of the mushroom body are termed "inferior protocerebrum" or "clasp" (Ito et al., 2014; Pereanu et al., 2010; IPa, I, m, p; Figs. 2F, L3–L5 and S4B, C, F). The superior protocerebrum (SP), comprising a superior lateral (SLP) and superior medial (SMP) domain, forms the dorsal compartments of the brain (Figs. 2C–F, K3, K4, L2, L3 and S4G, H).

A system of longitudinal fascicles interconnects neuropil domains of the insect ventral nerve cord (VNC) at different anteroposterior levels (Power, 1948; Tyrer and Gregory, 1982). These fascicles, which in *Drosophila* are commonly marked by the expression of the adhesion protein Fasciclin II (FasII; Grenningloh et al., 1991), include a regularly spaced medial, intermediate, and lateral system (Fig. 3). Anti-Neuroglian, which more globally labels primary axons, also faintly visualizes these fiber systems (Fig. 3A–C). Medial and lateral tracts each have a dorsal (DMT, DLT) and ventral component (VMT, VLT), respectively. The intermediate fascicle has several components extending along the center of the VNC neuropil (CIT1-3) (Nassif et al., 2003; Landgraf et al., 2003b). Anteriorly, the long axon tracts of the ventral nerve cord anastomose with each other and continue towards the brain (Nassif et al., 2003). They form three main bundles, termed medial cervical tract (MCT), lateral cervical tract (LCT), and posterior cervical tract (PCT). Each of these fiber systems, which carry ascending and descending axons connecting brain and VNC, splits up into smaller branches shown in Fig. 3B–F. A small number of these FasII-positive connectives associate with discrete primary lineages, which contain FasII-positive neurons (for specific detail, see below).

3.4. *Synopsis of neuro-anatomical features of the early larval brain provided by lineage-associated tracts*

We will in the following sections present detailed descriptions of all of the lineage-associated PATs labeled by the global marker anti-Neuroglian, including their position of entry into the neuropil (entry portals) and trajectory within the neuropil. For didactic reasons, we will proceed by breaking down lineages into their topologically defined groups. Before going into this detail, we present first a summary of our findings in Fig. 4 and Table 2. Overall, we can distinguish 68 discrete fiber bundles that enter the brain. As indicated in the second column (B) of Table 2, these

Table 1
Abbreviations for fiber tracts and neuropil compartments of the *Drosophila* early larval brain.

Fiber tracts	Abbr.	Fiber tracts (cont'd.)	Abbr.	Compartments	Abbr.
Anterior-dorsal commissure	ADC	Supraellipsoid body commissure	SEC	Lateral appendix of medial lobe	LAML
Antennal lobe commissure	ALC	Subellipsoid body commissure	SuEC	Antennal lobe	AL
Antennal lobe tract	ALT	Transverse superior anterior fasicle	trSA	Anterior optic tubercle	AOTU (CPLd[a])
Antennal nerve	AN	Intermediate superior transverse fascicle	trSI	Inner optic anlage	IOA
Basolateral protocerebral tract	BLPT	Transverse superior posterior fascicle	trSP	Inferior protocerebrum	IP
Basomedial protocerebral tract	BMPT	Medial trSP	trSPm	Anterior inferior protocerebrum	IPa (CA[a])
Central intermediate tract	CIT1-3	Ventrolateral longitudinal tract	VLT	Lateral inferior protocerebrum	IPl (CPL[a])
Dorsal CIT	CITd	Ventromedial longitudinal tract	VMT	Medial inferior protocerebrum	IPm (CPM[a])
Ventral CIT	CITv	Ventral nerve cord	VNC	Posterior inferior protocerebrum	IPp (CPM[a])
Descending bundle	deCP	Vertical tract of the SLP	vSLPT	Lateral accessory lobe	LAL (BC[a])
Dorsolateral longitudinal tract	DLT			Lateral appendix of the medial lobe	LAML
Dorsomedial longitudinal tract	DMT			Lateral horn	LH (CPLd[a])
Dorso-posterior protocerebral tract	DPPT			Larval optic neuropil	LON
Frontomedial commissure	FrMC			Mushroom body	MB
Great commissure	GC			Calyx of MB	CA
Commissure of the lateral accessory lobe	LALC			Medial lobe of MB	ML
Lateral cervical tract	LCT			Peduncle of MB	PED
Lateral equatorial fascicle	LEF			Spur of MB	SP
Anterior LEF	LEFa			Vertical lobe of MB	VL
Posterior LEF	LEFp			Anterior periesophageal neuropil	PENPa (Bcv[a])
Longitudinal superior lateral fascicle	loSL			Dorsal PENPa (tritocerebrum)	TRd
Longitudinal superior medial fascicle	loSM			Ventral PENPa (tritocerebrum)	TRv
Anterior loSM	loSMa			Primordium of the fan-shaped body	prFB
Posterior loSM	loSMp			Subesophageal ganglion	SEG
Intermediate longitudinal ventral fascicle	loVI			Superior lateral protocerebrum	SLP (CPLd[a])
Lateral longitudinal ventral fascicle	loVL			Lateral SLP	SLPl
Medial longitudinal ventral fascicle	loVM			Posterior SLP	SLPp
Posterior-lateral longitudinal ventral fascicle	loVP			Latero-posterior SLP	SLPpl
Median bundle	MBDL			Medio-posterior SLP	SLPpm
Medical cervical tract	MCT			Superior medial protocerebrum	SMP (DA/DP[a])
Medial equatorial fascicle	MEF			Superior protocerebrum	SP
Anterior MEF	MEFa			Ventrolateral protocerebrum	VLP (BPL[a])
Medio-lateral antennal lobe tract	mlALT			Ventromedial cerebrum	VMC (BPM[a])
Second nerve of corpora cardiaca	NCC2				
Oblique posterior fascicle	obP				
Posterior cervical tract	PCT				
Posterior lateral fascicle	PLF				
Dorsal PLF	PLFd				
Ventral PLF	PLFv				
Commissure of the PLP	PLPC				
Pharyngeal nerve	PN				
Superior arch commissure	SAC				

Column A: List of fiber tracts and associated abbreviations.
Column B: List of larval neuropil compartments and associated abbreviations.
[a] Indicates older version larval compartment nomenclature as described in Younossi-Hartenstein et al. (2003).

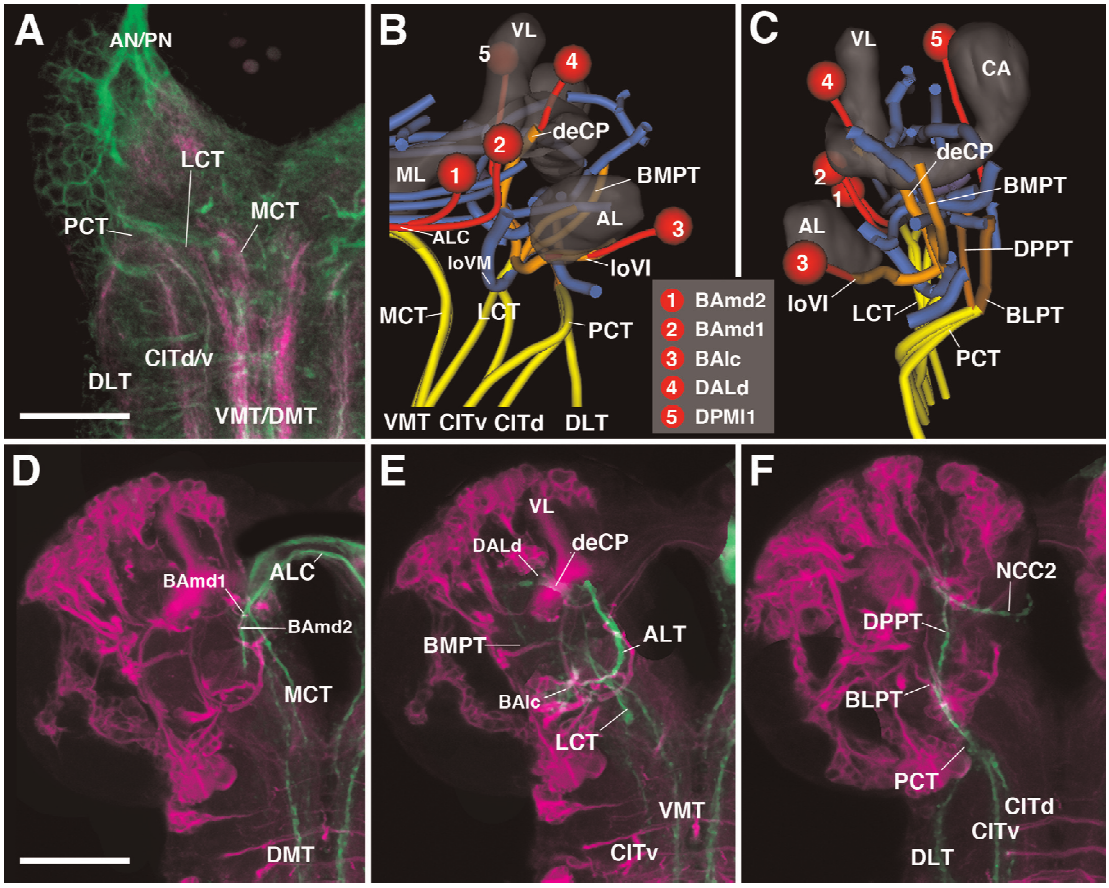

Fig. 3. Association of brain lineages and tracts with FasII-positive fiber bundles. (A) *z*-Projection of horizontal confocal sections of L1 larval anterior ventral nerve cord and basal brain, labeled with FasII-Gal4 (magenta) and anti-Neuroglian (BP104, green). FasII is expressed on each side in three pairs of long fiber tracts (CITd/v dorsal and ventral component of central intermediate tract; DLT dorsal lateral tract; VMT/DMT ventral and dorsal medial tract). These tracts anastomose in the anterior nerve cord (subesophageal ganglion, SEG) and continue as the cervical tracts into the basal brain (LCT lateral cervical tract; MCT medial cervical tract; PCT posterior cervical tract). (B and C) 3D digital model of FasII-positive tracts (yellow, orange) in spatial relationship to central brain neuropil tracts (blue), selected lineages (red) and central brain neuropil compartments.Anterior view (B) and lateral view (C). (D–F) *z*-Projections of frontal confocal section of third instar brain labeled with *insc*-Gal4, UAS-chRFP-Tub (magenta; labels secondary lineages) and anti-FasII (green). The three cervical tracts and their projections in the brain are shown separately [D: medial cervical tract (MCT); E: lateral cervical tract (LCT); F: posterior cervical tract (PCT)]. For abbreviations of compartments and tracts see Table 1. Bars: 20 µm (A); 50 µm (D–F).

bundles can correspond to: one lineage (e.g., BAmd1), small sets of adjacent lineages (e.g., BAla3/BAla4), single hemi/sublineages (e.g., DPMpm1a), or two hemilineages of neighboring lineages (e.g., DALcm1m/DALcm2m). Within the neuropil, these fiber bundles form larger fascicles that can be classified, by their main orientation according to body axis, into longitudinal, transverse, and vertical (ascending/descending) fascicles. These fascicles could be identified with their counterparts described for the brain at later stages of development (late larva to adult; Pereanu et al., 2010; Lovick et al., 2013). Table 2 and Fig. 4 represent these fascicles, color coded and assigned to the lineages that contribute to them. The basal-anterior (BA) lineages, according to previous studies (Kuert et al., 2012; Kumar et al., 2009), belong predominantly to the deuterocerebrum; two lineages, BAlv and BAlp4, in addition to three other subesophageal lineages not considered here, are positive for the Hox gene *labial*, a marker of the tritocerebrum. BA lineages form a set of longitudinal fascicles (loVM, loVI, loVL; dark blue), as well as two ascending fiber systems (red): the antennal lobe tract (ALT; formed by BAla1, BAlc, BAmv3, BAlp4) connecting the antennal lobe and neighboring territories to the dorso-posterior protocerebrum, and (part of) the median bundle (MBDL, dark red; formed by BAmas1/2) that leads from the PENPa to the dorso-anterior protocerebrum (Fig. 4A top, B, F, D, H). Lineages of the DAL and DAM group form the anterior protocerebrum (note that "anterior," relative to the body axis, corresponds to "ventral" relative to the neuraxis; see Ito et al., 2014). DAL lineages, in addition to the dorsal most BA lineages (BAmd1/BAmd2), mainly form systems of transverse fiber bundles and commissures flanking the lobes of the mushroom body and the surrounding IPa compartment (ALC, FrMC, SuEC; green in Fig. 4A top, B, F). The lineage DALd, and part of DALcm1/2, form the major descending bundle (deCP; orange in Fig. 4A) projecting from the protocerebrum to the ventral brain and SEG (Fig. 4A, B, F, G). DAM lineages enter the anterior part of the SMP (superior medial protocerebrum) compartment and form commissural (ADC, green) as well as longitudinal fibers (loSMa; blue in Fig. 4A, B, F, H).

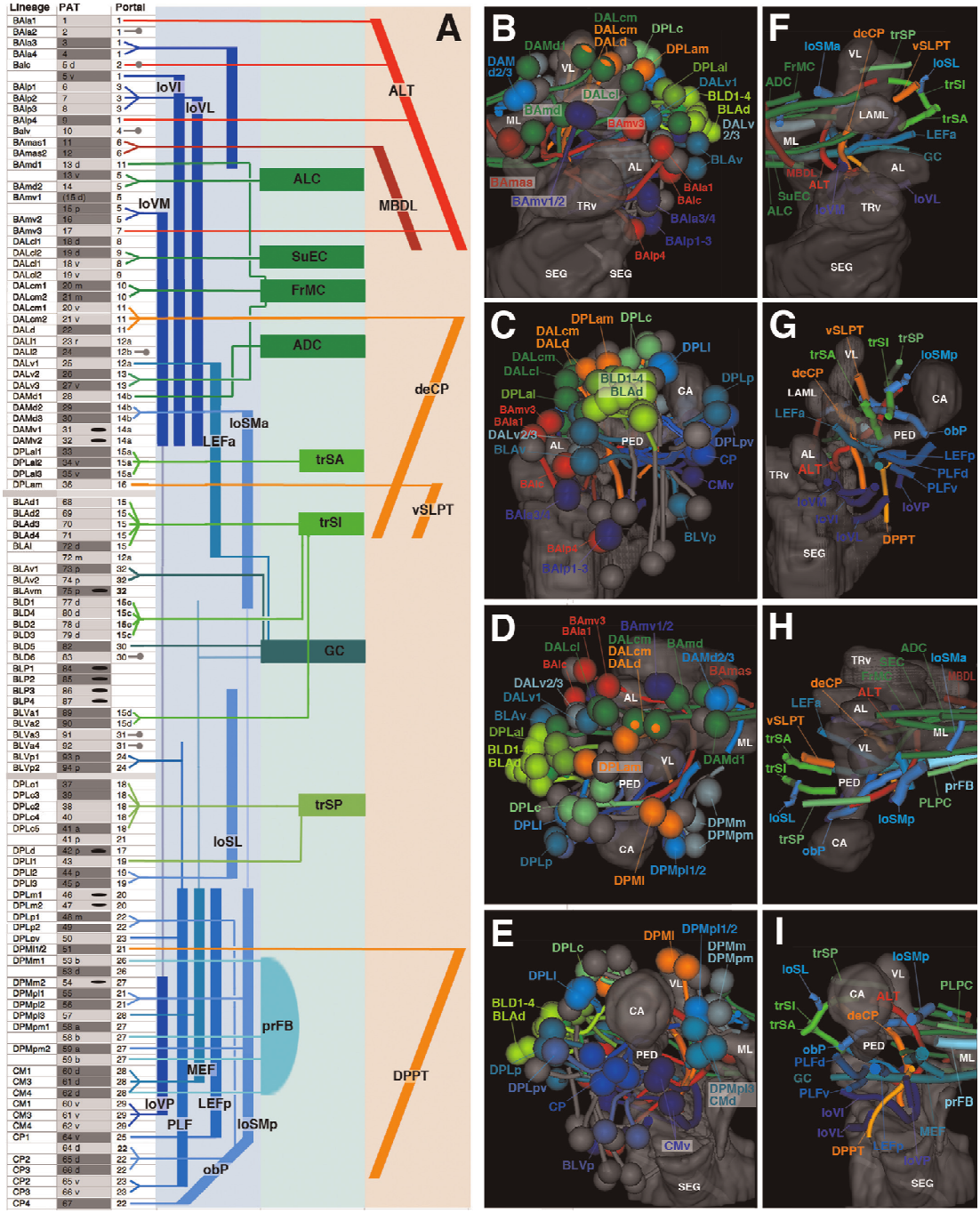

Fig. 4. Synopsis of lineages and neuropil tracts. (A) List of lineages (first column), associated PAT tracts (second column), and neuropil entry portals (third column). Neuropil fiber tracts are represented by colored bars at the right of panels; longitudinal tracts are in blue, transverse tracts/commissures in green, ascending and descending tracts in red and orange, respectively. Lines connect individual lineages (left) with the appropriate neuropil tracts (right). Lineages that project locally (according to specific labeling) are indicated by short gray lines and circles (third column); lineages for which no clear information exists are indicated by black oval in second column. (B–I) Digital 3D models of lineages (B–E) and tracts (F–I). Mushroom body and ventral brain neuropil compartments are shown semi-transparently for reference. Anterior view (B, F; medial to the left), lateral view (C, G; anterior to the left); dorsal view (D, H; medial to the right); posterior view (E, I; medial to the right). Coloring of lineages reflects their projection along longitudinal fiber system (blue), transverse system (green), or ascending/descending system (red or orange, respectively). For abbreviations of fiber tracts and compartments see Table 1.

Table 2
Lineages of the *Drosophila* early larval brain.

A Lineage	B #	C Gal4	D Portal	E #	F Tract
BAla1	1	Per[a]	AL vl	1	mlALT
BAla2	2	OK371[b]	AL vl	1	
BAla3	3	En[a]	AL vl	1	
BAla4	4		AL vl	1	
BAlc	5 d	GH146[a] R75C05(s)[c]	AL l	2	mALT
	5 v		AL vl	1	loVl4GC
BAlp1	6		VLP vm	3	
BAlp2	7		VLP vm	3	loVL
BAlp3	8		VLP vm	3	loVL4vP
BAlp4	9	R46C11[c]	AL vl	1	mALT
BAlv	10		VLCi v	4	0
BAmas1	11		AL vm	6	MBDL
BAmas2	12	Ems[d]	AL vm	6	MBDL
BAmd1	13 d		VL vm	11	FrMC
	13 v	R58F02(v)[c]	AL v	5	ALC
BAmd2	14	R34C01, R58F02(v)[c]	AL v	5	ALC
BAmv1	15 p	Per[a]	AL v	5	loVM
BAmv2	16	R33C10, R76B11[c]	AL v	5	loVM
BAmv3	17	GH146[a], R74A02, R46C11[c]	AL d	7	mALT
DALcl1	18 d	STAT[a], R82E10[c]	SP d	9	
DALcl2	19 d		SP d	9	SuEC
DALcl1	18 v		SP v	8	SuEC
DALcl2	19 v		SP v	8	LEa
DALcm1	20 m		VL vm	11	FrMC
DALcm2	21 m		VL vm	11	FrMC
DALcm1	20 v		VL vl	10	deCP
DALcm2	21 v		VL vl	10	deCP
DALd	22		VL vl	10	deCP
DALl1	23 r	R46C11[c]	VLP dm	12	trSli?
DALl2	24		VLP dm	12	
DALv1	25	R58F02[c]	VLP dm	12	LEFa4GC
DALv2	26	Per[a], R48B12[c]	LAL v	13	LEa
DALv3	27	En[a]	LAL v	13	
DAMd1	28		VL dm	14	ADC
DAMd2	29		VL dm	14	loSMa
DAMd3	30		VL dm	14	
DAMv1	31		VL dm	14	
DAMv2	32			14	
DPLal1	33	R36C09[c]	SLP l	15 a	trSA
DPLal2	34 v		SLP l	15 a	trSA
DPLal3	35 v		SLP l	15 a	trSA
DPLam	36	En[a]	SLP a	16	vSLPT
DPLc1	37		SLP pm	18	trSPm
DPLc3	39		SLP pm	18	trSPm
DPLc2	38		SLP pm	18	
DPLc4	40		SLP pm	18	
DPLc5	41 a		SLP pm	18	trSPm
	41 p		CA m	21	
DPLd	42		VL dl	17	
DPLl1	43		SLP pl	19	trSPl
DPLl2	44 p		SLP pl	19	loSLp
DPLl3	45 p		SLP pl	19	loSLp
DPLm1	46		SLP p	20	0
DPLm2	47		SLP p	20	0
DPLp1	48 m		CA l	22	obP4sPLPC
DPLp2	49		CA l	22	
DPLpv	50		PLP ps	23	PLFdl
DPMl1	51		CA m	21	DPPT
DPMm1	53 b	9D11, R13A10[c]	PB dm		prFB
	53 d		PB dm	26	
DPMm2	54		PB dl	27	
DPMpl1	55		CA m	21	loSMp
DPMpl2	56		CA m	21	loSMp
DPMpl3	57		PB v	28	MEF4GC
DPMpm1	58 a	9D11, R13A10[c]	PB dl	27	mALT
	58 b		PB dl	27	dlrFB
DPMpm2	59 a	9D11, R13A10[c]	PB dl	27	loSMp
	59 b		PB dl	27	dlrFB
CM1	60 d	9D11, R13A10[c]	PB v	28	MEF4LALC
CM3	61 d	9D11, R13A10, R81B07(s)[c]	PB v	28	MEF
CM4	62 d	9D11, R13A10, R81B07(s)[c]	PB v	28	MEF
CM1	60 v		VMC po	29	loVP
CM3	61 v		VMC po	29	loVP4(pPLPC)
CM4	62 v		VMC po	29	loVP4pPLPC
(CM5)	63		PB v		
CP1	64 d	R34A04, R34G03, R76A10[c]	CA l	22	MBDLchi
	64 v		CA v	25	LEF
CP2	65 d		CA l	22	obP4loSM
CP3	66 d		CA l	22	obP4loSM
CP2	65 v		PLP ps	23	PLF d
CP3	66 v		PLP ps	23	PLF d
CP4	67		CA l	22	obP4loSM
BLAd1	68		SLP l	15 a	trSl
BLAd2	69		SLP l	15 a	trSl
BLAd3	70		SLP l	15 a	trSl
BLAd4	71		SLP l	15 a	
BLAl	72 d		SLP l	15 a	trSl
	72 m		VLP dm	12	
BLAv1	73 p		VLP dl	32	GC
BLAv2	74 p	R46C11(s)[c]	VLP dl	32	GC
BLAvm	75 p	R81B07, R46C11(s)[c]	VLP dl	32	
BLD1	77 d		SLP l	15 c	trSl
BLD4	80 d		SLP l	15 c	trSl
BLD2	78 d		SLP l	15 c	trSl
BLD3	79 d		SLP l	15 c	trSl
BLD5	82	Ato[a], R67A11[c]	PLP l	30	GC
BLD6	83	R67A11[c]	PLP l	30	
BLP1	84				
BLP2	85				
BLP3	86				
BLP4	87				
BLVa1	89	So[a]	LH a	15d	
BLVa2	90	So[a]	LH a	15d	
BLVa3	91	R67A11[c]	VLP vli	31	
BLVa4	92	R67A11[c]	VLP vli	31	
BLVp1	93 p	R75B09[c]	PLP pi	24	PLFv4GC
BLVp2	94 p	R75B09[c]	PLP pi	24	PLFv4SEC

Column A: Lineage names based on topology (Pereanu and Hartenstein, 2006). Bracketing of CM5 indicates that no primary lineage tract could be identified for this lineage.
Column B: Number identifying lineage-associated tracts (PATs) in Fig. 1. In lineages with multiple hemilineage tracts or sublineage tracts, these are individually listed (e.g., dorsal hemilineage tract of BAlc is identified as "5d", ventral hemilineage tract as "5v"). Differential light and dark shading indicates lineage tracts that have merged into a single bundle; for example, a single PAT is formed by BAmv1 and BAmv2, or for the dorsal hemilineages 18d and 19d of DALcl1 and DALcl2, respectively.
Column C: Markers for lineages.
Column D: Entry portal of lineage-associated tracts. For abbreviations see Table 1.
Column E: Number identifying entry portals in Figs. 2, 5–10, and 12.
Column F: Neuropil fascicle joined by lineage-associated tracts. For abbreviations of fascicle names see Table 1.

[a] Reviewed in Spindler and Hartenstein (2010).
[b] Das et al. (2013).
[c] Jenett et al. (2012).
[d] Lichtneckert et al. (2007).

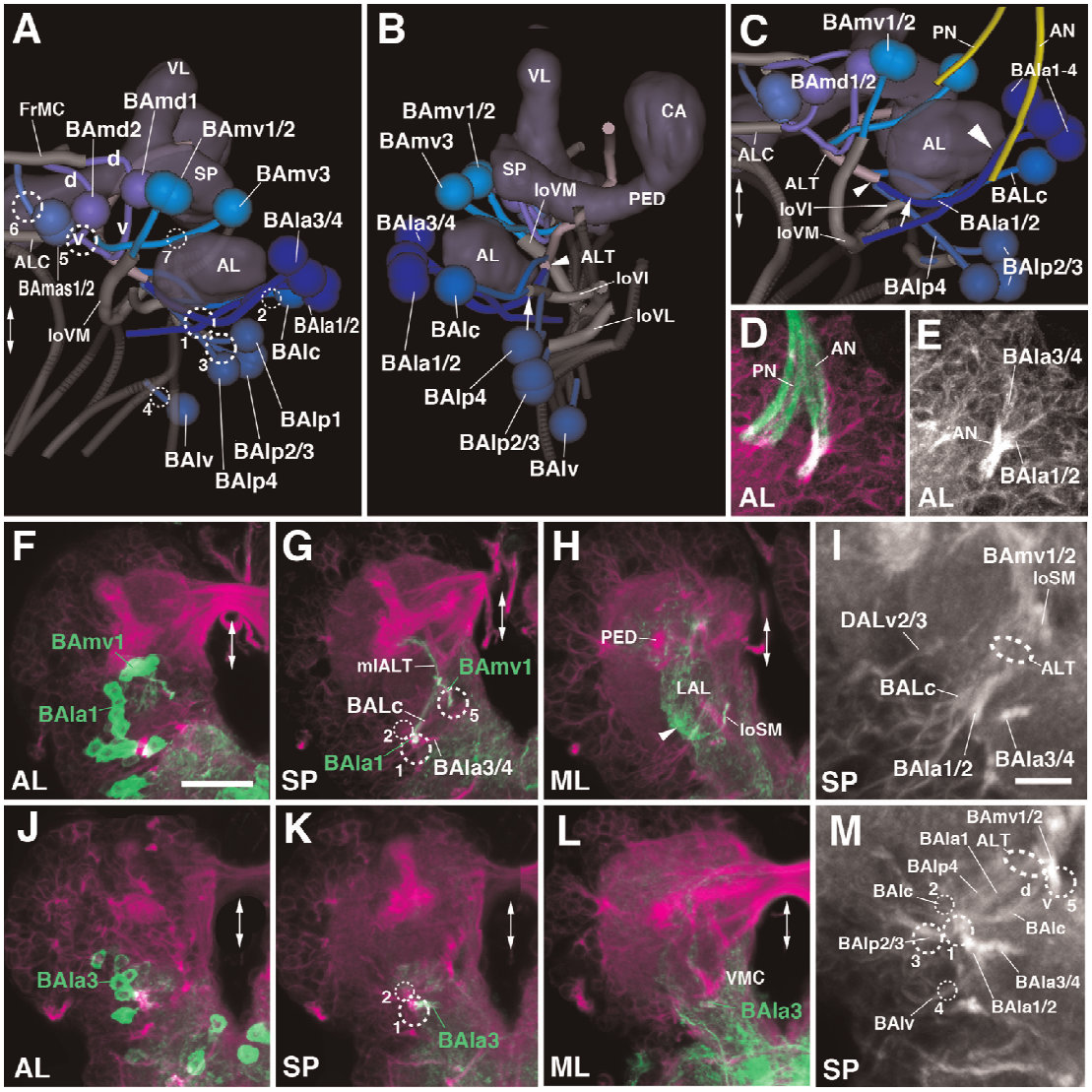

Fig. 5. Tracts associated with baso-anterior (BA) lineages. (A–C) Digital 3D models of BA lineages and tracts in a single L1 brain hemisphere. Anterior view (A), lateral view (B), ventro-anterior view (C). Centers of cell body clusters of lineages are depicted as spheres; lineage-associated axon tracts are shown as lines. Mushroom body and antennal lobe (blue-gray) and FasII-positive tracts (dark gray) are shown for reference. Fiber bundles of neuropil formed by BA lineage tracts are shown in light gray. Numbered hatched circles in (A) and other panels represent entry portals of lineage-associated tracts. "d" and "v" in (A) indicate dorsal and ventral hemilineage tracts of BAmd1 and BAmd2, respectively. Arrow in (B, C) points at entry of ventral hemilineage of BAlc into loVl tract; small arrowhead in (B, C) indicates convergence of tracts of BAla1, BAlc, and BAlp4 into the antennal lobe tract (ALT); large arrowhead in (C) points at close parallel entry of antennal nerve (AN) and tracts of BAla1-4. Double-headed arrow in (A, C) and all other panels indicates brain midline. (D–M) z-Projections of frontal confocal sections of a single L1 brain hemisphere. Antero-posterior levels shown by z-projections are indicated by letters (AL, SP, ML) at lower left corner (for definition of levels, see Fig. 2). Primary neurons and tracts are labeled by anti-Neuroglian (BP104; magenta in panels D, F–H, J–L; white in panels E, I, M). BP104-positive antennal nerve (AN) and pharyngeal nerve (PN) is highlighted in green in panel (D). Lineages BAmv1 and BAla1 are labeled by *per*-Gal4-4-UAS-mcd8::GFP (green in F–H); BAla3 is labeled by *en*-Gal4-4-UAS-mcd8::GFP (green in J–L). Panels (I) and (M) are high magnifications of central parts of (G) and (K), respectively. For abbreviations of compartments and fiber tracts see Table 1; for numbering of entry portals see Table 2. Bars: 10 µm (D, E, I, M); 20 µm (F–H, J–L).

DPL, BLA, and BLD lineages are associated with the dorsolateral protocerebrum. Many of these lineages converge on three transverse fiber systems (trSA: DPLal1-3; trSl: BLAd1-4, BLAl, BLD1-4; trSP: DPLc1-5, DPLl1) located in the superior lateral protocerebrum (SLP; light green in Fig. 4A center, B–I). BLAv1/2, as well as the posterior-lateral lineages BLVp1/2, forms the main ventral commissural system, the great commissure (GC, dark green; Fig. 4A center, F, I). The GC is also joined anteriorly by fibers of the DALv1 lineage and posteriorly by the CM group (see below; Fig. 4A, F, I). The pair DPLl2/3 forms a longitudinal fiber system

(loSL) in the SLP compartment.

DPM, CM, and CP lineages belong to the dorso-medial and posterior protocerebrums and mainly contribute to longitudinal fiber systems connecting the posterior protocerebrum with the anterior protocerebrum and deuterocerebrum. These include dorsal bundles (loSMp, formed by DPMpl1/2 and part of DPMpm2; Fig. 4A bottom, D, E, H, I), as well as ventral bundles. Most prominent among these is the medial equatorial fascicle (MEF), which forms a thick fascicle running medially of and parallel to the peduncle of the mushroom body. It is formed by dorsal components of the CM lineages, as well as DPMpl3 (Fig. 4A bottom, E, I). Further laterally are the lateral equatorial fascicle (LEFp, formed by CP1; Fig. 4A bottom, E, I), the postero-lateral fascicle (PLFd, formed by ventral components of CP lineages and DPLpv; PLFv, formed by BLVp1 and 2; Fig. 4A bottom, E, I), and the posterior ventral longitudinal fascicle (loVP, associated with ventral parts of the CM lineages; Fig. 4A bottom, E, I). Dorsal components of the CP group and DPLp1/2 form the conspicuous oblique posterior fascicle (obP), which crosses over the peduncle where it emerges from the calyx (Fig. 4A bottom, H, I); the obP turns anteriorly and joins the loSM bundle (Fig. 4A bottom, H). Two lineages, DPMl1/2, form a descending tract towards the SEG (DPPT; Fig. 4A bottom, E, I).

Compartments missing from the larval brain are those of the central complex, a prominent structure of the adult brain. The main (secondary) lineages contributing to the adult central complex are the four posterior lineages: DPMm1, DPMpm1/2, CM4 (fan-shaped body), and DALv2 (ellipsoid body). Several other lineages, including BAmv1 also contribute to the fan-shaped body (Wong et al., 2013). Based on a recent study (Riebli et al., 2013), primary neurons of DPMm1, DPMpm1/2, and CM4 form a commissural tract that, in the late larva, grows into a distinct fan-shaped body primordium. This commissural system is already visible in the early larval brain (Fig. 4A bottom, D, E, H, I; for details see below). No corresponding primordium of the ellipsoid body can be discerned; primary DALv2 neurons, whose secondary neurons form the ring-shaped volume of the adult ellipsoid body, project to the LAL and medial lobe of the mushroom body (see below). Midline-crossing fibers of DALv2/3 form a thin commissural system joining the FrMC commissure, which demarcates the location where the ellipsoid body will form during early metamorphosis (Fig. 4A center).

3.5. *Antero-ventral lineages: the BA group*

The BA cluster contains 17 lineages which form 11 bundles entering the anterior neuropil in the vicinity of the antennal lobe (AL). BAla1-4 form an antero-lateral BA subgroup with PATs that pass over the AL surface and converge at an entry point at the antero-lateral boundary of the AL, closely attached to the antennal nerve (entry portal AL vl, #1; Figs. 2G, I, K1, K2 and 5A–E). The BAla1/2 tract turns medially along the posterior boundary of the AL (Fig. 5B). The BAla2 lineage includes local interneurons (Das et al., 2013) that terminate within the AL. BAla1, marked by several known Gal4 driver lines, including *per*-Gal4 (Larsen et al., 2009; Fig. 5F–H), represents one of the four antennal lobe projection lineages. Its tract turns dorsally, forming part of the antennal lobe tract (ALT) that leaves the antennal lobe at its posterior boundary (Fig. 5B, G). The BAla1 tract soon exits the ALT towards laterally, approaches the peduncle, and terminates in the inferior protocerebrum surrounding the peduncle (Das et al., 2013; Fig. 5G, H). This peculiar pathway, which matches the corresponding BAla1 secondary axon tract in the adult brain, represents the medio-lateral antennal lobe tract (mlALT; Das et al., 2013; Lovick et al.,2013). BAla3 is marked by *en*-Gal4 (Kumar et al., 2009; Fig. 5J–M). The BAla3/4 tract projects postero-medially, passes the large loVM bundle (see below) at its ventral surface, and branches in the ventromedial cerebrum (VMC; Fig. 5K, L).

BAlc, located posterior of the BAla1-4 cluster, enters the posterior AL at a position dorsal of BAla1/2 (entry portal AL l, #2; Figs. 2G, I, K1, K2 and 5B, I). Similar to the corresponding secondary tract in the late larva and adult, the BAlc tract bifurcates with one branch projecting dorso-medially and the other one ventro-medially (Fig. 2K2; arrow and arrowhead in Fig. 5B). The dorso-medial branch joins BAla1 towards the antennal lobe tract (ALT; arrowhead in Fig. 5B, C). Primary BAlc neurons with this dorsal trajectory were described as local antennal interneurons, as well as atypical projection neurons (Das et al., 2013). In the adult brain, the dorsal BAlc neurons form a hemilineage of uni-glomerular projection neurons (Lai et al., 2008). The ventral branch of BAlc, similar to its secondary counterpart at a later stage, converges upon the ventral longitudinal fiber system, forming the loVl (longitudinal ventral intermediate) fascicle, and projecting posteriorly towards the boundary between the ventromedial cerebrum and ventrolateral protocerebrum (VMC and VLP; arrow in Fig. 5B, C).

BAlp1-4 are located postero-ventrally of BAla1-4 (Figs. 2K2, K3 and 5A–C). BAlp1-3 converge upon a single, short, posteriorly-directed bundle entering the neuropil in the cleft between the lateral accessory lobe (LAL) and VLP compartments (entry portal VLP vm, #3). This trajectory corresponds to the longitudinal ventral lateral fascicle (loVL; Figs. 2K3 and 5A, C). BAlp4, marked by the Gal4 driver R46C11 (Table 2), contains atypical antennal lobe projection neurons (Das et al., 2013). The BAlp4 tract projects straight dorso-medially along the posterior boundary of the antennal lobe (AL), to join BAla1 and BAlc at the root of the antennal lobe tract (ALT; entry portal AL vl, #1; Fig. 5A–C, M). BAlv is located ventrally of the BAlp cluster and projects a short tract medially towards the boundary between VLP and subesophageal ganglion (SEG; entry portal VLCi v, #4; Figs. 2K3 and 5A, B, M). This entry point marks the position where a distinct compartment, the inferior ventrolateral cerebrum (VLC) which receives BAlv projections, will emerge (Lovick et al., 2013).

BAmas1/2 form a pair with a joined tract entering at the dorso-medial border of the anterior periesophageal ganglion (PENPa), medially of the antennal lobe (entry portal AL vm, #6), and projecting dorsally towards the superior medial protocerebrum (SMP; Figs. 2K1 and 5A). Located dorsolaterally of BAmas1/2 and medially of the lateral appendix of the medial lobe (LAML) are two lineages, BAmd1 and BAmd2. Both tracts project straight posteriorly towards the medial lobe of the mushroom body with the BAmd1 tracts entering slightly laterally of BAmd2 (entry portal ALv; #5; Figs. 2K1 and 5A). Similar to its secondary counterpart, BAmd1 bifurcates into a dorsal and ventral branch. The dorsal branch approaches the dorsal surface of the medial lobe (ML) and makes a sharp medial turn, joining the medially-directed tract of the DALcm1/2 lineage (see below). The joined tracts of the medial DALcm1/2 and dorsal BAmd1 cross the midline in the fronto-medial commissure (FrMC; Fig. 5A). The ventral branch of BAmd1 approaches the ventral surface of the ML, turns medially, and crosses the midline as the antennal lobe commissure (ALC; Fig. 5A, C). The BAmd2 tract, entering medially and ventrally of BAmd1, also turns ventrally and then medially as part of the ALC (Fig. 5A, C). The ventral components of both BAmd1 and BAmd2 and their commissural tract express Fasciclin II (Fig. 3B–D). Markers for BAmd2 (e.g., R34C01-Gal4; Table 2) and GFP-labeled clones (Lovick et al., 2015) reveal that BAmd2 also possesses a second, dorsally-directed branch (not visible with anti-Neuroglian alone), similar to BAmd1 (Fig. 5A).

The last group of BA lineages, BAmv1-3, is located dorsally of the antennal lobe (AL; Fig. 5A–C). Together, the BAmv1/2 lineages form a common, thick tract that projects postero-ventrally and enters medially of the AL (entry portal AL v, #5; Figs. 2G, K1, K2

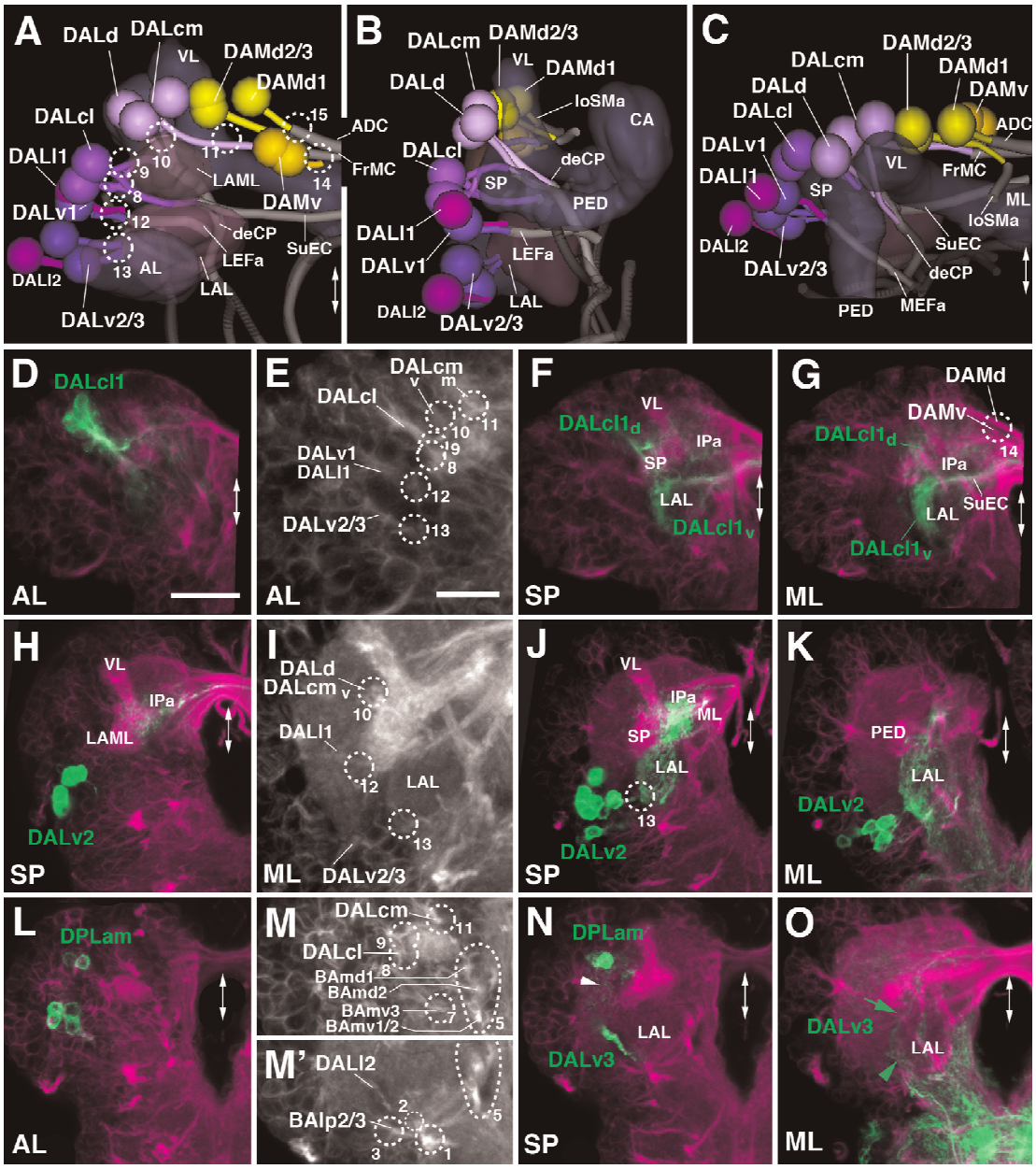

Fig. 6. Tracts associated with dorso-anterior lateral (DAL) and dorso-anterior medial (DAM) lineages. (A–C) Digital 3D models of DAL and DAM lineages and tracts in a single L1 brain hemisphere. Anterior view (A), lateral view (B), dorsal view (C). Aside from mushroom body and antennal lobe (blue-gray) and FasII-positive tracts (dark gray), the lateral accessory lobe (LAL) and lateral appendix of the medial lobe (LAML; both in magenta-gray) are shown for reference. Fiber bundles of neuropil formed by DAL lineage tracts are shown in light gray. Numbered hatched circles in (A) and other panels represent entry portals of lineage-associated tracts. Double-headed arrow in (A, C) and all other panels indicate brain midline. (D–O) z-Projections of frontal confocal sections of a single L1 brain hemisphere. Antero-posterior levels shown by z-projections are indicated by letters (AL, SP, ML) at lower left corner (for definition of levels, see Fig. 2). Primary neurons and tracts are labeled by anti-Neuroglian (BP104; magenta in panels D, F–H, J–L, N, O; white in panels E, I, M/M'). Lineage DALcl1 is labeled by R82E10-Gal4-UAS-mcd8::GFP (green in D, F, G); DALv2 is labeled by *per*-Gal4-UAS-mcd8::GFP (green in H, J, K); DALv3 and DPLam are labeled by *en*-Gal4-UAS-mcd8::GFP (green in L, N, O). Panels (E), (I), (M) and (M') are high magnifications of central parts of (D), (J) and (N), respectively. For abbreviations of compartments and fiber tracts see Table 1; for numbering of entry portals see Table 2. Bars: 20 µm (D, F, G, H, J–O); 10 µm (E, I).

and 5A). The tract, defining the medial longitudinal ventral fascicle (loVM), continues posteriorly, first along the boundary between the lateral accessory lobe (LAL) and anterior periesophageal ganglion (PENPa), then towards the boundary between the ventromedial cerebrum (VMC) and ventrolateral protocerebrum (VLP; Figs. 2K2, K3 and 5A–C, G). BAmv1 is marked by *per*-Gal4 (Larsen et al., 2009; Fig. 5F–I; Table 2), which reveals additional detail about the trajectory of this lineage. As described for the secondary BAmv1 lineage, primary BAmv1 gives off a crescent-shaped branch projecting dorsally along the lateral boundary of the LAL (Fig. 5H, arrowhead). BAmv3 constitutes the fourth antennal lobe projection neuron lineage; it contains all of the 20 or so projection neurons connecting the larval AL to the calyx and lateral horn (Das et al., 2013; Ramaekers et al., 2005). BAmv3 can be marked by several reporter lines, among them GH146-Gal4 (Stocker et al., 1997; Table 2). The BAmv3 tract (which is difficult to discern solely by anti-Neuroglian) enters the AL from a dorso-medial position, projecting medially right in front of the downward path of the ventral BAmd1 tract, and then turning posteriorly to join BAla1/BAlc/BAlp at the root of the antennal lobe tract (ALT; entry portal AL d, #7; Fig. 5A–C).

3.6. *Antero-dorsal lineages: DAL and DAM*

The DAL group possesses 10 lineages located anterior and lateral of the spur (SP) and vertical lobe (VL) of the mushroom body (Fig. 6A–C). DALcl1/2 forms a paired cluster which flanks the SP and emits a dorsal and a ventral tract (Figs. 2K1, K2 and 6A, B, D–G). DALcl1 is marked by the expression of R82E10-Gal4 (Table 2; Fig. 6D–G). The ventral tracts of DALcl1/2 project medially, passing the lateral appendix of the medial lobe (LAML) and entering medially of this compartment via the portal SPv (#8; Fig. 6A, E, M) As shown by marker R82E10, the ventral tract of DALcl1 continues medially and crosses the midline in a commissure that we interpret as the forerunner of the adult subellipsoid commissure (SuEC; Fig. 6A, F, G), as defined by the secondary DALcl1 tract (Lovick et al., 2013). The dorsal DALcl1/2 tract extends posteriorly and medially, crosses the peduncle at its dorsal surface, then turns ventrally (entry portal SP d, #9; Fig. 6A, E, M). These trajectories of DALcl1/2 primary axons resembles the pattern of secondary DALcl1/2 tracts (Lovick et al., 2013). Terminal arborizations of the dorsal DALcl1 tract (labeled by R82E10-Gal4) fill the anterior and medial inferior protocerebrums (IPa, IPm), posterior to the elbow formed by the lobes of the mushroom body (Fig. 6F, G); branching of the ventral tract occurs in the LAL (Fig. 6F, G).

DALcm1/2 and DALd are located medially of DALcl1/2, flanking the antero-lateral surface of the vertical lobe (VL; Figs. 2K1, K2 and 6A–C). The DALcm1/2 lineages form a cluster that produces a medial tract and a ventral tract. The medially-directed tract passes in front of the VL and is directed towards the midline; its crossing defines the forerunner of the frontomedial commissure (FrMC; entry portal VL vm, #11; Fig. 6A, B, E, I). The posterior tract curves around the lateral and posterior surface of the VL and then turns ventrally, joining the single tract of DALd which forms the descending deCP tract (entry portal VL vl, #10; Figs. 2K2 and 6A, B, E, I).

Three DALv lineages are located ventrally of DALcl1/2 (Figs. 2K2 and 6A–C). The DALv1 tract projects postero-medially into the space in between the lateral accessory lobe (LAL), ventrolateral protocerebrum (VLP), and spur (SP; entry portal VLP dm, #12; Figs. 2K2, L2 and 6A, B, E, I). It is closely attached to the ventromedial surface of the peduncle and continues posteriorly towards the great commissure, defining the anterior LEF fascicle (LEFa; Figs. 2K2, K3 and 6B, C). DALv2/3 form a cluster ventral of DALv1 (arrowhead in Figs. 2K2 and 6A, H–K). DALv2 is marked by *per*-Gal4 (Spindler and Hartenstein, 2010, 2011) and *poxn*-Gal4 (Boll and Noll, 2002; Minocha, 2010); DALv3 by *en*-Gal4 (Kumar et al., 2009; Larsen et al., 2009; Fig. 6L, N, O). The DALv2/3 tracts, which express Neurotactin only faintly, approach the lateral surface of the LAL, where they form terminal arborizations (entry portal LAL v, #13; Fig. 6A, B, E, I, J). The DALv2 tract (labeled by specific markers) then turns dorso-medially and forms dense arborizations in the LAL and surrounding the medial lobe of the mushroom body (Fig. 6J, K). Some axons cross the midline with the FrMC commissure and terminate in the medial lobe of the contralateral hemisphere (not shown).

Two lineages, DALl1/2, form the DALl group among the secondary lineages, and are located laterally of DALv1-3 (Cardona et al., 2010a; Lovick et al., 2013). Secondary DALl2 axons enter the antero-medial surface of the ventrolateral protocerebrum (VLP) in a very short tract. A cluster of neurons, that we interpret as DALl2, with axons converging onto the medial VLP close to entry portal VLPdm (#12) is also apparent in the L1 brain (Fig. 6A–C). DALl1, whose secondary component has a highly characteristic trajectory along the lateral surface of the peduncle and then backward to the anterior anterior optic tubercle (Lovick et al., 2013) was difficult to follow backward to the L1 stage. A primary lineage closely associated with DALv1, its tract running parallel to the DALv1 tract, is the only candidate for the primary DALl1 (entry portal VLP dm, #12; Figs. 2J2 and 6A, B).

A group of five DAM lineages is located medially of the mushroom body vertical lobe (Figs. 2K1–K3 and 6A–C). The most ventral component, DAMv1/2, projects two adjacent, thin tracts posteriorly into the superior medial protocerebrum (SMP; entry portal VL dm, #14; Figs. 2K1 and 6A, G). The DAMd lineages are located dorso-posteriorly of DAMv and enter the neuropil through the VL dm entry portal (#14 in Figs. 2 and 6). A medial group of neurons, interpreted as DAMd1, has medially-directed axons which reach the dorsal midline, defining the anterior-dorsal commissure (ADC; Fig. 6A, C, G). Secondary neurons of DAMd2/3 project posteriorly, forming the anterior longitudinal superior medial fascicle (loSMa; Lovick et al., 2013). Fibers emitted from the primary DAMd2/3 cluster which follow a similar posterior route are only faintly visible in some preparations (indicated as "loSMa" in Fig. 6A–C).

3.7. *Dorso-lateral lineages: the DPL group*

DPL lineages are widely dispersed over the dorso-lateral surface of the superior protocerebrum. One can distinguish the following subgroups with characteristic tract entry points: an antero-lateral DPLal with an adjacent DPLam and a DPLd cluster; a postero-lateral DPLl cluster; a posterior DPLp cluster; a dorsal DPLc cluster; and a dorso-posterior DPLm cluster. The DPLal cluster, presumably formed by three lineages, DPLal1-3, enters the superior lateral protocerebrum laterally (SLP; entry portal SLP l, #15a; Figs. 2G–I, K3 and 7A) and projects a thick bundle, the transverse superior anterior fascicle (trSA), ventro-medially towards the peduncle (PED; Figs. 2K3 and 7A, D, H, L). The trSA tract demarcates the boundary between the SLP compartment (above) and ventrolateral protocerebrum (VLP; below). DPLam is marked by the expression of *en*-Gal4 (Kumar et al., 2009; Fig. 6L, N). The short DPLam tract enters the SLP compartment medially of the trSA (entry portal SLP a, #16; Figs. 2G–I, K3 and 7A, B) and forms terminal arborizations in the SLP and the lateral inferior protocerebrum (IPl; Fig. 6N, arrowhead).

The DPLl group, which consists of three uniquely identifiable secondary lineages (DPLl1-3), is located posterior of DPLal. It forms a short tract entering the superior lateral protocerebrum (SLP) compartment latero-posteriorly (entry portal SLP pl, #19; Figs. 2H, I, K4 and 7B, C) and projects anteriorly, forming the longitudinal superior lateral fascicle (loSL; Figs. 2K4 and 7B, C, G, K, O). Even

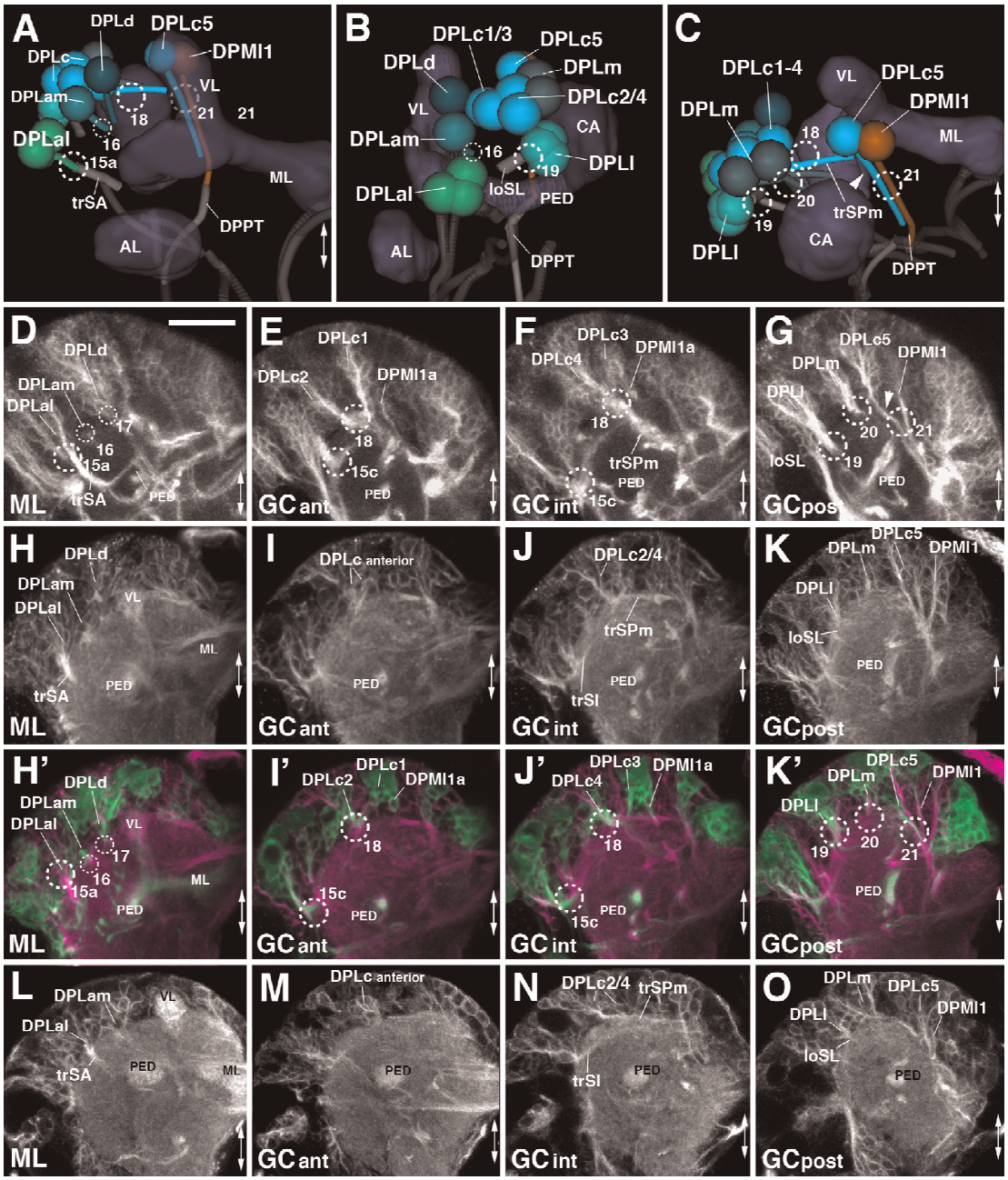

Fig. 7. Tracts associated with dorso-posterior lateral (DPL) lineages. (A–C) Digital 3D models of DPL lineages and tracts in a single L1 brain hemisphere. Anterior view (A), lateral view (B), dorsal view (C). Mushroom body and antennal lobe (blue-gray) and FasII-positive tracts (dark gray) are shown for reference. Numbered hatched circles in (A) and other panels represent entry portals of lineage-associated tracts. Double-headed arrow in (A, C) and all other panels indicates brain midline. (D–O) z-Projections of frontal confocal sections of a single brain hemisphere of early L3 (64 h; D–G), late L2 (48 h; H–K′), and L1 (12 h; L–O). Antero-posterior levels shown by z-projections are indicated by letters [ML, anterior GC level (GCant), intermediate GC level (GCint), posterior GC level (GCpost)] at lower left corner (for definition of levels, see Fig. 2). Secondary lineages are labeled by anti-Neurotactin (BP106; white in D–G) or *insc*-Gal4⋅UAS-chRFP-Tub (green in H′–K′); primary neurons and tracts are labeled by anti-Neuroglian (BP104; white in H–K and L–O; magenta in H′–K′). For abbreviations of compartments and fiber tracts see Table 1; for numbering of entry portals see Table 2. Bar: 20 μm (D–O).

further posteriorly and ventrally one finds the DPLp group, which, because of their close association with the CP lineages, is discussed along with these (see below).

DPLc includes five lineages (DPLc1-5) at the secondary stage (second to third larval instar; Fig. 7D–G). The cell body clusters are spread out over a fairly wide area topping the superior lateral protocerebrum (SLP); tracts converge on a thick bundle (called the medial transverse superior posterior fascicle; trSPm) that forms a conspicuous entry portal at the boundary between the SLP and superior medial protocerebrum (SMP; Pereanu and Hartenstein, 2006; Lovick et al., 2013; Fig. 7F). Within the neuropil, DPLc tracts have a medially directed trajectory that passes towards and then underneath the longitudinal superior medial fascicle (loSM). DPLc2 and 4 reach the neuropil from a more lateral position, and form a more posterior tract than DPLc1/3/5 (Fig. 7D–G). The cell body clusters of DPLc2 and DPLc1 (Fig. 7E) are located anteriorly of DPLc3/4/5 (Fig. 7F, G). A characteristic feature of DPLc5 is its possession of a second, ventrally directed tract (Fig. 7C, G, arrowhead) which enters the posterior neuropil at the CA m portal (#21 in Figs. 2J and 7C, K′). This configuration of DPLc lineages can be followed backward from late L3 to approximately 48 h post-hatching, when secondary tracts start to elongate (Fig. 7H-K′). Prior to this stage, primary DPLc tracts form one thick bundle that passes superficially from laterally to medially over the SLP (trSPm in Figs. 2K4 and 7A, C, N). This bundle, fed by a more lateral and a more medial cluster, corresponds to the DPLc2/4 tract. Expression of FasIII in DPLc2/4 throughout the larval period (Supplementary Fig. S5) helps identifying these DPLc members in the early larval brain. Further anteriorly are clusters with very short axon bundles directed towards the DPLc2/4 tract; these clusters (DPLc anterior in Fig. 7I, M) are interpreted as DPLc1/3. For DPLc5, a substantial ventrally-directed tract, which projects parallel to the descending DPMI1 tract (Fig. 7A, C, G, K/K′, O; see also below) can be distinguished.

DPLm1/2 form a pair located posterior of the DPLc group, laterally adjacent to the calyx (Figs. 2K4, K5 and 7B, C, G, K, O). A short tract enters at SLP p (#20 in Figs. 2H, I and 7C, G, K′) and projects anteriorly at the boundary between the superior lateral and superior medial protocerebrums (SLP, SMP). One remaining DPL lineage, DPLd, is difficult to identify in the L1 brain. The secondary DPLd lineage enters laterally adjacent to the tip of the vertical lobe (entry portal VL dl, #17 in Fig. 7D, H′), and has a characteristic branched tract, with one branch projecting medially around the tip of the VL towards the midline, and the other branch directed postero-laterally towards the intermediate superior transverse fascicle (trSI). In the L1 brain, we can only identify a small cell cluster located laterally to the VL tip that corresponds in position to DPLd (Fig. 7A, H/H′).

3.8. *Posterior-medial lineages: DPM and CM*

The DPM and CM lineages are clustered along the dorso-medial-posterior edge of the superior medial protocerebrum (SMP). Among the DPMs, one can further distinguish, based on distinct projection pattern, a medial group (DPMm1/m2, DPMpm1/2) from two lateral groups (DPMl1/2, DPMpl1-3). The medial DPM lineages (except for DPMm2) are marked by the expression of several known driver lines (9D11-Gal4, Bayraktar et al., 2010; Riebli et al., 2013 and R13A10-Gal4 (see Table 2)) and represent Type II lineages which, at the secondary stage, produce much larger progeny by means of intermediate progenitors (Bello et al., 2008; Yang et al., 2013). DPMpm1 and DPMpm2 also express Fasciclin III throughout larval development (Supplementary Fig. S5B, C, E, F). These lineages, together with CM4 (see below), generate the columnar neurons of the central complex; following the nomenclature of Bello et al. (2008) they were called DM1-4, respectively). In the L1 brain, DPMm1, DPMpm1/2, and CM4 form already larger clusters than other (Type I) lineages. DPMm1/DM1 enters close to the dorsal midline at the PB m entry portal (#26 in Figs. 2J and 8A–C). Towards posterior-laterally it is followed by DPMpm1/DM2 and DPMpm2/DM3 which form the PB dl portal (#27 in Figs. 2J and 8A–D). These two lineages are also positive for the adhesion molecule Fasciclin III, which is expressed in a discrete subset of lineages throughout larval development (Fig. S2B, C, E, F).

Each one of the three medial DPM Type II lineages has a tract that follows an antero-ventral trajectory into the posterior inferior protocerebrum (IPp), before turning medially towards the midline (Figs. 2K4, K5 and 8A, B). The convergence of medially-directed fibers of DPMm1, DPMpm1/2, and CM4 (see below) represents the primordium of the fan-shaped body (prFB), as recently defined by Riebli et al. (2013) who used a Gal4 driver line specifically expressed in primary neurons of these four lineages. Aside from the tract destined for the primordium of the fan-shaped body, DPMpm1/2 produce a second axon bundle that has a projection identical to that described for the corresponding secondary lineages (Lovick et al., 2013): DPMpm2 axons project antero-laterally into the longitudinal superior medial fascicle (loSM); DPMpm1 axons follow the antennal lobe tract antero-ventrally (ALT; Fig. 8A). DPMm1 also forms a second tract, directed medially and crossing the midline at a level posterior to the primordium of the fan-shaped body (Fig. 8A, B). A similar tract is formed by the secondary DPMm1 lineage (Lovick et al., 2013), in addition to several other tracts that are not distinguishable in the early larva. The fourth member of the medial DPMs, DPMm2, is located lateral of DPMpm1 and enters at PB dl (#27); it is negative for the Type II lineage marker 9D11-Gal4 and projects medially (Fig. 8A–D).

Two lineages, DPMpl1 and DPMpl2, are situated postero-laterally adjacent to DPMpm2. Their entry portal, CA m (#21 in Figs. 2H, J and 8A, B, D), is located right next to the PB dl entry portal. Axons of DPMpl1/2 (which form a single cell cluster at the L1 stage) converge onto a forward directed tract that defines the longitudinal superior medial fascicle (loSM; Fig. 8A–E). DPMpm2 also sends a branch into this fascicle (arrow in Fig. 8D), similar to DPMpm2 at the secondary stage (Lovick et al., 2013). The third DPMpl lineage, DPMpl3, is located ventrally of DPMpl1/2 and projects its tract along the medial equatorial fascicle (MEF; entry portal PB v, #28; Figs. 2J, K5 and 8A, B, D, E, H).

The second lateral DPM group, DPMI, is represented by one lineage (DPMI1) with a thick, highly visible tract. DPMI1 is located at the level of DPMpl1/2 and DPMpm1/2, and extends its axons straight vertically, entering along with DPMpl1/2 via CA m (#21 in Figs. 2H, J and 8A, B, D). The DPMI1 axons define the FasII-positive dorso-posterior protecerebral tract (DPPT; a subset of DPMI1 neurons are positive for FasII; see Fig. 3C, F). The DPPT is accompanied by the equally massive axon bundle of DPLc5, which runs laterally parallel to it (Fig. 7C, G, K′). A thin fiber bundle converges on the DPMI1 tract from anteriorly. The cell body cluster, designated DPMI1a in Fig. 7E, F, I′, J′, giving rise to this bundle lies directly anterior to DPMI1. A definitive secondary lineage (represented by a clone) had not been defined previously; it is possible that DPMI1a represents a second primary lineage.

The CM lineages CM1, CM3, and CM4 are Type II lineages located at the postero-medial surface of the brain. Their short axon bundles converge upon two entry portals, a dorsal one (PB v; #28 in Figs. 2H, J, K5 and Fig. 8A, B, D, E) and a ventral one (VMC po; #29 in Figs. 2J, K5 and 8A, B, D, E). The dorsal convergence (CMd; Fig. 8A, B) is mostly formed by fibers of CM4, the fourth Type II lineage that, during the secondary stage, generates the columnar neurons of the central complex. CM4 axons form a thick bundle extending forward into the inferior protocerebrum; this bundle defines the medial equatorial fascicle (MEF; Figs. 2K4 and 8A–H). A branch of these forward-directed axons turns medially towards

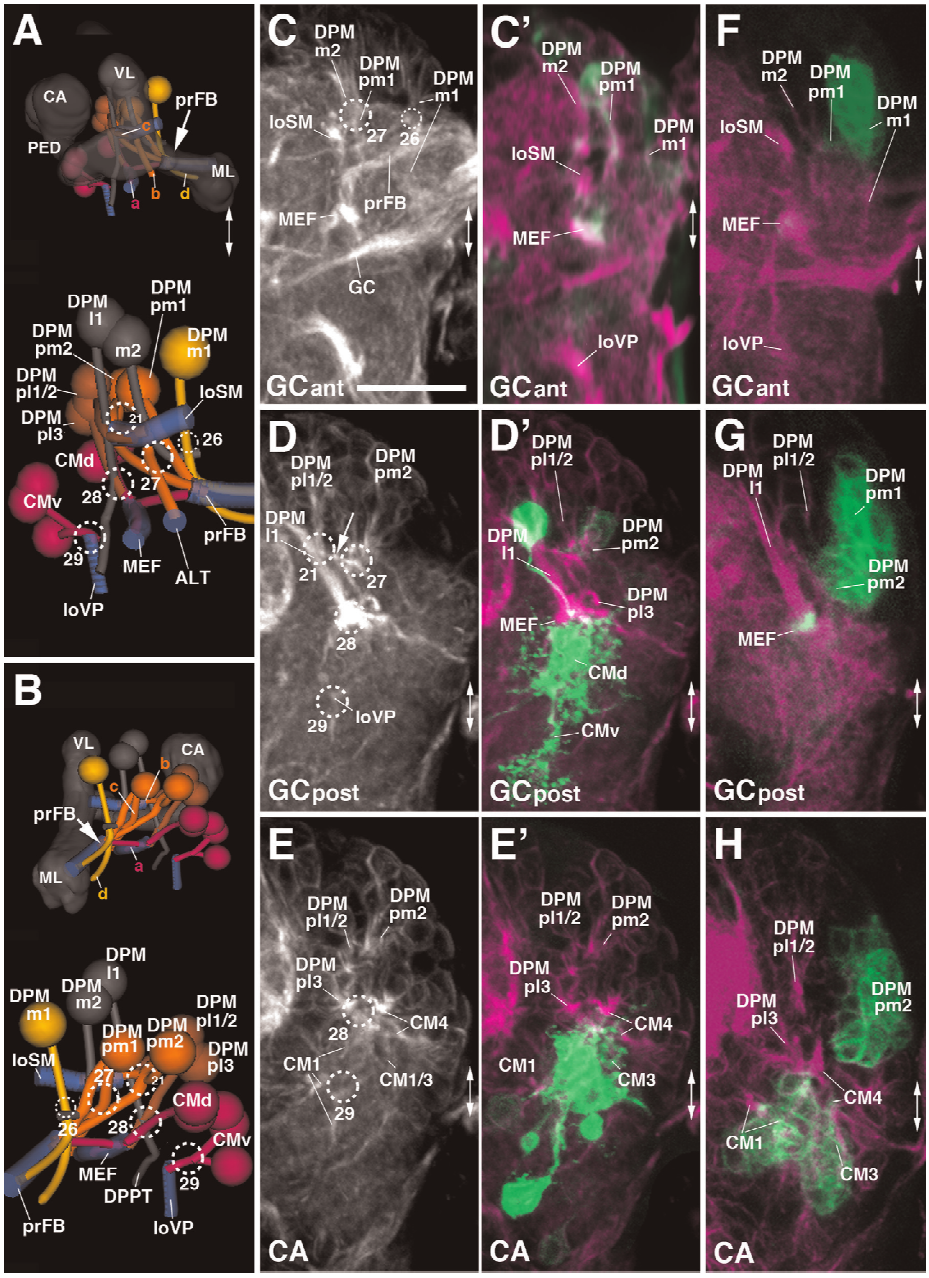

Fig. 8. Tracts associated with dorso-posterior medial (DPM) and centro-medial (CM) lineages. (A, B) Digital 3D models of DPM and CM lineages and tracts in a single L1 brain hemisphere. Anterior view (A), medial view (B). At top of each panel, lineages are shown in relationship to mushroom body (gray) for spatial orientation; bottom of panels shows higher magnification of lineages and neuropil tracts (light blue). Numbered hatched circles in (A) and other panels represent entry portals of lineage-associated tracts. Arrows in (A) and (B) point at convergence of tracts of DPMm1, DPMpm1/2, and CM4 to form a commissural tract that represents the primordium of the fan-shaped body (prFB). Letters "a"–"d" indicate additional tracts formed by these lineages (see text). Double-headed arrow in (A, C) and all other panels indicates brain midline. (C–H) z-Projections of frontal confocal sections of medial half of a L1 brain hemisphere (24 h; C–E′) and L2 larva (48 h; F–H). Antero-posterior levels shown by z-projections are indicated by letters (GCant, GCpost, CA) at lower left corner (for definition of levels, see Fig. 2). Primary neurons and tracts are labeled by anti-Neuroglian (BP104; white in panels C–E; magenta in C′-H). Primary neurons representing the Type II lineages DPMm1, DPMpm1/2, CM1/3/4 are labeled by 9D11-Gal4-4-UAS-mcd8::GFP (green in C′–E′); from L2 onward, the same marker labels secondary neurons of these lineages (green in panels F–H). For abbreviations of compartments and fiber tracts see Table 1; for numbering of entry portals see Table 2. Bar: 20 μm (C–H).

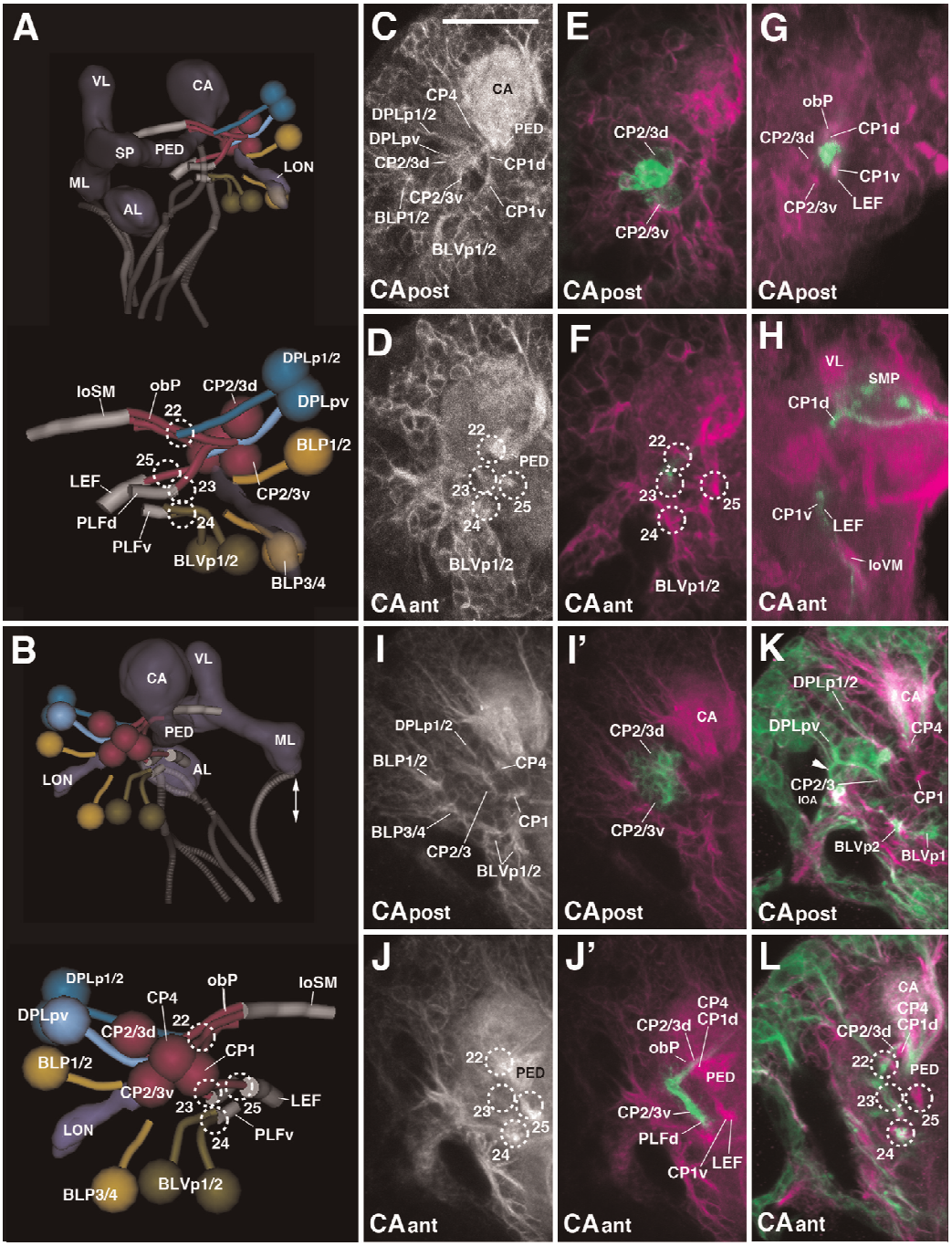

Fig. 9. Tracts associated with posterior lineages (CP, BLP, DPLp). (A, B) Digital 3D models of posterior lineages and tracts of a single L1 brain hemisphere. Lateral view (A), posterior view (B). At the top of each panel, lineages are shown in relationship to mushroom body (blue-gray) for spatial orientation; bottom of panels shows higher magnification of lineages and neuropil tracts (light blue). Numbered hatched circles in (A) and other panels represent entry portals of lineage-associated tracts. Double-headed arrow in (B) indicates brain midline. (C–L) *z*-Projections of frontal confocal sections of lateral half of brain hemisphere of L1 larva (24 h; C–H), L2 larva (48 h; I, J'), and early L3 larva (56 h; K, L). Lateral in all panels is to the left. Antero-posterior levels shown by *z*-projections are indicated by letters (CAant, CApost) at lower left corner (for definition of levels, see Fig. 2). Primary neurons and tracts are labeled by anti-Neuroglian (BP104; white in panels C, D, I, J; magenta in all other panels). Primary neurons representing the Type II lineages CP2 and CP3 are labeled by 9D11-Gal4.4-UAS-mcd8::GFP (green in E, F); from L2 onward, the same marker labels secondary neurons of these lineages (green in panels I', J'). Primary neurons of CP1 are labeled by R76A11-Gal4.4-UAS-mcd8::GFP (green in G, H). Secondary neurons are globally labeled by *insc*-Gal4.4-UAS-chRFP-Tub (green in K, L). For abbreviations of compartments and fiber tracts see Table 1; for numbering of entry portals see Table 2. Bar: 20 μm (C–L).

the primordium of the fan-shaped body (prFB; Fig. 8A, B). A second lineage projecting into the MEF is DPMpl3, located dorsally adjacent to CM4 (see above; Fig. 8A, B, E/E′, H). Extending anteriorly, the MEF splits up into branches that turn ventrally towards the great commissure (GC; Fig. 2K4), and antero-laterally towards the lateral accessory lobe (LAL; not shown).

Located ventrally and laterally of the origin of the medial equatorial fascicle (MEF) two clusters, interpreted as CM1 and CM3, have axons that contribute to the MEF, but mainly converge on the VMC po portal (#29) They project forward and ventrally, forming the longitudinal ventral posterior fascicle (loVP; Figs. 2J, K5 and 8A, B, D, E). The fifth CM lineage, CM5, a small Type I lineage located ventro-posteriorly extending its tract medially adjacent to CM4 at the secondary stage, could not be identified in L1 with certainty.

3.9. Posterior-lateral lineages: CP, DPLp, BLP, BLVp

The CP group comprises four lineages, CP1-4. Based on their expression of 9D11-Gal4, CP2 and CP3 represent Type II lineages (Bayraktar et al., 2010). CP2/3 form a thick tract that is located at the ventro-lateral boundary of the calyx and bifurcates into a dorsal and ventral branch (Figs. 2K5 and 9A–C, I, J′). The dorsal branch enters the neuropil at the CA I portal (#22 in Figs. 2I, J, K5 and 9A, B, D, F, J, L), and projects dorsomedially, forming the oblique posterior tract (obP; Fig. 9A, B, J′, L). The ventral branch projects anteriorly, parallel to the peduncle. This tract enters at the PLP ps portal (#23 in Figs. 2I, J, K5 and 9A, B, D, F, J, L) and forms the dorsal component of the posterior-lateral fascicle (PLFd; Fig. 9A, J′). CP1, marked by the expression of R76A11-Gal4 (Fig. 9G, H) enters medially of CP2/3 and also forms a branched tract (entry portal CA I, #22; Figs. 2I, J, K5 and 9B–D, F, G, J, L). The dorsal CP1 tract joins the obP, forming the ventral component of this thick bundle (Fig. 9A, B, J′, L). The ventral CP1 branch, which projects forward, medially of the ventral CP2/3 branch, enters at the CA v portal (#25 in Figs. 2J, K5 and 9A–D, J/J′, L) and forms part of the lateral equatorial fascicle (LEF; Figs. 2K4 and 9A, B, G, H, J′). The fourth CP lineage, CP4 (as defined at the secondary stage in the late larva), also projects along the obP, close to CP1; CP4 neurons and their primary tract are located dorsally of CP1 (entry portal CA I, #22; Figs. 2I, J, K5 and 9A–C, I, J/J′, K, L).

Three lineages of the DPL group, DPLp1/2 and DPLpv, are close to the CP clusters in location and projection. The DPLp1/2 cluster is located dorsally of CP2/3, laterally of the calyx (entry portal CA I; #22; Figs. 2I, J, K5 and 9A–D, F, I–L). The DPLp1/2 tract converges onto the dorsal CP2/3 tract as it turns into the oblique posterior tract (obP). DPLpv is located ventro-laterally of DPLp1/2, bordering the inner optic anlage of the optic lobe primordium (entry portal PLP ps, #23; Figs. 2I, J and 9D, F, J–L). At the secondary stage, DPLpv has a characteristic, bifurcated tract, with one short lateral branch towards the optic neuropil, and a medial branch that projects anteriorly along the posterior-lateral fascicle (PLFd), together with the CP2/3 axons (Fig. 9K, arrowhead). A primary cluster with a short, simple tract, projecting ventrally of the DPLp1/2 tract, can be followed back towards the L1 stage and has been tentatively defined as DPLpv (Fig. 9A–C).

BLP lineages are located at the postero-lateral brain surface, posteriorly of the optic lobe primordium. Their axon tracts approach the lateral neuropil surface (more precisely: the point where the lateral surface of the ventrolateral protocerebrum (VLP) is joined by the larval optic neuropil) from posteriorly (Pereanu and Hartenstein, 2006). At the secondary stage, BLPs form two lineage pairs with similar projection: BLP1/2, whose cell body clusters are located further dorsally, extend their axons antero-ventrally towards the lateral surface of the VLP compartment. BLP3/4, located further ventrally, project upward towards the lateral superior lateral protocerebrum (SLP; Lovick et al., 2013). Two BLP clusters with similar location and axonal trajectory can be followed backward towards the L1 stage: one cluster (termed BLP1/2) approaches the junction between the larval optic neuropil (LON) and VLP from postero-dorsally, the other one (BLP3/4) from postero-ventrally (Figs. 2I, J, K5 and 9A–D, F, I, J, L). Tracts cannot be followed any further anteriorly, and their entry portals into the brain neuropil cannot clearly be defined.

BLV lineages are located ventrolaterally of the optic lobe primordium. The two posterior-most members of this group, BLVp1/2, are located ventrally adjacent to CP2/3, and have closely apposed axon tracts that converge on the posterior-lateral fascicle carrying the ventral CP2/3 axons (PLF; Figs. 2K5 and 9A–D, I–L). BLVp1/2 tracts form a separate entry point (PLP pi; #24 in Figs. 2I, J, K5 and 9A–D, F, J, L) and continue as the ventral component of the PLF (PLFv) that projects anteriorly towards the lateral inferior protocerebrum.

3.10. Lateral lineages: BLA, BLD, BLV

BLA lineages are located along the anterior edge of the optic lobe primordium. At the secondary stage, they comprise a ventral group of 3 lineages (BLAv1/2, BLAvm) and a dorsal group of five lineages (BLAd1-4, BLAl). The BLAv lineages can be individually followed backward towards the L1 stage; primary BLAv lineages form three separate tracts that project posteriorly towards the lateral surface of the ventrolateral protocerebrum (VLP). Only BLAv1 is labeled by R67A11-Gal4 (Fig.10D/D′). The BLAv lineage tracts turn medially and enter the VLP neuropil (entry portal VLP dl, #32; Figs. 2I and 10A, B, D, E, G, H′, J, K); BLAv1/2 fibers continue medially as part of the great commissure (GC; Figs. 2K3 and 10A, B, D, E, G′, H′). BLAd lineages form a cluster dorsally of the BLAv lineages. Three to four short, posteriorly-directed tracts converge on a thick bundle which enters the superior lateral protocerebrum (SLP) at a position directly underneath the transverse superior anterior fascicle (trSA) formed by DPLal (entry portal SLP l, #15b; Figs. 2G–I, K3 and 10A–D, G/G′, J). Right posterior of the trSA, the BLAd bundle turns dorso-medially, forming the transverse superior intermediate fascicle (trSI; Fig. 10A–D). The BLAl lineage, located at the medial edge of the BLAd cluster, has a characteristic bifurcated tract that sends one branch postero-laterally, the other one antero-medially. The posterior branch follows the neuropil surface to join the axon bundle formed by BLAd; the antero-medial branch extends around the anterior neuropil surface along the boundary between the superior lateral protocerebrum (SLP) and ventrolateral protocerebrum (VLP), and approaches the spur of the mushroom body (Figs. 2K2, K3 and 10A, C).

BLD lineages are located dorsally of the optic lobe primordium and project tracts ventrally towards the lateral surface of the neuropil. At the secondary stage, six lineages, further subdivided into three pairs with similar trajectories, were identified. The posterior pair, BLD5/6, has long, vertically-oriented tracts that are directed towards the junction between the larval optic neuropil (LON) and the ventrolateral protocerebrum (VLP). Here, tracts turn medially in or near the great commissure (GC). The BLD5/6 pair, located furthest posteriorly and marked by R67A11-Gal4, can be followed backwards to the L1 stage (Figs. 2K4 and 10B, C, F/F′, I/I′, L). The PAT of this pair projects straight ventrally and enters the lateral neuropil immediately dorsal of the larval optic neuropil (LON; PLP l entry portal, #30; Figs. 2I and 10B, F, I/I′, L). The four anterior BLD lineages, BLD1-4, have tracts that approach the lateral surface and make a characteristic sharp turn towards dorso-medially, joining the transverse superior intermediate fascicle (trSI) formed by BLAd (see above). At the secondary stage, the BLD1-4 lineages have characteristic branching patterns, which do

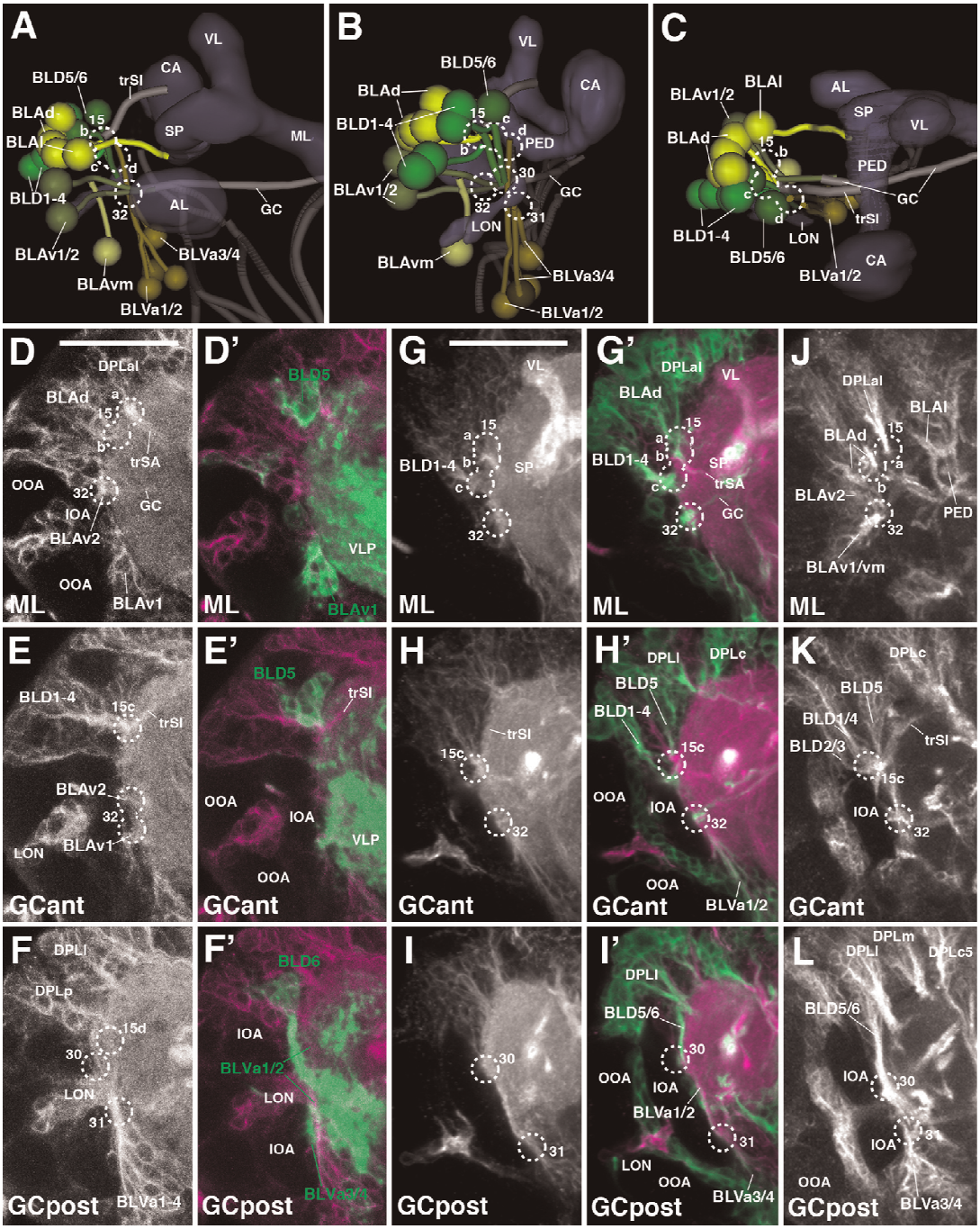

Fig. 10. Tracts associated with lateral lineages (BLA, BLD, BLV). (A–C) Digital 3D models of BL lineages and tracts in a single L1 brain hemisphere. Anterior view (A), postero-lateral view (B), dorsal view (C). Aside from mushroom body and antennal lobe (blue-gray) and FasII-positive tracts (dark gray), the larval optic neuropil (LON) is shown for reference. Fiber bundles of neuropil to which BL lineage tracts contribute are shown in light gray. Numbered hatched circles in (A) and other panels represent entry portals of lineage-associated tracts. (D–L) z-Projections of frontal confocal sections of lateral half of L1 brain hemisphere (24 h; D–F′) and early L3 larva (64 h; G–L). Lateral in all panels is to the left. Antero-posterior levels shown by z-projections are indicated by letters (ML, GCant, GCpost) at lower left corner (for definition of levels, see Fig. 2). Primary neurons and tracts are labeled by anti-Neuroglian (BP104; white in panels D–F and G–I; magenta in D′–F′ and D′–I′). Primary neurons of BLD5, BLD6, BLVa3, and BLVa4 are labeled by R67A11-Gal4-UAS-mcd8::GFP (green in D′–F′). Secondary neurons are globally labeled by *insc*-Gal4-UAS-chRFP-Tub (green in G′–I′) and anti-Neurotactin (BP106; white in J–L). On all panels, parts of larval optic lobe neuropil (LON) are shown close to left margin (IOA inner optic anlage; OOA outer optic anlage). For abbreviations of compartments and fiber tracts see Table 1; for numbering of entry portals see Table 2. Bar: 20 µm (D–F′); 50 µm (G–I′).

not exist at the primary stage in the L1 brain. Here, BLD1-4 form a lateral and a medial pair, directly adjacent to the dorsal edge of the optic lobe primordium (inner optic anlage, IOA; Fig. 10B, C, E, H/H′, K); axons of both clusters converge and enter the superior lateral protocerebrum (SLP) right next to the DPLal and BLAd tracts (SLP I entry portal, #15c; Figs. 2G, I and 10B, C, E, H/H′, K). BLD1-4 tracts continue along the trSI fascicle.

BLV lineages are grouped around the ventral edge of the optic lobe primordium and project their tracts dorsally, into the cleft formed in between the inner optic anlage (IOA) and the ventral lateral protocerebrum neuropil (VLP; Figs. 2K4 and 10A, B, F/F′, I/I′, L). The two posterior BLVs (BLVp1/2) were discussed in the previous section (see above). The remaining, anterior BLV lineages form two pairs, BLVa1/2 and BLVa3/4. The BLVa3/4 pair is located posteriorly and medially of the BLVa1/2 pair. As described for the corresponding secondary lineages, the primary BLVa3/4 tract is shorter, ending below the LON–VLP junction at the lateral surface of the VLP (entry portal VLP vl, #31; Figs. 2I, K4 and Fig. 10A, B, F/F′, I/I′, L). The BLVa1/2 tract extends further dorsally, passing anterior of the LON–VLP junction towards the superior lateral protocerebrum (SLP; entry portal LH a, #15d; Figs. 2G–I, K4 and 10A, B, F/F′, I/I′, L).

4. Discussion

4.1. The use of pan-neuronal markers in reconstructing brain architecture

The brain neuropil of insects and most other invertebrates is composed of the thin processes of neurons and glial cells. One can distinguish neuropil domains where terminal axonal and dendritic branches form synaptic connections (synaptic neuropil) from bundles of long processes (tracts or fascicles) that interconnect different domains of synaptic neuropil. Globally expressed neuronal membrane proteins, such as Neuroglian or Neurotactin, are concentrated in long axon bundles and, when labeled by protein-specific antibodies, they stand out against the surrounding synaptic neuropil. It is important to note that many known pan-neuronal proteins are expressed dynamically (Fung et al., 2008). Both Neurotactin and Neuroglian appear at high levels in young neurons that send out their initial axon during embryonic development (Bieber et al., 1989; Hortsch et al., 1990). As shown in the present study, the proteins are still highly expressed by all primary neurons in the early larva, but there are already differences in expression level which are most likely correlated with the birthdate of neurons. Thus, the intensity of labeling of neuronal cell bodies in the cortex is not identical for all cells; clusters of strongly labeled cell bodies, always closely associated with the beginning of the lineage axon tract (PAT), are surrounded by more weakly labeled cell bodies (see, for example, clusters indicated by arrows in Fig. 2L2). We suspect that the cells with higher expression levels are the late born neurons and that their strongly labeled axon tracts form the visible "backbone" of the PATs visible in the L1 brain. In the late larval brain, primary neuron expression of Neurotactin and (to a lesser extent), Neuroglian, wanes, while expression of these markers in secondary axon tracts is very robust. Secondary tracts maintain expression of Neurotactin and Neuroglian throughout early metamorphosis; at late pupal stages, Neuroglian remains strong all the way into adulthood, which makes it possible to relate the long axon tracts of the larva to those of the adult (Lovick et al., 2013).

One needs to point out that, aside from the lineage-associated axon bundles, there exists a second type of tract or fascicle which consists of less tightly packed parallel fibers with interspersed short terminal branches and synapses. A prominent example are the longitudinal, FasII-positive axon tracts of the ventral nerve cord and the lobes of the mushroom body. The long nerve fibers that scaffold these domains, also called "tract neuropils" (Virtual Fly Brain; Milyaev et al., 2012), are not necessarily related by lineage. This is very clear in case of the longitudinal tracts of the VNC, where lineage associated tracts form predominantly transverse (commissural) or vertical bundles (Kuert et al., 2014; Truman et al., 2004), but do not become part of the FasII-positive longitudinal fascicles. Instead, these fascicles are most likely formed by single or small subsets ("sublineages") of axons belonging to several different lineages. In the embryo, FasII is expressed in groups of neurons that are born and differentiate early and thereby establish neuropil "pioneer" or "founder" tracts (Goodman and Doe, 1993; Nassif et al., 1998). The exact relationship of the FasII-positive neuron clusters to lineages has not yet been established; however, it seems clear that these clusters are derived from multiple lineages.

4.2. Factors controlling the spatial pattern of lineages and lineage-associated tracts

The pattern of PATs reflects in part the pattern of neuroblasts that had generated the lineages giving rise to the PATs. Based on clonal analysis, neuronal cell bodies belonging to one lineage cluster around their mother neuroblast and the PAT begins at the base of each cluster (Bossing et al., 1996; Larsen et al., 2009; Schmidt et al., 1997). There is no large scale migration of cell bodies away from the location in which they were placed at birth. The differences that one observes between the position of lineages in early and late embryos are brought about by a general movement of the brain primordium as a whole, whereby the neuraxis tilts posteriorly. For example, neuroblasts of lineages that are located dorso-posteriorly in the larval brain (e.g., mushroom body) start out quite anteriorly in the neuroblast map of the stage 11 embryo (Chang et al., 2003; Kunz et al., 2012; Noveen et al., 2000). It is not known what kind of morphogenetic mechanisms cause this shift; most likely, forces outside the brain primordium itself, such as the moving foregut and head epidermis, are involved. However, in terms of local neighborhood relationships between individual neuroblasts and the clusters of neurons they give rise to, there do not appear to be major changes between early and late embryonic stages (Chang et al., 2003; Sprecher et al., 2007).

Aside from neuroblast location, another determining factor of the pattern of PATs appears to be affinities of certain lineages to each other. Thus, PATs of most lineages do not enter the neuropil as individual bundles, but travel together in groups of 2–4 members. Such groups of entering PATs form "entry portals" that represent distinct landmarks at the neuropil surface. They appear as funnel-shaped depressions, or as clefts, in volume renderings of confocal stacks of preparations where the neuropil is labeled by global markers such as DN-cadherin (Figs. 2 and 11). Many portals form part of the boundaries between neuropil compartments; examples are the portals that surround the antennal lobe at the anterior neuropil surface. Importantly, the combinations of lineages that group together during the primary phase of neurogenesis remain in contact during secondary neurogenesis in the late larva. In other words, the entry portals defined by PATs in the L1 larva correspond to those formed by SATs in the adult brain (Lovick et al., 2013; Wong et al., 2013), which makes the entry portals a useful structural feature to follow neuropil morphogenesis throughout development (see below).

What do lineages that adhere together and enter the neuropil at the same portal have in common? Part of the answer probably lies in similarities in projection and connectivity mediated by the joined lineages. In the majority of cases, joined lineages project along the same fascicle within the neuropil, and therefore connect

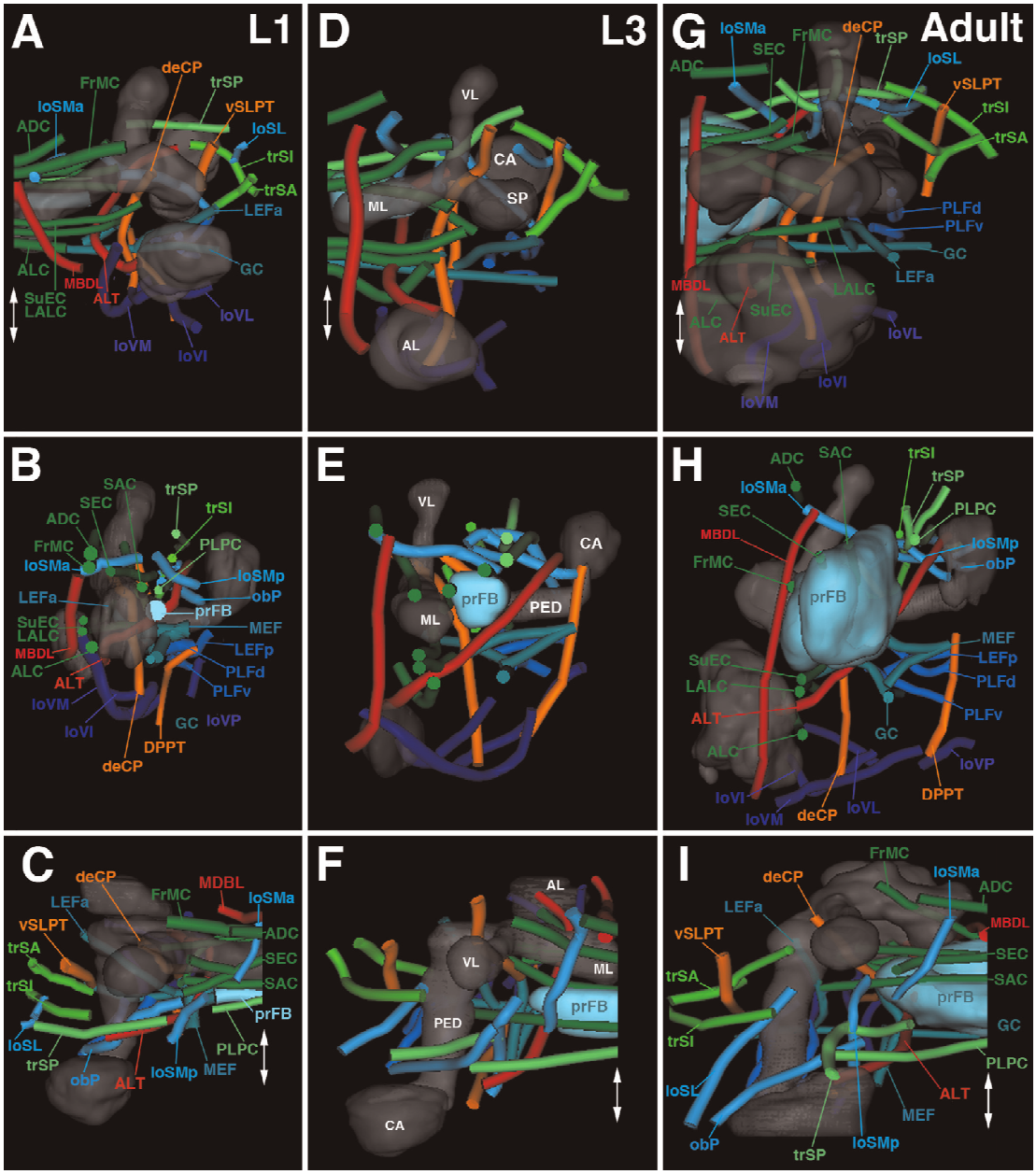

Fig. 11. Digital 3D models of lineage-associated neuropil tracts in a single hemisphere of the L1 larval brain, (A–C), L3 larval brain (D–F) and adult brain (G–I). Anterior view (upper row; A, D, G; medial to the left); medial view (intermediate row; B, E, H; anterior to the left); dorsal view (bottom row; C, F, I; medial to the right). Mushroom body and antennal lobe shown for reference (gray). Rendering of tracts follows color scheme used in Fig. 4 (longitudinal tracts: blue; transverse tracts/commissures: green; ascending tracts: red; descending tracts: orange). The fan-shaped body primordium is rendered in light blue. Double-headed arrow indicates midline. Bars: 20 µm (A–C); 25 µm (D–F); 50 µm (G–I).

overlapping or closely adjacent neuropil domains. Examples are BAmv1/2, BAlp2/3, BAla3/4, DALcl1/2 (hemilineages), DALcm1/2/DALd (hemilineages), DPLal1-3, DPLc1-5, DPLl1-3, BLAd1-4, BLP3/4, and BLV3/4. The secondary components of all of these lineages have been visualized as GFP-labeled clones, and show not only common tracts, but also similar, largely overlapping domains of terminal arborization (Ito et al., 2013; Wong et al., 2013; Yu et al., 2013). It will be interesting to establish for these groups of lineages

the corresponding neuroblasts and their genetic identities; one would expect that the commonalities in anatomical properties of a group are reflected in the expression of similar genes during early development.

4.3. *Structural elements of the L1 and adult brain: a comparison*

We had documented in previous studies (Nassif et al., 1998, 2003; Pereanu et al., 2010; Younossi-Hartenstein et al., 2006) that many structural elements of the adult brain can be already

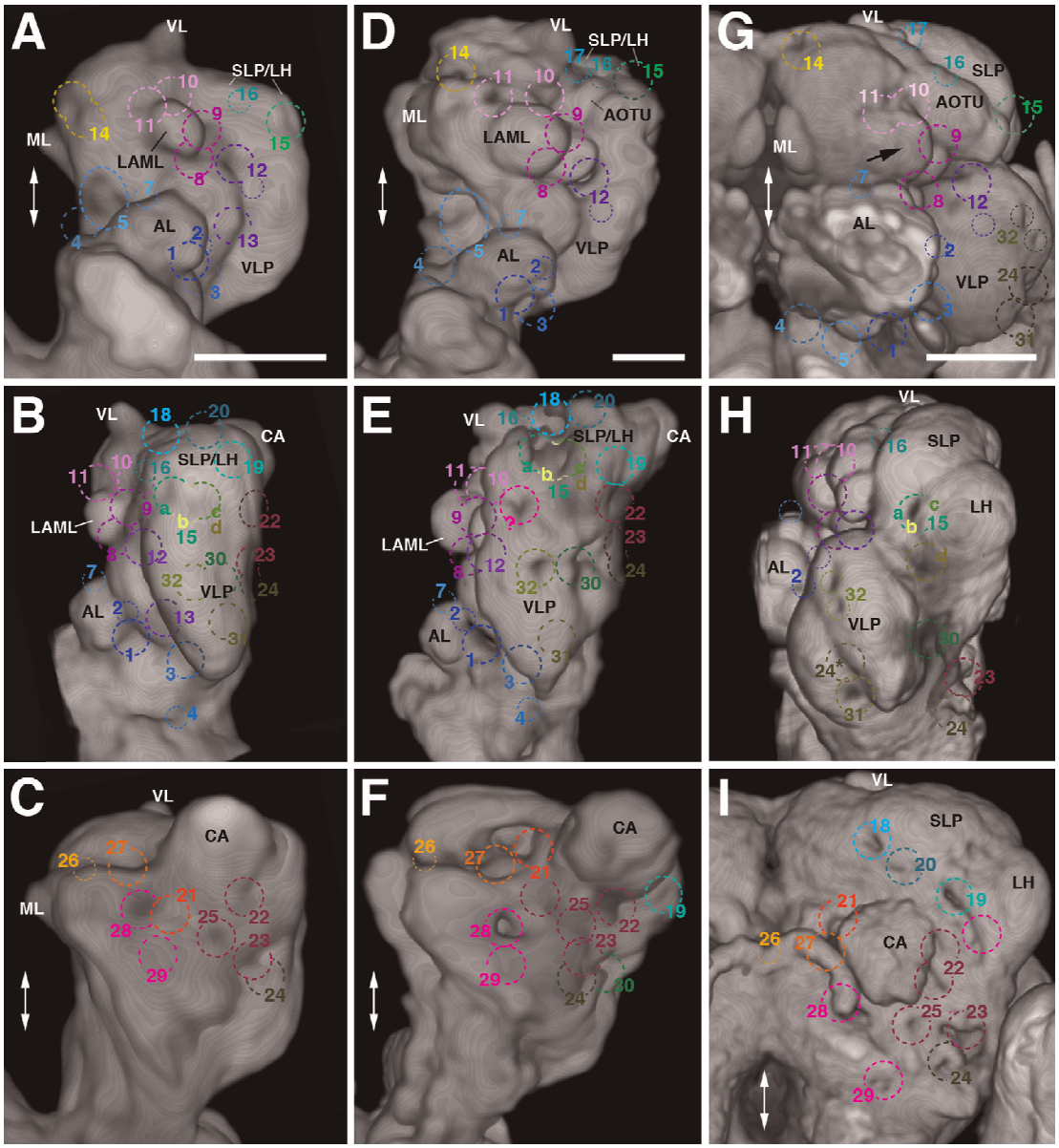

Fig. 12. Entry portals of lineage-associated tracts (numbered hatched circles in the L1 larval brain (A–C), L3 larval brain (D–F), and adult brain (G–I)). Each panel shows volume rendering of anti-DN-cadherin-labeled (L1) or anti-bruchpilot (L3, adult) brain hemisphere, highlighting relief of neuropil surface. Anterior view (upper row; A, D, G; medial to the left); lateral view (intermediate row; B, E, H; anterior to the left); posterior view (bottom row; C, F, I; medial to the left). Double-headed arrow in (A) and all other panels indicates brain midline. Rendering of entry portals follows color scheme used to differentiate between groups of lineages in Figs. 1 and 5–10.

recognized at the early larval stage. The identification of lineages and their associated tracts add many new details to these findings. Thus, the change in distances between fiber tracts (Fig. 11) and lineage entry portals (Fig. 12) that occur during development reflect the changes in neuropil growth that occurs during larval and pupal development. This growth is due to the enlargement of primary neuronal arbors (from early to late larva) and the addition of secondary neurons (from early larva to adult). Neuropil growth is highly anisotropic: some compartments grow much more than others. Compartments that grow most are related to the highly increased number of sensory afferents that characterizes the transition from larva to adult (12 photoreceptors in the larva, $6000 photoreceptors in the adult; 21 antennal olfactory afferents in the larva; $1300 in the adult (Laissue and Vosshall, 2008)), and to the control of complex motor acts the adult fly is capable of. Neuropil growth is most pronounced in four regions of the central brain: (1) the ventrolateral protocerebrum and anterior anterior optic tubercle which receives higher order input from the optic lobe (visual system); (2) the antennal lobe, a primary sensory center for olfaction; (3) the superior lateral protocerebrum and lateral horn, which presumably serve as multimodal association centers; (4) the central complex which controls locomotor behavior.

(1) The growth of the ventrolateral protocerebrum can be best appreciated in the anterior and lateral/medial views of the neuropil presented in Figs. 11A–F and 12A–F, respectively. Note the increase in distance between the vertically oriented tracts deCP and DPPT, and in length of the longitudinally oriented ventral fascicles (loVL, loVM, loVP; Fig. 11D–F). The portals of the laterally entering lineages BLVa3/4 (#31) and BLVp1/2 (#24), which are right next to each other in the L1 brain (Fig. 12D), are pushed apart (Fig. 12E, F); the same change occurs for the entries of BLAv1/2 (#32) and BLD5/6 (#30). The anterior anterior optic tubercle (AAOTU) bulges out of the anterior surface of the larval SLP compartment (Fig. 12C).
(2) The adult antennal lobe develops at the dorsal margin of its larval counterpart, as described in previous works (ref). The enormous growth of this compartment can be appreciated by the increasing vertical and horizontal distance between the entry portals of dorsal projection neuron lineage BAmv3 (#7) and the ventrolateral lineages BAla1/2 (#1; Fig. 12A–C). The portal of BAmv1/2 (#5), and the location of the ventral longitudinal medial fascicle (loVM) formed by these lineages, shifts to a ventral position (Figs. 11A–C and 12A–C). The BAmas1/2 portal (#6) is also pushed ventrally and the median bundle (MBDL) formed by the BAmas1/2 lineages lengthens (Fig. 11A–C).
(3) The neuropil domain located dorso-laterally of the peduncle is relatively underdeveloped in the larval brain, compared to the adult. Here, the neuropil forms prominent bulges, the superior lateral protocerebrum (SLP) and lateral horn (LH). By contrast, in the larva, the corresponding domain ("SLP/LH" in Fig. 12C, F, I) is represented by a thin layer of neuropil. The growth of these compartments is reflected in the increasing distances between the entry portals of anterior DPL lineages [DPLal (#15), DPLam (#16)] and posterior DPL lineages [DPLc (#18), DPLm (#19), DPLl (#20); see Fig. 12D, E, I]. The DPLc and DPLl portals, occupying a lateral position in the larva (Figs. 11G, H and 12 D, E), have been pushed towards the posterior brain surface by the outgrowing SLP and LH (Figs. 11I and 12I).
(4) The central complex develops during metamorphosis, primarily through the differentiation of the massive number of columnar/small field neurons generated by the type II lineages DPMm1/DM1, DPMpm1/DM2, DPMpm2/DM3, and CM4/DM4 (Riebli et al., 2013; Yang et al., 2013). In the early larval brain, primary neurons of these lineages form a commissural bundle that crosses the midline right behind the medial lobe of the mushroom body (Fig. 11D, G). This commissure, which grows into a sizeable primordium of the fan-shaped body by the third larval instar (Riebli et al., 2013; Fig. 11E, H), foreshadows the position of the central complex as a set of compartments formed during pupal development by elaborate branching of secondary commissural fibers that "squeeze" in between the commissures formed by previously established primary neurons (the SuEC/LALC antero-ventrally, SEC and SAC antero-dorsally, GC ventrally, and PLPC postero-dorsally; Fig. 11D–F). An anteriorly located lineage, DALv2, contributes the (large field) ring neurons of the ellipsoid body that represents the anterior part of the central complex (Fig. 11F).

Acknowledgments

We thank Dr. J. Truman for generous help in the screen for Gal-4 lines with expression in larval brain lineages. This work was supported by NIH Grant R01 NS054814 to V.H.

Appendix A. Supplementary material

Supplementary data associated with this article can be found in the online version at http://dx.doi.org/10.1016/j.bios.2014.05.063.

References

Asburner M., Drosophila: A Laboratory Manual, 1989, Cold Spring Harbor Laboratory Press, Cold Spring Harbor, NY.
Bayraktar, O.A., Boone, J.Q., Drummond, M.L., Doe, C.Q., 2010. Drosophila type II neuroblast lineages keep Prospero levels low to generate large clones that contribute to the adult brain central complex. Neural Dev. 5, 26. http://dx.doi.org/10.1186/1749-8104-5-26.
Bello, B.C., Izergina, N., Caussinus, E., Reichert, H., 2008. Amplification of neural stem cell proliferation by intermediate progenitor cells in Drosophila brain development. Neural Dev. 3, 5. http://dx.doi.org/10.1186/1749-8104-3-5.
Betschinger, J., Mechtler, K., Knoblich, J.A., 2006. Asymmetric segregation of the tumor suppressor brat regulates self-renewal in Drosophila neural stem cells. Cell 124, 1241–1253.
Bieber, A.J., Snow, P.M., Hortsch, M., Patel, N.H., Jacobs, J.R., Traquina, Z.R., Schilling, J., Goodman, C.S., 1989. Drosophila neuroglian: a member of the immunoglobulin superfamily with extensive homology to the vertebrate neural adhesion molecule L1. Cell 59, 447–460.
Birkholz, O., Rickert, C., Nowak, J., Cobanl, C., Technau, G.M., 2015. Bridging the gap between postembryonic cell lineages and identified embryonic neuroblasts in the ventral nerve cord of *Drosophila melanogaster*. Biol. Open 4 (4), 420–434.
Boll, W., Noll, M., 2002. The Drosophila Pox neuro gene: control of male courtship behavior and fertility as revealed by a complete dissection of all enhancers. Development 129, 5667–5681.
Bossing, T., Udolph, G., Doe, C.Q., Technau G.M., 1996. The embryonic central nervous system lineages of *Drosophila melanogaster*. I. Neuroblast lineages derived from the ventral half of the neuroectoderm. Dev. Biol. 179, 41–64.
Brody, T., Odenwald, W.F., 2005. Regulation of temporal identities during Drosophila neuroblast lineage development. Curr. Opin. Cell Biol. 17, 672–675.
Caldwell, J.C., Miller, M.M., Wing, S., Soll, D.R., Eberl, D.F., 2003. Dynamic analysis of larval locomotion in Drosophila chordotonal organ mutants. Proc. Natl. Acad. Sci. U.S.A. 100, 16053–16058.
Cardona, A., Saalfeld, S., Arganda, I., Pereanu, W., Schindelin, J., Hartenstein, V., 2010a. Identifying neuronal lineages of Drosophila by sequence analysis of their axon tracts. J. Neurosci. 30, 7538–7553.
Cardona, A., Saalfeld, S., Preibisch, S., Schmid, B., Cheng, A., Pulokas, J., Tomancak, P., Hartenstein, V., 2010b. An integrated micro- and macroarchitectural analysis of the Drosophila brain by computer-assisted serial electron microscopy. PLoS Biol. 8, e1000502.
Cardona, A., Saalfeld, S., Schindelin, J., Arganda-Carreras, I., Preibisch, S., Longair, M., Tomancak, P., Hartenstein, V., Douglas, R.J., 2012. TrakEM2 software for neural circuit reconstruction. PLoS One. 7, e38011.
Chang, T., Younossi-Hartenstein, A., Hartenstein, V., 2003. Development of neural lineages derived from the sine oculis positive eye field of Drosophila. Arthropod. Struct. Dev. 32, 303–317.
Choi, J.C., Park, D., Griffith, L.C., 2004. Electrophysiological and morphological

characterization of identified motor neurons in the Drosophila third instar larva central nervous system. J. Neurophysiol. 91, 2353–2365.
Colomb, J., Grillenzoni, N., Ramaekers, A., Stocker, R.F., 2007. Architecture of the primary taste center of *Drosophila melanogaster* larvae. J. Comp. Neurol. 502, 834–847.
Das, A., Gupta, T., Davla, S., Prieto-Godino, L.L., Diegelmann, S., Reddy, O.V., Raghavan, K.V., Reichert, H., Lovick, J., Hartenstein, V., 2013. Neuroblast lineage-specific origin of the neurons of the Drosophila larval olfactory system. Dev. Biol. 373, 322–337.
de la Escalera, S., Bockamp, E.O., Moya, F., Piovant, M., Jiménez, F., 1990. Characterization and gene cloning of neurotactin, a Drosophila transmembrane protein related to cholinesterases. EMBO J. 9, 3593–3601.
Dumstrei, K., Wang, F., Nassif, C., Hartenstein, V., 2003. Early development of the Drosophila brain. V. Pattern of postembryonic neuronal lineages expressing Shg/DE-cadherin. J. Comp. Neurol. 455, 451–462.
Friggi-Grelin, F., Coulom, H., Meller, M., Gomez, D., Hirsh, J., Birman, S., 2003. Targeted gene expression in Drosophila dopaminergic cells using regulatory sequences from tyrosine hydroxylase. J. Neurobiol. 54, 618–627.
Fung, S., Wang, F., Chase, M., Godt, D., Hartenstein, V., 2008. Expression profile of the cadherin family in the developing Drosophila brain. J. Comp. Neurol. 506, 469–488.
Gerber, B., Stocker, R.F., 2007. The Drosophila larva as a model for studying chemosensation and chemosensory learning: a review. Chem. Senses 32, 65–89.
Ghysen, A., Dambly-Chaudière, C., Jan, L.Y., Jan, Y.N., 1993. Cell interactions and gene interactions in peripheral neurogenesis. Genes Dev. 7, 723–733.
Goodman, C.S., Doe, C.Q., 1993. Embryonic development of the Drosophila central nervous system. In: Bate, M., Martinez-Arias, A. (Eds.), In the Development of *Drosophila melanogaster*. Cold Spring Harbor: Cold Spring Harbor Press, pp. 941–1012.
Grenningloh, G., Rehm E., J., Goodman, C.S., 1991. Genetic analysis of growth-cone guidance in Drosophila: fasciclin II functions as a neuronal recognition molecule. Cell 67, 45–57.
Hartenstein, V., 1988. Development of the Drosophila larval sensory organs: spatiotemporal pattern of sensory neurones, peripheral axonal pathways, and sensilla differentiation. Development 102, 869–886.
Hartenstein, V., Spindler, S., Pereanu, W., Fung, S., 2008. The development of the Drosophila larval brain. Adv. Exp. Med Biol. 628, 1–31.
Hayashi, S., Ito, K., Sado, Y., Taniguchi, M., Akimoto, A., Takeuchi, H., Aigaki, T., Matsuzaki, F., Nakagoshi, H., Tanimura, T., Ueda, R., Uemura, T., Yoshihara, M., Goto, S., 2002. GETDB, a database compiling expression patterns and molecular locations of a collection of Gal4 enhancer traps. Genesis 34, 58–61.
Hortsch, M., Patel, N.H., Bieber, A.J., Traquina, Z.R., Goodman, C.S., 1990. Drosophila neurotactin, a surface glycoprotein with homology to serine esterases, is dynamically expressed during embryogenesis. Development 110, 1327–1340.
Ito, K., Hotta, Y., 1992. Proliferation pattern of postembryonic neuroblasts in the brain of *Drosophila melanogaster*. Dev. Biol. 149, 134–148.
Ito, M., Masuda, N., Shinomiya, K., Endo, K., Ito, K., 2013. Systematic analysis of neural projections reveals clonal composition of the Drosophila brain. Curr. Biol. 23, 644–655.
Ito, K., Shinomiya, K., Ito, M., Armstrong, J.D., Boyan, G., Hartenstein, V., Harzsch, S., Heisenberg, M., Homberg, U., Jenett, A., Keshishian, H., Restifo, L.L., Rössler, W., Simpson, J.H., Strausfeld, N.J., Strauss, R., Vosshall, L.B., 2014. A systematic nomenclature for the insect brain. Neuron 81, 755–765.
Jenett, A., Rubin, G.M., Ngo, T.T., Shepherd, D., Murphy, C., Dionne, H., Pfeiffer, B.D., Cavallaro, A., Hall, D., Jeter, J., Iyer, N., Fetter, D., Hausenfluck, J.H., Peng, H., Trautman, E.T., Svirskas, R.R., Myers, E.W., Iwinski, Z.R., Aso, Y., DePasquale, G. M., Enos, A., Hulamm, P., Lam, S.C., Li, H.H., Laverty, T.R., Long, F., Qu, L., Murphy, S.D., Rokicki, K., Safford, T., Shaw, K., Simpson, J.H., Sowell, A., Tae, S., Yu, Y., Zugates, C.T., 2012. A GAL4-driver line resource for Drosophila neurobiology. Cell Rep. 2, 991–1001.
Johansen, J., Halpern, M.E., Keshishian, H., 1989. Axonal guidance and the development of muscle fiber-specific innervation in Drosophila embryos. J. Neurosci. 9, 4318–4332.
Kaneko, M., Hall, J.C., 2000. Neuroanatomy of cells expressing clock genes in Drosophila: transgenic manipulation of the period and timeless genes to mark the perikarya of circadian pacemaker neurons and their projections. J. Comp. Neurol 422, 66–94.
Kim, M.D., Wen, Y., Jan, Y.N., 2009. Patterning and organization of motor neuron dendrites in the Drosophila larva. Dev. Biol. 336, 213–221.
Kohsaka, H., Okusawa, S., Itakura, Y., Fushiki, A., Nose, A., 2012. Development of larval motor circuits in Drosophila. Dev. Growth Differ. 54, 408–419.
Kuert, P.A., Bello, B.C., Reichert, H., 2012. The labial gene is required to terminate proliferation of identified neuroblasts in postembryonic development of the Drosophila brain. Biol. Open. 1, 1006–1015.
Kuert, P.A., Hartenstein, V., Bello, B.C., Lovick, J.K., Reichert, H., 2014. Neuroblast lineage identification and lineage-specific Hox gene action during postembryonic development of the subesophageal ganglion in the Drosophila central brain. Dev. Biol. 390, 102–115.
Kumar, A., Fung, S., Lichtneckert, R., Reichert, H., Hartenstein, V., 2009. Arborization pattern of engrailed-positive neural lineages reveal neuromere boundaries in the Drosophila brain neuropil. J. Comp. Neurol. 517, 87–104.
Kwon, J.Y., Dahanukar, A., Weiss, L.A., Carlson, J.R., 2011. Molecular and cellular organization of the taste system in the Drosophila larva. J. Neurosci. 31, 15300–15309.
Kunz, T., Kraft, K.F., Technau, G.M., Urbach, R., 2012. Origin of Drosophila mushroom body neuroblasts and generation of divergent embryonic lineages. Development 139, 2510–2522.
Lai, S.L., Awasaki, T., Ito, K., Lee, T., 2008. Clonal analysis of Drosophila antennal lobe neurons: diverse neuronal architectures in the lateral neuroblast lineage. Development 135, 2883–2893.
Laissue, P.P., Vosshall, L.B., 2008. The olfactory sensory map in Drosophila. Adv. Exp. Med. Biol. 628, 102–114.
Landgraf, M., Jeffrey, V., Fujioka, M., Jaynes, J.B., Bate, M., 2003a. Embryonic origins of a motor system: motor dendrites form a myotopic map in Drosophila. PLoS Biol. 1, E41.
Landgraf, M., Sánchez-Soriano, N., Technau, G.M., Urban, J., Prokop, A., 2003b. Charting the Drosophila neuropile: a strategy for the standardised characterisation of genetically amenable neurites. Dev. Biol. 260, 207–225.
Larsen, C., Shy, D., Spindler, S., Fung, S., Younossi-Hartenstein, A., Hartenstein, V., 2009. Patterns of growth, axonal extension and axonal arborization of neuronal lineages in the developing Drosophila brain. Dev. Biol. 335, 289–304.
Lee, T., Lee, A., Luo, L., 1999. Development of the Drosophila mushroom bodies: sequential generation of three distinct types of neurons from a neuroblast. Development 126, 4065–4076.
Liu, L., Yermolaieva, O., Johnson, W.A., Abboud, F.M., Welsh, M.J., 2003. Identification and function of thermosensory neurons in Drosophila larvae. Nat. Neurosci. 6, 267–273.
Lichtneckert, R., Bello, B., Reichert, H., 2007. Cell lineage-specific expression and function of the empty spiracles gene in adult brain development of *Drosophila melanogaster*. Development 134, 1291–1300.
Lovick, J.K., Ngo, K.T., Omoto, J.J., Wong, D.C., Nguyen, J.D., Hartenstein, V., 2013. Postembryonic lineages of the Drosophila brain: I. Development of the lineage-associated fiber tracts. Dev. Biol. 384, 228–257.
Lovick J.K., Kong A., Omoto J.J., Ngo K.T., Younossi-Hartenstein A., Hartenstein V., 2015. Patterns of growth and tract formation during the early development of secondary lineages in the Drosophila larval brain, Devel Neurobio. http://dx.doi.org/10.1002/dneu.22325.
Masuda-Nakagawa, L.M., Tanaka, N.K., O'Kane, C.J., 2005. Stereotypic and random patterns of connectivity in the larval mushroom body calyx of Drosophila. Proc. Natl. Acad. Sci. U.S.A. 102, 19027–19032.
Masuda-Nakagawa, L.M., Gendre, N., O'Kane, C.J., Stocker, R.F., 2009. Localized olfactory representation in mushroom bodies of Drosophila larvae. Proc. Natl. Acad. Sci. U.S.A. 106, 10314–10319.
Milyaev, N., Osumi-Sutherland, D., Reeve, S., Burton, N., Baldock, R.A., Armstrong, J. D., 2012. The virtual fly brain browser and query interface. Bioinformatics 28, 411–415.
Minocha, S., 2010. A Role of Pox Neuro in the Developing Drosophila Brain: Determination of Large-Field Neurons Essential for Ellipsoid Body Formation and of Ventral Projection Neurons (Doctoral dissertation). Retrieved from Zurich Open Repository and Archive.
Nassif, C., Noveen, A., Hartenstein, V., 1998. Embryonic development of the Drosophila brain I. The pattern of pioneer tracts. J. Comp. Neurol. 402, 10–31.
Nassif, C., Noveen, A., Hartenstein, V., 2003. Early development of the Drosophila brain III. The pattern of neuropile founder tracts during the larval period. J. Comp. Neurol. 455, 417–434.
Noveen, A., Daniel, A., Hartenstein, V., 2000. The role of eyeless in the embryonic development of the Drosophila mushroom body. Development 127, 3475–3488.
Pearson, B.J., Doe, C.Q., 2004. Specification of temporal identity in the developing nervous system. Annu. Rev. Cell Dev. Biol. 20, 619–647.
Pereanu, W., Hartenstein, V., 2006. Neural lineages of the Drosophila brain: a 3D digital atlas of the pattern of lineage location and projection at the late larval stage. J. Neurosci. 26, 5534–5553.
Pereanu, W., Kumar, A., Jenett, A., Reichert, H., Hartenstein, V., 2010. Development-based compartmentalization of the Drosophila central brain. J. Comp. Neurol. 518, 2996–3023.
Power, M.E., 1948. The thoraco-abdominal nervous system of an adult insect *Drosophila melanogaster*. J. Comp. Neurol. 88, 347–409.
Python, F., Stocker, R.F., 2002. Adult-like complexity of the larval antennal lobe of *D. melanogaster* despite markedly low numbers of odorant receptor neurons. J. Comp. Neurol. 445, 374–387.
Rajashekhar, K.P., Singh, R.N., 1994. Neuroarchitecture of the tritocerebrum of *Drosophila melanogaster*. J. Comp. Neurol. 349, 633–645.
Ramaekers, A., Magnenat, E., Marin, E.C., Gendre, N., Jefferis, G.S., Luo, L., Stocker, R. F., 2005. Glomerular maps without cellular redundancy at successive levels of the Drosophila larval olfactory circuit. Curr. Biol. 15, 982–992.
Riebli, N., Viktorin, G., Reichert, H., 2013. Early-born neurons in type II neuroblast lineages establish a larval primordium and integrate into adult circuitry during central complex development in Drosophila. Neural Dev. 8, 6. http://dx.doi.org/10.1186/1749-8104-8-6.
Rusan, N.M., Peifer, M., 2007. A role for novel centrosome cycle in asymmetric cell division. J. Cell Biol. 177, 13–20.
Siebert, M., Banovic, D., Goellner, B., Aberle, H., 2009. Drosophila motor axons recognize and follow a Sidestep-labeled substrate pathway to reach their target fields. Genes Dev 23, 1052–1062.
Selcho, M., Pauls, D., Han, K.A., Stocker, R.F., Thum, A.S., 2009. The role of dopamine in Drosophila larval classical olfactory conditioning. PLoS One 4, e5897.
Schindelin, J., Arganda-Carreras, I., Frise, E., Kaynig, V., Longair, M., Pietzsch, T., Preibisch, S., Rueden, C., Saalfeld, S., Schmid, B., Tinevez, J.Y., White, D.J., Hartenstein, V., Eliceiri, K., Tomancak, P., Cardona, A., 2012. Fiji: an open-source platform for biological-image analysis. Nat. Methods 9, 676–682.
Schleyer, M., Saumweber, T., Nahrendorf, W., Fischer, B., von Alpen, D., Pauls, D.,

Thum, T., Gerber, B., 2011. A behavior-based circuit model of how outcome expectations organize learned behavior in larval Drosophila. Learn. Mem. 18, 639–653.
Schmidt, H., Rickert, C., Bossing, T., Vef, O., Urban, J., Technau, G.M., 1997. Dev Biol. 189, 186–204.
Schrader, S., Merritt, D.J., 2000. Central projections of Drosophila sensory neurons in the transition from embryo to larva. J. Comp. Neurol. 425, 34–44.
Sink, H., Whitington, P.M., 1991. Early ablation of target muscles modulates the arborisation pattern of an identified embryonic Drosophila motor axon. Development 113, 701–707.
Spindler, S.R., Hartenstein, V., 2010. The Drosophila neural lineages: a model system to study brain development and circuitry. Dev. Genes Evol. 220, 1–10.
Spindler, S.R., Hartenstein, V., 2011. Bazooka mediates secondary axon morphology in Drosophila brain lineages. Neural Dev. 6, 16. http://dx.doi.org/10.1186/1749-8104-6-16.
Sprecher, S., Reichert, H., Hartenstein, V., 2007. Gene expression patterns in primary neuronal clusters of the Drosophila embryonic brain. Gene Expr. Patterns 7, 584–595.
Sprecher, S.G., Cardona, A., Hartenstein, V., 2011. The Drosophila larval visual system: high-resolution analysis of a simple visual neuropil. Dev. Biol. 358, 33–43.
Stocker, R.F., Heimbeck, G., Gendre, N., de Belle, J.S., 1997. Neuroblast ablation in Drosophila P[Gal4] lines reveals origins of olfactory interneurons. J. Neurobiol. 32, 443–456.
Tabata, T., Schwartz, C., Gustavson, E., Ali, Z., Kornberg, T.B., 1995. Creating a Drosophila wing de novo, the role of engrailed, and the compartment border hypothesis. Development 121, 3359–3369.
Truman, J.W., Bate, M., 1988. Spatial and temporal patterns of neurogenesis in the central nervous system of *Drosophila melanogaster*. Dev. Biol. 125, 145–157.
Truman, J.W., Schuppe, H., Shepherd, D., Williams, D.W., 2004. Developmental architecture of adult-specific lineages in the ventral CNS of Drosophila. Development 131, 5167–5184.
Tyrer, N.M., Gregory, G.E., 1982. A guide to the neuroanatomy of locust suboesophageal and thoracic ganglia. Philos. Trans. R. Soc. Lond. B 297, 91–123.
Urbach, R., Technau, G.M., 2003. Molecular markers for identified neuroblasts in the developing brain of Drosophila. Development 130, 3621–3637.
Urbach, R., Technau, G.M., 2004. Neuroblast formation and patterning during early brain development in Drosophila. Bioessays 26, 739–751.
Vactor, D.V., Sink, H., Fambrough, D., Tsoo, R., Goodman, C.S., 1993. Genes that control neuromuscular specificity in Drosophila. Cell 73, 1137–1153.
Wong, D.C., Lovick, J.K., Ngo, K.T., Borisuthirattana, W., Omoto, J.J., Hartenstein, V., 2013. Postembryonic lineages of the Drosophila brain: II. Identification of lineage projection patterns based on MARCM clones. Dev. Biol. 384, 258–289.
Yang, J.S., Awasaki, T., Yu, H.H., He, Y., Ding, P., Kao, J.C., Lee, T., 2013. Diverse neuronal lineages make stereotyped contributions to the Drosophila locomotor control center, the central complex. J. Comp. Neurol. 521, 2645–2662 (Spc1).
Younossi-Hartenstein, A., Nassif, C., Hartenstein, V., 1996. Early neurogenesis of the Drosophila brain. J. Comp. Neurol. 370, 313–329.
Younossi-Hartenstein, A., Salvaterra, P., Hartenstein, V., 2003. Early development of the Drosophila brain IV. Larval neuropile compartments defined by glial septa. J. Comp. Neurol. 455, 435–450.
Younossi-Hartenstein, A., Shy, D., Hartenstein, V., 2006. The embryonic formation of the Drosophila brain neuropile. J. Comp. Neurol. 497, 981–998.
Yu, H.H., Awasaki, T., Schroeder, M.D., Long, F., Yang, J.S., He, Y., Ding, P., Kao, J.C., Wu, G.Y., Peng, H., Myers, G., Lee, T., 2013. Clonal development and organization of the adult Drosophila central brain. Curr. Biol. 23, 633–

Chapter 3

Hydroxyurea-mediated neuroblast ablation establishes birth dates of secondary lineages an addresses neuronal interactions in the developing *Drosophila* brain

Hydroxyurea-mediated neuroblast ablation establishes birth dates of secondary lineages and addresses neuronal interactions in the developing *Drosophila* brain

Jennifer K. Lovick, Volker Hartenstein[n]

article info

Article history:
Received 16 December 2014
Received in revised form
27 February 2015
Accepted 5 March 2015
Available online 13 March 2015

Keywords:
Ablation
Brain
Development
Drosophila
Lineage

abstract

The *Drosophila* brain is comprised of neurons formed by approximately 100 lineages, each of which is derived from a stereotyped, asymmetrically dividing neuroblast. Lineages serve as structural and developmental units of *Drosophila* brain anatomy and reconstruction of lineage projection patterns represents a suitable map of *Drosophila* brain circuitry at the level of neuron populations ("macro-circuitry"). Two phases of neuroblast proliferation, the first in the embryo and the second during the larval phase (following a period of mitotic quiescence), produce primary and secondary lineages, respectively. Using temporally controlled pulses of hydroxyurea (HU) to ablate neuroblasts and their corresponding secondary lineages during the larval phase, we analyzed the effect on development of primary and secondary lineages in the late larval and adult brain. Our findings indicate that timing of neuroblast re-activation is highly stereotyped, allowing us to establish "birth dates" for all secondary lineages. Furthermore, our results demonstrate that, whereas the trajectory and projection pattern of primary and secondary lineages is established in a largely independent manner, the final branching pattern of secondary neurons is dependent upon the presence of appropriate neuronal targets. Taken together, our data provide new insights into the degree of neuronal plasticity during *Drosophila* brain development.

Introduction

The *Drosophila* brain develops from a stereotyped set of embryonically-born stem cells, called neuroblasts. Each neuroblast is defined by its expression of a unique combination of transcriptional regulators (Skeath and Thor, 2003; Urbach and Technau, 2003b). Neuroblasts divide asymmetrically, each mitotic division resulting in a self-renewing neuroblast and a "ganglion mother cell," which divides once more giving rise to two postmitotic neurons. In holometabolous insects, such as *Drosophila*, neuroblasts undergo two phases of proliferation. The first phase occurs during the embryonic period; the second one takes place in the larva. In the embryo, a neuroblast divides five to eight times, producing groups ("lineages") of 10–20 embryonic ("primary") neurons each (Larsen et al., 2009). Neurons belonging to the same lineage share a number of fundamental morphological characteristics: cell bodies remain clustered together in the outer layer (cortex) of the brain and their axons fasciculate into a common tract (primary axon tract; PAT). In cases where clones of differentiated primary neurons have been labeled it became apparent that neurons of one lineage also share one or a few specific brain compartments in which they form synaptic contacts. For example, four lineages (MB1–4) are restricted to the calyx and lobes of the mushroom body (Ito et al., 1997) and one lineage (BAmv3) forms the projection neurons of the larval antennal lobe (Das et al., 2013; Python and Stocker, 2002; Ramaekers et al., 2005).

At the end of embryogenesis, most neuroblasts enter a period of quiescence. Only five neuroblasts (MB1–4, BAlc/LNb) continuously divide between embryogenesis and early metamorphosis (Ito and Hotta, 1992; Ito et al., 1997; Stocker et al., 1997). All other neuroblasts exit the quiescent phase and re-enter the cell cycle between approximately 20 and 48 h after hatching (Ito and Hotta, 1992). During this secondary phase of proliferation, which lasts to the end of the larval stage, most neuroblasts generate an average of 150 postembryonic ("secondary") neurons (Bello et al., 2008). Similar to primary neurons, secondary neurons of a given lineage form coherent clusters of neuronal cell bodies and project axons which bundle together as the secondary axon tract (SAT). Secondary axon tracts form a stereotyped, conspicuous pattern that is visible from the larva through metamorphosis into the adult stage (Lovick et al., 2013; Wong et al., 2013). Differentiation of secondary

http://dx.doi.org/10.1016/j.ydbio.2015.03.005
0012-1606/

neurons (i.e. sprouting of branches and formation of synapses) occurs during metamorphosis, along with remodeling of primary neurons; both secondary neurons and remodeled primary neurons form the adult brain circuitry.

The mechanism triggering the larval ("secondary") phase of proliferation involves signals derived from the surface glia surrounding the neuroblasts (Ebens et al., 1993). The insulin pathway, which links larval growth in general to the nutritional state, plays an important role in secondary neuroblast proliferation as well (Chell and Brand, 2010). Many aspects of how secondary neuroblast proliferation is initiated remain unknown. In particular, it is not clear whether and how the identity of a neuroblast influences the time point at which it enters mitosis. The time period over which neuroblasts start to divide lasts for more than 24 h, though the order in which neuroblasts resume proliferation and produce their respective secondary lineages has not been documented. In other words, in any given larva, some neuroblasts enter mitosis considerably earlier than others. Given the high degree of stereotypy of neuroblasts in the embryo (Urbach and Technau, 2003a; Younossi-Hartenstein et al., 1996), and of lineages and their SATs in the late larva (Pereanu and Hartenstein, 2006), we assumed that the birth order of secondary lineages is also highly invariant: a neuroblast of a given identity will always re-enter mitosis at the same time point. To test this hypothesis we used the drug hydroxyurea (HU), a compound known to arrest actively dividing cells, to ablate proliferating neuroblasts and therefore secondary neurons (lineages) they give rise to (de Belle and Heisenberg, 1994; Prokop and Technau, 1994). If our assumption is correct, applying HU at a specific time point should always affect the same set of lineages. We systematically administered short HU pulses during and after the 20–48 h period when neuroblasts enter their larval phase of proliferation and analyzed the effect on the development of secondary lineages in the late larval and adult brain using global markers for SATs (anti-Neurotactin/BP106, anti-Neuroglian/BP104), as well as several lineage-specific Gal4 lines.

Our data demonstrate that the time points at which secondary neuroblasts start to divide are indeed fairly stereotyped, allowing us to reconstruct a "birth calendar" for all lineages. Knowing the birth date of a lineage is of importance for future experiments targeting that particular lineage for ablation or lineage-specific manipulation by mosaic analysis. Aside from establishing lineage birth dates, our results also provide new insights into the degree of plasticity in *Drosophila* brain development. Trajectories of secondary axon tracts appear to be established largely independently of each other. Similarly, the structure of primary neurons in the larval and adult brain is mostly unaffected by the loss of secondary lineages. In contrast to the apparent rigid nature in which axonal trajectories are established, the final patterning of terminal arbors by secondary lineages appears to depend upon the presence of corresponding neuronal targets (loss of target tissue leads to the absence of terminal arbors by surviving secondary lineages in that region).

Materials and methods

Genetics

Flies were grown at 25 1C using standard fly media unless otherwise noted. *per*-Gal4 (Kaneko and Hall, 2000), *en*-Gal4 (Tabata et al., 1995), *ple*-Gal4 (TH-Gal4; Friggi-Grelin et al., 2003; #8848, Bloomington *Drosophila* Stock Center, University of Indiana, IN, USA), GH146-Gal4 (a gift from R.F. Stocker, University of Fribourg, Switzerland; Stocker et al., 1997), UAS-mcd8::GFP (Lee et al., 1999; #5137, BDSC).

Immunohistochemistry

Samples were fixed in 4% formaldehyde or 4% methanol-free formaldehyde in phosphate buffer saline (PBS, Fisher-Scientific, pH¼7.4; Cat No. #BP399-4). Tissues were permeabilized in PBT (PBS with 0.1–0.3% Triton X-100, pH¼7.4) and immunohistochemistry was performed using standard procedures (Ashburner, 1989). The following antibodies were provided by the Developmental Studies Hybridoma Bank (Iowa City, IA): mouse anti-Bruchpilot (Brp, 1:20), mouse anti-Neurotactin (BP106, 1:10), rat anti-DN-Cadherin (DN-EX #8, 1:20), and mouse anti-Neuroglian (BP104, 1:30). Secondary antibodies, IgG_1 (Jackson ImmunoResearch; Molecular Probes) were used at the following dilutions: Cy5-conjugated anti-rat Ig (1:100), Cy3-conjugated anti-mouse Ig (1:200), Cy5-conjugated anti-mouse Ig (1:250), Alexa 546-conjugated anti-mouse (1:500), DynaLight 649-conjugated anti-rat (1:400), Alexa 568-conjugated anti-mouse (1:500).

Hydroxyurea (HU) ablation experiments

Hydroxyurea (HU, Sigma) acts as a DNA-synthesis inhibitor which blocks the normal function of nucleotide reductase (Timson, 1975) and is lethal to S-phase cells (Furst and Mahowald, 1985). HU has been used in *Drosophila* to ablate adult muscle precursors (Broadie and Bate, 1991) as well as central brain neuroblasts (de Belle and Heisenberg, 1994; Stocker et al., 1997). Procedure for preparation of HU was adapted from Broadie and Bate (1991). HU was administered to fly larvae through the diet. Briefly, HU was dissolved in distilled water at a concentration of 50 mg/ml. The dissolved HU was then added to partially cool melted fly media to achieve a final concentration of 5 mg/ml. After thorough mixing, the HU media was poured onto 60 •• 15 mm Petri dishes to cool. Food plates were made fresh (o1 day beforehand) for each experiment.

To ablate neuroblasts, staged larvae were allowed to grow on standard media at 25 1C in Petri dishes until time of ablation. Larvae were quickly transferred via blunted forceps to food plates containing 5 mg/ml of HU for 4 h. This is sufficient time for the HU to accumulate to doses high enough to kill actively dividing neuroblasts (Broadie and Bate, 1991; Truman and Bate, 1988; White and Kankel, 1978). After 4 h, larvae were transferred to Petri dishes containing standard media and grown until dissected as either wandering L3 or adults. Fly stocks and larvae for experiments were grown at 25 1C.

Confocal microscopy

Staged *Drosophila* larval and adult brains labeled with suitable markers were viewed as whole-mounts by confocal microscopy [LSM 700 Imager M2 using Zen 2009 (Carl Zeiss Inc.); lenses: 40 •• oil (numerical aperture 1.3)]. Complete series of optical sections were taken at 2-μm intervals. Captured images were processed by ImageJ or FIJI (National Institutes of Health, http://rsbweb.nih.gov/ij/ and http://fiji.sc/) and Adobe Photoshop.

Generation of three-dimensional models

Digitized images of confocal sections were imported into FIJI (Schindelin et al., 2012; http://fiji.sc/). Complete series of optical sections were taken at 2-mm intervals. Since sections were taken from focal planes of one and the same preparation, there was no need for alignment of different sections. Models were generated using the 3-dimensional viewer as part of the FIJI software package. Digitized images of confocal sections were imported using TrakEM2 plugin in FIJI software (Cardona et al., 2012). Surface renderings of larval brains stained with anti-Bruchpilot

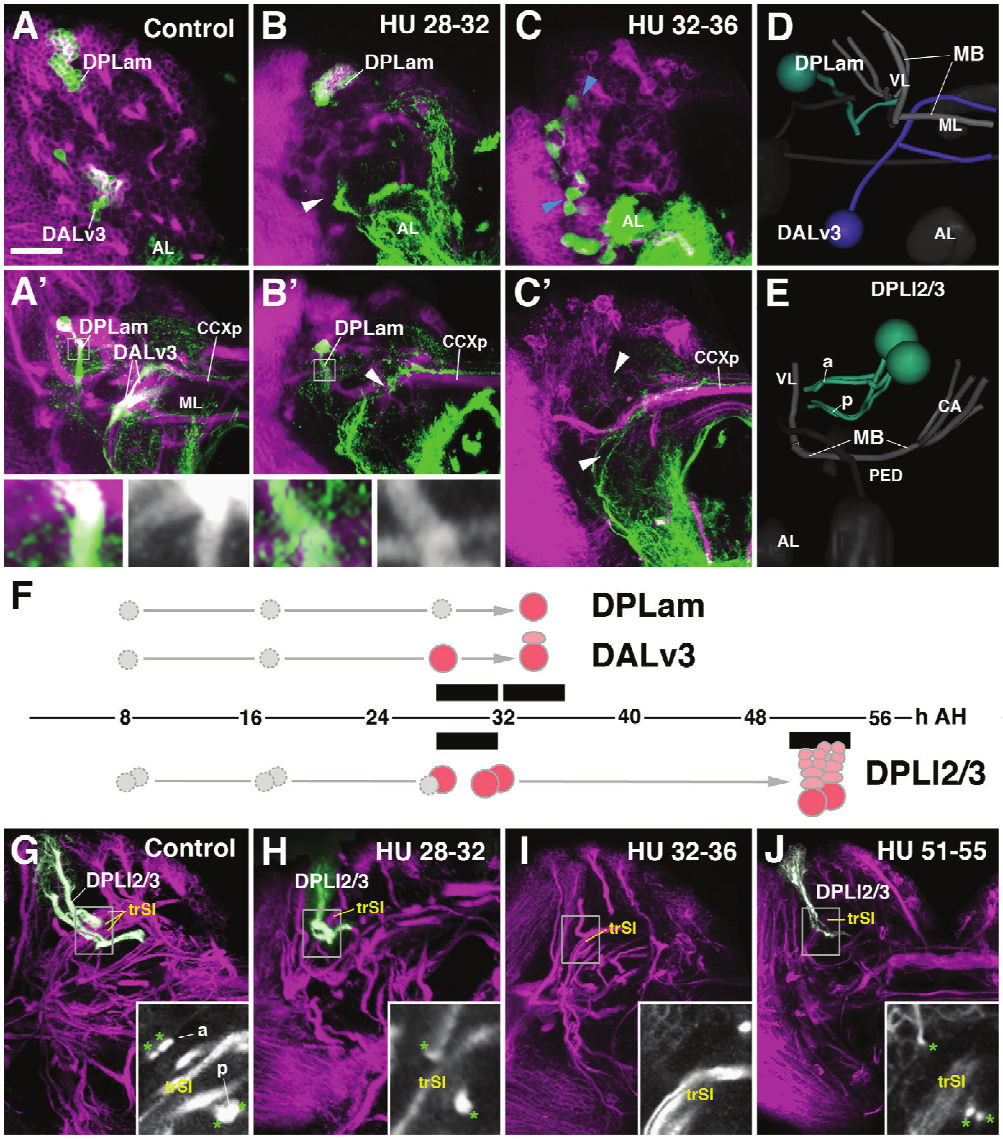

Fig. 1. Hydroxyurea (HU) ablates neural lineages in a time-dependent manner. Panels A–C^{I} and G–J show z-projections of confocal sections of late larval brain, labeled with anti-Neurotactin (BP106, magenta). In A–C^{I}, two lineages, DPLam and DALv3, are labeled by GFP driven by *engrailed*-Gal4 (green). Panels of the upper row (A–C) show a section of the anterior brain cortex; A^{I}–C^{I} depict a brain section at the level of the mushroom body medial lobe (ML) and the primordium of the central complex (CCXp). In G–J, the lineage pair DPLI2/3 is highlighted (green). 3D digital models in panels D and E illustrate location and tracts of lineages DPLam, DALv3, and DPLI2/3 within a single brain hemisphere (D: anterior view; E: lateral view). The mushroom body (MB) and antennal lobe (AL) are shown for reference. Panel F represents a time line (hours after hatching, AH) where intervals at which HU was administered are shown as black bars. Symbols flanking the time line above and below represent the onset of proliferation (red circles) of the neuroblasts forming lineages DPLam, DALv3, and DPLI2/3, deduced from HU effects shown in this figure. Thus, pulses of HU at 28–32 h AH (B, B^{I}) results in ablation of DALv3; note cluster of *en*-positive neurons present in brain cortex of control (A), absent in HU-treated animal (arrowhead in B). Likewise, the branched axon tract of DALv3 (A^{I}) is absent in HU-treated animal (arrowhead in B^{I}). By contrast, lineage DPLam is unaffected by HU administration between 28 and 32 h. Insets in A^{I} and B^{I} show the characteristic, vertically-oriented axon tract of DPLam in control (A^{I}) and experimental animal (B^{I}). Application of HU at 32–36 h ablates both DALv3 and DPLam secondary neurons (white arrowheads in C^{I}). Note that primary neurons of both lineages, which also express *en*-Gal4-driven GFP, are not affected by the HU pulse (blue arrowheads in C). DPLI2 and 3 form a pair of neighboring lineages in the dorso-lateral brain cortex (E, G). Each has two hemilineages, one (a) projects along the dorsal brain surface before entering the neuropil, the other (p) invades the neuropil after a short distance. Note presence of all four hemilineage tracts, marked by green asterisks, in inset of panel G. The intermediate transverse superior fascicle (trSI) is shown as reference. HU pulses from 28 to 32 h eliminated one of the DPLI lineages (note a single a and p hemilineage tract in inset of panel H). HU application from 32 to 36 generally ablated both DPLI lineages (inset of panel I). Later HU pulses (e.g., from 51 to 55 h, as shown in panel J) resulted in truncated lineages, since the neuroblasts were able to generate part of their progeny before being blocked by HU. For abbreviations of compartments and fascicles see Table 1. Scale bar: 25 mm.

were generated as volumes in the 3-dimensional viewer in FIJI. Cell body clusters were indicated on surface renderings using TrakEM2. Digital atlas models of cell body clusters and SATs were created by manually labeling each lineage and its approximate cell body cluster location in TrakEM2.

Results

HU pulses applied at a defined time interval ablate distinct secondary lineages without altering the projection of other lineages

Engrailed (*en*)-Gal4 is expressed, among others, in two brain lineages, DPLam and DALv3 (Kumar et al., 2009; Fig. 1A–D). HU application prior to 28 h after-hatching (AH) has no effect on either of these lineages. Pulses from 28 to 32 h AH ablated DALv3 in many specimens, leading to the absence of the cluster of cell bodies in the cortex and the secondary axon tract in the neuropil (arrowheads in Fig. 1B, B$^{\prime}$). The second *en*-Gal4-positive lineage, DPLam, is never affected by 28–32 h HU pulses; its cell body cluster is present at its normal location (Fig. 1B) and its secondary axon tract follows its normal trajectory (Fig. 1B$^{\prime}$, see inset). Both DALv3 and DPLam are consistently ablated when applying HU at 32–36 h AH (Fig. 1C, C$^{\prime}$, F). These results indicate that secondary lineages have fairly invariant birth dates, defined by the time at which the secondary neuroblast enters its larval phase of proliferation. The results further demonstrate that the ablation of subsets of lineages leaves the development of other lineages unaffected, making it possible to identify these lineages based on their location and axonal trajectory. Some lineages, like DALv3, seem to have a more sharply defined birth date, in that HU prior to a certain time point (e.g., 28 h AH) leaves the lineage intact in all cases, whereas it always ablates that lineage in the subsequent interval (e.g., 28–32 h AH). However, most lineages, like DPLam, show more variability, where HU at one interval ablates a lineage only in a certain fraction of cases; applying HU at the subsequent interval would enhance the fraction, or move it to 100% (see also below).

Whereas ablating a neuroblast at the time before it enters its first mitosis should result in the absence of the entire lineage, later HU pulses should give the neuroblast time to start proliferating and produce a certain number of neurons before arresting it, which would result in the formation of small ("truncated") lineages. This hypothesis could be confirmed for most lineages and is illustrated in Fig. 1F–J. DPLI2 and DPLI3 form a pair of secondary lineages whose tracts extend close to each other; they are easily recognized because of their bifurcated axon tracts which pass the trSI fascicle at its dorsal and ventral side, respectively (Cardona et al., 2010; Lovick et al., 2013; Fig. 1E and G). HU pulses from 36–40 h AH consistently ablated both of these lineages (not shown); pulses from 28–32 h or 32 - 36 h ablated one or both lineages (Fig. 1H and I), indicating there is a degree of variability to the time of birth of DPLI2/3 and other lineages (see also below). If HU pulses were applied after 50 h AH, truncated versions of DPLI2/ 3 and most other lineages can be observed at their normal position and with normal axon trajectory (Fig. 1J).

Larval HU pulses do not hinder the development of primary neurons or glial cells during the larval period

Primary neurons and glia are born and differentiate during the embryonic phase. In the late larva, primary neurons can be distinguished from secondary neurons by their large cell bodies located deep in the cortex and by the fact that they form branched neurites in the neuropil. The *en*-Gal4 driver is expressed in both primary and secondary components of DPLam and DALv3. HU pulses at 32–36 h AH ablated secondary neurons, but left primary neurons intact (Fig. 1C). To confirm that larval HU pulses do not prevent the proper projection of primary neurons we used the TH-Gal4 driver line which is expressed in a small number of dopaminergic (D) neurons belonging to seven primary lineages whose projections in the larval brain are known (Blanco et al., 2011; L.C. and V.H., unpublished observation). Supplementary Fig. S1 shows DA clusters DL1 (lineages CP2/3), DL2a (lineages BLVa1/2), and DM1b (lineage DPMl1) in the late larval brain of a control animal (Fig. S1A–C) and a HU treated animal (Fig. S1D–F). Location and number of DA neurons as well as their axonal projection and arborization occurs normally in the HU treated animal. Note, for example, profuse arborization of the DL1 cluster in the anterior compartments (SMP, IPa, LAL) surrounding the lobes of the mushroom body in the control and experiment (Fig. S1A and D). Note also the characteristic trajectory of DL1 axons which form part of the obP fascicle. In the control, these axons are sandwiched between the secondary tracts of CP2/3 and CP1/4 (Fig. S1B, inset); in the experiment (Fig. S1E, inset), the secondary CP2/3 tract is ablated (arrowhead), but primary DL1 axons appear at their normal position dorsal of CP1/4, whose secondary neurons are born after 32 h AH and are not affected by the 28–32 h HU pulse applied in this experiment.

Neurons of the larval brain are invested by several types of glial cells, including two types of neuropil glia: cortex glia and surface glia (for review, see Hartenstein, 2011). These cells are born as primary glia in the embryo. Additional, secondary glia are produced by a few select lineages, notably some of the dorsomedial type II lineages (Izergina et al., 2009; Viktorin et al., 2011; Omoto et al., 2015). However, these additional glial cells, recognizable by the specific marker Repo, do not begin to differentiate until late larval stages, thus primary glia are solely responsible for forming a stable scaffold around neurons and proliferating neuroblasts. Similar to primary neurons, these primary glia were not affected by the early larval pulses of HU (data not shown), suggesting that the time-dependent ablation of lineages described in this work is most likely due to a direct effect of HU on neuroblasts as they re-enter mitosis.

Calendar of birth dates of secondary lineages

Following treatments with HU at defined intervals, brains dissected at the late larval stage and labeled with anti-Neurotactin (BP106) to visualize secondary axon tracts were assayed for the presence or absence of specific lineages. Given their characteristic shape and position (see Fig.1G–J), tracts remaining in HU treated animals could be assigned to specific lineages in most cases (Figs.2, 3). Taking the earliest time interval at which application of HU ablates a lineage as a rough birth date of that lineage we established a temporal chart of birth dates for all secondary lineages (Fig.4A). As explained above, most lineages show a certain degree of variability. The variability could in part be artifactual, reflecting merely that the level of HU (which depends on the feeding of the larva) reached a critical threshold somewhat later in one case versus another. This idea is supported by the observation that by slightly shifting the interval of HU application (e.g., 33–37 h AH vs. 32–36 h AH) one obtained, for selected lineages, different ratios of ablated vs. non-ablated. For example, BAla3, not affected by application at 32–36 h, was affected in about half of the cases at 33–37 h; likewise, DALcm1/2 and DPLI2/3, ablated in a fraction of cases with HU pulses between 32–36 h, were always gone with 33–37 h pulses (data not shown).

With the exception of the four MB lineages and the BAlc/IAL lineage (which reportedly never cease their proliferative activity; Ito and Hotta, 1992), all lineages have a birth date between 20 and 40 h AH. Lineages born early or late during this interval are

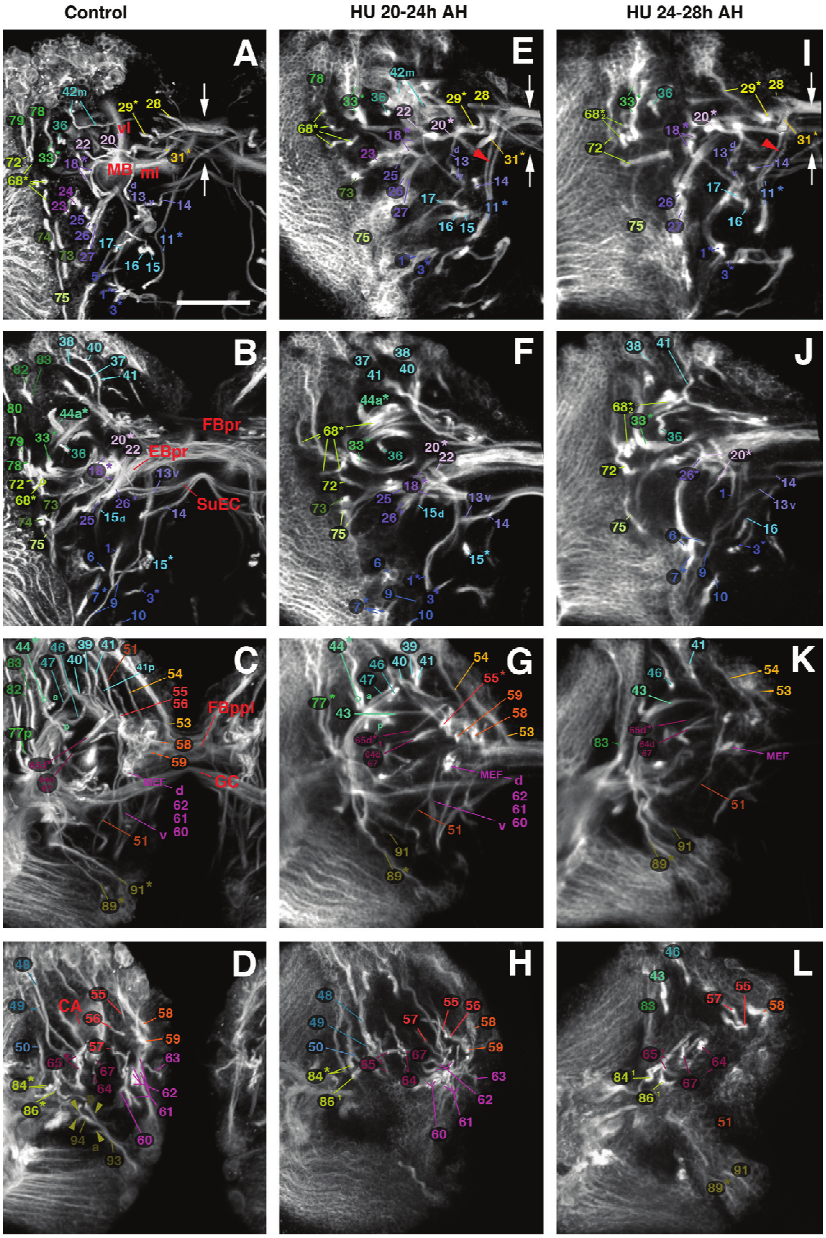

Fig. 2. Ablation of secondary lineages by timed 4 h pulses of hydroxyurea (HU). All panels of this and the following figure, Fig. 3, show z-projections of contiguous confocal sections of a late third instar larval left brain hemisphere labeled with BP106, representing brain slices of 15–20 μm thickness. Panels of both Figs. 2 and 3 are arranged in four rows and three columns. Pairs of vertical arrows indicate the midline. Z-projections of the first row (A, E, and I) correspond to an anterior level (mushroom body lobes; MB). Panels of the second row (B, F, and J) represent a "subanterior" level (FBpr primordium of fan-shaped body; EBpr primordium of ellipsoid body). The third row (C, G, and K) corresponds to the level of the great commissure (GC) and dorsal commissural tracts forming the posterior plexus of the fan-shaped body (FBppl). The fourth row (D, H, and L) represents a posterior level (CA calyx of mushroom body). All panels of one column show brain of larva subjected to a specific HU regimen (Fig. 2A–D:control; Fig. 2E–H: HU pulse at 20–24 h after hatching (AH); Fig. 2I–L: HU pulse at 24–28 h AH; Fig. 3A–D: HU at 28–32 h AH; Fig. 3E–H: HU at 32–36 h AH; Fig. 3I–L: HU at 55–60 h AH). Secondary axon tracts (SATs) of individual lineages are annotated with a unique numerical identifier (for tabulated listing of lineages see Fig.4A). Numbers followed by an asterisk indicate tracts formed by more than one SAT (typically two SATs), which cannot be followed separately. For example, "20*" stands for "20 and 21." Lower case letters "d" and "v" indicate dorsal or ventral hemi-/sublineage tracts formed by the CP lineages and CM lineages. Subscripted "1" or "2" indicate cases where the SAT of a closely spaced lineage pair or group of lineages is still identifiable in experimental animals, but is reduced in size. Compare, for example the SAT pair formed by BAmas1/2 ("11*" in Fig. 2A, E, I; point where the two tracts split is indicated by red arrowhead in E and I) with the thin tract ("11_1"; lack of split indicated by green arrowhead) resulting from HU pulse at 28–32 h AH (Fig. 3A). For abbreviations of compartments and fascicles see Table 1. Scale bar: 50 μm. Other abbreviations: BLx BL lineage group.

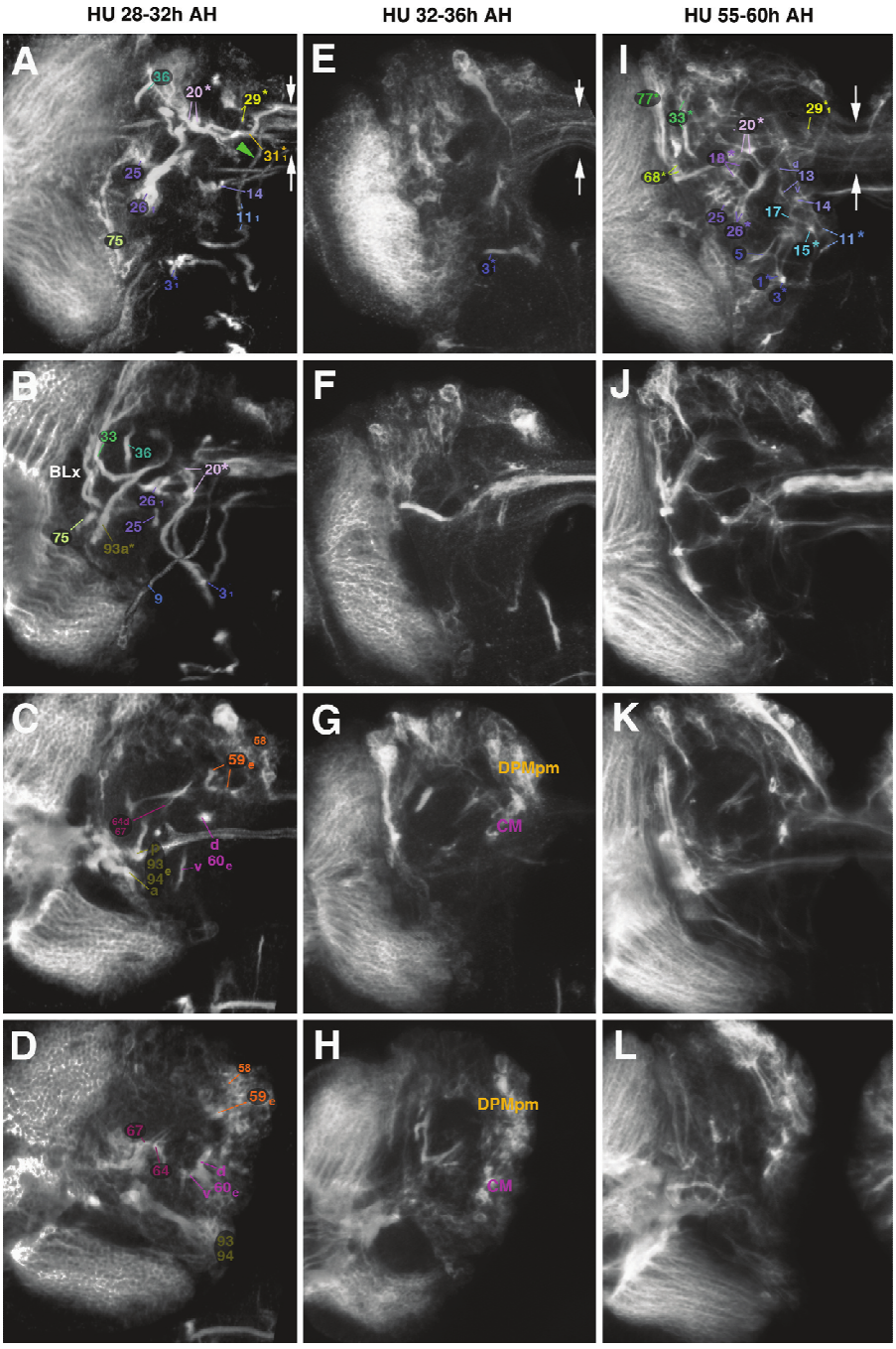

Fig. 3. Ablation of secondary lineages by timed 4 h pulses of hydroxyurea (HU) (continued). For explanation of panels, see legend to Fig. 2.

generally intermingled and show no clear topological pattern (Fig. 4B). Possible exceptions are lineages located dorso-medially in the anterior brain, including the five DAM lineages (DAMd1–3, 28–30; DAMv1–2, 31–32) and the medial DAL lineages (DALcm1–2, 20–21; DALd, 22), which are among the latest born lineages (32–36 h AH; Fig.3E, Fig.4B), and the postero-medially located Type II lineages

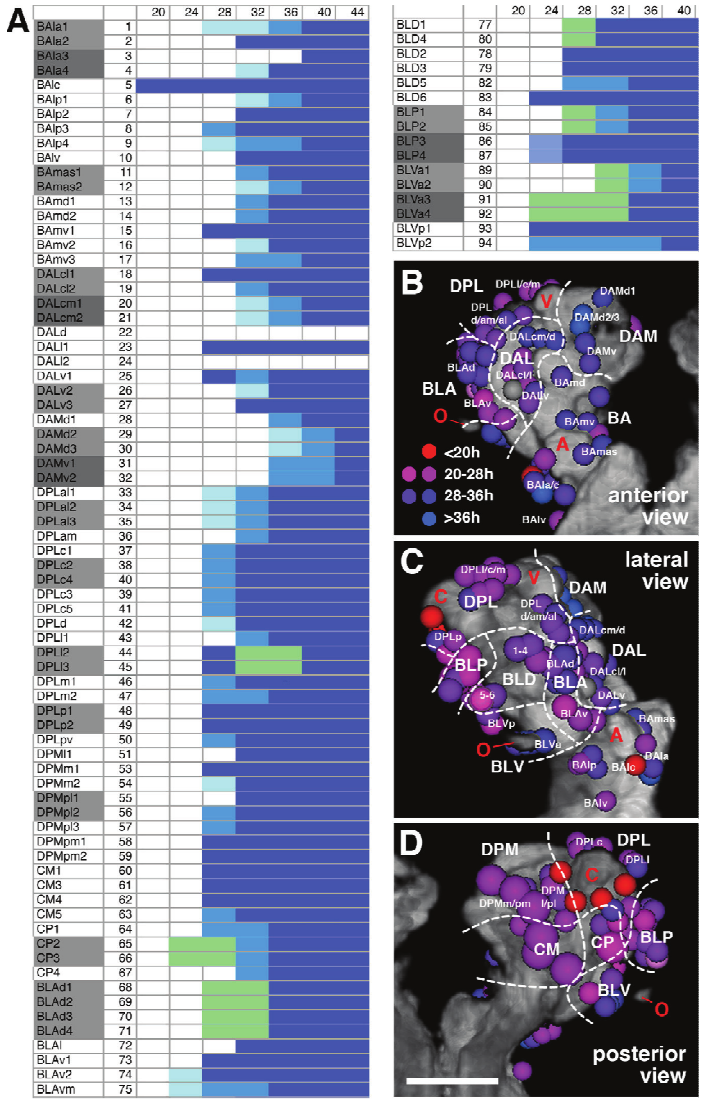

Fig. 4. (A) Secondary lineage birth dates. All lineages are listed at the left; for lineage abbreviations in this panel and in panels (B–D), see Table 1, and Lovick et al. (2013). The horizontal axis represents the time axis, subdivided into 4 h intervals. Numbers at the top indicate hours after hatching. Onset of blue shading indicates time interval at which the corresponding secondary lineage is ablated by HU pulse (dark blue¼ablation in ~90% of cases; medium blue¼ablation in 50–90%; light blue¼ablation in 10–50%). Gray shading in left column points out lineage pairs with highly similar or identical axonal trajectory in larval brain. Green shading is applied in cases where one member of a lineage pair was consistently ablated in a high fraction of cases, whereas the other member was spared. For example, during a 20–24 or 24–28 h interval, one lineage of the CP2/CP3 pair is ablated; due to the identical axonal trajectory of CP2 and CP3, it is not possible to determine which of the two was affected. (B–D): Correlation of birth date and location of a lineage. Digital three-dimensional models of larval brain hemispheres, showing position of neuropil entrypoints of lineages (colored spheres) in relationship to neuropil topography (gray). The neuropil surface model was generated by volume-rendering of a series of confocal sections of a brain hemisphere labeled with the synaptic marker nc82 (Brp; see Lovick et al., 2013). Four prominent elements of the neuropil surface are indicated in red lettering (A: antennal lobe; C: calyx; V: tip of vertical lobe; O: optic lobe). The three panels represent different view points (B: anterior; C: lateral; D: posterior). White hatched lines demarcate territories occupied by the different lineage groups that are annotated in white lettering (e.g. BA, BLA). Coloring of a lineage indicates its birth date based on time point when it was ablated by a 4 h HU pulse. Color key (see panel B): red¼birth date before 20 h; magenta¼birth date 20–28 h; violet¼birth date 28–36 h; blue¼birth date 36–44 h. Scale bar: 50 mm.

(DPMm1, 53; DPMpm1–2, 58–59; CM1–4, 60–62), which form a coherent group born relatively early (24–28 h AH; Table 1; Fig.2L, Fig.4B). The very first born lineages (birth date 20–24 h AH) are clustered laterally around the optic lobe and comprise one or two representatives each of the four BL groups (BLA: BLAv2–vm, 74–75; BLD: BLD6, 83; BLP: BLP3–4, 86–87; BLV: BLVa3–4, p1–2, 91–94; Fig.2F–H, Fig.4B). Also one lineage of the CP2/3 pair is consistently affected with HU pulses as early as 20–24 h AH [compare thick tract "65d^{D}", formed by the two lineages CP2/3, in control (Fig. 2C) with thin corresponding tract, "65$_{1}^{n}$" in Fig. 2G]. Aside from CP2/3, several other lineages form pairs or small groups, whereby the cell body clusters are neighbors in the brain cortex and the axon tracts extend

Table 1
List of abbreviations of neuropil fascicles and larval neuropil compartments (left) and adult neuropil compartments (center, right).

Fascicles	Abbr.	Compartments (adult)	Abbr.	Compartments (adult) cont'd	Abbr.
Commissure of the lateral accessory lobe	LALC	Antennal lobe	AL	Posteriorlateral protocerebrum	PLP
Dorsolateral root of the fan-shaped body	dlrFB	Antenno-mechanosensory	AMMC	Anterior periesophageal neuropil	PENPa
Dorsomedial root of the fan-shaped body	dmrFB	and motor center		Protocerebral bridge	PB
Great commissure	GC	Anterior optic tubercle	AOTU	Subesophageal ganglion	SEG
Intermediate superior transverse fascicle	trSI	Bulb	BU	Superior intermediate	SIP
Longitudinal superior medial fascicle	loSM	Ellipsoid body	EB	protocerebrum	
Anterior loSM	loSMa	Fan-shaped body	FB	Superior lateral protocerebrum	SLP
Posterior loSM	loSMp	Inferior protocerebrum	IP	Anterior SLP	SLPa
Medial antennal lobe tract	mALT	Anterior IP	IPa	Posterior SLP	SLPp
Medial equatorial fascicle	MEF	Lateral IP	IPl	Superior medial protocerebrum	SMP
Oblique posterior fascicle	obP	Medial IP	IPm	Inferior ventrolateral cerebrum	VLCi
Posterior lateral fascicle	PLF	Posterior IP	IPp	Ventrolateral protocerebrum	VLP
Subellipsoid body commissure	SuEC	Lateral accessory lobe	LAL	Anterior VLP	VLPa
		Lateral horn	LH	Posterior VLP	VLPp
Compartments (larval)	Abbr.	Mushroom body	MB	Ventromedial cerebrum	VMC
Central complex primordium	CCXp	Calyx	CA	Anterior VMC	VMCa
Ellipsoid body primordium	EBpr	Medial lobe	ML	Infracommissural VMC	VMCi
Fan-shaped body primordium	FBpr	Pedunculus	PED	Postcommissural VMC	VMCpo
		Spur	SPU	Precommissural VMC	VMCpr
		Vertical lobe	VL	Supracommissural VMC	VMCs
		Noduli	NO		

very close to each other, or even merge, so that they cannot be distinguished in the neuropil of the larval brain. These paired/clustered lineages include BAla1/2, BAla3/4, BAlp2/3, BAmas1/2, BAmv1/2, DALcl1/2, DALcm1/2, DALv2/3, DAMd2/3, DAMv1/2, DPLal1-3, DPLc2/4, DPLl2/3, DPLp1/2, DPMpl1/2, CP2/3, BLAd1–4, BLP1/2, BLP3/4, BLVa1/2, and BLVa3/4. It is noteworthy that, almost without exception, individual members of these pairs/clusters have different birth dates. For example, following HU treatment from 20–24 h AH, one out of the two CP2/3 lineages or BLP3/4 lineages was ablated (Fig.4A). HU pulses at 24–28 h AH consistently ablated two out of the four BLAd1-4 lineages (68–71; Fig.2I, Fig.4A). Pulses from 28–32 h ablated one lineage of the BAmas1/2 and BAla3/4 pair, and two of the DPLal1-3 triplet (11–12, 3–4, and 33–35, respectively; Fig.3A–B, Fig.4 A).

Differences in the birth dates of secondary lineages also do not seem to reflect gross differences in projection pattern. According to the recent mapping of the projection of secondary lineages in the adult brain (Ito et al., 2013; Wong et al., 2013; Yu et al., 2013) one can clearly recognize lineages with local projections (one or two neighboring compartments) from other lineages with far flung projections (e.g., the antennal lobe lineages connecting the ventral deuterocerebrum with the dorsal protocerebrum or the lineages with long commissural axons connecting the ventrolateral protocerebrum of both hemispheres). Members of both classes, small local and large projection, are found among the early-born or the late-born lineages. For example, the DAMd2/3 pair which forms widespread connections between the superior medial protocerebrum and the posterior ventromedial cerebrum is born around the same time as the DAMv1/2 pair which develops only local projections in the superior medial protocerebrum (Wong et al., 2013). Born during the earliest interval (20–24 h AH), the CP2/3 pair forms large projections between posterior dorso-lateral compartments (lateral horn, superior lateral protocerebrum) and anterior-medial compartments (mushroom body lobes, fan-shaped body; Wong et al., 2013). The BLP3/4 pair, born as early as CP2/3, has restricted arborizations in the lateral horn.

Ablation of secondary lineages causes strong effects on adult neuropil organization

Given the size of primary vs. secondary lineages (Bello et al., 2008; Larsen et al., 2009), the secondary neurons account for 80–90% of the neurons of the adult central brain. Hence it stands to reason that the volume of the neuropil compartments, formed by neuronal arborizations and synapses, also depends largely on the secondary neurons, and would be decreased if secondary neurons were absent. The analysis of adult brains of animals treated with HU during the larval stage confirms this notion: the loss of neuropil volume is correlated with the time of HU application, and time points between 32–36 h and 36–40 h AH, causing the virtual absence of secondary lineages in the larva (see above), lead to the strongest effects in the adult brain (Fig. 5). Despite this, many animals underwent metamorphosis and were able to eclose (approximately 86% 32–36 h and 30% 36–40 h HU treated animals were sub-viable and were dissected out of the pupal case (data not shown)). Eclosing adults were essentially immobile, exhibiting little or no spontaneous movement or reflex action (J.L., unpublished observation).

Compartments affected most strongly following neuroblast ablation are those known to be formed mostly of secondary neurons (e.g. the mushroom body, whose α/β and α'/β' neurons are all born post-embryonically) and compartments that are newly formed during metamorphosis and therefore are likely comprised preferentially of secondary neurons, including the central complex (ellipsoid body/EB, fan-shaped body/FB, noduli; arrowhead in Fig. 5D and J) and anterior optic tubercle (AOTU; arrowhead in Fig.5B and N). Aside from the AOTU, other compartments closely associated with the input from the optic lobe, whose neurons differentiate during metamorphosis, are also strongly affected by larval HU treatment; these compartments include the ventrolateral protocerebrum (VLPa, VLPp; Fig.5 D, F, and N) and the lateral horn (LH; Fig.5 H). Least affected are compartments whose volume normally does not increase significantly during metamorphosis, including the inferior protocerebrum (IPa, IPl, IPm, IPp; Fig.5 B, F, H, and N) and ventromedial cerebrum (VMCpo, VMCpr; Fig.5 F and H; Pereanu et al., 2010).

HU-induced defects of the central complex, illustrated in more detail in Fig.6, are most severe. The central complex, and particularly the ellipsoid body, is formed by a small number of lineages. DALv2 includes large field (ring) neurons of the ellipsoid body (EB) and the dorsal Type II lineages DPm1/DM1, DPMpm1/DM2, DPMpm2/DM3, and CM4/DM4 form the small field (columnar) neurons connecting the EB with the fan-shaped body (FB) and protocerebral bridge (Wong et al., 2013; Yang et al., 2013). The ablation of DALv2, labeled by *per*-Gal4 (Fig.6A, arrowhead in D, G, arrowhead in H), is always associated with the elimination of

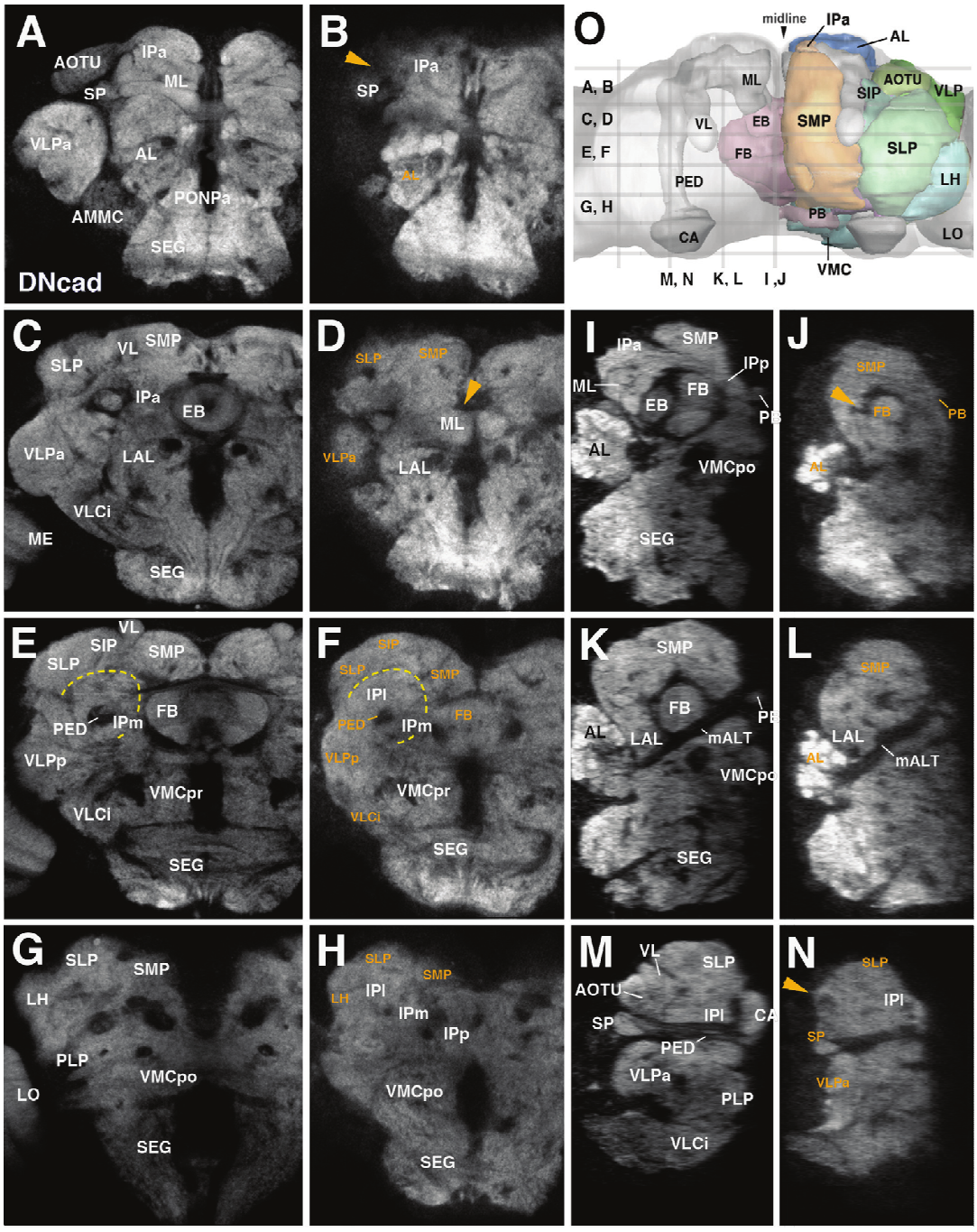

Fig. 5. Effects of HU-mediated ablation of secondary lineages on adult brain neuropils. Z–projections of frontal (A–H) and sagittal (I–N) confocal sections of brains of control (left column: A, C, E, G; third column: I, K, M) and HU treated animals (second column: B, D, F, H; right column: J, L, N). HU was applied during 32–36 h interval after hatching. Brain neuropil is labeled with anti-DNcad. Compartments are annotated in white lettering; orange lettering highlights compartments most strongly affected by HU treatment. Level of sections are indicated in panel O, which shows central brain neuropil in a dorsal view. Compartments of mushroom body and central complex are outlined and annotated for left hemisphere; right hemisphere shows outlines and names of other compartments that are visible in dorsal view. Orange arrowheads throughout the figure point at locations where compartments were completely ablated by HU pulse (AOTU in panels B and N, EB in panels D and J). Dashed yellow line in panels E and F outlines the inferior protcerebrum (IP), a region largely unaffected by HU treatment. For abbreviations of compartments and fascicles see Table 1. Scale bar: 50 μm. Other abbreviations: LO lobula of the optic lobe.

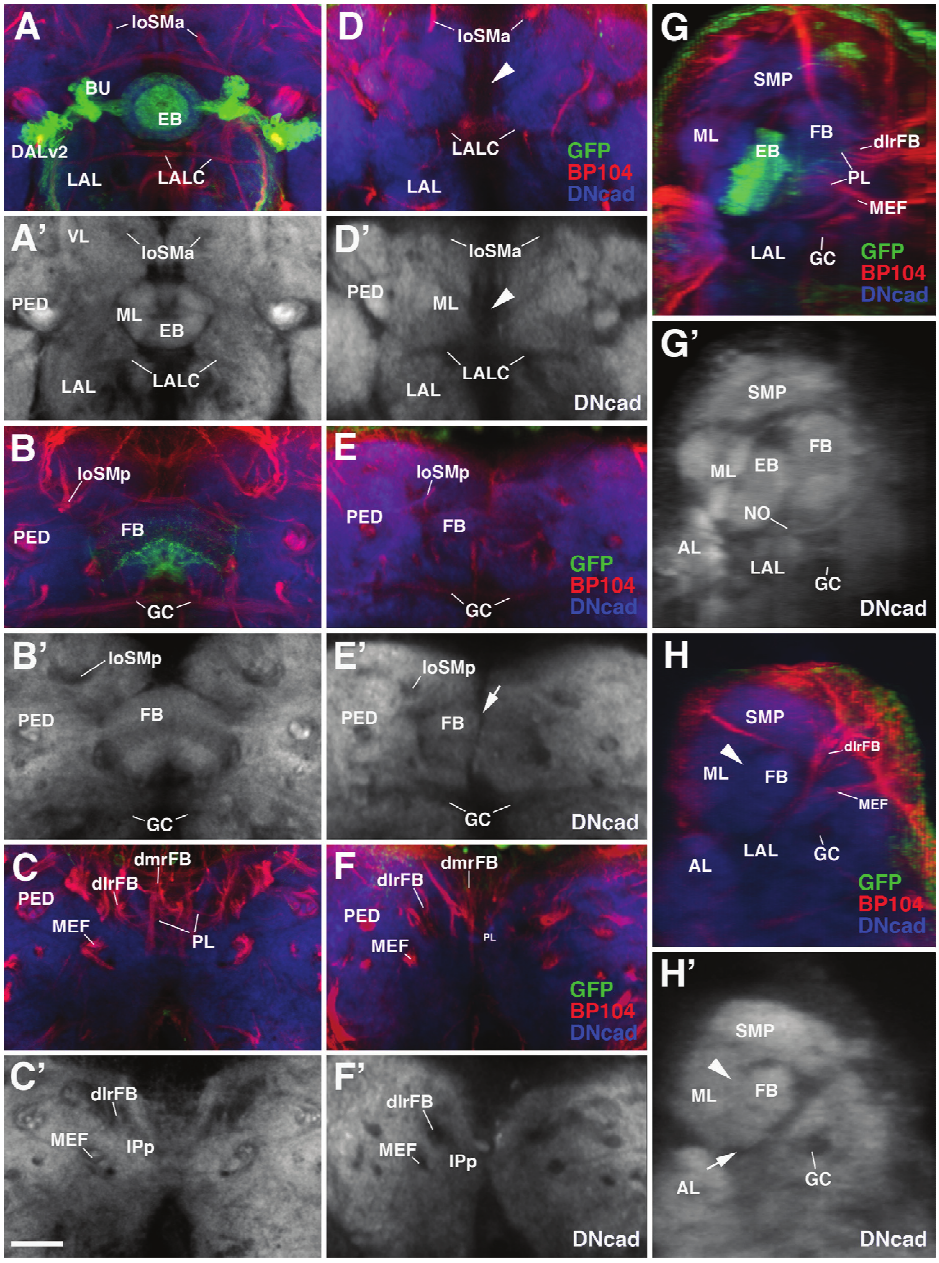

Fig. 6. Defects of the central complex following HU-mediated ablation of secondary lineages. Z-projections of frontal (A–F^{I}) and sagittal (G–H^{I}) confocal sections of brains of control (left column: A–C^{I}; right column: G, G^{I}) and HU-treated animals (middle column: D–F^{I}; right column: H, H^{I}). Rows represent corresponding planes of sections along the antero-posterior axis or medio-lateral axis (A/A^{I}, D/D^{I}: ellipsoid body; B/B^{I}, E/E^{I}: fan-shaped body; C/C^{I}, F/F^{I}: posterior roots of the central complex; G/G^{I}, H/H^{I}: 5 mm lateral of midline). HU was applied during 28–32 h interval after hatching. Axon fascicles formed by secondary axon tracts are globally labeled by anti-Neuroglian (BP104; red in A–H). Brain neuropil is labeled with anti-DNcad (blue in A-H; white in A^{I}–H^{I}). The DALv2 lineage, forming wide field (R-) neurons of the ellipsoid body and fan-shaped body is labeled by GFP driven by *per*-Gal4 (green in A, B, C, D, E, F, G, H). Ablation of secondary lineages, including DALv2, by the HU pulse leads to complete elimination of the ellipsoid body (EB in A/A^{I}, G/G^{I}; arrowhead in D/D^{I}, H/H^{I}). The fan-shaped body and the posterior roots of the central complex (FB in B/B^{I}, E/E^{I}, G/G^{I}, H/H^{I}; dlrFB and dmrFB in C/C^{I}, F/F^{I}, G, H) are strongly reduced. Note vertical cleft in midline of reduced fan-shaped body in experimental animals (arrow in E^{I}). For abbreviations of compartments and fascicles see Table 1. Scale bar: 25 mm. Other abbreviations: PL plexus of the fan-shaped body.

the EB as defined by synaptic markers such as DNcad or Nc82 (Fig.6A$^{\prime}$, arrowhead in D$^{\prime}$, G$^{\prime}$, arrowhead in H$^{\prime}$). The same holds true for the noduli, formed by the columnar neurons of the dorsal Type II lineages, which are not detectable in adult brains where these lineages were ablated (not shown). By contrast, a strongly reduced FB is always present in HU treated animals (Fig.6E, E$^{\prime}$, H, and H$^{\prime}$). Interestingly, the FB in experimental animals is commonly split in the midline (arrowhead in Fig.6E$^{\prime}$). This might be due to the fact that (among all of the Type II lineages) the crossed axons of DPMm1/DM1 and DPMpm1/DM2, both of which innervate the contralateral half of the FB, are missing; as a result, the cohesion between the left and right half of the FB could be compromised.

Effects of the ablation of secondary lineages on neuronal branching morphogenesis

HU pulses between 24 and 32 h AH frequently result in brain asymmetries, ablating a given lineage on one side, but not the other. This effect can be explained in light of the more or less pronounced variability in the birth dates of lineages: whereas the neuroblast of a lineage might start to divide at 24 h in the left hemisphere, its counterpart in the opposite hemisphere might be delayed by a few hours. An example is shown in Fig.7A–C, where DALv2 is ablated on the left, but not the right. This unilateral ablation resulted in a rudimentary, misshapen "hemi-ellipsoid body" which is closely attached to the ventral surface of the (rudimentary) right fan-shaped body (Fig.7B and B$^{\prime}$). Furthermore, in this and the three other cases of unilateral DALv2 ablation we were able to observe, the terminal arborizations of the non-ablated DALv2 showed a pattern that significantly deviated from the normal pattern. Thus, terminal fibers formed regularly spaced aggregates, separated by signal-free gaps, as opposed to a normal ellipsoid body (created by the overlap of neuronal arborizations of neurons on both sides) where the DALv2 terminal arbors fill a smooth and continuous, ring-shaped volume (Fig.7C). We conclude that interactions between DALv2 axons and their contralateral counterparts determine the pattern and spacing of terminal branches of this lineage.

A significant branching defect of one secondary lineage in reaction to the lack of another lineage could also be observed for the antennal projection lineages BAmv3/adNB and BAlc/INB, both of which are labeled by GH146-Gal4 (Das et al., 2013; Lai et al., 2008; Stocker et al., 1997). BAmv3 and BAlc project along the mALT towards the calyx (CA) and lateral horn (LH; Fig.7D–F). As the mALT passes along the anterior surface of the calyx, BAlc/BAmv3 axons send short branches into the calyx (Fig.7F). Early HU treatment ablates the secondary MB lineages, resulting in the strong reduction or absence of the CA (Fig.7I and I$^{\prime}$). In these animals, no side branches emerge from the BAlc/BAmv3 axons (Fig. 7I), indicating that signals specific to the CA are required to induce branching off the main BAlc/BAmv3 axons.

To test the effect of widespread ablation of secondary lineages on the differentiation of primary neurons we analyzed the structure of the TH-Gal4-positive neurons in adult brains of animals treated with HU between 32 and 36 h AH. Previous studies had shown that primary neurons prune back their neurite tree at the onset of metamorphosis (Blanco et al., 2011; Consoulas et al., 2000; Marin et al., 2005; Roy et al., 2007; Weeks, 1999). Subsequently, a new neurite tree is reassembled that often resembles the primary tree, but also can show new, adult-specific features. As shown in Fig.8 and Supplementary Fig.S2, TH-Gal4-positive neurons of HU treated animals appear in their normal pattern (compare Fig.S2F–J with Fig.S2A–E) and exhibit a densely branched neurite tree, as shown in Fig.S2F$^{\prime}$/G$^{\prime}$ for the superior medial protocerebrum (SMP), the (rudimentary) medial lobe (ML), and the anterior inferior protocerebrum (IPa) surrounding the medial lobe. Terminal arborizations of the PPM3 neurons, which predominantly innervate the central complex, are present, but are abnormally shaped. For example, terminal branches of PPM3 neurons innervating the ellipsoid body (EB) follow the circular shape of this compartment (Fig.8A and A$^{\prime}$; L.C. and V.H., unpublished observation). In the absence of the secondary DALv2 lineage that scaffolds the EB, PPM3 axons follow the trajectory towards the position where the EB would normally appear (Fig.8B$^{\prime}$). However, terminal branches sprouting from these axons are arranged along a horizontal line, rather than a circle (arrows in Fig.8B$^{\prime}$).

Discussion

Hydroxyurea-mediated ablation of neural lineages

In this study we used hydroxyurea (HU) to ablate secondary neural lineages, following the previously published regimen of HU application that was established to kill mushroom body neuroblasts (de Belle and Heisenberg, 1994; Prokop and Technau, 1994). HU blocks DNA synthesis by inhibiting ribonucleotide reductase and causes cell death in S-phase. Since HU does not affect gene transcription or protein synthesis and therefore specifically targets dividing cells, it is used as an anti-neoplastic drug in a number of different cancers. As a means to block cell division and/or ablate specific lineages, HU has been applied in several previous studies in both vertebrates (e.g., *Xenopus*: Harris and Hartenstein, 1991) and invertebrates (e.g., Becker et al., 1998; Broadie and Bate, 1991; Malun, 1998; Pfister et al., 2007). In *Drosophila*, a short pulse of HU given right after hatching ablates the four mushroom body lineages (as well as one other lineage of antennal lobe projection neurons (BAlc/INB)), which allows for the study of different aspects of mushroom body function in *Drosophila* larvae and adults (Sweeney et al., 2012). The reason why HU specifically targets neuroblast lineages, rather than all dividing cell populations in the larva, lies in the peculiar, stem cell-like mode of neuroblast mitosis (generation of neuronal progeny through a series of asymmetric divisions). On the other hand, adult progenitors in other tissues, such as the imaginal discs, the intestine, or the musculature, divide symmetrically and asynchronously or parasynchronously. During any given 4 h time interval, some of these progenitors are in the S-phase of mitosis (and thereby sensitive to HU), but most will not be, and will continue to proliferate. Since adult progenitors show a great deal of regulative capacity (e.g. the imaginal leg disc: Kiehle and Schubiger, 1985; imaginal wing disc: Milán et al., 1997; Neufeld et al., 1998; Wartlick et al., 2011), organ size will be affected little or not at all following a HU pulse. By contrast, a neural lineage results from a single, asymmetrically dividing neuroblast, and will be missing in its entirety once the neuroblast is ablated.

Applying BrdU, Ito and Hotta (1992) had documented the time course of appearance of dividing neuroblasts. Their data showed a roughly linear increase in the number of BrdU positive clusters at the brain surface from 20 to 50 h AH, a finding that is matched by our data presented in this study. Since all neuroblasts re-enter mitosis within a relatively short time period of about 20 h it is not possible to delete individual lineages, using 4 h pulses. Based on our data (Fig. 4), a HU pulse administered from 20–24 h AH resulted in the ablation of an average of six lineages (in addition to the MB lineages and BAlc). A pulse from 24–28 h added another 33 lineages to that number, indicating that most secondary lineages are born during this time window. An average of 22 lineages appear in the 28–32 h interval, 19 in the 32–36 h interval, and only 2 after 36 h (Fig.4). For one lineage, DALl2, we could not

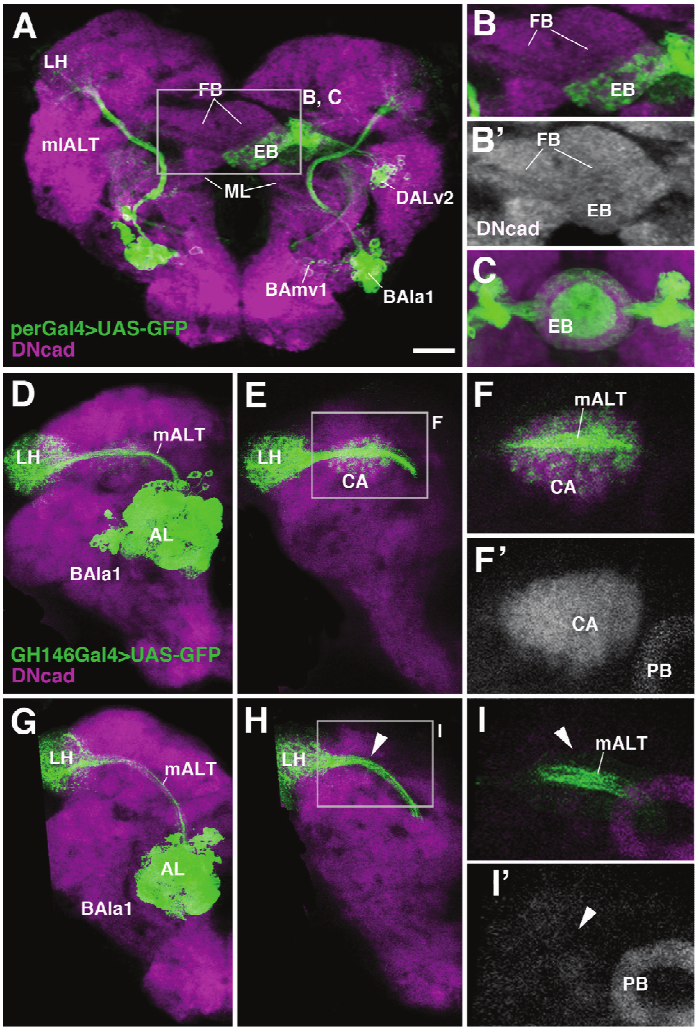

Fig. 7. HU-mediated ablation of secondary lineages reveals neuronal interactions. (A, B, B^{l}): Unilateral ablation of the DALv2 lineage, labeled by *per*-Gal4 (green), in left brain hemisphere. All panels show z-projections of frontal confocal sections at level of central complex (EB ellipsoid body; FB fan-shaped body). Neuropil is labeled by anti-DNcad (magenta or white) Note asymmetric axonal arborization of remaining right hemispheric DALv2 (EB in A, B/B^{l}), and coarse-grained texture of terminal fibers (B) compared to control (C). (D–I) Terminal arborization of ventral antennal lobe projection neurons of lineage BAla1 (labeled by GH146-Gal4) in the mushroom body calyx (CA) and lateral horn (LH) of control animal (D–F^{l}) and HU-treated animal (G–I^{l}; pulse between 0 and 4 h after hatching). (D) and (G) show z-projections of confocal sections including both anterior levels (AL antennal lobe), which contain BAla1 cell bodies and dendrites, and posterior levels (LH lateral horn; CA calyx) where BAla1 axons terminate. (E–F^{l}) and (H–I^{l}) focus on the posterior level for better resolution. Note dense, evenly-spaced terminal arbors of BAla1 in both lateral horn and calyx of control (E–F^{l}). In HU-treated animal (G–I^{l}), the calyx is ablated (arrowhead in I^{l}), and terminal branches of BAla1 towards this structure are absent (arrowheads in H, I). By contrast, the projection to the lateral horn (LH) is undisturbed (H). For abbreviations of compartments and fascicles see Table 1. Scale bar: 25 mm.

establish a birth date. DALl2 has a short tract that only touches the surface of the VLP compartment before terminating, therefore not providing a distinctive enough pattern that would allow us to determine whether this lineage is present in an experimental brain where many surrounding tracts are missing.

As expected from earlier works on the four MB lineages and BAlc/INB, secondary lineages in general have a fairly invariant birth date. For example, among the lineages ablated by the 20–24 h HU pulse are always BLD6, BLVp1, one of the CP2/3 pair, and one of the BLP3/4 pair. Lineages affected last (36–40 h) include the DAMd2/3 and the DAMv1/2 pairs. The birth dates established by the HU application, for these and all other secondary lineages, correlate well with the labeling of developing lineages using *insc*-Gal4 (Lovick et al., 2015b). The HU data further suggest that the time of birth is fixed more precisely for some lineages than for others. Thus, lineages such as BAmv1 or DALcl1 were never affected with 20–24 h (or earlier) HU pulses, and were always absent following 24–28 h (or later) pulses (Fig.4), suggesting that the birth date of these lineages invariably falls into the 24–28 h interval. In contrast, most lineages were affected with increasing severity over a longer period. For example, lineages DPLal1/2 were infrequently ablated with 24–28 h HU pulses; they were absent

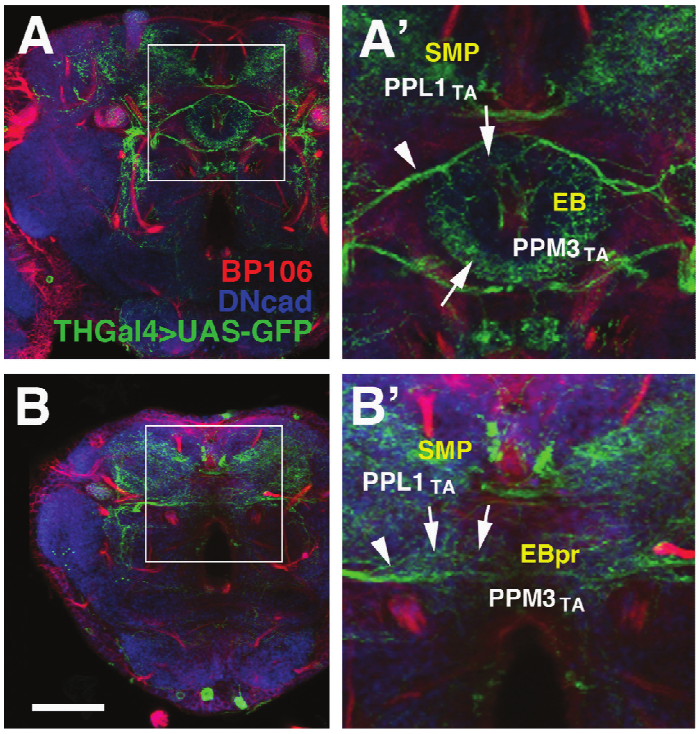

Fig. 8. HU-mediated ablation of secondary lineages does not affect the adult differentiation of dopaminergic primary neurons expressing TH-Gal4. Axon fascicles formed by secondary lineages are globally labeled by anti-Neuroglian (BP104, red), and neuropil is labeled by anti-DNcad (blue). (A, A^{i}): z-projection of frontal confocal sections of control animal at level of ellipsoid body (EB). (B, B^{i}): Corresponding z-projection of HU-treated animal (HU pulse at 32–36 h AH). White arrows indicate terminal arbors and white arrowheads point to long axons. Shown are terminal arborizations of the dopaminergic neuronal groups PPL1 ($PPL1_{TA}$), which innervates the superior medial protocerebrum (SMP) and PPM3 ($PPM3_{TA}$), which normally follows the ring shape of the ellipsoid body (EB). In HU treated animal, the EB is rudimentary ("EBpr" in panel B^{i}) and PPM3 projections follow a straight course across the midline. Scale bar: 50 μm.

most of the time following 28–32 h pulses, and always gone with pulses 32–36 h or later (Fig.4). This finding points at a certain variability in the timing of reactivation of the DPLal neuroblasts. We can only speculate why the variability in birth date seems higher in some vs. other lineages. It is possible that certain neuroblasts are more sensitive to the HU: if applied at a given interval, HU would reach a concentration that, due to variability in feeding or other factors, falls in a range (x1–x2). x1 is sufficient to arrest neuroblast A, whereas another neuroblast, B, requires level x2. In that case, HU application at that time interval will always ablate lineage A, but variably B. To address this question, more detailed studies, focusing on a few, selected lineages, would be required.

Mechanisms involved in the asynchronous reactivation of neuroblasts

Our findings demonstrate that neurons of central brain secondary lineages arise asynchronously during early larval development. Secondary neuroblasts sequentially reactivate (exit quiescence) over a period of approximately 20 h extending from 20–40 h post-hatching. With the exception of five pairs of neuroblasts, which continuously divide (BAlc/INB and the four MB neuroblasts), central brain neuroblasts resume proliferation beginning with those located most laterally, near to the optic lobe (BLAv2/vm, BLD6, BLP3/4, BLVa3/4, BLVp1/2). This observation matches previous reports in the ventral nerve cord that neuroblasts located most laterally exit quiescence first (Chell and Brand, 2010; Ito and Hotta, 1992; Truman and Bate, 1988).

The fact that neuroblasts reactivate at different time points, rather than simultaneously, is a curious phenomenon, given that extrinsic factors seem to be primarily responsible to drive neuroblast re-entry into the cell cycle. Recent findings showed that amino acids, which activate the Tor pathway in the fat body, and insulin from cortex glia which activates PI3K/Akt signaling within the neuroblasts themselves (Chell and Brand, 2010; Sousa-Nunes et al., 2011), are responsible for neuroblast reactivation. Additional extrinsic factors have also been implicated in regulating exit from quiescence. These include the cell adhesion molecule E-Cadherin expressed by glia/neuroblast lineages (Dumstrei et al., 2003), which promotes neuroblast proliferation, the glia-secreted glycoprotein Anachronism (Ana; Ebens et al., 1993), which prevents cell-cycle re-entry after quiescence, and the ECM molecule Terribly Reduced Optic Lobes (Trol; Voigt et al., 2002), which counteracts Ana and enhances exit from quiescence, possibly through positive regulation of FGF and Hedgehog signaling pathways in neuroblasts (Barrett et al., 2008; Park et al., 2003). Given that all neuroblasts should have equal access to any of these hemolymph- and glia-derived stimuli, the question arises why they react to them in different ways, some neuroblasts re-entering mitosis earlier than others.

There are a number of explanations for this phenomenon. First, there might be subtle quantitative differences in the density of

glial cells or glia-neuroblast contacts which could account for the fact that signals passed between glia and neuroblasts have a different strength at different locations. This possibility is not likely, given that (with the exception of the DAM/DALcm lineages which, as a cohesive group, reactivate relatively late) in most locations, early and late re-activating neuroblasts are neighbors. Another explanation would be to postulate the existence of intrinsic factors within the neuroblast that modulate the effect of how neuroblasts at different locations react to extrinsic re-entry stimuli. Along this line, it has been shown that precocious VNC neuroblast re-activation through overexpression of PI3K within neuroblasts does not alter the order in which the neuroblasts begin dividing (lateral to medial; Chell and Brand, 2010) or the duration of time in which they divide, suggesting that neuroblasts have a cell intrinsic timer which dictates the timing and duration of neuroblast proliferation. The importance and molecular nature of intrinsically timed factors for controlling cell fate and neuroblast proliferation has been amply documented. A stereotyped sequence of transcription factors, Hb, Kr, Pdm, Cas, and Grh is expressed in many embryonic neuroblasts and acts to control the fate of neurons born at the respective time points when these molecules are present (Brody and Odenwald, 2005; Pearson and Doe, 2004). In many lineages the sequence of transcription factors resumes in the larva. For example, the VNC neuroblast Nb 3-3 ends on Cas in the embryo and becomes quiescent; subsequently, it re-activates in the early larva with the expression of Cas, and then switches to Svp (Tsuji et al., 2008). Abdominal Nb3-3 neuroblasts, as a result of expression of the Hox gene AbdA, do not become quiescent; they switch from Cas to Svp already in the late embryo. These results indicate that neuroblasts have an intrinsic timer (responsible for switching between different transcription factors) that is "remembered" throughout the phase of quiescence. This timer could be responsible to modulate a neuroblast's response to the "wake-up" stimuli acting on it from the outside during the larval phase.

We would like to point out that one aspect of the mitosis re-entry pattern of neuroblasts could be most easily explained by assuming local cell–cell interactions. This is the finding that in many of the cases where lineages are neighbors and have similar or identical trajectory (e.g., DALcl1/2, CP2/3, BLVa3/4), one member of the pair/small group is born earlier than the other member (s). For example, 24–28 h HU pulses consistently ablated one of the DALcl1/2 pair (DALcl1) and two of the BLAd1–4 group. This slight difference in birth date among members of a lineage pair is corroborated by an independent analysis where the early larval development of secondary lineages was imaged directly (Lovick et al., 2015b). It is possible that in these cases, cell–cell interactions between neighboring neuroblasts of a lineage pair plays a role in tuning the exact time point when they re-enter mitosis.

Ablation of secondary lineages reveals extrinsic mechanisms controlling neuronal differentiation

The targeted ablation of specific brain compartments, or populations of neurons, has been an important means to study questions of neuronal development, function, and plasticity. Typically, these ablation studies relied on surgically disrupting cohesive fiber bundles, such as sensory nerves or central brain tracts, and then assaying the effects on other populations of neurons that formed pre- or postsynaptic connections with the ablated fibers. Among many other results, these experiments demonstrated the high degree of plasticity in the nervous system of both vertebrates and invertebrates. For example, dendrites, deprived of one of their normal inputs, reacted by reshaping their branching pattern whereby they gained access to other inputs (Mizrahi and Libersat, 2001; Murphey and Chiba, 1990). Due to its small size, *Drosophila* has not been used frequently as a model to address neural development by surgical means. However, "genetic ablation" can substitute for surgery, and a number of important insights were gained from genetically removing certain cell types, or tissues, and study the effect on the remaining cells of the nervous system. For example, genetically ablating all sensory neurons in embryos did not prevent the structural and functional differentiation of basic motor circuits underlying peristaltic behavior (Suster and Bate, 2002), indicating that the presence of sensory afferents (or activity) is not required for the proper wiring of motor neurons and many interneurons.

The present study allows several conclusions in the context of neuronal interactions taking place during brain metamorphosis. First, targeting and arborization of antennal projection neurons depends on extrinsic signals from the target tissues. Two lineages, BAmv3 and BAlc, form projections towards the lateral horn and give off collateral branches towards the calyx. In the absence of the secondary MB lineages, where the calyx is reduced by 90%, BAmv3 does not emit any axon collaterals towards the region where the calyx would normally reside, implying that this projection depends on target-derived signals. There is abundant evidence for extrinsic, target-derived signals triggering or directing axonal growth during the embryonic stage, where cells at the midline of the nervous system control the pattern of commissural axons, emitting repulsive (e.g., Slit, Ephrins) or attractive signals (e.g., Netrins). These signaling pathways show a high degree of conservation between invertebrate models (*Drosophila*, *C. elegans*) and vertebrates (Judas et al., 2003; Killeen and Sybingco, 2008). Well-studied cases of axon–target interactions at later stages of brain development are rare, in both vertebrate systems and *Drosophila*. An example from mammalian brain that bears a certain degree of similarity to the antenno-calycal projection discussed here is the cerebro-spinal tract, which forms collaterals to the pontine nuclei in the brain stem. This collateral projection depends on signals from the pons; removal of the pons results in failure of collaterals to form, and ectopic pontine neurons evoke supernumerary collaterals (O'Leary et al., 1991). The molecular nature of the signaling mechanism underlying the cortico-pontine collateral attraction has not yet been elucidated. The interaction between calyx and antenno-calycal afferents described in this study might present an opportunity to screen for elements of the underlying molecular mechanisms controlling axonal collateral growth.

Partial ablation of secondary lineages also revealed the role of extrinsic mechanisms shaping the branching pattern of primary neurons. A small set of primary dopaminergic neurons, the PPM3 neurons, that form part of the CM4 lineage, establish widespread arborizations in the fan-shaped body and the ellipsoid body (L.C. and V.H., unpublished observation). Rudimentary PPM3 projections invading the midline neuropil at the position where the central complex normally develops are still recognizable following HU pulses between 28 and 36 h AH, which ablated secondary lineages that form the major bulk of the volume of the central complex compartments. However, the highly ordered, ring-shaped or layered trajectory of PPM3 terminal branches is absent in the HU treated brains (Fig.8), indicating that interactions with secondary neurons of the central complex is crucial in shaping the neurite tree of primary neurons.

In conclusion, the temporally controlled HU-mediated ablation of secondary neuroblasts and their lineages provides a set of data that is important for developmental studies of the *Drosophila* brain. Knowing the exact birth date of a lineage is one of the essential prerequisites when planning to specifically label or genetically manipulate that lineage in a spatiotemporally restricted manner (e.g. Gal4/Gal80ts or other binary repression systems). Our findings will also stimulate further research into the genetic mechanism controlling neuroblast proliferation and quiescence, as well as axonal pathfinding and branching.

Acknowledgments

We thank the members of the Hartenstein laboratory for critical discussions during the preparation of this manuscript. We thank K.T. Ngo, J.J. Omoto, and T. Shenoy for their assistance in several hydroxyurea ablation experiments. We are grateful to the Bloomington Stock Center and R.F. Stocker for fly strains and the Developmental Studies Hybridoma Bank for antibodies. This work was supported by National Institutes of Health, NIH, United States (R01 NS29357-15). J.K. Lovick was supported by the USPHS National Research Service Award GM07104.

Appendix A. Supporting information

Supplementary data associated with this article can be found in the online version at http://dx.doi.org/10.1016/j.ydbio.2015.03.005.

References

Ashburner, M., 1989. Drosophila. A Laboratory Manual. Cold Spring Harbor Laboratory Press, Cold Spring Harbor, NY, pp. 214–217.

Barrett, A.L., Krueger, S., Datta, S., 2008. Branchless and Hedgehog operate in a positive feedback loop to regulate the initiation of neuroblast division in the Drosophila larval brain. Dev. Biol. 317, 234–245.

Becker, T., Bothe, G., Harley, A.R., Macagno, E.R., 1998. Cell proliferation in a peripheral target is required for the induction of central neurogenesis in the leech. J. Neurobiol. 34, 295–303.

Bello, B.C., Izergina, N., Caussinus, E., Reichert, H., 2008. Amplification of neural stem cell proliferation by intermediate progenitor cells in Drosophila brain development. Neural Dev. 3, 5.

Blanco, J., Pandey, R., Wasser, M., Udolph, G., 2011. Orthodenticle is necessary for survival of a cluster of clonally related dopaminergic neurons in the Drosophila larval and adult brain. Neural Dev. 6, 34.

Broadie, K.S., Bate, M., 1991. The development of adult muscles in Drosophila: ablation of identified muscle precursor cells. Development 113, 103–118.

Brody, T., Odenwald, W.F., 2005. Regulation of temporal identities during Drosophila neuroblast lineage development. Curr. Opin. Cell Biol. 17, 672–675.

Cardona, A., Saalfeld, S., Arganda, I., Pereanu, W., Schindelin, J., Hartenstein, V., 2010. Identifying neuronal lineages of Drosophila by sequence analysis of their axon tracts. J. Neurosci. 30, 7538–7553.

Cardona, A., Saalfeld, S., Schindelin, J., Arganda-Carreras, I., Preibisch, S., Longair, M., Tomancak, P., Hartenstein, V., Douglas, R.J., 2012. TrakEM2 software for neural circuit reconstruction. PLoS ONE 7 (6), e38011. http://dx.doi.org/10.1371/journal.pone.0038011.

Chell, J.M., Brand, A.H., 2010. Nutrition-responsive glia control exit of neural stem cells from quiescence. Cell 143, 1161–1173.

Consoulas, C., Duch, C., Bayline, R.J., Levine, R.B., 2000. Behavioral transformations during metamorphosis: remodeling of neural and motor systems. Brain Res. Bull. 53, 571–583.

Das, A., Gupta, T., Davla, S., Prieto-Godino, L.L., Diegelmann, S., Reddy, O.V., Raghavan, K.V., Reichert, H., Lovick, J., Hartenstein, V., 2013. Neuroblast lineage-specific origin of the neurons of the Drosophila larval olfactory system. Dev. Biol. 373, 322–337.

de Belle, J.S., Heisenberg, M., 1994. Associative odor learning in Drosophila abolished by chemical ablation of mushroom bodies. Science 1994 (263), 692–695.

Dumstrei, K., Wang, F., Hartenstein, V., 2003. Role of DE-cadherin in neuroblast proliferation, neural morphogenesis, and axon tract formation in Drosophila larval brain development. J. Neurosci. 23, 3325–3335.

Ebens, A.J., Garren, H., Cheyette, B.N., Zipursky, S.L., 1993. The Drosophila anachronism locus: a glycoprotein secreted by glia inhibits neuroblast proliferation. Cell 74, 15–27.

Friggi-Grelin, F., Coulom, H., Meller, M., Gomez, D., Hirsh, J., Birman, S., 2003. Targeted gene expression in Drosophila dopaminergic cells using regulatory sequences from tyrosine hydroxylase. J. Neurobiol. 54, 618–627.

Furst, A., Mahowald, A.P., 1985. Cell division cycle of cultured neural precursor cells from Drosophila. Dev. Biol. 112, 467–476.

Harris, W.A., Hartenstein, V., 1991. Neuronal determination without cell division in Xenopus embryos. Neuron 6, 499–515.

Hartenstein, V., 2011. Morphological diversity and development of glia in Drosophila. Glia 59, 1237–1252.

Ito, K., Hotta, Y., 1992. Proliferation pattern of postembryonic neuroblasts in the brain of Drosophila melanogaster. Dev. Biol. 149, 134–148.

Ito, K., Awano, W., Suzuki, K., Hiromi, Y., Yamamoto, D., 1997. The Drosophila mushroom body is a quadruple structure of clonal units each of which contains a virtually identical set of neurones and glial cells. Development 124, 761–771.

Ito, M., Masuda, N., Shinomiya, K., Endo, K., Ito, K., 2013. Systematic analysis of neural projections reveals clonal composition of the Drosophila brain. Curr. Biol. 23, 644–655.

Izergina, N., Balmer, J., Bello, B., Reichert, H., 2009. Postembryonic development of transit amplifying neuroblast lineages in the Drosophila brain. Neural Dev. 4 (44), http://dx.doi.org/10.1186/1749-8104-4-44.

Judas, M., Milosević, N.J., Rasin, M.R., Heffer-Lauc, M., Kostović, I., 2003. Complex patterns and simple architects: molecular guidance cues for developing axonal pathways in the telencephalon. Prog. Mol. Subcell. Biol. 32, 1–32.

Kaneko, M., Hall, J.C., 2000. Neuroanatomy of cells expressing clock genes in Drosophila: transgenic manipulation of the period and timeless genes to mark the perikarya of circadian pacemaker neurons and their projections. J. Comp. Neurol. 422, 66–94.

Kiehle, C.P., Schubiger, G., 1985. Cell proliferation changes during pattern regulation in imaginal leg discs of Drosophila melanogaster. Dev. Biol. 109, 336–346.

Killeen, M.T., Sybingco, S.S., 2008. Netrin, Slit and Wnt recepetors allow axons to choose the axis of migration. Dev. Biol. 323, 143–151.

Kumar, A., Fung, S., Lichtneckert, R., Reichert, H., Hartenstein, V., 2009. Arborization pattern of engrailed-positive neural lineages reveal neuromere boundaries in the Drosophila brain neuropil. J. Comp. Neurol. 517, 87–104.

Lai, S.L., Awasaki, T., Ito, K., Lee, T., 2008. Clonal analysis of Drosophila antennal lobe neurons: diverse neuronal architectures in the lateral neuroblast lineage. Development 135, 2883–2893.

Larsen, C., Shy, D., Spindler, S., Fung, S., Younossi-Hartenstein, A., Hartenstein, V., 2009. Patterns of growth, axonal extension and axonal arborization of neuronal lineages in the developing Drosophila brain. Dev. Biol. 335, 289–304.

Lee, T., Lee, A., Luo, L., 1999. Development of the Drosophila mushroom bodies: sequential generation of three distinct types of neurons from a neuroblast. Development 126, 4065–4076.

Lovick, J.K., Ngo, K.T., Omoto, J.J., Wong, D.C., Nguyen, J.D., Hartenstein, V., 2013. Postembryonic lineages of the Drosophila brain: I. Development of the lineage-associated fiber tracts. Dev. Biol. 384, 228–257.

Lovick J.K., Kong A., Omoto J.J., Ngo K.T., Younossi-Hartenstein A., Hartenstein V., 2015b. Patterns of growth and tract formation during the early development of secondary lineages in the Drosophila larval brain. Submitted.

Malun, D., 1998. Early development of mushroom bodies in the brain of the honeybee *Apis mellifera* as revealed by BrdU incorporation and ablation experiments. Learn. Mem. 5, 90–101.

Marin, E.C., Watts, R.J., Tanaka, N.K., Ito, K., Luo, L., 2005. Developmentally programmed remodeling of the Drosophila olfactory circuit. Development 132, 725–737.

Milán, M., Campuzano, S., García-Bellido, A., 1997. Developmental parameters of cell death in the wing disc of Drosophila. Proc. Natl. Acad. Sci. USA 94, 5691–5696.

Mizrahi, A., Libersat, F., 2001. Synaptic reorganization induced by selective photoablation of an identified neuron. J. Neurosci. 21, 9280–9290.

Murphey, R.K., Chiba, A., 1990. Assembly of the cricket cercal sensory system: genetic and epigenetic control. J. Neurobiol. 21, 120–137.

Neufeld, T.P., de la Cruz, A.F., Johnston, L.A., Edgar, B.A., 1998. Coordination of growth and cell division in the Drosophila wing. Cell 93, 1183–1993.

O'Leary, D.D., Heffner, C.D., Kutka, L., López-Mascaraque, L., Missias, A., Reinoso, B.S., 1991. A target-derived chemoattractant controls the development of the corticopontine projection by a novel mechanism of axon targeting. Development 2, 123–130.

Omoto J.J., Yogi P., Hartenstein V., Origin and development of neuropil glia of the drosophila larval and adult brain: Two distinct glial populations derived from separate progenitors. Dev. Biol. 2015, pii: S0012-1606(15)00111-6, http://dx.doi.org/10.1016/j.ydbio.2015.03.004.

Park, Y., Rangel, C., Reynolds, M.M., Caldwell, M.C., Johns, M., Nayak, M., Welsh, C.J., McDermott, S., Datta, S., 2003. Drosophila perlecan modulates FGF and hedgehog signals to activate neural stem cell division. Dev. Biol. 253, 247–257.

Pearson, B.J., Doe, C.Q., 2004. Specification of temporal identity in the developing nervous system. Annu. Rev. Cell Dev. Biol. 20, 619–647.

Pereanu, W., Hartenstein, V., 2006. Neural lineages of the Drosophila brain: a three-dimensional digital atlas of the pattern of lineage location and projection at the late larval stage. J. Neurosci. 26, 5534–5553.

Pereanu, W., Kumar, A., Jenett, A., Reichert, H., Hartenstein, V., 2010. Development-based compartmentalization of the Drosophila central brain. J. Comp. Neurol. 518, 2996–3023.

Pfister, D., De Mulder, K., Philipp, I., Kuales, G., Hrouda, M., Eichberger, P., Borgonie, G., Hartenstein, V., Ladumer, P., 2007. The exceptional stem cell system of Macrostomum lignano: screening for gene expression and studying cell proliferation by hydroxyurea treatment and irradiation. Front. Zool. 9, 4–9.

Prokop, A., Technau, G.M., 1994. Normal function of the mushroom body defect gene of Drosophila is required for the regulation of the number and proliferation of neuroblasts. Dev. Biol. 161, 321–337.

Python, F., Stocker, R.F., 2002. Adult-like complexity of the larval antennal lobe of *D. melanogaster* despite markedly low numbers of odorant receptor neurons. J. Comp. Neurol. 445, 374–387.

Ramaekers, A., Magnenat, E., Marin, E.C., Gendre, N., Jefferis, G.S., Luo, L., Stocker, R. F., 2005. Glomerular maps without cellular redundancy at successive levels of the Drosophila larval olfactory circuit. Curr. Biol. 15, 982–992.

Roy, B., Singh, A.P., Shetty, C., Chaudhary, V., North, A., Landgraf, M., Vijayraghavan, K., Rodrigues, V., 2007. Metamorphosis of an identified serotonergic neuron in the Drosophila olfactory system. Neural Dev. 24, 2–20.

Schindelin, J., Arganda-Carreras, I., Frise, E., Kaynig, V., Longair, M., Pietzsch, T., Preibisch, S., Rueden, C., Saalfeld, S., Schmid, B., Tinevez, J.Y., White, D.J., Hartenstein, V., Eliceiri, K., Tomancak, P., Cardona, A., 2012. Fiji: an open-source platform for biological-image analysis. Nat. Methods 9, 676–682.

Skeath, J.B., Thor, S., 2003. Genetic control of Drosophila nerve cord development. Curr. Opin. Neurobiol. 13, 8–15.
Sousa-Nunes, R., Yee, L.L., Gould, A.P., 2011. Fat cells reactivate quiescent neuroblasts via TOR and glial insulin relays in Drosophila. Nature 471, 508–512.
Stocker, R.F., Heimbeck, G., Gendre, N., de Belle, J.S., 1997. Neuroblast ablation in Drosophila P[GAL4] lines reveals origins of olfactory interneurons. J. Neurobiol. 32, 443–456.
Suster, M.L., Bate, M., 2002. Embryonic assembly of a central pattern generator without sensory input. Nature 416, 174–178.
Sweeney, S.T., Hidalgo, A., de Belle, J.S., Keshishian, H., 2012. Hydroxyurea ablation of mushroom bodies in Drosophila. Cold Spring Harb. Protoc. 2012, 231–234.
Tabata, T., Schwartz, C., Gustavson, E., Ali, Z., Kornberg, T.B., 1995. Creating a Drosophila wing de novo, the role of engrailed, and the compartment border hypothesis *Development* 121, 3359–3369.
Timson, J., 1975. Hydroxyurea. Mutat. Res. 32, 115–132.
Truman, J.W., Bate, M., 1988. Spatial and temporal patterns of neurogenesis in the central nervous system of *Drosophila melanogaster*. Dev. Biol. 125, 145–157.
Tsuji, T., Hasegawa, E., Isshiki, T., 2008. Neuroblast entry into quiescence is regulated intrinsically by the combined action of spatial Hox proteins and temporal identity factors. Development 135, 3859–3869.
Urbach, R., Technau, G.M., 2003a. Molecular markers for identified neuroblasts in the developing brain of Drosophila. Development 130, 3621–3637.
Urbach, R., Technau, G.M., 2003b. Early steps in building the insect brain: neuroblast formation and segmental patterning in the developing brain of different insect species. Arthropod Struct. Dev. 32, 103–123.
Voigt, A., Pflanz, R., Schäfer, U., Jäckle, H., 2002. Perlecan participates in proliferation activation of quiescent Drosophila neuroblasts. Dev. Dyn. 224, 403–412.
Viktorin, G., Riebli, N., Popkova, A., Giangrande, A., Reichert, H., 2011. Multipotent neural stem cells generate glial cells of the central complex through transit amplifying intermediate progenitors in Drosophila brain development. Dev. Biol. 356, 553–565.
Wartlick, O., Mumcu, P., Kicheva, A., Bittig, T., Seum, C., Jülicher, F., González-Gaitán, M., 2011. Dynamics of Dpp signaling and proliferation control. Science 331, 1154–1159.
Weeks, J.C., 1999. Steroid hormones, dendritic remodeling and neuronal death: insights from instect metamorphosis. Brain Behav. Evol. 54, 51–60.
White, K., Kankel, D.R., 1978. Patterns of cell division and cell movement in the formation of the imaginal nervous system in *Drosophila melanogaster*. Dev. Biol. 65, 296–321.
Wong, D.C., Lovick, J.K., Ngo, K.T., Borisuthirattana, W., Omoto, J.J., Hartenstein, V., 2013. Postembryonic lineages of the Drosophila brain: II. Identification of lineage projection patterns based on MARCM clones. Dev. Biol. 384, 258–289. Yang, J.S., Awasaki, T., Yu, H.H., He, Y., Ding, P., Kao, J.C., Lee, T., 2013. Diverse neuronal lineages make stereotyped contributions to the Drosophila locomotor control center, the central complex. J. Comp. Neurol. 521, 2645–2662.
Younossi-Hartenstein, A., Nassif, C., Green, P., Hartenstein, V., 1996. Early neurogenesis of the Drosophila brain. J. Comp. Neurol. 370, 313–329.
Yu, H.H., Awasaki, T., Schroeder, M.D., Long, F., Yang, J.S., He, Y., Ding, P., Kao, J.C., Wu, G.Y., Peng, H., Myers, G., Lee, T., 2013. Clonal development and organization of the adult Drosophila central brain. Curr. Biol. 23, 633–643.

Chapter 4

Patterns of Growth and Tract Formation During the Early Development of Secondary Lineages in the *Drosophila* Larval Brain

Patterns of Growth and Tract Formation During the Early Development of Secondary Lineages in the *Drosophila* Larval Brain

Jennifer K. Lovick, Angel Kong, Jaison J. Omoto, Kathy T. Ngo, Amelia Younossi-Hartenstein, Volker Hartenstein*

Department of Molecular Cell and Developmental Biology, University of California Los Angeles, Los Angeles, California 90095

Received 29 May 2015; revised 9 July 2015; accepted 10 July 2015

ABSTRACT: The *Drosophila* brain consists of a relatively small number of invariant, genetically determined lineages which provide a model to study the relationship between gene function and neuronal architecture. In following this long-term goal, we reconstruct the morphology (projection pattern and connectivity) and gene expression patterns of brain lineages throughout development. In this article, we focus on the secondary phase of lineage morphogenesis, from the reactivation of neuroblast proliferation in the first larval instar to the time when proliferation ends and secondary axon tracts have fully extended in the late third larval instar. We have reconstructed the location and projection of secondary lineages at close (4 h) intervals and produced a detailed map in the form of confocal z-projections and digital three-dimensional models of all lineages at successive larval stages. Based on these reconstructions, we could compare the spatio-temporal pattern of axon formation and morphogenetic movements of different lineages in normal brain development. In addition to wild type, we reconstructed lineage morphology in two mutant conditions. (1) Expressing the construct UAS-p35 which rescues programmed cell death we could systematically determine which lineages normally lose hemilineages to apoptosis. (2) *so*-Gal4-driven expression of dominant-negative EGFR ablated the optic lobe, which allowed us to conclude that the global centrifugal movement normally affecting the cell bodies of lateral lineages in the late larva is causally related to the expansion of the optic lobe, and that the central pattern of axonal projections of these lineages is independent of the presence or absence of the optic lobe. Develop Neurobiol 00: 000–000, 2015

Keywords: brain; development; *Drosophila*; larval; lineage

INTRODUCTION

Highly ordered connections of neurons represent the structural basis of the complex brain circuitry controlling behavior. Neuronal connectivity is contingent on morphological and functional properties of individual neurons ("wiring properties"), which are shaped during development. A fundamental task of developmental neurobiology is to elucidate the genetic mechanisms that control neuronal wiring properties. A number of transcriptional regulators that exert a profound effect on neuronal shapes and target selection have come to light, many of them in genetic studies

Correspondence to: V. Hartenstein (volkerh@mcdb.ucla.edu).

Contract grant sponsor: NIH; contract grant number: 1 R01 NS054814.

Contract grant sponsor: USPHS National Research Service Award; contract grant number: GM07104 (to J.K.L.).

Contract grant sponsor: Ruth L. Kirschstein National Research Service Award; contract grant number: GM007185 (to J.J.O.).

Contract grant sponsor: NSF Graduate Research Fellowship Program; contract grant number: DGE-0707424 (to K.T.N.).

Additional Supporting Information may be found in the online version of this article.

Published online 00 Month 2015 in Wiley Online Library (wileyonlinelibrary.com).
DOI 10.1002/dneu.22325

of *Drosophila* neurons (Jan and Jan, 2010). Despite this progress, our understanding of how genetic networks regulate neuronal wiring is still in its infancy.

Drosophila represents a favorable model system to address the relationship between gene function and neuronal architecture. Aside from the genetic and molecular tools that have been developed, *Drosophila* offers the advantage that its nervous system is built by a relatively small number of genetically and structurally defined modules, the neural lineages (Hartenstein et al., 2008; Ito et al., 2013; Wong et al., 2013; Yu et al., 2013). Most lineages (Type I) possess approximately 100–150 neurons that are produced by a single, stem cell-like neuroblast. A small number of lineages restricted to the dorsomedial brain (Type II lineages) are much larger (~500 neurons; Bello et al., 2008). Neuroblasts first appear in the early embryo and proliferate in a characteristic, stem cell-like mode. A neuroblast divides asymmetrically into a large daughter cell that continuously divides (self-renewal) and a second, smaller daughter cell (ganglion mother cell; GMC), which divides once more to produce two postmitotic cells that differentiate into two neurons or glial cells. In this manner, each embryonic neuroblast initially produces a lineage of 10–20 primary neurons that form the larval brain (Hartenstein et al., 1987; Larsen et al., 2009). Most neuroblasts become mitotically quiescent in the late embryo and reactivate proliferation during the larval stage (Truman and Bate, 1988; Prokop and Technau, 1991; Ito and Hotta, 1992; Prokop et al., 1998). Continuing to divide throughout the larval period, neuroblasts produce sets of secondary neurons which, together with remodeled primary neurons, give rise to the adult brain. Unlike Type I neuroblasts, those which give rise to Type II lineages exhibit a more complex pattern of proliferation; rather than generating GMCs, Type II neuroblasts divide into a series of intermediate progenitors, which themselves undergo several rounds of asymmetric divisions, much like Type I neuroblasts (Kang and Reichert, 2015).

During the embryonic phase, neuroblasts express specific and invariant combinations of transcription factors, which have been mapped in considerable detail (Urbach and Technau, 2003a). Several of the early expressed transcription factors remain active also during the secondary phase of neuroblast proliferation (Lichtneckert et al., 2007; Kumar et al., 2009a,b; Sen et al., 2014). It is thought that a neuroblast, by the set of transcription factors it expresses, is provided with a specific "genetic address," which plays a role in shaping the connectivity and function of the neurons it produces (Skeath and Thor, 2003; Urbach and Technau, 2003b). This notion bears well with the fact that neurons of the same lineage generally project together in one or two coherent fiber tracts, implying that they react in the same way to positional information controlling axonal pathfinding (Lœhr et al., 2002). In addition, on differentiation, neurons of the same lineage typically target one or a few, spatially-restricted brain compartments. This is particularly true for the secondary lineages, as documented in a detailed clonal analyses of the projection patterns of MARCM clones in the adult brain (Ito et al., 2013; Wong et al., 2013; Yu et al., 2013). By contrast, primary neurons of a given lineage, in particular those born early in the embryo, show a higher degree of diversity in terms of target selection.

Lineages are further subdivided into smaller units, called hemilineages and sublineages. Hemilineages are the result of the division of GMCs. In many, if not all lineages, the neurons resulting from one GMC are not equal, but form an "A" and a "B" neuron (Truman et al., 2010). Studies of secondary lineages showed that A-neurons and B-neurons systematically differ with respect to their axonal trajectory, whereby all A-neurons bundle into one tract and B-neurons into another. The branched secondary axon tracts (SATs) described for a number of lineages of both ventral cord (Truman et al., 2004, 2010; Kuert et al., 2012, 2014) and brain (Pereanu and Hartenstein, 2006; Cardona et al., 2010) in actuality represent the A-tract and B-tract combined. In many, if not all cases with an unbranched SAT, one hemilineage is eliminated by apoptotic cell death (Kumar et al., 2009a; Truman et al., 2010). Sublineages represent groups of neurons born sequentially during a certain time interval. In some cases, sublineages may differ with regard to their terminal arborization. They may all project along the same SAT, but choose different targets (e.g., layers; glomeruli) in the area of terminal arborization. This has been shown in detail for the four mushroom body (MB) lineages, where neurons born during different time intervals generate the *c*-lobe, *a*/*b*-lobe, and a^0/b^0-lobe, respectively (Lee et al., 1999; Lin and Lee, 2012).

To use lineages for genetic studies, it is essential to provide detailed knowledge of the morphology of lineages throughout development. Quite extensive information exists for the lineages forming the MB and the antennal lobe (e.g., Lee et al., 1999; Jefferis et al., 2002, 2005; Zhu et al., 2003; Yu et al., 2010; Lin et al., 2012, 2013; Das et al., 2013). For other lineages, our knowledge is restricted to the above referenced maps that were generated for embryonic neuroblasts and for secondary lineages at the late larval stage and the adult stage. The developmental

changes that shape the structure of lineages between the time when they first appear in the late embryo and the time of neuronal differentiation have not yet been elucidated for most lineages.

In this article, we have analyzed the early secondary phase of lineage morphogenesis, encompassing the time interval when neuroblasts resume proliferation (first larval instar) to the time point when SATs have fully extended (third larval instar). The focus was on the larval brain (supraesophageal ganglion); a similar analysis of the ventral nerve cord (subesophageal ganglion, thoracic ganglia) is underway (Kuert et al., in preparation). Our analysis produced a detailed map, in the form of digital three-dimensional (3D) models, of lineages at successive larval stages which allowed us to study axon growth and morphogenetic movements of lineage cell body clusters. Finally, we identified those brain lineages that lose hemilineages by cell death, using the apoptosis-inhibiting construct UAS-p35 (Yoo et al., 2002). Our results will assist future investigations addressing the mechanisms that control neuronal fate and differentiation in the *Drosphila* brain.

MATERIAL AND METHODS

Fly Lines

Flies were grown at 25°C using standard fly media unless otherwise noted. *asense (ase)*-Gal4 (Zhu et al., 2006), *engrailed (en)*-Gal4 (Tabata et al., 1995; #30564, Bloomington *Drosophila* Stock Center (BDSC), University of Indiana, IN), *inscuteable (insc)*-Gal4 (Mz1407; Betschinger et al, 2006; #8751, BDSC), *sine oculis (so)*-Gal4 (Chang et al., 2003a,b), UAS-chRFP-Tub (Rusan and Peifer, 2007; #25774, BDSC), UAS-mcd8::GFP (Lee et al., 1999; #5137, BDSC), UAS-p35 (on third; Yoo et al., 2002), UAS-dnEGFR (Chang et al., 2003a).

Clonal Analysis and Lineage Tracing Experiments

Primary lineage flp-out clones were generated using flies bearing the genotype: *hs-FLP*^{1}, *UAS-mCD8-GFP*/1; *UAS-mCD8-GFP*/1; *tub-FRT-GAL80-FRT-GAL4* (Zecca and Struhl, 2002). *Briefly, embryos were* heat-shocked at 38°C for 5 min and raised at 18°C until wandering third instar larva; third instar larval brains were dissected and processed for immunohistochemistry (see below).

Immunohistochemistry

Samples were fixed in 4% formaldehyde or 4% methanol-free formaldehyde in phosphate buffer saline (PBS, Fisher-Scientific, pH 5 7.4; Cat No. #BP399-4). Tissues were permeabilized in PBT (PBS with 0.1–0.3% Triton X-100, pH 5 7.4) and immunohistochemistry was performed using standard procedures (Ashburner 1989). The following primary antibodies were provided by the Developmental Studies Hybridoma Bank (Iowa City, IA): mouse anti-bruchpilot (nc82; 1:20); rat anti-DN-Cadherin (DN-EX #8, 1:20), and mouse anti-Neurotactin (BP106, 1:10). Additional primary antibodies: rabbit anti-Deadpan (Dpn; Bier et al., 1992). Secondary antibodies, IgG_1 (Jackson ImmunoResearch; Molecular Probes) were used at the following dilutions: Cy5-conjugated anti-rat Ig (1:100), Cy3-conjugated anti-mouse Ig (1:200), Cy5-conjugated anti-mouse Ig (1:250); Alexa 546-conjugated anti-mouse (1:500), DynaLight 649-conjugated anti-rat (1:400), Alexa 568-conjugated anti-mouse (1:500).

Confocal Microscopy

Staged *Drosophila* larval and adult brains labeled with suitable markers were viewed as whole-mounts by confocal microscopy [LSM 700 Imager M2 using Zen 2009 (Carl Zeiss); lenses: 403 oil (numerical aperture 1.3)]. Complete series of optical sections were taken at 2-µm intervals. Captured images were processed by ImageJ or FIJI (National Institutes of Health, http://rsbweb.nih.gov/ij/and http://fiji.sc/) and Adobe Photoshop.

Digital Removal of Background Fluorescence

For clarity in some panels, background fluorescence and/or fluorescence from other lineages (visualized with Gal4 drivers or clones) were digitally removed using FIJI (Schindelin et al., 2012; http://fiji.sc/) or Adobe Photoshop.

Electron Microscopy

For electron microscopy, larval brains were dissected and fixed in 2% glutaraldehyde in PBS for 20 min, followed by a postfixation for 30 min in a mixture of 1% osmium tetroxide and 2% glutaraldehyde in 0.15 *M* cacodylate buffer (on ice). Specimens were washed several times in PBS and dehydrated in graded ethanol and acetone (all steps on ice). Preparations were left overnight in a 1:1 mixture of Epon and acetone and then for 5–10 h in unpolymerized Epon. They were transferred to molds, oriented and placed at 60°C for 24 h to permit polymerization of the Epon. Blocks were sectioned (0.1 Am). Sections were mounted on net grids (Ted Pella) and treated with uranyl acetate and lead citrate. A JEOL 100CX transmission electron microscope was used for observation.

Morphological Criteria for Staging of Larval Brains

Animals were staged by placing larvae hatched from the egg within a 1 h period on food plates under noncrowded

conditions at 25°C. As even when larvae are reared at low density to guarantee optimal food supply, there is considerable variability (in the order of 10%) in brain growth of larvae of the same age. We, therefore, defined specific morphogenetic parameters of the rapidly expanding optic lobe as structural hallmarks of the larval brain. These parameters include the ratio of optic lobe diameter (OOA) to neuropil diameter (OOA/NP), the ratio of neuroblasts versus epithelium within the outer optic anlage (NB/NB 1 E), and the thickness of the layer of medulla neurons (Supporting Information Fig. S1).

Generation of Three-Dimensional Models

Digitized images of confocal sections were imported into FIJI (Schindelin et al., 2012; http://fiji.sc/). Complete series of optical sections were taken at 2-μm intervals. As sections were taken from focal planes of one and the same preparation, there was no need for alignment of different sections. Models were generated using the 3D viewer as part of the FIJI software package. Digitized images of confocal sections were imported using TrakEM2 plugin in FIJI software (Cardona et al., 2012). Surface renderings of larval brains stained with anti-DNCad were generated as volumes in the 3D viewer in FIJI. Cell body clusters were indicated on surface renderings using TrakEM2. Digital atlas models of cell body clusters were created by manually labeling each lineage and its approximate cell body cluster location in TrakEM2.

RESULTS

Reconstruction of Secondary Axon Tracts in the Early Larval Brain

Using an antibody against the adhesion protein Neurotactin (de la Escalera et al., 1990) and the Gal4 driver line *insc*-Gal4 (Betschinger et al., 2006), which is expressed specifically in secondary lineages from the time of their appearance onward, we reconstructed the pattern of larval secondary lineages at short temporal intervals between hatching and 96 h after hatching (AH). By analyzing the different aspects of the pattern of secondary lineages, including location of the tract entry points and characteristic trajectory and branching within the neuropil, at sequential, closely spaced time intervals, it was possible to identify individual lineages, or lineage pairs, at all stages (Hartenstein et al., 2015; Supporting Information Fig. S2, S3, Table 1). During the first larval instar, as described in previous works (Ito and Hotta, 1992), only five neuroblasts are mitotically active and are strongly labeled by *insc*-Gal4 and Deadpan (Dpn). These include the four neuroblasts of the MB located in the posterior brain and the neuroblast generating the BAlc lineage that flanks the antero-lateral neuropil ["3" in Fig. 1(A)]. Neuroblasts of all other lineages are small cells, also marked by the expression of Deadpan (Dpn; Bier et al., 1992), which are scattered throughout the brain cortex, either close to the surface ["1" in Fig. 1(A)] or at deeper levels ["2" in Fig. 1(A)]. Many neuroblasts already express low levels of *insc*-Gal4>UAS-chRFP-Tub, which allows one to recognize thin basal processes connecting the cell body to the neuropil surface [as in the case of "1" in Fig. 1(A); BAlp1/2 and DPLc neuroblasts in Fig. 1(B)]. This peculiar phenomenon had already been described for the early larval neuroblasts of the ventral nerve cord (Truman and Bate, 1988; Chell and Brand, 2010); the connection between cell body and neuropil [green arrows in Fig. 1(B)] may serve as a structure that anchors those neuroblasts which are remote from the neuropil to the site where the primary axon tract enters the neuropil [magenta arrows in Fig. 1(B)].

All neuroblasts re-enter the cell cycle between 20 and 40 h AH in a stereotyped temporal order (Ito and Hotta, 1992; Lovick and Hartenstein, 2015). This is accompanied by an increase in cell size, an increase in expression of *insc*-Gal4, and relocation to the brain surface [Fig. 1(C)]. The appearance of these morphological and genetic changes defines the "time of birth" for a secondary lineage and closely corresponds to the birth date deduced from experiments where neuroblasts were systematically ablated, at short intervals, using the drug hydroxyurea (HU; Lovick and Hartenstein, 2015; Table 1). The first lineages to appear around 20 h AH are DALv1, BLAv2, BLD6, and BLVp1 (Table 1). Around 24–27 h more than half of the secondary lineages can be detected; the last ones to be born are several lineages located in the antero-dorsal brain (DAMv, DAMd, DALcm).

Secondary Axons Follow the Tracts Laid Down by Primary Lineages

Following their birth during the late first/early second larval instar, secondary lineages undergo a rather uniform phase of growth and axonogenesis. During the first 2–4 h following their enlargement, neuroblasts perform one to two cell divisions. At this stage, lineages appear as small clusters of *insc*-positive cells, with one large superficial neuroblast accompanied by two to four smaller progeny [GMC, neurons; see for example DAMd1 in Fig. 2(K)]. Subsequently, with the onset of axonogenesis in the first-born neurons, SATs make their appearance as short stubs connecting the cell body cluster with the neuropil surface

Table 1 Steps in the Development of Secondary Lineages

		20	24	28	32	36	40	44			20	24	28	32	36	40	44
BAla1	1			b				c	DPLm2	47		a	b				c
BAla2	2			b				c	DPLp1	48		a	b				c
BAla3	3							b	DPLp2	49		a	b				c
BAla4	4			a				b	DPLpv	50		a	b				c
Balc	5	c							DPMl1	51			b				c
BAlp1	6							c	DPMl34				b				c
BAlp2	7		a	b				c	DPMm1	53		a	b				c
BAlp3	8		a	b				c	DPMm2	54			a				c
BAlp4	9			b				c	DPMpl1	55			a				c
Balv	10			b				c	DPMpl2	56			a				c
BAmas1	11			a				c	DPMpl3	57			a				c
BAmas2	12							a	DPMpm1	58		a	b				c
BAmd1	13			a				b	DPMpm2	59		a	b				c
BAmd2	14			a				b	CM1	60		a	b				c
BAmv1	15		a	c					CM3	61		a	b				c
BAmv2	16			b				c	CM4	62		a	b				c
BAmv3	17			b				c	CM5	63			a				c
DALcl1	18		a	b				c	CP1	64		a	b				c
DALcl2	19			a				c	CP2	65		(a)	(b)				c
DALcm1	20							b	CP3	66		(a)	(b)				c
DALcm2	21							b	CP4	67			a				
DALd	22			a				c	BLAd1	68		(a)	(b)				c
DALl1	23		a	b				c	BLAd2	69		(a)	(b)				c
DALl2	24		a	b				c	BLAd3	70		(a)	(b)				c
DALv1	25		b					c	BLAd4	71		(a)	(b)				c
DALv2	26			b				c	BLAl	72			(b)				c
DALv3	27		a	b				c	BLAv1	73		a	b				c
DAMd1	28			a				b	BLAv2	74		a	b				c
DAMd2	29			a				b	BLAvm	75		a	b				c
DAMd3	30			a				b	BLD1	77		a	b				c
DAMv1	31			a				b	BLD4	80		a	b				c
DAMv2	32			a				b	BLD2	78		a	b				c
DPLal1	33		a	b				c	BLD3	79		a	b				c
DPLal2	34		a	b				c	BLD5	82		a	b				c
DPLal3	35		a	b				c	BLD6	83		b	c				
DPLam	36			b				c	BLP1	84			(b)				c
DPLc1	37		a	b				c	BLP2	85			(b)				c
DPLc2	38		a	b				c	BLP3	86			(b)				c
DPLc4	40		a	b				c	BLP4	87			(b)				c
DPLc3	39		a	b				c	BLVa1	89			(a)				c
DPLc5	41			b				c	BLVa2	90			(a)				c
DPLd	42			a				c	BLVa3	91		(a)	(b)				c
DPLl1	43			a				c	BLVa4	92		(a)	(b)				c
DPLl2	44		a	b				c	BLVp1	93		b	c				
DPLl3	45		a	b				c	BLVp2	94							c
DPLm1	46		a	b				c	MB1-4		c						

All Lineages are listed at the left. The horizontal axis represents the time axis, subdivided into 4 h intervals. Numbers at the top indicate hours AH. Onset of blue shading indicates time interval at which the corresponding secondary lineage is ablated by HU pulse (see Lovick and Hartenstein, 2015; dark blue 5 ablation in >90% of cases; medium blue 5 ablation in 50–90%; light blue 5 ablation in 10–50%). Gray shading in left column points out lineage pairs with highly similar or identical axonal trajectory in larval brain. Lower case letters (a–c) signify stages in secondary lineage development, based on their appearance in preparations of brains expressing the secondary lineage marker insc-Gal4>UAS-mcd8-GFP (see Fig. 1). Letter "a" indicates presence of neuroblast at/prior to entering mitosis; "b" signifies stage shortly after onset of proliferation when lineage consists of neuroblast and small cluster of progeny; at stage marked "c," lineage has formed axon tract entering neuropil. [Color table can be viewed in the online issue, which is available at wileyonlinelibrary.com.]

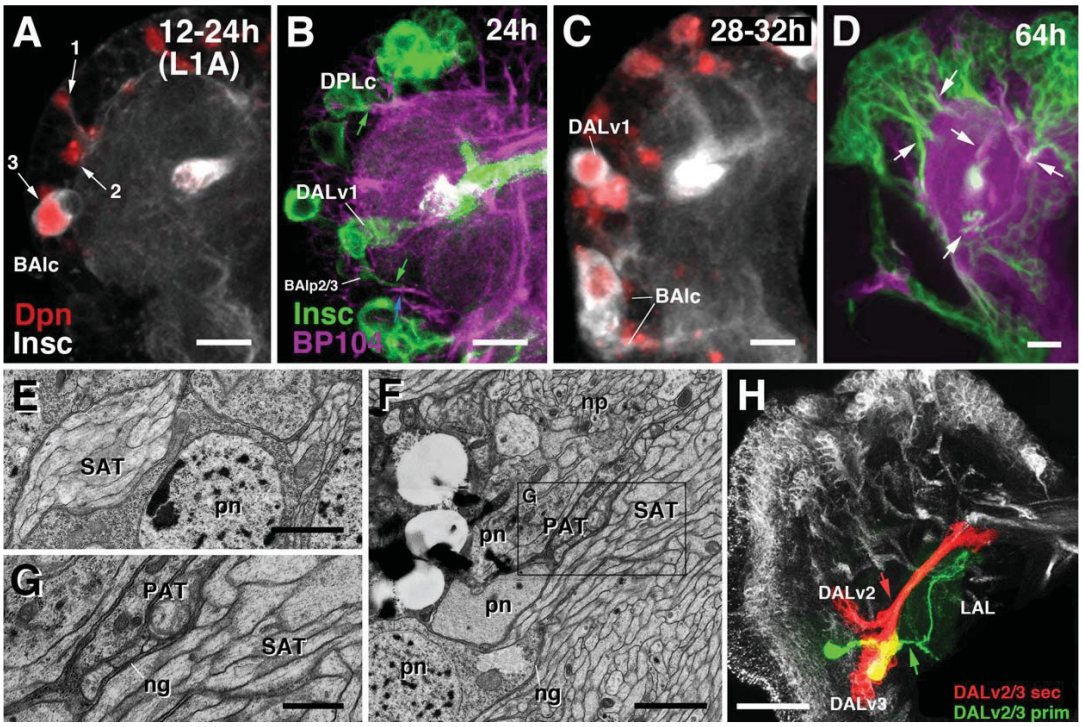

Figure 1 Early development of secondary lineages in the larval brain. (A–D) Expression of *insc*-Gal4 (Insc; white in panels A, C; green in panels B, D) in secondary lineages. Panels are z-projections of confocal sections of larval brain hemispheres (midline at right margins) fixed at different stages of development (A: 12–24 h AH; morphologically stage L1A [see Supporting Information Fig. S1]; B: 24 h AH [stage L1B]; C: 28–32 h AH [stage L2A]; D: 64 h AH [stage L3A]). (A): Insc is turned on in neuroblasts, co-labeled with anti-Deadpan (red), shortly before onset of secondary phase of proliferation. Arrow (1) points at neuroblast with superficially located cell body and basal process contacting neuropil surface; arrow (2) indicates neuroblast with deep cell body; neuroblast marked by arrow 3 (lineage BAlc) is large, strongly Insc-positive, and has commenced proliferation. Following onset of proliferation, neuroblasts upregulate Insc-expression, enlarge, and move to periphery of cortex (C). (B, D) Co-labeling of incipient secondary lineages (Insc, green) and primary axon tracts (BP104, magenta). Note close association of primary (magenta) and secondary (green) axon tracts [examples shown by white arrows in panel (D)]. In panel (B), blue arrow points at neuropil entry point of PAT of lineages BAlp2/3; green arrow indicates fiber emitted by secondary BAlp2/3 neuroblasts toward this entry point. (E–G): Transmission electron micrographs of section of mid-third larval instar brain. (E): shows SAT in deep layer of brain cortex, surrounded by cell bodies of primary neurons (pn). (F): SAT entering the neuropil (np; upper right half of image). Group of primary neurons (pn lower left) form primary axon tract (PAT); SAT follows PAT. Thin lamella of neuropil glia (ng) surrounds primary axon tract. Profiles of primary axons are slightly thicker and more electron dense than secondary axons (G). (H) z-projection of frontal confocal sections of late third larval instar brain, showing lineage pair DALv2/3 labeled by *engrailed*-Gal4>UAS-mcd8::GFP. Secondary lineage tracts are globally labeled by anti-Neurotactin (BP106; white). Primary neurons, distinguishable from undifferentiated secondary neurons by their large cell bodies and branched axons, were rendered green; secondary neurons red. Note separate entries and trajectories of primary and SATs (arrows). Scale bars: 10 μm (A–D); 1 μm (E, F); 0.5 μm (G); 40 μm (H).

[Fig. 2(A,I,L)]. SATs then extend into the neuropil, following in almost all cases the pattern that is prefigured by the primary axon tracts [PATs; arrows in Fig. 1(D) indicate representative examples]. PATs are labeled by anti-Neuroglian (BP104) in the early larval brain, and a comprehensive map of PATs and their corresponding lineages has been generated (Hartenstein et al., in press). The direct contact between SATs and PATs at the neuropil entry points can also be appreciated electron microscopically [Fig. 1(E–G)].

The only case where entry point and trajectory of PAT and SAT differed markedly is the lineage pair DALv2/3, labeled by the expression of *engrailed*-Gal4 [Kumar et al., 2009b; Fig. 1(H)]. Primary DALv2/3 neurons enter the neuropil at the ventro-lateral surface of the lateral accessory lobe (LAL) and fill this compartment with terminal

arborizations [Fig. 1(H); see also Hartenstein et al., 2015]. Secondary DALv2/3 axons form a thick bundle that skirts the anterior surface of the LAL, and enters the neuropil close to the medial lobe of the MB. These axons will differentiate into the large-field neurons of the ellipsoid body, a compartment that has no counterpart in the larval brain.

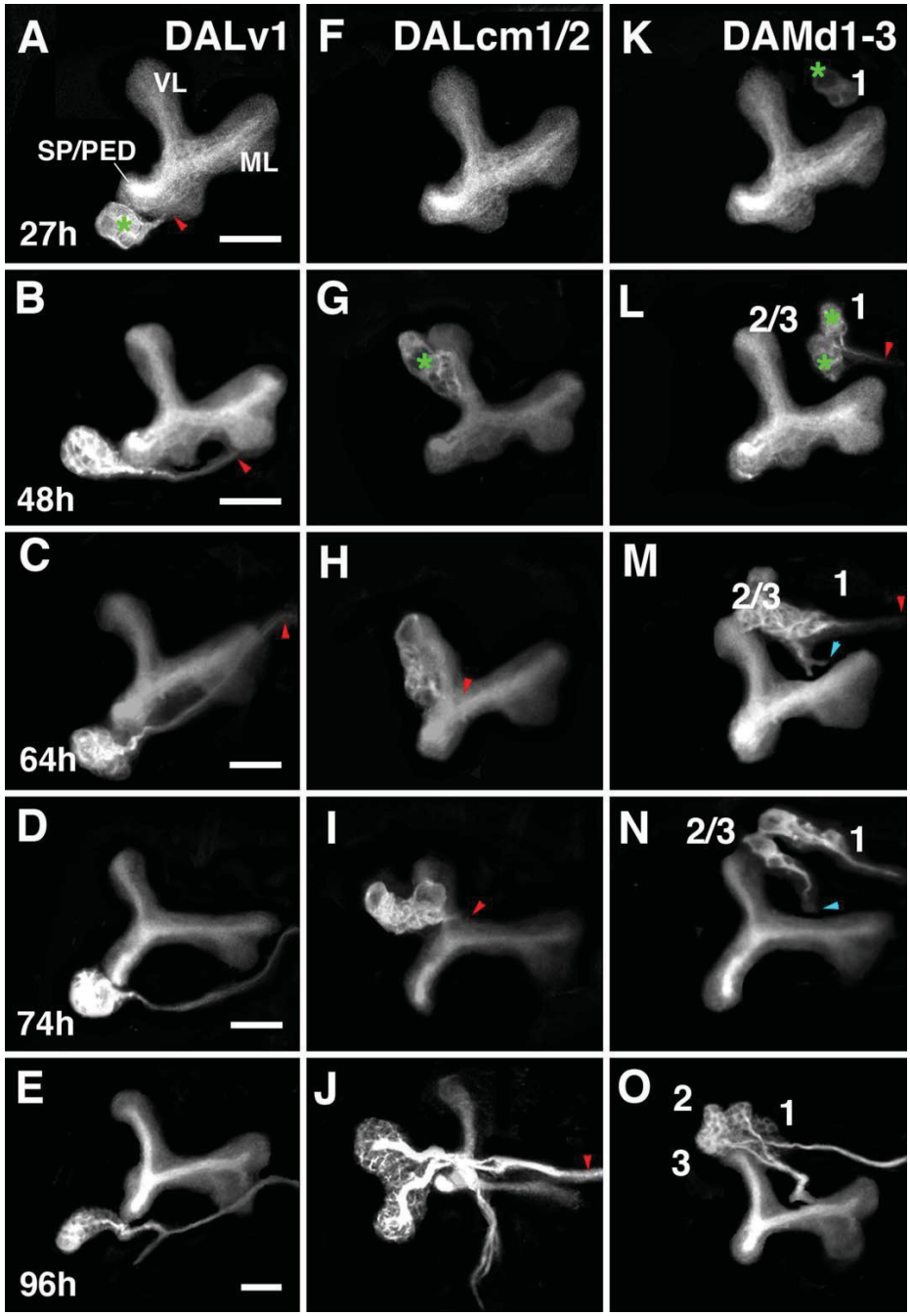

The Sequence at Which Secondary Axon Tracts Extend Follows the Birth Order of Lineages

The time of onset of axonogenesis and the time course of axon extension seems to correlate with the birth date of a lineage. In other words, neurons extend their axon at a fixed time interval following their birth; an early born lineage such as DALv1 has a well-established SAT at 27 h AH [Fig. 2(A)]. The DALv1 SAT reaches across the midline around 64 h AH [Fig. 2(C)]. By contrast, a late born lineage such as DALcm1/2 produces short axons at 64 h AH [Fig. 2(H)] and reaches the midline after 80 h AH [Fig. 2(J)]. The DAMd group of lineages consists of three members; one of them, DAMd1, has a slightly earlier time of birth than DAMd2/3 [Table 1; Fig. 2(K,L)]. The DAMd1 tract extends toward the brain midline around 48 h AH [Fig. 2(L)]; the longitudinally directed DAMd2/3 tract follows suit several hours later [Fig. 2(M)]. This temporally staggered extension of SATs is in striking contrast to the near simultaneous sprouting of branches and formation of synaptic connections, events that do not occur for any secondary lineage (except the MB) during the larval stage. Instead, secondary lineages, independent of birth date, appear to branch and form terminal arborizations in a temporally coordinated manner during the late pupal stage (Larsen et al., 2009).

The Majority of Type I Secondary Brain Lineages Lose a Hemilineage to Programmed Cell Death

Previous work focusing mostly on the ventral nerve cord had shown that in many, if not all, secondary Type I lineages, the mitosis of each GMC is asymmetric, generating an "A" daughter neuron and a "B" daughter neuron (Truman et al., 2010). "A" neurons and "B" neurons each constitute their own A and B hemilineage and their axons gather in two separate bundles or tracts. When a lineage only has a single tract, the assumption is that one hemilineage is present and that the other has been removed via programmed cell death. This was confirmed for a number of secondary lineages of the ventral nerve cord (VNC) (Truman et al., 2010) and the brain (Kumar et al., 2009a), where the majority of Type I lineages (50 out of 87) possess only one tract (called "Type I 1H lineages" in the following; Table 2). To establish whether these lineages lose hemilineages due to programmed cell death we inhibited cell death in Type I lineages during the larval period by expressing a UAS-p35 construct (Yoo et al., 2002) under the control of the *ase*-Gal4 driver line (Zhu et al., 2006). Following this treatment, none of the lineages which normally possess two tracts ("Type I 2H lineages") showed structural abnormalities. By contrast, most of the Type I 1H lineages developed an additional tract (Table 2). In these lineages, the normal SAT was fully formed and followed the normal trajectory, but a second, often thinner bundle branched off the normal tract. In most cases, the branching occurred proximally, close to the point where the SAT entered the neuropil [arrowhead in Fig. 3(H)]; sometimes, the SAT was split already in the cortex and an additional cell cluster was visible (data not shown). In other cases, the supernumerary tract branched off the SAT at a more distal location within the neuropil. The trajectory of the supernumerary branch was relatively stereotyped for a given lineage; it either closely followed the path of a neighboring SAT or formed a novel pathway not normally followed by any lineage (Table 2). A representative example for each of these two behaviors is provided by Figure 3(A–H). In the first case, the lineage BAmas1 whose regular SAT turns dorsally toward the superior medial protocerebrum (SMP) compartment, forms a branch that follows the pathway of TRdm (a lineage of the subesophageal ganglion) into the anterior subesophageal ganglion [arrowhead in Fig. 3(A–D)]. The second scenario is represented by DPLam that enters the neuropil from antero-

Figure 2 Elongation of SATs. Panels show parts of z-projections of frontal confocal sections of larval brain hemispheres imaged at sequential stages (panels of first row: 27 h AH; second row: 48 h AH; third row: 64 h AH; fourth row: 74 h AH; bottom row: 96 h AH). Brains were labeled with *insc*-Gal4>UAS-mcd8::GFP, visualizing secondary lineages. For each column, one lineage and MB (as reference; ML: medial lobe; SP/PED: spur/peduncle; VL: vertical lobe) were graphically isolated using the FIJI paint tool to manually erase all labeled lineages except the one to be illustrated. Green asterisk indicates cell body cluster; red and blue arrowheads point at tip of advancing axon tracts. Left column (A–E) shows lineage DALv1 which has started to extend its axon tract already at 27 h (A) and has reached midline by 64 h (C). Center column (F–J) illustrates lineage pair DALcm1/2, which makes its first appearance at 48 h (G) and starts to emit axons at 64 h (H), reaching midline in the late third instar larva (J). Right column (K–O) shows lineages DAMd1-3. DAMd1 is represented by faintly *insc*-positive neuroblast at 27 h (K) and emits a medially directed tract around 48 h (L). The pair DAMd2/3 produces a posteriorly directed tract at 64 h (M, blue arrowhead). Scale bar: 20 μm.

Table 2 Secondary Lineage Tracts

A Lineage	B #	C Type	D Tracts	E p35	F p35	A Lineage	B #	C Type	D Tracts	E p35	F p35
BAla1	1	I H1		1	BAla3/4	DPLm2	47	I H2	u	2	
BAla2	2	I H1				DPLp1	48	I H2	Ma	2	
BAla3	3	I H1		1	n	DPLp2	49	I H1		1	CP2/3
BAla4	4	I H1				DPLpv	50	I H2	u	2	
Balc	5	I H2	dv	2		DPMl1	51	I H2	u	2	
BAlp1	6	I H1		1	p *	DPMl34		I 2	u	2	
BAlp2	7	I H1		1	p *	DPMm1	53	II			
BAlp3	8	I H1		1	n *	DPMm2	54	I H1		1	p
BAlp4	9	I H1		2		DPMpl1	55	I H1		2	
Balv	10	I H1		2		DPMpl2	56	I H1		1	n
BAmas1	11	I H1		1	TRdm	DPMpl3	57	I H1		1	p *
BAmas2	12	I H1		1	p *	DPMpm1	58	II			
BAmd1	13	I H2	dv	2		DPMpm2	59	II			
BAmd2	14	I H1		1	DAMd2/3	CM1	60	II			
BAmv1	15	I H2	Pd	2		CM3	61	II			
BAmv2	16	I H1		2		CM4	62	II			
BAmv3	17	I H1		2		CM5	63	I H1		2	
DALcl1	18	I H2	dV	2		CP1	64	I H2	Dv	2	
DALcl2	19	I H2		2		CP2	65	II			
DALcm1	20	I H2	Mv	2		CP3	66	II			
DALcm2	21	I H2		2		CP4	67	I H1		2	
DALd	22	I H1		2		BLAd1	68	I H1		1	p
DALl1	23	I H2	u	2		BLAd2	69	I H1			
DALl2	24	I H1		1	DALl1	BLAd3	70	I H1			
DALv1	25	I H1		1	p *	BLAd4	71	I H1			
DALv2	26	I H1		1	DALcl1/2	BLAl	72	I H2	u	2	
DALv3	27	I H2		2		BLAv1	73	I H2	mP	2	
DAMd1	28	I H1		1	p	BLAv2	74	I H2	mP	2	
DAMd2	29	1		1	n *	BLAvm	75	I H2	mP	2	
DAMd3	30	1				BLD1	77	I H2	u	2	
DAMv1	31	I H2	u	2		BLD4	80	I H2	u	2	
DAMv2	32	I H2		2		BLD2	78	I H1		n	
DPLal1	33	I H1		1	DPLal2/3	BLD3	79	I H2	u	2	
DPLal2	34	I H2	Dv	2		BLD5	82	I H1		1	BLAl
DPLal3	35	I H2		2		BLD6	83	I H1		1	p
DPLam	36	I H1		1	n	BLP1	84	I H1		2	
DPLc1	37	I H1		2		BLP2	85	I H1		1	p
DPLc2	38	I H1		v	p	BLP3	86	I H1		2	
DPLc4	40	I H2	u	2		BLP4	87	I H1		2	
DPLc3	39	I H1		2		BLVa1	89	I H1		u	
DPLc5	41	I H2	aP	2		BLVa2	90	I H1		u	
DPLd	42	I H2	mP	2		BLVa3	91	I H1		1	BLVa1/2
DPLl1	43	I H1		2		BLVa4	92	I H1			
DPLl2	44	I H2	u	2		BLVp1	93	I H2	Dv	2	
DPLl3	45	I H2		2		BLVp2	94	I H2	u	2	
DPLm1	46	I H1		1	n *						

Column (A): lineage name; column (B) number used for lineage in Supporting Information Figures S2 and S3. Column (C): classification of lineage (I H1: type I lineage with one axon tract; I H2: type I lineage with two tracts; II: type II lineage). Column (D): designation of lineage tracts (see Lovick et al., 2013, Table 2; a or A: anterior; d or D dorsal; m or M: medial; p or P posterior; v or V ventral). If capital letter is used, corresponding tract extended earlier than its partner written in lower case (e.g., "Dv" in lineage pair DPLal2/3 indicates that the dorsal tract of DPLal2/3 appeared earlier than the ventral tract). Letter "u" indicates that order of appearance of tracts remains undetermined. Column (E) reports effect of expression of UAS-p35 in corresponding lineage (1 supernumerary tract present; 2 no supernumerary tract). Dark gray shading marks lineages where no supernumerary tract was observed despite the fact that only a single tract exists in wild type (see column C). Light gray shading labels members of lineage pairs/groups where presence or absence of supernumerary tracts could not be ascertained. Column (F): trajectories of supernumerary tracts caused by UAS-p35. If tract followed another, established lineage tract, the corresponding lineage name is given. Letter "p" stands for cases where supernumerary tract extended parallel to the regular tract of corresponding lineage; "n" indicates novel trajectories (not encountered in wild type brains). Asterisks marks cases where supernumerary tracts appeared in only a fraction of preparations analyzed.

dorsally and projects through the characteristic crescent formed by the tract of lineages DPLal1-3 toward the domain surrounding the peduncle of the MB [Fig. 3(E,F)]. In animals over-expressing p35 in secondary neurons, an additional branch emerged from DPLam that projected laterally, following a trajectory that does not exist in normal brains [arrowhead in Fig. 3(G,H)].

In some lineages, supernumerary tracts follow pathways that are prefigured by their corresponding primary neurons. The concept is schematically illustrated in Figure 3(O) and exemplified in Figure 3(I–N). The example shown is lineage BAmd2 whose secondary neurons follow a single tract directed ventro-medially into the antennal lobe commissure, following the ventral ("v") tract of BAmd1 [Fig. 3(I,J)]. Following p35

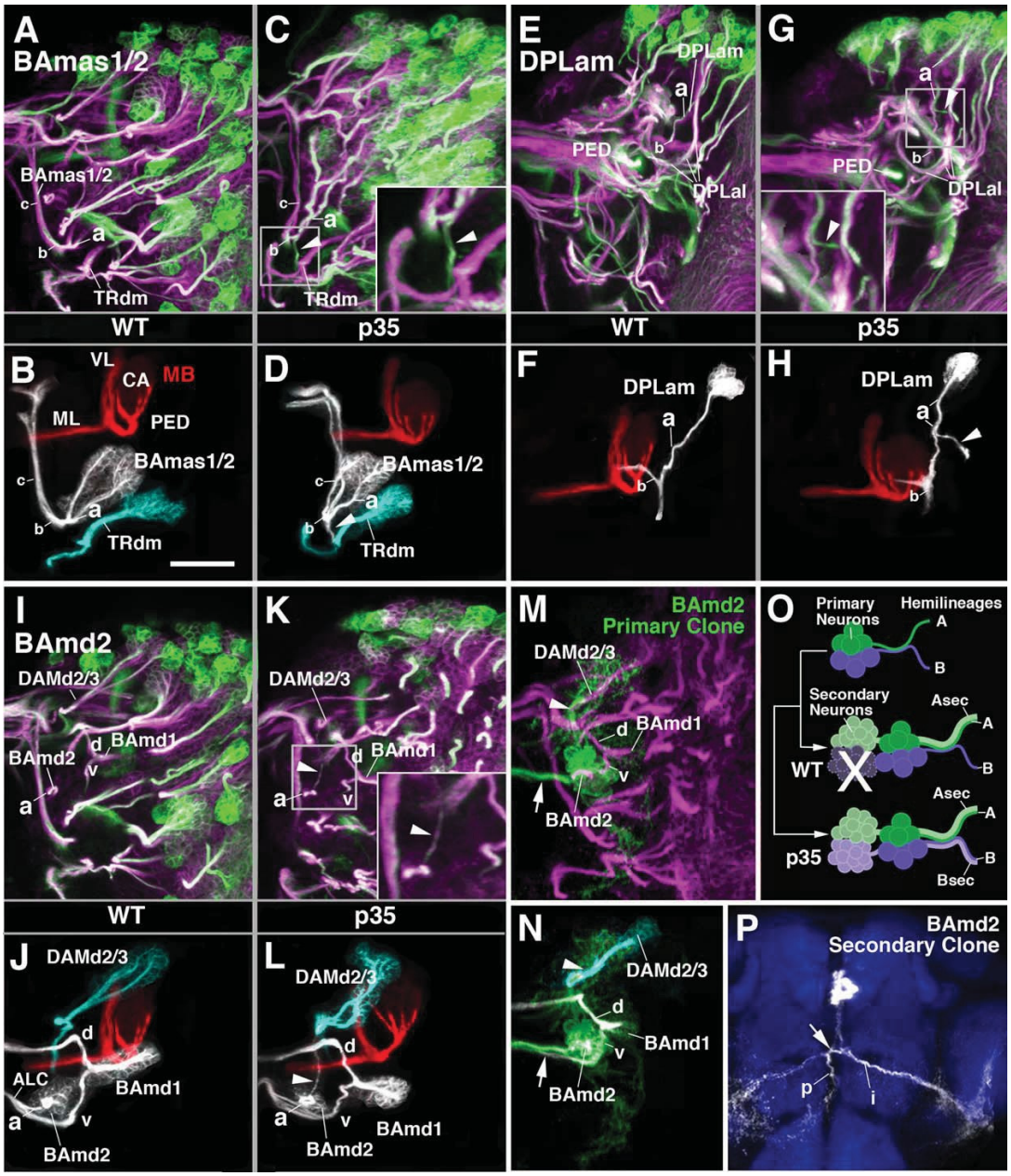

over-expression, a thin supernumerary tract branches off the BAmd2 tract and projects dorso-posteriorly, following the axon bundle formed by the DAMd2/3 lineages [arrowhead in Fig. 3(K,L)]. A GFP-labeled clone of primary neurons of BAmd2 showed axons that followed both the ventral pathway [arrow in Fig. 3(M,N)] and dorsal pathway [arrowhead in Fig. 3(M,N)]; a clone of secondary neurons, as expected, has only neurons projecting ventrally [arrow in Fig. 3(P)]. We surmise that the two pathways of primary neurons correspond to the two primary hemilineages of BAmd2, as suggested schematically in Figure 3(O) (top). Taken together, these findings imply that during the primary phase of BAmd2 proliferation in the embryo, both hemilineages (A and B) survive and differentiate [Fig. 3(O), top]. During the secondary phase of proliferation, one hemilineage [arbitrarily called B in Fig. 3(O), center] undergoes cell death, so that the SAT of BAmd2 has only an A-component. When p35 is over-expressed, the B component does not die and forms a supernumerary axon tract [Fig. 3(O), bottom].

Hemilineages of a Given Lineage Extend Axon Tracts at Different Time Points

In most Type I 2H lineages, extension of the hemilineage-associated SATs occurs at different time points (Table 2, Fig. 4). The pair DPLal2/3 forms a dorsal tract, shared with DPLal1, that grows out between 48 and 74 h AH [red arrowhead in Fig. 4(B,C)], and a ventral tract that appears later, between 74 and 96 h AH [cyan arrowhead in Fig. 4(D)]. Two similar examples are illustrated in Figure 4(E–H): The pair DALcl1/2 forms a ventral tract passing underneath the spur of the MB (red arrowhead) and a dorsal tract passing above the peduncle (cyan arrowhead); the former forms between 20 and 48 h AH, the latter between 64 and 96 h AH. The lineages BLAv1 and BLAvm each possess a posterior tract extending posteriorly between 20 and 48 h AH (yellow arrowheads) and a medial tract passing medially over the anterior surface of the ventrolateral protocerebrum (VLP) between 74 and 96 h AH (magenta arrowheads).

Morphogenetic Movements of Lineages During Larval Brain Growth

Between hatching and the third larval instar, the brain undergoes a substantial increase in volume due to the proliferation of secondary lineages, the growth of the optic lobe, and continued branching of primary neurons. As a result of these events, the cell body clusters of many secondary lineages and, in some cases also the point of entry of SATs, shift in position (Fig. 5, Supporting Information Fig. S3). The most

---

Figure 3 Identification of hemilineages that undergo programmed cell death during normal development. (A–L) z-projections of frontal confocal sections of late third instar brain hemispheres (medial to the left) in which secondary lineages are labeled by *ase*-Gal4>UAS-mcd8::GFP (green) and anti-Neurotactin (BP106; magenta). Panels are organized in sets of four (A–D, E–H, I–L) focusing on a specific lineage (A–D: BAmas1/2; E–H: DPLam; I–L: BAmd2). In lower pair of each quartet (B/D, F/H, J/L), the lineage or lineage pair was graphically isolated and is shown in white; isolated mushroom body (MB; CA calyx; ML medial lobe; PED peduncle; VL vertical lobe) is shown in red for reference. Left two panels of each quartet (A/B; E/F; I/J) show wild-type, right ones (C/D, G/H, K/L) illustrate phenotype following *ase*-Gal4-driven expression of UAS-p35. (A–D) Trajectory of the paired tract of BAmas1/2 is indicated by letters "a" (proximal segment), "b" (turn), and "c" (distal, ascending segment). In brain expressing p35 (C, D) an ectopic tract branches off the turn "b" (arrowhead in C, D; see inset in C for higher magnification) and joins the SAT of lineage TRdm (shown in cyan). (E–H) Proximal and distal segment of tract of DPLam is marked by letters "a" and "b," respectively. Ectopic branch (arrowhead in G, H) projects laterally in p35 brain. (I–L) Lineages BAmd1 and BAmd2 enter the anterior neuropil at a location right underneath the medial lobe. BAmd1 branches into a dorsal (d) and ventral (v) tract; BAmd2, in wild type, has only a ventral tract (a). In p35 brain, BAmd2 forms ectopic dorsal branch (arrowhead in K, L) which joins the SAT of DAMd2/3 (shown in cyan). (M–P) Ectopic secondary branch of BAmd2 follows a trajectory established by primary BAmd2 lineage. (M, N) z-projection of frontal confocal sections of third larval instar brain in which the primary BAmd2 lineage is visualized as a GFP-labeled flp-out clone (green; see Material and Methods). Secondary lineages are globally labeled by BP106 (magenta). Note that primary BAmd2 emits a ventral branch (arrow) and a dorsal branch (arrowhead). The dorsal branch follows the same, posteriorly-directed pathway as DAMd2/3 (cyan in panel N). (O) Schematic presenting development of BAmd2 (and, possibly other) lineages: Primary neurons include two hemilineages, called (arbitrarily) A and B; following secondary phase of proliferation, only one secondary hemilineage ("Asec") differentiates and follows the pathway of the corresponding primary hemilineage, whereas the other one ("Bsec") undergoes programmed cell death. "Bsec" is rescued by expression of p35. (P) MARCM clone of differentiated secondary BAmd2 lineage in adult brain (white; neuropil labeled by anti-DNcad [blue]; from Wong et al., 2013). BAmd2 possesses only a ventral tract (arrow) that gives off a posterior contralateral branch (p) and an ipsilateral branch (i). Scale bar: 40 μm (for all panels).

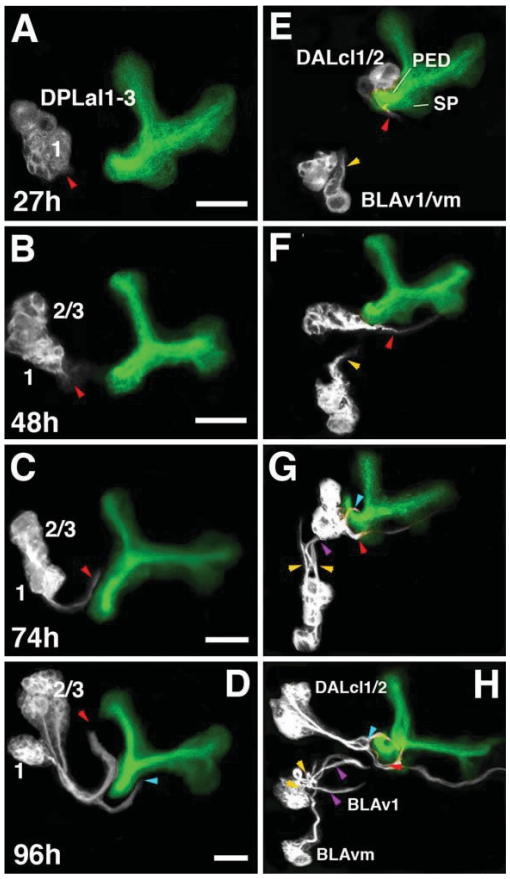

Figure 4 Hemilineage tracts of a given lineage extend at different time points. Panels show parts of z-projections of frontal confocal sections of larval brain hemispheres imaged at sequential stages (panels of first row: 27 h AH; second row: 48 h AH; third row: 74 h AH; bottom row: 96 h AH). Brains were labeled with *insc*-Gal4>UAS-mcd8::GFP, visualizing secondary lineages. For each column, one or two lineage(s) and MB (as reference; green) were graphically isolated (see Material and Methods). Red and blue arrowheads point at tip of advancing hemilineage tracts. Left column (A–D) shows lineages DPLal1-3. In late larva (D), all three of these have a hemilineage extending a crescent-shaped, dorsally-directed hemilineage tract (red arrowhead; see also Lovick et al., 2013; Wong et al., 2013). In addition, DPLal2/3 form a ventral hemilineage tract (cyan arrowhead). Between 27 and 74 h AH (A–C), only the dorsal tract is present. Right column (E–H) illustrates lineage pairs DALcl1/2 and BLAv1/vm. In late larva (H), DALcl1/2 possess two hemilineage tracts, one passing underneath (red arrowhead), the other over (cyan arrowhead) the MB peduncle. The ventral tract extends at an early stage (27 h; E), the dorsal one later (74 h; G). Similarly, BLAv1/vm form posteriorly directed tracts (yellow arrowheads) before medially directed ones (magenta arrowheads). Scale bar: 20 /m.

significant movements of lineage clusters can be observed in the lateral brain, where the optic lobe neuropils and the fiber systems connecting the optic lobe to the central brain emerge. Here, lineages that initially emerge at the lateral surface of the brain [BAlp, BLA, BLD, BLP, BLV; Fig. 5(A)] are displaced toward anteriorly (BAlp, BLA), dorsally (BLD), or posteriorly [BLP, BLV; Fig. 5(B)]. Likewise, the antennal lobe and lineages grouped around it (BAla, BAmas, BAmv), start out at a fairly lateral position (Supporting Information Fig. S4D) and shift medially in the late larva (Supporting Information Fig. S4J). Growth of the LAL and the lateral appendix of the medial lobe are accompanied by a moving-apart of lineages of the BA and DAL groups (compare distance between DALcl, DALv, and BAmv in Supporting Information Fig. S4D vs. J). At the dorsal brain surface, the expansion of the superior protocerebrum is accompanied by a shift toward posterior of the DPM lineages (note increasing gap between the DPM and the DAM group in Supporting Information Fig. S4F,I,L).

To test whether the movement of lineage clusters could be altered by blocking growth of certain parts of the brain, we ablated the optic lobe by expressing a dominant negative construct of EGFR in the embryonic anlage of the optic lobe, using the driver line *so*-Gal4 (Chang et al., 2003a,b; Fig. 5). Following this genetic manipulation, late larval brains lack the epithelial optic lobe anlagen (IOA, OOA) and the neurons produced by them [compare Fig. 5(C,F)]. Lineages of the central brain develop their normal trajectories [Fig. 5(F)], even though lineage clusters, in particular those of the lateral half of the brain, have a location that is significantly different from that of the wild type [compare Fig. 5(E)]. This finding implies that the growth of the optic lobe is causally related to the displacement of the cell bodies of central brain lineages that occurs during normal development; it also implies that the SAT trajectories do not react measurably if the normal displacement is blocked.

DISCUSSION

Secondary Neuroblasts at the Onset of Proliferation

Secondary lineages, visualized with global markers, can be traced from the time of their first appearance in the early larva throughout the remainder of the larval period. Analysis of larval brains labeled with global markers at close intervals enabled us to

reconstruct the early "life history" of most secondary lineages. *insc*-Gal4 appears in neuroblasts several hours prior to their first mitosis. Premitotic, spindle-shaped neuroblasts, labeled by *insc*-Gal4, and the gene *deadpan* (Bier et al., 1992), are located at various depths within the cortex and emit a thin basal process toward the surface of the neuropil, much like early secondary neuroblasts of the larval ventral

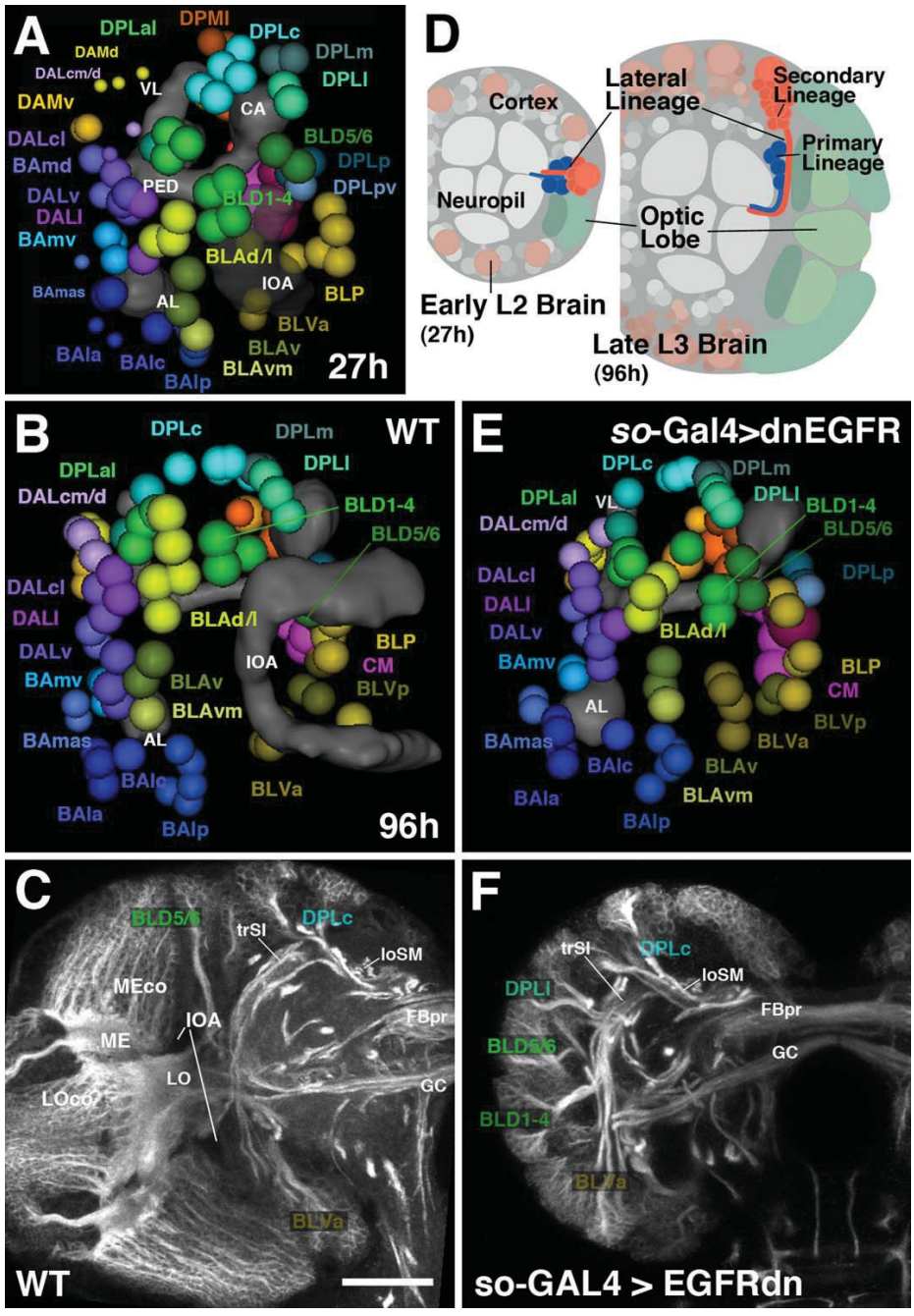

nerve cord (Truman and Bate, 1988; Chell and Brand, 2010). Embryonic (primary) neuroblasts do not possess a basal process, suggesting that this structure is not required for neuroblast proliferation, but may be important for the guidance of secondary neurons. Thus, basal processes attach to the neuropil at the entry point of primary axon tracts and serve to not only anchor the neuroblast in the cortex, but also allow secondary neurons, which are born in close contact with their older (primary) siblings, to extend their axons along the primary axon tract.

From an evolutionary/developmental perspective, it is tempting to speculate that the basal process hints at the "neuronal nature" of a neuroblast. In this view, a neuroblast might be seen as a neuron inhibited from differentiation and instead prompted to proliferate. After blocking cell division through mutations in the cell cycle regulator *string*, embryonic neuroblasts differentiate into neurons, expressing neuronal markers and producing axonal processes (Hartenstein and Posakony, 1990; Harris and Hartenstein, 1991). The basal process formed by neuroblasts during their time of mitotic quiescence could represent a rudimentary axon which then is retracted on entry into the mitotic cycle.

In a previous study (Lovick and Hartenstein, 2015), we determined the time-point at which individual secondary lineages are born, defined by the onset of proliferation of the corresponding neuroblast, by applying the mitosis inhibitor HU, which selectively ablates proliferating neuroblasts and their neuronal progeny. Birth dates determined using the HU method closely match those found in this study. In the majority of cases, one can detect the neuroblast by its expression of *insc*-Gal4 several hours before the time at which it is ablated using HU (Table 1). The validated time table of the reactivation of neuroblast proliferation will assist us and others in developing strategies that target specific lineages for genetic manipulations.

Hemilineages of Most Brain Lineages are Lost Through Programmed Cell Death

Previous studies had indicated that axon tracts of hemilineages in the ventral nerve cord and brain typically enter the neuropil together, but then follow different pathways within the neuropil. Furthermore, in cases where a lineage, observed in the late larva or adult, emits only a single tract, this is the result of programmed cell death of one of the hemilineages (Kumar et al., 2009a; Truman et al., 2010). We provide evidence that, in most brain lineages with a single tract, one hemilineage undergoes cell death. Over expression of the caspase inhibitor p35 (Clem et al., 1991), which inhibits cell death in these lineages, results in the appearance of an additional secondary tract. Supernumerary tracts are typically smaller than "regular" tracts and could be due to a delay in the action of p35 in inhibiting programmed cell death. Alternatively, neurons of "rescued" hemilineages may suffer from intrinsic defects in specification that cause them to lag behind in differentiation. It is significant that in all cases, supernumerary axons bundle together and form a single, highly invariant tract supporting the idea that these are a cohesive group (hemilineage) of cells rescued from programmed cell death. Furthermore, our data suggests that this supernumerary tract may reflect the pathway taken by the corresponding primary hemilineage tract. We directly show this for the lineage BAmd2. Primary clones demonstrate that BAmd2

Figure 5 Morphogenetic movements of secondary lineages during the larval period. (A–C) Wild-type. Panels A and B show digital 3D models of larval brain hemispheres at two sequential stages (A: 27 h AH; B: 96 h AH; both lateral view, anterior to the left). Models are based on confocal stacks of brains in which secondary lineages are labeled by *insc*-Gal4>UAS-mcd8::GFP (see Supporting Information Figs. S1 and S2). Centers of cell body clusters of lineages are depicted as colored spheres. Differential coloring associates lineages to particular, topologically defined groups (for color key and more comprehensive representation of lineages at consecutive larval stages, see Supporting Information Fig. S3). Mushroom body (CA calyx; ML medial lobe; PED peduncle; SP spur; VL vertical lobe), antennal lobe (AL), and inner optic anlage (IOA) are shown for reference (gray). Panel (C) represents z-projection of frontal confocal sections at level of great commissure (GC) and fan-shaped body primordium (FBpr). Secondary lineages are labeled by anti-Neurotactin (BP106). In late larva (B, C), the optic lobe primordium (LO lobula neuropile; LOco lobula cortex; ME medulla neuropil; MEco medulla cortex) has grown to cover the entire lateral surface of the brain. Lineages located in the lateral brain hemisphere at an early stage (A) shift centrifugally to more anterior (BLA lineages), dorsal (BLD and DPLl/DPLc lineages), posterior (BLP and DPLp lineages), or ventral (BLV) positions. This morphogenetic shift is shown schematically in panel (D). (E, F): Topology of secondary lineages in 96h larval brain following ablation of optic lobe primordium by *so*-Gal4>UAS-dnEGFR. Panels show digital 3D model of lineages (E) and z-projection of BP106-labeled brain (F) at same orientation and magnification as those in adjacent (B) and (C), respectively. Notice absents of optic lobe primordium in (F); compare to (C). Scale bar: 40 μm (for all panels). Additional abbreviations: loSM longitudinal superior medial fascicle; trSI intermediate superior transverse fascicle.

projects a ventral and a dorsal (hemilineage) primary tract, whereas the secondary BAmd2 has only a ventral tract. When cell death is inhibited, the supernumerary secondary tract extends along a dorsal trajectory, much like the dorsal primary tract. This implies that (1) BAmd2 forms two intact hemilineages in the embryo; (2) initiates both hemilineages, with tracts identical to the primary ones, during the secondary phase of proliferation; (3) completely eliminates the dorsal hemilineage via programmed cell death. We anticipate that clonal analysis of primary brain lineages (Jaison Omoto, Jennifer Lovick, and Volker Hartenstein in preparation) will reveal that this phenomenon of "secondary hemilineage elimination" applies to many brain lineages.

Differential expression of Notch has been shown to be important for delineating hemilineages in the ventral nerve cord (Truman et al., 2010) as well as subsets of lineages in the brain (Lin et al., 2010, 2012). Briefly, the Notch inhibitor Numb is segregated into one set of daughter cells, resulting in $Notch^{ON}$ (Notch signaling active; "A" fate) and $Notch^{OFF}$ (Notch signaling inhibited; "B" fate) sibling neurons. Most, if not all, lineages consist of A and B fated cells: in some lineages, Notch expression determines whether or not neurons undergo programmed cell death (Karcavich and Doe, 2005; S´anchez-Soriano et al., 2005; Kumar et al., 2009a; Lin et al., 2010, 2012; Truman et al., 2010) or it determines what type of neural fate a cell will adopt ($Notch^{ON}$ 5 local interneurons; $Notch^{OFF}$ 5 projection neurons; Lin et al., 2010, 2012). Notch has also been shown in numerous contexts to inhibit differentiation (e.g., high Notch activity in vertebrate neuroepithelial cells promotes proliferation and inhibits neuronal differentiation; Austin et al., 1995; Dorsky et al., 1995). We speculate that our finding that hemilineages of a given lineage (e.g., DALcl1/2, DPLal2/3; see Fig. 4) emit tracts at slightly different time points may also be the result of differential Notch activity in the corresponding neurons. It is possible that GMC daughter cells receiving high Notch activity are temporarily inhibited to differentiate and, as a result, lag behind their siblings in regard to axon extension. Systematic studies that correlate high versus low Notch levels with hemilineages of all lineages are required to substantiate this idea.

Movement of Secondary Neuroblasts and Lineages

In vertebrates, brain formation is accompanied by active migrations of undifferentiated neuronal precursors. Neurons are born apically within the pseudostratified neuroepithelium that forms the wall of the neural tube. Subsequently, neural precursors lose contact to the apical surface and migrate radially along the elongated neuroepithelial cells (at that point called radial glia) toward basally. In the brain, more widespread active migrations (or migratory streams) occur at certain locations, such as the rhombic lip (formation of the cerebellum; Wullimann et al., 2011) and the subpallium (inhibitory interneurons; Sultan et al., 2013). For a vertebrate neuron, the location of its cell body is of central importance for the structural properties of the network the neuron is engaged in. Thus, the cell body is the "center" from which dendritic and axonal processes sprout; if, for example, the cell body of a neuron is located in a deep cortical layer, dendrites of these cells are also typically focused in this region.

Circuit design is different in many invertebrates, including *Drosophila*, where the cell body of a neuron remains at the periphery of the neuropil, and dendritic or axonal branches occur at various distances from the cell body (S´anchez-Soriano et al., 2005). This implies that the location of the cell body is not as crucial for wiring as in vertebrates. Accordingly, active migration of neuronal cell bodies to reach defined positions at a distance from the location where they were born has not yet been documented. In most cases described in the literature (e.g., embryonic neurons: Lekven et al., 1998; lineages in the larval or adult brain: Pereanu and Hartenstein, 2006; Ito et al., 2013; Wong et al., 2013; Yu et al., 2013; this study), neurons born by the same neuroblast remain relatively close to each other. However, in some cases, substantial displacement of cell bodies, typically of entire hemilineages, has been observed (for example, lineages DPLl2/3 and BLVp1/2; Lovick et al., 2013; Wong et al., 2013). What remained constant is the location where axons entered (rather than merely touched) the neuropil. We speculate that at this location (as well as inside the neuropil) strong adhesive contacts are formed between the axons and its microenvironment (e.g., glia; other neurons). Once the neuropil grows during pupal development, the entry portals of the hemilineages shift further apart. Assuming that cell bodies are tethered to the portal by their proximal axon segments (i.e., the length of fiber between cell body and entry portal), one can imagine that the cell bodies are pulled along as the portals shift in position.

It is possible to interpret the large-scale displacement of lateral lineage clusters, which accompanies growth of the optic lobe, along similar lines. At an early stage of larval development (approximately

24–40 h post hatching) secondary neurons of lineages that are located in the lateral brain cortex, surrounding the small primordium of the optic lobe, emit axons that, following a short, straight path, enter the neuropil [Fig. 5(D)]. As the optic lobe grows, cell body clusters of these lineages are "pushed out of the way" toward more dorsal, ventral, anterior, and posterior positions. At the same time, the proximal segments of the axon tracts, bridging the distance between cell bodies and neuropil surface, lengthen [Fig. 5(D)]. Following ablation of the optic lobe primordium, cell bodies of lateral lineages remain at their original position, supporting the conclusion that these cells move passively as a result of the growing optic lobe primordium. The fact that the central trajectories of the axon tracts of lateral lineages are not altered despite gross abnormalities in cell body position supports the idea that pathfinding of secondary axons heavily depends on the primary tracts, as already proposed in previous studies (e.g., Spindler et al., 2009). Once the first secondary axons have latched on to the primary tract at the neuropil entry portal, the secondary tract is stabilized; later outgrowing axons merely follow their younger siblings.

The authors thank the members of the Hartenstein laboratory for critical discussions during the preparation of this manuscript. Authors are grateful to the Bloomington Stock Center and the Developmental Studies Hybridoma Bank for fly strains and antibodies. The authors declare no conflict of interest.

REFERENCES

Ashburner M. 1989. Drosophila. A Laboratory Manual. Cold Spring Harbor, NY: Cold Spring Harbor Laboratory Press. 214–217 p.

Austin CP, Feldman DE, Ida JA Jr, Cepko CL. 1995. Vertebrate retinal ganglion cells are selected from competent progenitors by the action of Notch. Development 121: 3637–3650.

Bello BC, Izergina N, Caussinus E, Reichert H. 2008. Amplification of neural stem cell proliferation by intermediate progenitor cells in Drosophila brain development. Neural Dev 3:5. doi:10.1186/1749-8104-3-5.

Betschinger J, Mechtler K, Knoblich JA. 2006. Asymmetric segregation of the tumor suppressor brat regulates self-renewal in Drosophila neural stem cells. Cell 124:1241–1253.

Bier E, Vaessin H, Younger-Shepherd S, Jan LY, Jan YN. 1992. Deadpan, an essential pan-neural gene in Drosophila, encodes a helix-loop-helix protein similar to the hairy gene product. Genes Dev 6:2137–2151.

Cardona A, Saalfeld S, Arganda I, Pereanu W, Schindelin J, Hartenstein V. 2010. Identifying neuronal lineages of Drosophila by sequence analysis of their axon tracts. J Neurosci 30:7538–7553.

Cardona A, Saalfeld S, Schindelin J, Arganda-Carreras I, Preibisch S, Longair M, Tomancak P, et al. 2012. TrakEM2 software for neural circuit reconstruction. PLoS One 7:e38011.

Chang T, Shy D, Hartenstein V. 2003a. Antagonistic relationship between Dpp and EGFR signaling in Drosophila head patterning. Dev Biol 263:103–113.

Chang T, Younossi-Hartenstein A, Hartenstein V. 2003b. Development of neural lineages derived from the sine oculis positive eye field of Drosophila. Arthropod Struct Dev 32:303–317.

Chell JM, Brand AH. 2010. Nutrition-responsive glia control exit of neural stem cells from quiescence. Cell 143: 1161–1173.

Clem RJ, Fechheimer M, Miller LK. 1991. Prevention of apoptosis by a baculovirus gene during infection of insect cells. Science 254:1388–1390.

Das A, Gupta T, Davla S, Prieto-Godino LL, Diegelmann S, Reddy OV, Raghavan KV, et al. 2013. Neuroblast lineage-specific origin of the neurons of the Drosophila larval olfactory system. Dev Biol 373:322–337.

de la Escalera S, Bockamp EO, Moya F, Piovant M, Jim´enez F. 1990. Characterization and gene cloning of neurotactin, a Drosophila transmembrane protein related to cholinesterases. Embo J 9:3593–3601.

Dorsky RI, Rapaport DH, Harris WA. 1995. Xotch inhibitis cell differentiation in the Xenopus retina. Neuron 14: 487–496.

Harris WA, Hartenstein V. 1991. Neuronal determination without cell division in Xenopus embryos. Neuron 6: 499–515.

Hartenstein V, Posakony JW. 1990. Sensillum development in the absence of cell division: The sensillum phenotype of the Drosophila mutant string. Dev Biol 138:147–158.

Hartenstein V, Rudloff E, Campos-Ortega JA. 1987. The pattern of proliferation of the neuroblasts in the wildtype embryo of Drosophila melanogaster. Wilhelm Roux's Arch Dev Biol 196:473–485.

Hartenstein V, Spindler S, Pereanu W, Fung S. 2008. The development of the Drosophila larval brain. Adv Exp Med Biol 628:1–31.

Hartenstein V, Younossi-Hartenstein A, Lovick J, Kong A, Omoto J, Ngo K, Viktorin G. Lineage-associated tracts defining the anatomy of the Drosophila first instar larval brain. Dev Biol. 2015 Jun 30. pii: S0012-1606(15)30027-0. doi: 10.1016/j.ydbio.2015.06.021. [Epub ahead of print]. PMID:26141956.

Ito K, Hotta Y. 1992. Proliferation pattern of postembryonic neuroblasts in the brain of Drosophila melanogaster. Dev Biol 149:134–148.

Ito M, Masuda N, Shinomiya K, Endo K, Ito K. 2013. Systematic analysis of neural projections reveals clonal composition of the Drosophila brain. Curr Biol 23:644–655.

Jan YN, Jan LY. 2010. Branching out: Mechanisms of dendritic arborization. Nat Rev Neurosci 11:316–328.

Jefferis GS, Marin EC, Komiyama T, Zhu H, Chihara T, Berdnik D, Luo L. 2005. Development of wiring specificity of the Drosophila olfactory system. Chem Senses Suppl1:i94.

Jefferis GS, Marin EC, Watts RJ, Luo L. 2002. Development of neuronal connectivity in Drosophila antennal lobes and mushroom bodies. Curr Opin Neurobiol 12:80–86.

Kang KH, Reichert H. 2015. Control of neural stem cell self-renewal and differentiation in Drosophila. Cell Tissue Res 359:33–45.

Karcavich R, Doe CQ. 2005. Drosophila neuroblast 7-3 cell lineage: A model system for studying programmed cell death, Notch/Numb signaling, and sequential specification of ganglion mother cell identity. J Comp Neurol 481: 240–251.

Kuert PA, Bello BC, Reichert H. 2012. The labial gene is required to terminate proliferation of identified neuroblasts in postembryonic development of the Drosophila brain. Biol Open 1:1006–1015.

Kuert PA, Hartenstein V, Bello BC, Lovick JK, Reichert H. 2014. Neuroblast lineage identification and lineage-specific Hox gene action during postembryonic development of the subesophageal ganglion in the Drosophila central brain. Dev Biol 390:102–115.

Kumar A, Bello B, Reichert H. 2009a. Lineage-specific cell death in postembryonic brain development of Drosophila. Development 136:3433–3442.

Kumar A, Fung S, Lichtneckert R, Reichert H, Hartenstein V. 2009b. The arborization pattern of engrailed-positive neural lineages reveal neuromere boundaries in the Drosophila brain neuropile. J Comp Neurol 517:87–104.

Larsen C, Shy D, Spindler S, Fung S, Younossi-Hartenstein A, Hartenstein V. 2009. Patterns of growth, axonal extension and axonal arborization of neuronal lineages in the developing Drosophila brain. Dev Biol 335:289–304.

Lee T, Lee A, Luo L. 1999. Development of the Drosophial mushroom bodies: Sequential generation of three distinct types of neurons from a neuroblast. Development 126: 4065–4076.

Lekven AC, Tepass U, Keshmeshian M, Hartenstein V. 1998. Faint sausage encodes a novel extracellular protein of the immunoglobulin superfamily required for cell migration and the establishment of normal axonal pathways in the Drosophila nervous system. Development 125:2747–2758.

Lichtneckert R, Bello B, Reichert H. 2007. Cell lineage-specific expression and function of the empty spiracles gene in adult brain development of Drosophila melanogaster. Development 134:1291–1300.

Lin S, Kao CF, Yu HH, Huang Y, Lee T. 2012. Lineage analysis of Drosophila lateral antennal lobe neurons reveals notch-dependent binary temporal fate decisions. PLoS Biol 10:e1001425.

Lin S, Lai SL, Yu HH, Chihara T, Luo L, Lee T. 2010. Lineage-specific effects of Notch/Numb signaling in post-embryonic development of the Drosophila brain. Development 137:43–51.

Lin S, Lee T. 2012. Generating neuronal diversity in the Drosophila central nervous system. Dev Dyn 241:57–68.

Lin S, Marin EC, Yang CP, Kao CF, Apenteng BA, Huang Y, O'Connor MB, et al. 2013. Extremes of lineage plasticity in the Drosophila brain. Curr Biol 23:1908–1913.

Lüdhr R, Godenschwege T, Buchner E, Prokop A. 2002. Compartmentalisation of central neurons in Drosophila: A new strategy of mosaic analysis reveals localization of pre-synaptic sites to specific segments of neurites. J Neurosci 22:10357–10367.

Lovick JK, Ngo KT, Omoto JJ, Wong DC, Nguyen JD, Hartenstein V. 2013. Postembryonic lineages of the Drosophila brain: I. Development of the lineage-associated fiber tracts. Dev Biol 384:228–257.

Lovick J, Hartenstein V. 2015. Hydroxyurea-mediated neuroblast ablation establishes birthdates of secondary lineages and addresses neuronal interactions in the developing Drosophila brain. Dev Biol 402:32–47.

Pereanu W, Hartenstein V. 2006. Neural lineages of the Drosophila brain: A 3D digital atlas of the pattern of lineage location and projection at the late larval stage. J Neurosci 26:5534–5553.

Prokop A, Bray S, Harrison E, Technau GM. 1998. Homeotic regulation of segment-specific differences in neuroblast numbers and proliferation in the Drosophila central nervous system. Mech Dev 74:99–110.

Prokop A, Technau GM. 1991. The origin of postembryonic neuroblasts in the ventral nerve cord of Drosophila melanogaster. Development 111:79–88.

Rusan NM, Peifer M. 2007. A role for a novel centrosome cycle in asymmetric cell division. J Cell Biol 9:13–20.

Sánchez-Soriano N, Lüdhr R, Bottenberg W, Haessler U, Kerassoviti A, Knust E, Fiala A, et al. 2005. Are dendrites in Drosophila homologous to vertebrate dendrites?. Dev Biol 288:126–138.

Schindelin J, Arganda-Carreras I, Frise E, Kaynig V, Longair M, Pietzsch T, Preibisch S, Rueden C, Saalfeld S, Schmid B, Tinevez JY, White DJ, Hartenstein V, Eliceiri K, Tomancak P, Cardona A. 2012. Fiji: an open-source platform for biological-image analysis. Nat Methods 9: 676–682.

Sen S, Cao D, Choudhary R, Biagini S, Wang JW, Reichert H, VijayRaghavan K. 2014. Genetic transformation of structural and functional circuitry rewires the Drosophila brain. eLife 2014;3:e04407.

Skeath JB, Thor S. 2003. Genetic control of Drosophila nerve cord development. Curr Opin Neurobiol 13:8–15.

Spindler SR, Ortiz I, Fung S, Takashima S, Hartenstein V. 2009. Drosophila cortex and neuropile glia influence secondary axon tract growth, pathfinding, and fasciculation in the developing larval brain. Dev Biol 334:355–368.

Sultan KT, Brown KN, Shi SH. 2013. Production and organization of neocortical interneurons. Front Cell Neurosci 7:221. doi: 10.3389/fncel.2013/00221.

Tabata T, Schwartz C, Gustavson E, Ali Z, Kornberg TB. 1995. Creating a Drosophila wing de novo, the role of

engrailed, and the compartment border hypothesis. Development 121:3359–3369.

Truman JW, Bate M. 1988. Spatial and temporal patterns of neurogenesis in the central nervous system of Drosophila melanogaster. Dev Biol 125:145–157.

Truman JW, Moats W, Altman J, Marin EC, Williams DW. 2010. Role of Notch signaling in establishing the hemilineages of secondary neurons in Drosophila melanogaster. Development 137:53–61.

Truman JW, Schuppe H, Shepherd D, Williams DW. 2004. Developmental architecture of adult-specific lineages in the ventral CNS of Drosophila. Development 131:5167–5184.

Urbach R, Technau GM. 2003a. Molecular markers for identified neuroblasts in the developing brain of Drosophila. Development 130:3621–3637.

Urbach R, Technau GM. 2003b. Early steps in building the insect brain: Neuroblast formation and segmental patterning in the developing brain of different insect species. Arthropod Struct Dev 32:103–123.

Wong DC, Lovick JK, Ngo KT, Borisuthirattana W, Omoto JJ, Hartenstein V. 2013. Postembryonic lineages of the Drosophila brain: II. Identification of lineage projection patterns based on MARCM clones. Dev Biol 384: 258–289.

Wullimann MF, Mueller T, Distel M, Babaryka A, Grothe B, K€oster RW. 2011. The long adventurous journey of rhombic lip cells in jawed vertebrates: A comparative developmental analysis. Front Neuroanat 5:27. doi: 10.3389/fnana.2011.00027.

Yoo SJ, Huh JR, Muro I, Yu H, Wang L, Wang SL, Feldman RM, et al. 2002. Hid, Rpr and Grim negatively regulate DIAP1 levels through distinct mechanisms. Nat Cell Biol 4:416–424.

Yu HH, Awasaki T, Schroeder MD, Long F, Yang JS, He Y, Ding P, et al. 2013. Clonal development and organization of the adult Drosophila central brain. Curr Biol 23: 633–643.

Yu HH, Kao CF, He Y, Ding P, Kao JC, Lee T. 2010. A complete developmental sequence of a Drosophila neuronal lineage as revealed by twin-spot MARCM. PLoS Biol 8:e1000461. pii:

Zecca M, Struhl G. 2002. Subdivision of the Drosophila wing imaginal disc by EGFR-mediated signaling. Development 129:1357–1368.

Zhu S, Chiang AS, Lee T. 2003. Development of the Drosophila mushroom bodies: Elaboration, remodeling and spatial organization of dendrites in the calyx. Development 130:2603–2610.

Zhu S, Lin S, Kao CF, Awasaki T, Chiang AS, Lee T. 2006. Gradients of the Drosophila Chinmo BTB-zinc finger protein govern neuronal temporal identity. Cell 127: 409–422.

Chapter 5

Postembryonic lineages of the *Drosophila* brain: I. Development of the lineage-associated fiber tracts

Postembryonic lineages of the *Drosophila* brain: I. Development of the lineage-associated fiber tracts

Jennifer K. Lovick, Kathy T. Ngo, Jaison J. Omoto, Darren C. Wong, Joseph D. Nguyen, Volker Hartenstein [n]

article info

Article history:
Received 27 March 2013
Received in revised form
11 July 2013
Accepted 11 July 2013
Available online 20 July 2013

Keywords:
Brain
Lineage
Circuitry
Drosophila
Mapping
Metamorphosis

abstract

Neurons of the *Drosophila* central brain fall into approximately 100 paired groups, termed lineages. Each lineage is derived from a single asymmetrically-dividing neuroblast. Embryonic neuroblasts produce 1,500 primary neurons (per hemisphere) that make up the larval CNS followed by a second mitotic period in the larva that generates approximately 10,000 secondary, adult-specific neurons. Clonal analyses based on previous works using lineage-specific Gal4 drivers have established that such lineages form highly invariant morphological units. All neurons of a lineage project as one or a few axon tracts (secondary axon tracts, SATs) with characteristic trajectories, thereby representing unique hallmarks. In the neuropil, SATs assemble into larger fiber bundles (fascicles) which interconnect different neuropil compartments. We have analyzed the SATs and fascicles formed by lineages during larval, pupal, and adult stages using antibodies against membrane molecules (Neurotactin/Neuroglian) and synaptic proteins (Bruchpilot/N-Cadherin). The use of these markers allows one to identify fiber bundles of the adult brain and associate them with SATs and fascicles of the larval brain. This work lays the foundation for assigning the lineage identity of GFP-labeled MARCM clones on the basis of their close association with specific SATs and neuropil fascicles, as described in the accompanying paper (Wong et al., 2013. Postembryonic lineages of the Drosophila brain: II. Identification of lineage projection patterns based on MARCM clones. Submitted.).

Introduction

The central brain and ventral ganglion of *Drosophila* is formed by an estimated 30,000 neurons which are generated from a pool of embryonically-derived stem cells, called neuroblasts, in a fixed lineage mechanism. This means that each neuroblast represents a genetically-distinct cell, characterized by the expression of a specific set of transcription factors (Doe, 1992; Urbach et al., 2003; Urbach and Technau, 2003a, 2003b). Each neuroblast gives rise to a group of neurons that is consistent in type and number across all individuals. Embryonic neuroblasts undergo several (5–10) rounds of asymmetric divisions, generating lineages of primary neurons that differentiate and make up the functional larval CNS (Larsen et al., 2009). After a period of mitotic quiescence that extends from late embryogenesis to the end of the first larval instar, neuroblasts enter a second, longer phase of proliferation which gives rise to adult-specific secondary neurons. Lineages constitute units, not only in terms of development (shared gene expression with the parent neuroblast), but also in terms of morphology. In most cases, all neurons of a given lineage extend their axons as one or two coherent fiber bundles along invariant trajectories in the brain neuropil and innervate a specific set of neuropil compartments (Hartenstein et al., 2008; Ito and Awasaki, 2008). Well-described examples are the four mushroom body lineages (Crittenden et al., 1998; Ito et al., 1997) and the four lineages that interconnect the antennal lobe (olfactory center) with the mushroom body input domain, the calyx (Das et al., 2008, 2013; Lai et al., 2008; Stocker et al., 1990; Yu et al., 2010). The development and anatomical projection of most lineages remains largely unknown; ascertaining this knowledge and using it to generate an accurate map of *Drosophila* brain circuitry at the level of neuron populations ("macro-circuitry") is an important project followed by us and others over the past several years.

Previous studies have provided detailed analyses of the lineages of the central brain, ventral ganglion ("ventral nerve cord"), and optic lobe at the embryonic and late larval stage, as well as of specific neural subtypes in the adult CNS (Bausenwein et al., 1992; Fischbach and Dittrich, 1989; Helfrich-Förster et al., 2007; Huser et al., 2012; Kunz et al., 2012; Mao and Davis, 2009; Pereanu and Hartenstein, 2006; Schmidt et al., 1997; Seibert and

0012-1606/$ - see front matter
http://dx.doi.org/10.1016/j.ydbio.2013.07.008

Urbach, 2010; Shafer et al., 2006; Sprecher et al., 2011; Stocker et al., 1990; Truman et al., 2004). In the embryo, lineages are represented by their parent neuroblasts, which have been mapped with respect to gene expression patterns and several anatomical landmarks (Doe, 1992; Hartenstein and Campos-Ortega, 1984; Urbach et al., 2003; Urbach and Technau, 2003a, 2003b; Younossi-Hartenstein et al., 1996). Systematic dye-labeling of neuroblasts has been used to image primary lineages of the ventral nerve cord at the late embryonic stage (Bossing et al., 1996; Schmid et al., 1999; Schmidt et al., 1997). Detailed knowledge of lineages also exists for the late larval stage, where maps of the secondary lineages of the ventral nerve cord (Truman et al., 2004) and brain (Cardona et al., 2010a; Dumstrei et al., 2003a; Pereanu and Hartenstein, 2006) were generated. At the late larval stage, antibody markers reveal secondary neuronal cell bodies and their characteristic fiber bundles (secondary axon tracts or SATs), most of which have been born by this time. Lineages are defined by several traits: the position at which an SAT enters the neuropil and the pathway it follows, giving each a distinct morphological profile. MARCM labeling (Lee and Luo, 2001) of secondary lineages provided an additional level of detail. Furthermore, for a small number of lineages, identified lacZ and Gal4 reporters (Brand and Perrimon, 1993), which mark single or very few lineages, have been used to follow their development, in some cases, all the way from embryo to adult stages (Kumar et al., 2009a; Pereanu et al., 2010; Spindler and Hartenstein, 2010; Spindler and Hartenstein, 2011). These studies made it clear that individual SATs, or small sets of SATs of neighboring lineages, form the "gross anatomical" fiber bundles (fascicles) of the brain. Fascicles, often accompanied by agglomerations of glial processes, can be recognized in brain confocal sections labeled with antibodies against neuronal membrane molecules and synaptically-localized proteins (Bieber et al., 1989; Hortsch et al., 1990; Iwai et al., 1997; Wagh et al., 2006). In the latter case (e.g. N-Cadherin), fascicles appear as signal-negative spaces, since they exclude synapses. Our group has previously established a map of the most prominent fascicles for the larval and adult brain (Pereanu et al., 2010). In this and the accompanying paper (Wong et al., 2013), extending upon our previous works, we will (1) assign the SATs of all secondary lineages defined in the larva to distinct neuropil fascicles; (2) follow SATs through pupal stages into the adult; and (3) use the SAT map of the adult brain to identify MARCM clones with their corresponding secondary lineages.

A major prerequisite for our project is to recognize SATs and neuropil fascicles throughout metamorphosis. The anatomy of the pupal brain of *Drosophila* or any other holometabolous insect has so far not been described in great detail. With a focus on individually-labeled cells in the *Manduca* CNS it was shown several decades ago that primary neurons, including motor neurons and interneurons, undergo a remodeling process whereby most neurite branches are first pruned back during early metamorphosis and then regrow in a new, adult-specific pattern (reviewed in Levine, 1984; Levine and Truman, 1985; Libersat and Duch, 2002; Tissot and Stocker, 2000; Truman and Booker, 1986; Truman and Reiss, 1988; Weeks, 2003). The same process was observed for the *Drosophila* embryonically-born Kenyon cells or mushroom body neurons (reviewed in Jefferis et al., 2002; Technau and Heisenberg, 1982). Secondary neurons, which represent the vast majority of neurons in the adult brain, begin to differentiate approximately one day after the onset of metamorphosis, sending out branches with terminal fibers and forming synapses (Dumstrei et al., 2003a; reviewed in Hartenstein et al., 2008; Singh and Singh, 1999; Stocker et al., 1997). This process leads to a steady increase of neuropil volume. Volume measurements taken in *Drosophila* (Power, 1952) and other holometabolans (Nordlander and Edwards, 1969) show that at around 24 h after puparium formation (P24) the neuropil takes up less than 25% of the overall brain volume; around P48 this fraction has raised to almost 50% and at eclosion it is 53%.

Throughout metamorphosis in the pupal brain, secondary axon tracts defining the adult brain lineages remain intact as cohesive fiber bundles and can be visualized using antibody markers against neuronal membrane molecules, such as Neurotactin or Neuroglian (Pereanu et al., 2010). We present in this paper a detailed map of all SATs for the larva, pupa, and adult. The practical importance of this map is two-fold. First, the SAT/neuropil fascicles, together with the neuropil compartments, help to define an anatomical framework to which smaller structural units (individual neurons, synapses), functional phenomena, or mutant phenotypes can be related. Second, SATs represent the hallmarks by which MARCM clones of lineages can be identified. To-date, only a small minority of lineages that continuously express a known Gal4-driver in the brain have been followed throughout development. Several groups (Ito et al., 2013; Yu et al., 2013; Wong et al., 2013) have now generated collections of lineage-specific MARCM clones, induced at the early larval stage, thereby marking all secondary neurons of a particular lineage. In all clones, neuronal cell bodies and their fiber tracts are easily visible, making it possible to assign a given clone to the lineage it represents.

Materials and methods

Fly stocks

Flies were grown at 25 °C using standard fly media unless otherwise noted. For Figs. 8 and 11, *1407-Gal4* (Mz1407; Bloomington #8751), mapping out to the *insc* locus, was used as a driver line to visualize all secondary lineages at various stages of development ranging from L3 to P48.

Markers

The Bruchpilot (Brp) antibody (Developmental Studies Hybridoma Bank, DSHB; nc82) labels synapses and served as a marker for neuropil. It is a mouse monoclonal antibody from a large library generated against *Drosophila* head homegenates. The antibody recognizes the active zone protein Brp, which forms protein bands of 190 and 170 kDa in Western blots of homogenized *Drosophila* heads (Wagh et al., 2006).

The N-Cadherin antibody (DSHB; DN-EX No. 8), another marker for neuropil, is a mouse monoclonal antibody raised against a peptide encoded by Exon 8, amino acid residues 1210–1272 of the *Drosophila CadN* gene. The antibody detected two major bands of 300-kDa and 200-kDa molecular weights on Western blot of S2 cells only after transfection with a cDNA encoding the N-Cadherin protein (Iwai et al., 1997).

The Neurotactin antibody (DSHB; BP106) is a mouse monoclonal antibody generated in a screen for novel antigens expressed on the surface of developing neurons in the Drosophila embryo (Patel et al., 1987). The antibody was used to screen a 9–12-h embryonic *Drosophila* phage-gt11 cDNA library (Snow et al., 1987) that identified two phages containing a 435-bp EcoRI fragment that did not include the full open reading frame. A radiolabeled probe derived from this fragment was used to screen the cDNA library and identify a large open reading frame (Hortsch et al., 1990). The deduced amino-terminal sequence of this cDNA (11 amino acids) is identical to protein microsequence data from affinity-purified Neurotactin protein (de la Escalera et al., 1990).

The Neuroglian antibody (DSHB; BP104) labels secondary neurons and axons in the adult brain. It is a mouse monoclonal

antibody from a library generated against isolated *Drosophila* embryonic nerve cords (Bieber et al., 1989).

Immunohistochemistry

Samples were fixed in 4% methanol-free formaldehyde in phosphate buffer saline (PBS, Fisher-Scientific, pH¾ 7.4; Cat No. #BP399-4). Tissues were permeabilized in PBT (PBS with 0.3% Triton X-100, pH¾7.4) and immunohistochemistry was performed using standard procedures (Ashburner, 1989). The following antibodies were provided by the Developmental Studies Hybridoma Bank (Iowa City, IA): mouse anti-Neurotactin (BP106, 1:10), rat anti-DN-Cadherin (DN-EX #8, 1:20), mouse anti-Neuroglian (BP104, 1:30), and mouse anti-Bruchpilot (nc82, 1:30). Secondary antibodies, IgG_1 (Jackson ImmunoResearch; Molecular Probes) were used at the following dilutions: Alexa 546-conjugated anti-mouse (1:500), DynaLight 649-conjugated anti-rat (1:400), Alexa 568-conjugated anti-mouse (1:500).

Clonal analysis

Clones were generated by Flp-mediated mitotic recombination at homologous FRT sites. Larval neuroblast clones were generated by MARCM (Lee and Luo, 2001; see below) or the Flp-out construct (Zecca et al., 1996; Ito et al., 1997).

Mitotic clone generation by Flp-out

To generate secondary lineage clones in the larva using the Flp-out technique; flies bearing the genotype:

(1) *hsflp, elav^{C155}-Gal4/+; UAS-FRT-rCD2, y+, stop-FRT-mCD8::GFP*
(2) *hsflp; Act5C-FRT-stop,y+-FRT-Gal4, UAS-tauLacZ/UAS-src::EGFP*

Briefly, early larva with either of the above genotype were heatshocked at 38 1C for 30–40 min. ***elav^{C155}-Gal4*** is expressed in neurons as well as secondary neuroblasts. Third instar larval and
adult brains were dissected and processed for immunohistochemistry (as described above).

Mitotic clone generation by MARCM

Mitotic clones were induced during the late first instar/ early second instar stages by heat-shocking at 38 1C for 30 min to 1 h (approximately 12–44 h ALH). GFP-labeled MARCM clones contain
the following genotype:

Adult MARCM clones:

(1) *hsflp/+; FRTG13, UAS-mCD8GFP/FRTG13, tub-GAL80; tub-Gal4/+* or
(2) *FRT19A GAL80, hsflp, UAS-mCD8GFP/ elav^{C155}-Gal4, FRT19A; UAS-CD8GFP/+*

Larval MARCM clones:

hsflp, elav^{C155}-Gal4, FRTG13, UAS-mCD8GFP/Y or hsflp, elav^{C155}-Gal4, FRTG13, UAS-mCD8GFP/; FRT42D, tub-Gal80/FRT42D.

Confocal microscopy

Staged ***Drosophila*** larval and adult brains labeled with suitable markers were viewed as whole-mounts by confocal microscopy [LSM 700 Imager M2 using Zen 2009 (Carl Zeiss Inc.); lenses: 40 ~ oil (numerical aperture 1.3)]. Complete series of optical sections were taken at 2-μm intervals. Captured images were processed by ImageJ or FIJI (National Institutes of Health, http://rsbweb.nih.gov/ij/ and http://fiji.sc/) and Adobe Photoshop.

2D registration of clones to standard brain

Brains with MARCM clones were labeled with DN-cad and BP104 to image the SAT and projection envelope relative to the BP104-positive fascicles and DN-cad-positive neuropil compartments. Fasciculation of the SAT of a clone with a fascicle allowed for its identification with a lineage, or lineage pair. To generate the figure panels z-projections of the individual MARCM clones were registered digitally with z-projections of a standard brain labeled with DN-cad ("2D registration"). Additional details are provided in the accompanying paper (Wong et al., 2013).

Generation of three-dimensional models

Digitized images of confocal sections were imported into FIJI (Schindelin et al., 2012; http://fiji.sc/). Complete series of optical sections were taken at 2-mm intervals. Since sections were taken from focal planes of one and the same preparation, there was no need for alignment of different sections. Models were generated using the 3-dimensional viewer as part of the FIJI software package. Digitized images of confocal sections were imported using TrakEM2 plugin in FIJI software (Cardona et al., 2012). Surface renderings of larval and adult brains stained with anti-Bruchpilot were generated as volumes in the 3-dimensional viewer in FIJI. Cell body clusters were indicated on surface renderings using TrakEM2. Digital atlas models of cell body clusters and SATs were created by manually labeling each lineage and its approximate cell body cluster location in TrakEM2.

Results

The development of secondary lineages during metamorphosis

At the late larval stage, secondary lineages comprise elongated, radially-oriented clusters of approximately 150 cells that tile the brain cortex. Each cluster produces an axon bundle (secondary axon tract: SAT) whose entry point into the neuropil and pathway followed within the neuropil is distinctive and highly invariant (Fig. 1A and B). Pathways of most SATs can be individually followed within the neuropil; in some cases, two or more lineages form a bundle in which the individual SATs cannot be distinguished (Fig. 1C–E; Table 1). A number of neuroblasts generate lineages which give rise to two dissimilar SATs; these are assumed to be the axon bundles belonging to two hemilineages (HSATs; Fig. 1A–E, Table 1). Finally, the large type II lineages, numbering eight in total (reviewed in Brand and Livesey, 2011), are composed of multiple sub-lineages, each emitting a separate axon bundle (SSATs; Fig. 1F–J). Only the most conspicuous of these fascicles can be followed and are listed in Table 2.

Global neuronal markers such as Neuroglian (hereafter referred to as BP104) and, to a lesser extent, Neurotactin (in the following called BP106) remain expressed post-embryonically, making it possible to follow lineages and their SATs from the larval to the adult stage (Fig. 2). The analysis presented in this paper is based on the reconstruction of lineages from BP104- and BP106-labeled brains of staged pupae fixed at close intervals, including P6, P12, P18, P24, P32, P40, P48, and P72. Whereas the relative position of SAT entry points and pathways within the neuropil remains fairly constant, a number of morphogenetic changes can be observed for most lineages. These will be discussed in the following paragraphs, before focusing on individual lineages.

During the time that secondary neurons differentiate and generate axonal and dendritic branches the neuropil volume increases (eg. growth of the SLP compartment, Fig. 2E–H). At the same time, the number of neuronal cell bodies does not increase;

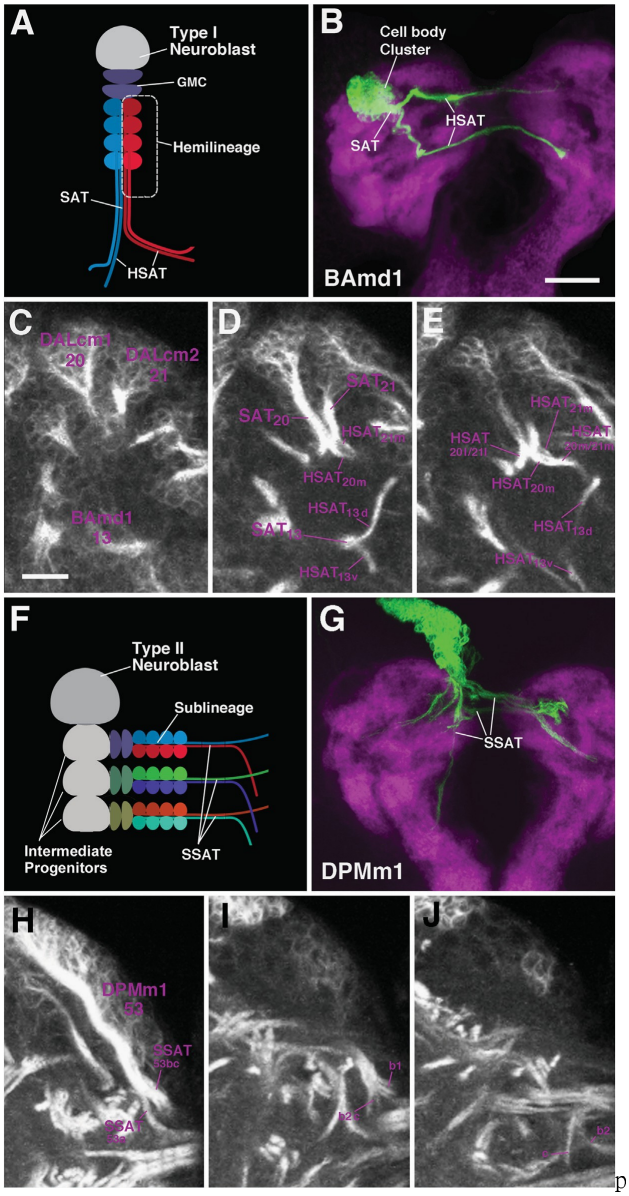

Fig. 1. Secondary lineages form SATs during larval development. (A) Schematic representation of a Type I lineage. A single neuroblast (in grey) undergoes several rounds of asymmetric division to produce an intermediate progenitor, the ganglion mother cell (GMC, navy blue). GMCs divide to produce two post-mitotic neurons. Neuronal somata remain in close proximity to the neuroblast and extend axonal fibers as a characteristic bundle (secondary axon tract, SAT) from the outer cortical region of the brain hemisphere to the inner region, the neuropil. On occasion, GMCs generate two sister populations of genetically distinct neurons, termed hemilineages, where each produces its own axon tract, HSAT (shown in red and blue in A). (B) Z-projection of frontal confocal section of a L3 MARCM neuroblast clone of the BAmd1 lineage induced during the larval period. BAmd1 contains two hemilineages where a large cell body cluster emits two fiber bundles, identifiable HSAT's. The larval neuropil is labeled in purple with N-Cadherin. ((C)–(E)) Three Z-projections, shown at different levels of the same BP106-labeled brain hemispheres. At the level shown in C, the cell body clusters and proximal SATs of three lineages, BAmd1 (#13), DALcm1 (#20) and DALcm2 (#21) are visible. In (D), the SAT of BAmd1 splits to form two HSATs (#13d and #13v). DALcm1 (#20), and DALcm2 (#21) are two neighboring lineages, each with HSATs (#20m/21m, #20l/21l), which come so close that they can no longer be distinguished. (F) Schematic of Type II lineage. A single neuroblast divides to generate multiple intermediate progenitor cells, each capable of undergoing several rounds of asymmetric divisions. Each asymmetrically dividing progenitor cell gives rise to symmetrically dividing GMCs to produce a sub-lineage and corresponding SAT (SSAT). Each SSAT is unique in composition and represented in different colors. ((G)–(J)) The Type II lineage DPMm1 (#53), as shown by a MARCM clone in an L3 brain ((G)); neuropil, in purple, labeled with anti-N-Cadherin and with the global marker BP106 ((H)–(J)). DPMm1 contains multiple SSAT's, all with different trajectories (note morphology of tracts #53a-c). Scale bars: 25 μm ((B) and (G)) and 10 μm ((C)–(E), (H)–(J)).

Table 1
List of abbreviations of neuropil fascicles (left), compartments (center), and entry portals of lineage-associated tracts (right).

Fascicles	Abbr.	Compartments	Abbr.	Entry portals	Abbr.
Anterior–dorsal commissure	ADC	Antennal lobe	AL	Anterior entry portal of the ML	ptML a
Antennal lobe commissure	ALC	Antenno-mechanosensory and motor center	AMMC	Anterior portal of the lateral horn	ptLH a
Antennal lobe tract	ALT	Anterior optic tubercle	AOTU	Anterior superior lateral protocerebrum portal	ptSLP a
Inner antennal lobe tract	iALT	Anterior periesophageal neuropil	PENPa	Antero-dorsal entry portal of the VLP	ptVLP ad
Medial antennal lobe tract	mALT	Bulb	BU	Dorrso-lateral superior ventro-lateral protocerebrum portal	ptVLP dls
Outer antennal lobe tract	oALT	Ellipsoid body	EB	Dorsal antennal lobe portal	ptAL d
Anterior optic tract	AOT	Fan-shaped body	FB	Dorsal spur portal	ptSP d
Anterior superior transverse fascicle	trSA	Inferior protocerebrum	IP	Dorso-lateral entry portal of the ML	ptML dl
Central protocerebral descending fascicle	deCP	Anterior IP	IPa	Dorso-lateral inferior ventro-lateral protocerebrum portal	ptVLP dli
Cervical Connective	CCT	Lateral IP	IPl	Dorso-lateral portal of protocerebral bridge	ptPB dl
Commisure of the lateral accessory lobe	LALC	Medial IP	IPm	Dorso-lateral vertical lobe portal	ptVL dl
Dorsal commissure of anterior subesophageal ganglion	DCSA	Posterior IP	IPp	Dorso-medial entry portal of the ML	ptML dm
Dorsolateral root of the fan-shaped body	dlrFB	Lateral accessory lobe	LAL	Dorso-medial portal of protocerebral bridge	ptPB dm
Fronto-medial commissure	FrMC	Lateral horn	LH	Dorso-medial ventro-lateral protocerebrum portal	ptVLP dm
Great commissure	GC	Mushroom body	MB	Dorso-medial vertical lobe portal	ptVL dm
Horizontal ventrolateral protocerebral tract	hVLPT	Calyx	CA	Lateral antennal lobe portal	ptAL l
Intermediate superior transverse fascicle	trSI	Medial lobe	ML	Lateral portal of calyx	ptCA l
Deep bundle of irSI	trSI d	Peduncle	PED/P	Lateral portal of the posterior lateral protocerebrum	ptPLP l
Superficial component of trSI	trSI s	Spur	SP	Lateral portal of the superior lateral protocerebrum	ptSLP l
Lateral ellipsoid fascicle	LE	Vertical lobe	VL	Medial portal of calyx	ptCA m
Anterior LE	LEa	Noduli	NO	Posterior inferior portal of the posterior lateral protocerebrum	ptPLP pi
Posterior LE	LEp	Posterior lateral protocerebrum	PLP	Posterior portal of superior lateral protocerebrum	ptSLP p
Lateral equatorial fascicle	LEF	Protocerebral bridge	PB	Posterior portal of the lateral horn	ptLH p
Anterior LEF	LEFa	Subesophageal ganglion	SEG	Posterior superior portal of the posterior lateral protocerebrum	ptPLP ps
Posterior LEF	LEFp	Superior protocerebrum	SP	Posterior ventro-medial cerebrum portal	ptVMCpo
Medial equatorial fascicle	MEF	Superior intermediate protocerebrum	SIP	Postero-lateral portal of superior lateral protocerebrum	ptSLP pl
Medial root of the fan-shaped body	mrFB	Superior lateral protocerebrum	SLP	Postero-medial portal of superior lateral protocerebrum	ptSLP pm
Median bundle	MBDL	Anterior SLP	SLPa	Ventral antennal lobe portal	ptAL v
Oblique posterior fascicle	obP	Posterior SLP	SLPp	Ventral entry portal of the VLCi	ptVLCi v
Posterior commissure of the posterior lateral protocerebrum	pPLPC	Superior medial protocerebrum	SMP	Ventral portal of calyx	ptCA v
Posterior lateral fascicle	PLF	Ventro-lateral cerebrum	VLC	Ventral portal of protocerebral bridge	ptPB v
External component of PLF	PLFe	Anterior VLC	VLCa	Ventral spur portal	ptSP v
Dorsolateral component of PLF	PLFdl	Inferior VLC	VLCi	Ventro-lateral antennal lobe portal	ptAL vl
Dorsomedial component of PLF	PLFdm	Lateral VLC	VLCl	Ventro-lateral inferior ventro-lateral protocerebrum portal	ptVLP vli
Ventral component of PLF	PLFv	Ventro-medial cerebrum	VMC	Ventro-lateral portal of calyx	ptCA vl
Posterior superior transverse fascicle	trSP	Anterior VMC	VMCa	Ventro-lateral superior ventro-lateral protocerebrum portal	ptVLP vls
Lateral trSP	trSPl	Inferior VMC	VMCi	Ventro-lateral vertical lobe portal	ptVL vl
Medial trSP	trSPm	Post-commissural VMC	VMCpo	Ventro-medial antennal lobe portal	ptAL vm
Sub-ellipsoid commissure	SuEC	Pre-commissural VMC	VMCpr	Ventro-medial ventro-lateral protocerebrum portal	ptVLP vm
Subesophageal-protocerebral system	SPS	Superior VMC	VMCs	Ventro-medial vertical lobe portal	ptVL vm
Superior arch commissure	SAC	Ventro-lateral protocerebrum	VLP		
Superior commissure of the posterior lateral protocerebrum	sPLPC	Anterior VLP	VLPa		
Superior lateral longitudinal fascicle	loSL	Posterior VLP	VLPp		
Anterior loSL	loSLa				
Posterior loSL	loSLp				
Superior medial longitudinal fascicle	loSM				
Anterior loSM	loSMa				
Posterior loSM	loSMp				
Supra-ellipsoid body commissure	SEC				
Ventral fibrous center	VFC				
Ventral longitudinal fascicle	loV				
Intermediate loV	loVIa				
Lateral loV	loVLa				
Medial loV	loVMa				
Posterior–lateral loV	loVP				
Vertical posterior fascicle	vP				
Vertical tract of the superior lateral protocerebrum	vSLPT				
Vertical tract of the ventro-lateral protocerebrum	vVLPT				

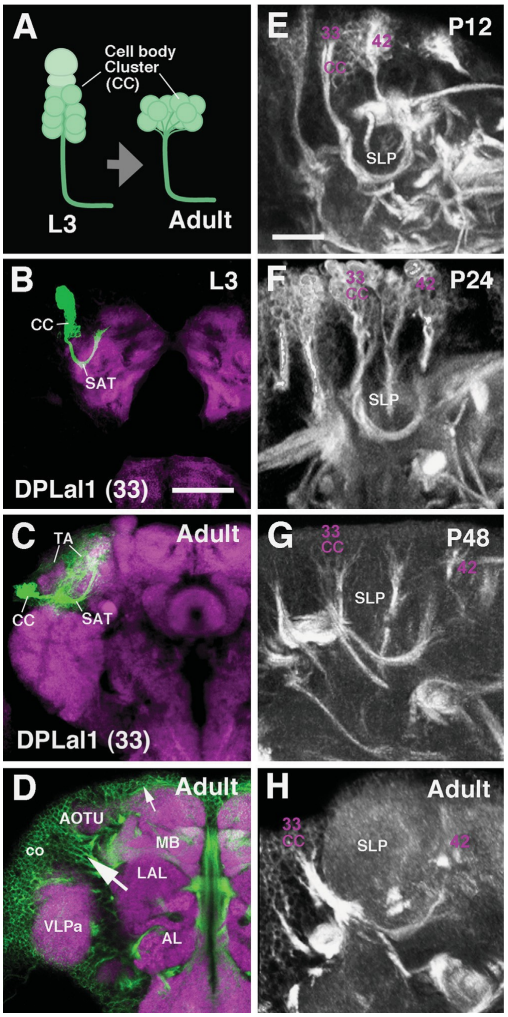

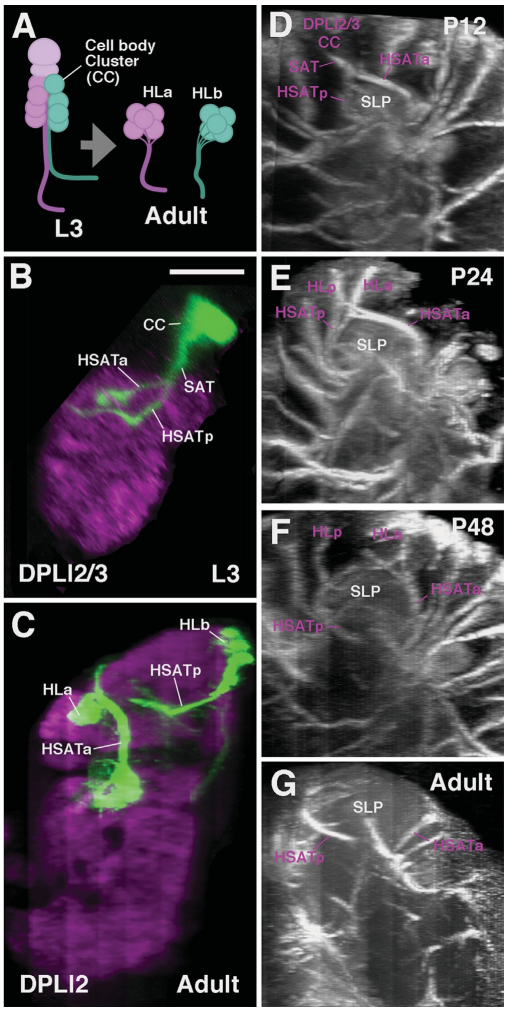

Fig. 2. Secondary lineages during metamorphosis. (A) Cell body clusters (CC) of lineages evolve from a columnar shape to a flattened shape in the adult due to a thinning of the cortex, but the general morphology of the SAT does not change dramatically. ((B) and (C)) Z-projections of a MARCM clone of the DPLal1 (#33) lineage at the L3 larval stage (B) and the adult stage (C). The SAT of this lineage extends along a crescent-shaped trajectory around the anterior tip of the superior lateral protocerebrum (SLP). In the adult, terminal arbors (TA) of DPLal1 and several other lineages result in a growth of this compartment while the SAT remains relatively unchanged. General changes include movement of the cell cluster (CC) from a more dorsal position to a more lateral position, decreases in cell number (most likely due to cell death), flattening of the CC, and elongation of the SAT crescent to extend around the ventral/anterior surface of the SLP. L3 and adult DPLal1 are represented by MARCM neuroblast clones induced during larval development. (D) Confocal section of adult brain hemisphere (anterior level), double-labeled with N-Cadherin (purple, neuropil) and BP104 (green, cortex), illustrating variances in the diameter of the cortex (co) at different locations. Small arrow points to a dorsal region where the cortex is thin; large arrow points to a region with thick cortex in the crevice formed between the antennal lobe (AL), lateral accessory lobe (LAL); anterior optic tubercle (AOTU); mushroom body (MB), and anterior ventrolateral protocerebrum (VLPa). ((E)–(H)) Z-projections of confocal sections of BP104/BP106-labeled brains (P12, P24, P48, adult) show the cell body clusters of DPLal1 (CC 33). In addition, the distance between DPLal1 and an adjacent lineage, DPLd (#42) increases as a result of the growth of the SLP compartment (compare location of #33 and #42 from (E) to (H)). Scale bars: 10 mm ((E)–(H)) and 25 mm ((B)–(D)).

Fig. 3. Hemilineage cell clusters and SAT neuropil entry points migrate away from each other during metamorphosis. (A) Cartoon depiction of the behavior seen in secondary lineages containing hemilineages. Hemilineage cell body clusters (CC, shown as spheres) and their corresponding axon tracts initially form adjacent to one another as seen at the late larval stage (L3). By adulthood, many hemilineages completely separate (CCs and HSATs) to form morphologically distinct elements (generically termed as HLα and HLβ, shown in orange and green, respectively). The extent to which hemilineages migrate apart varies between lineages. ((B)–(G)) Metamorphosis of the hemilineages of the DPLl2/3 secondary lineages. (B) and (C) are z-projections of confocal sections of single brain hemispheres containing GFP-labeled DPLl2/3 neuroblast clones, induced in the early larval period and fixed in the late larva (B) or adult (C). Neuropil (in purple) is labeled by N-Cadherin. ((D)–(G)) Z-projections of contiguous confocal sections of BP106/BP104-labeled brains (BP106 in (D)–(E); BP104 in (F) and (G)). Confocal stacks used in (B)–(G) were digitally rotated 90° to show the DPLl2/3 lineages from a lateral view. ((B), (D)) At the L3 and early pupal stage, DPLl2/3 appears as a pair of cell clusters (CC) whose axons come very close to each other and form a single SAT. This SAT splits into a posterior ventral (HSATp) and an anterior–dorsal (HSATa). These hemilineage tracts extend around the dorsal and lateral surfaces of the growing superior lateral protocerebrum (SLP) compartment during metamorphosis. ((E)–(G)) As the SLP grows ((E), P24; (F), P48; (G), adult), the hemilineage clusters HLa and HLp of the DPL2/3 lineage move away from each other. From P48 onward the clusters and HSATs are completely separated. Scale bar: 50 mm ((B)–(G)).

Table 2
List of secondary lineages of the ***Drosophila*** brain.

Lineage name	Lineage SAT number	Gal4 lineage marker	Entry portal	Separation of Hemilineages	Fascicle joined by lineage	Visibility of SAT	Commissure joined by lineage
BAla1	1	Per[1]	ptAL vl		mlALT	V v T	
BAla2	2	OK371[2]	ptAL vl		0	V v	
BAla3	3	En[1]	ptAL vl		0	V V O	
BAla4	4						
Balc	5d	GH146[1]	ptAL l	s	mALT	v v T	
	5v		ptAL vl		loVl	V V O	GC
BAlp1	6		ptVLP vm		0	V V O	
BAlp2	7		ptVLP vm		loVL	V V v	
BAlp3	8		ptVLP vm		loVL4vP	V V V	
BAlp4	9		ptAL vl		mALT	V V T	
Balv	10		ptVLCi v		0	V V	
BAmas1	11		ptAL vm		MBDL	V t	
BAmas2	12	Emc[3]	ptAL vm		MBDL		
BAmd1	13 d		ptVL vm	s	0	V O	FrMC
	13 v		ptAL d		0	V V	ALC
BAmd2	14				0	O O	ALC
BAmv1	15 d	Per[1]	ptAL v		loVM4LEp	V V T	
	15 p				loVM	V V V	
	15 dn					V	
BAmv2	16		ptAL v		loVM	V V T	
BAmv3	17	GH146[1]	ptAL d		mALT	O O T	
DALcl1	18 d	STAT[1]	ptSP d	a	0	V T	
	18 v		ptSP v		0	V V v	SuEC
	18 vn				MEF	O	
DALcl2	19 d		ptSP d	a	0	V T	SuEC
	19 v		ptSP v		LEa	V V T	
	19 dn				0	V	
DALcm1	20/21m		ptVL vm	a	0	V O	FrMC
	20/21 v		ptVL vl		deCP	V V v	
DALcm2				a			
DALd	22		ptVL vl		deCP	V V V	
DALl1	23 r		ptVLP dm		trSIi	V V O	
	23 v				0	V	
DALl2	24		ptVLP vm		0	v v	
DALv1	25		ptSP v		LEFa	V V V	GC
DALv2	26	Per[1]	ptSP v		LEa	V t	
DALv3	27 d	En[1]	ptSP v		LEa	V t	SEC
	27 v		ptSP v		LEa	V t	SuEC
DAMd1	28		ptVL dm		ADC	V V	FrMC
DAMd2	29		ptVL dm		loSMa	V V v	
DAMd3	30						
DAMv1	31		ptVL dm		0	V V	
DAMv2	32						
DPLal1	33		ptSLP l		trSA	V T	
DPLal2	34/35 d		ptSLP l	a	trSA	V T	
	34/35 v				0	V T	
DPLal3				a			
DPLam	36	En[1]	ptSLP a		vSLPT	V V V	
DPLc1	37		ptSLP pm		trSPm	VT	
DPLc2	38		ptSLP pm		trSPm	V T	
DPLc4	40					V T	
DPLc3	39		ptSLP pm		0	V V V	
DPLc5	41 a		ptSLP pm	S	trSPm	V T	
	41 p		ptPB v		0	O O	ADC
DPLd	42m		ptVL dl	s	0	V V V	ADC
	42 p		ptVL dl		loSLa4trSId	V V V	
DPLl1	43		ptSLP pl		trSPl	V t	
DPLl2	44 p		ptSLP pl	S	loSLp	V T	
	44 a		ptSLP a		vSLPT	V T	
DPLl3	45 p		ptSLP pl	S	loSLp	V T	
	45 a		ptSLP a		vSLPT	V T	
DPLm1	46		ptSLP p		0	V V	
DPLm2	47		ptSLP p		0	V V	
DPLp1	48m		ptCA l		obP	V O T	sPLPC
	48 v		ptSLP pl			v v	
	48 a		ptSLP pl		0	V V	
DPLp2	49						
DPLpv	50		ptPLP ps		PLFdl	V V V	

Table 2 (*continued*)

Lineage name	Lineage SAT number	Gal4 lineage marker	Entry portal	Separation of Hemilineages	Fascicle joined by lineage	Visibility of SAT	Commissure joined by lineage
DPMl1	51		ptCA v		DPPT	V O	
DPMm	53 a	9D11[4]	ptPB	s	loSMp	V O T	
	53 b		ptPB dm		mrFB	V V	
	53 c		ptPB dm		mrFB	V V	
	53 d		ptPB dm		0	V v O	0
DPMm2	54		ptPB dl		0	V V O	MBDLchi
DPMpl1	55		ptCA m		loSMp	V T	MBDLchi
DPMpl2	56		ptCA m		loSMp	V T	
DPMpl3	57		ptPB v		MEF	V T	GC
DPMpm1	58 a	9D11[4]	ptPB dl	a	mALT4MBDL	V O T	
	58 b		ptPB dl		dlrFB	V V	
DPMpm2	59 a	9D11[4]	ptPB dl	a	loSMp	V T	SEC chi
	59 b		ptPB dl		dlrFB	V V	
CM1	60 d	9D11[4]	ptPB v	S	MEF	v T	LALC
	60 v		ptVMCpo		loVP	v T	
CM3	61 a	9D11[4]	ptCA m	s	loSMp	v T	SEC
	61 d1		ptPB v		MEF	v T	
	61 d2		ptPB v		MEF	v T	
	61 v		ptVMCpo		loVP	v T	pPLPC
CM4	62 a	9D11[4]	ptPB v	S	loSMp	v T	
	62 d		ptPB v		MEF	v T	
	62 v		ptVMCpo		loVP	v T	pPLPC
CM5	63		ptPB v		0		
CP1	64 d		ptCA vl		obP4loSMp	V T	MBDLchi
	(64 v)		ptCA v			V T	
CP2	65 d		ptCA l	s	obP4loSMp4OE	V T	
	65 v		ptPLP ps		PLFdm	V T	
CP3	66 d		ptCA l	s	obP4loSMp	V T	SEC
	66 v		ptPLP ps		PLFdm	V T	
CP4	67		ptCA vl		obP4loSMp	V T	SEC
BLAd1	68		ptSLP l		trSId	V T	
BLAd2	69		ptSLP l		trSId	V T	
	69s				trSIs	V T	
BLAd3	70		ptSLP l		trSId	V T	
BLAd4	71		ptSLP l		trSIi	V T	
BLAl	72 d		ptSLP l	S	trSIs		
	72m		ptVLP dm		0		
BLAv1	73m		ptVLP dm	S	0	V V t	SAC
	73 p		ptVLP dli		0	V V O	GC
	73 pn				0	V	
BLAv2	74m		ptVLP dls	s	0	V V v	postCCX
	74 p		ptLH a		0	V V v	GC
	74 pn				0	v	
BLAvm	75m		ptVLP dm	S	0	V V	
	75 p		ptVLP dm		0	V V v	
BLD1	77 d		ptSLP l	S	trSIs	V T	
	77 p		ptPLP l		0	V V V	
BLD2	78 d		ptSLP l		trSIs	V T	
BLD3	79 d		ptSLP l	S	trSIs	V T	
	79 vn				0	V T	
	79 a		ptVLP dls		0	O	
BLD4	80 d		ptSLP l		trSIs	V T	
	80 v				0	v	
BLD5	82	Ato[1]	ptPLP l		0	V v	GC
BLD6	83		ptPLP l		0	V v	
BLP1	84		ptPLP ps		PLFe	V V	
BLP2	85				PLFe		
BLP3	86		ptLH p		0	V V	
BLP4	87				0		
BLVa1	89	So[1]	ptLH a		0	v v	
BLVa2	90	So[1]			0		
BLVa3	91		ptVLP vli		0	V V	
BLVa4	92				0		
BLVp1	93 p		ptPLP pi	S	PLFv	V V V	GC
	93 a		ptVLP vls		vVLPT	V V O	
BLVp2	94 p		ptPLP pi	S	PLFv	V V v	SEC
	94 a		ptVLP vls		vVLPT	V V O	SAC

Column A: Lineage names based on topology (Pereanu and Hartenstein, 2006). Shading indicates paired lineages with common tract. For lineage pairs shaded lightly, different MARCM clones were identified (see accompanying paper by Wong et al., 2013); dark shading indicates pairs for which only a single type of clone was found.
B: Number identifying lineage-associated tracts (SATs) on figures. In lineages with multiple hemilineage tracts or sublineage tracts, these are individually listed (e.g. dorsal hemilineage tract of BAlc is identified as "5d", ventral hemilineage tract as "5v").
C: Markers for lineages. References:
[1] reviewed in Spindler and Hartenstein (2010).
[2] Das et al. (2013).
[3] Lichtneckert et al. (2008).
[4] Pfeiffer et al. (2008).
D: Entry portal of lineage-associated tracts (for abbreviations, see Table 1).
E: Separation of hemilineages during metamorphosis. Lower case "a" signifies that hemilineage clusters and entry portals remain adjacent; lower case "s" indicates that hemilineage clusters separate; capital "S" stands for extensive shift of one or both hemilineages (separation of clusters ≥20 μm in adult).
F: Neuropile fascicle joined by lineage-associated tract. For abbreviations of fascicle names, see Table 1. "0" indicates that tract does not form part of any designated fascicle.
G: Traceability of lineage-associated tracts in BP104-labeled adult brain specimens. First letter refers to neuropil entry point; second letter represents proximal tract (≈20 μm away from entry point), third letter distal tract. Some tracts branch off another tract (e.g. BAmv1/#15dn branches off #15d); in these cases, letter representing neuropil entry point is omitted. In cases where lineage associated tract is short (e.g. BAlv/#10), third letter indicating distal tract is omitted. "V" stands for "clearly visible"; "v" for "faintly visible"; "0" for "not visible". "T" signifies that tract forms part off fascicle in which it cannot be distinguished from other components.
H: Commissure joined by lineage associated tract. For abbreviations, see Table 1. In cases where distal tract is not visible in adult brain (e.g. BAlc/#5v), entry into commissure is inferred from earlier, pupal specimens.

rather, for many lineages, it decreases, due to cell death (Booker and Truman, 1987a; Jiang and Reichert, 2012; Kumar et al., 2009b). As a result, the brain cortex becomes thinner and the clusters formed by individual lineages change in shape from radially-oriented "cylinders" to horizontally-flattened "plates" (Fig. 2A–C, e.g. DPLal1, #33). Depending on their position, some lineages are affected more than others by this flattening process. The cortex of the adult brain varies in diameter: it is thick at some locations where two outward-bulging compartments meet and deep "crevices" filled with neuronal cell bodies are formed (Fig. 2D, large arrow) or it is very thin or absent over the convexity of many different compartments (Fig. 2D, small arrow). A general morphological change is that the increase in neuropil volume causes lineage entry points and SATs to move away from each other (shown for DPLal1, #33; DPLd, #42 in Fig. 2E–H). However, the position of most lineages relative to each other remains constant, which is the prerequisite for following SATs throughout metamorphosis. Two processes, the separation of parts of lineages (presumably hemilineages) and the extension of additional fiber bundles, complicate the issue of identifying SATs during pupal stages for a number of lineages. In the late larva, the cell body clusters of hemilineages and the entry points of their HSATs are directly adjacent. During metamorphosis, hemilineages are drawn apart to a varying extent. In most cases, they remain close; in a few cases, they become far removed from each other (Fig. 3A; e.g. DPLl2/3). The example shown in Fig. 3B–G is the paired lineage DPLl2/3, whose HSATs at the larval and early pupal stages enter together at the dorso-posterior neuropil surface (Fig. 3B and D). During the course of metamorphosis (Fig. 3E and F), one hemilineage remains posteriorly, the other one moves anteriorly, resulting in two separate cell body clusters and two distinct entry points in the adult (Fig. 3C and G). This extreme separation of hemilineages, typically occurring between P12 and P40, affects several other lineages as well (see Table 1).

Development of nascent fiber bundles from a main SAT is the second mechanism by which the overall SAT structure of lineages is altered. As a rule, most lineages have fully extended their SAT (or HSATs/SSATs) by the late larval stage. For example, lineages of antennal lobe projection neurons, whose cell bodies are located in the antero-ventral brain close to the antennal lobe, extend their axons far posterior to the calyx (Das et al., 2013; Pereanu and Hartenstein, 2006). During pupal development, terminal arborizations sprout from these fiber bundles and accumulate in the antennal lobe and calyx/lateral horn. However, a number of lineages deviate slightly in that their SATs/HSATs acquire one or more major side branches, typically around 24–48 h of pupal development (P24–P48). This is shown in Fig. 4 for BAmv1, which in the late larva forms a dorsally-directed and a posteriorly-directed HSAT (HSATd and HSATp, Fig. 4B and D). Beginning around P24, the dorsal HSAT emits a laterally-directed branch (SAT_{late}, data not shown for P24). By P32, the aforementioned branching for the BAmv1 becomes more apparent (Fig. 4E), where the SAT_{late} reaches the VLPa compartment. The terminal arborization of SAT_{late} into the VLPa compartment is also observed in the adult stage (Fig. 4C and F). The most likely explanation is that branches added during the pupal period are formed by the axons belonging to a group of late-born neurons. In the late larva, these cells would not yet have extended an axon contributing to the larval SAT. When they extend their axons in the pupa, these fibers might not all follow the pre-existing larval SAT, but establish a novel trajectory (SAT_{late}) instead. Table 1 lists lineages forming prominent SAT branches during metamorphosis.

The pattern of fiber bundles in the brain neuropil

In the following presentation of lineages, SATs will be assigned to anatomically defined systems of fiber bundles (fascicles) in the brain neuropil. Fascicles are easily distinguished in the context of commonly used synaptic markers (eg. Bruchpilot, nc82; N-Cadherin, NCad; Syntaxin, 8C3) which label most neuropil regions in the brain because they appear as domains of low signal, since synapses are scarce or absent in fascicles. Components of most adult fascicles can also be positively labeled by BP104 (this work). The most prominent fascicles can be generally grouped into longitudinal, transverse, and vertical bundles, which are based on the cardinal axis they travel along. Most of these bundles extend along the surface of the inferior protocerebrum, which is the brain domain surrounding the peduncle and lobes of the mushroom body (Pereanu et al., 2010; Fig. 5). For a more comprehensive description of fascicles and neuropil compartments, visit our website, the Drosophila Brain Lineage Atlas: https://www.mcdb.ucla.edu/Research/Hartenstein/dbla/. Along the boundary between superior and inferior protocerebrum one further distinguishes a lateral and medial longitudinal superior fascicle (loSL and loSM, respectively; Fig. 5A–E; for alphabetical list of abbreviations of fascicles and compartments, see Table 2). The loSM can be subdivided into an anterior component, loSMa (Fig. 5A, B and E) and posterior component, loSMp (Fig. 5C, D and E). Among the transverse fascicles, we distinguish an anterior, intermediate, and

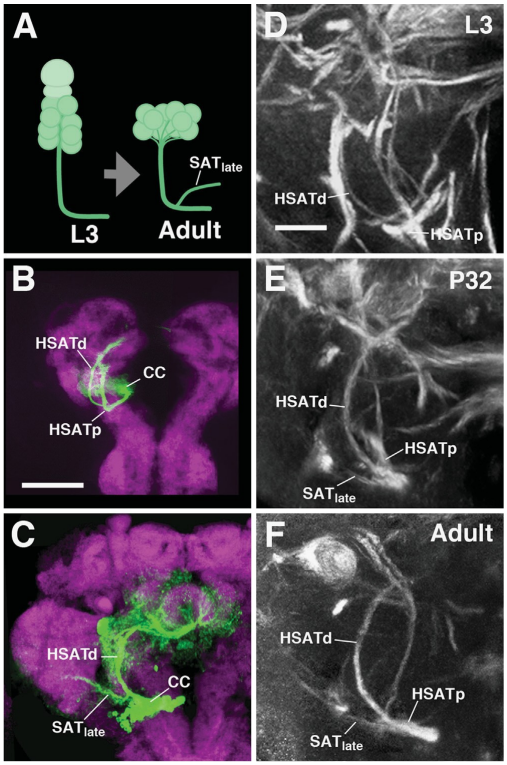

Fig. 4. Some secondary lineages acquire additional branches during metamorphosis. (A) Schematic illustrating that a fully extended SAT can produce an off-shoot (SAT_{late}) during metamorphosis, presumably generated by late-born secondary neurons that had not yet produced axonal fibers during larval development. The addition of branches does not affect the overall morphology of the main SAT. ((B) and (C)) Z-projections of confocal sections of brain hemispheres containing BAmv1-MARCM clones (fixed at larval stages in (B); at adult stages in (C)). BAmv1 has two HSATs, a dorsally-directed HSATd and posteriorly-directed HSATp by the L3 stage. In the adult, a third branch, SAT_{late}, is added to HSATd, and extends laterally into the VLPa compartment (neuropil is labeled by anti-DN-cadherin). ((D)–(F)) Z-projections of representative confocal sections of BP106/BP104-labeled pupal brains, highlighting the emergence of the SAT_{late} lateral branch, appearing between st. P24 (data not shown) and P32 (E). Of note, the collateral branch formed during metamorphosis follows a novel trajectory different from other SATs formed by the lineage during larval development. Scale bars: 50 μm ((B)–(G)) and 10 μm ((D)–(F)). Other abbreviations: cell body cluster CC.

posterior superior transverse fascicle (trSA, trSI, and trSP, respectively; Fig. 5B–E). More ventral and anterior is the lateral ellipsoid fascicle (LEa, LEp; Fig. 5A) that passes obliquely underneath the mushroom body medial lobe (Fig. 5A and E) and connects to the central complex. Fiber bundles entering the central complex from posterior form the medial and dorsolateral roots of the fan-shaped body (mrFB, dlrFB), as well as part of the medial equatorial fascicle (MEF; Fig. 5D and E; see below).

Longitudinal fascicles extending at the ventral surface of the inferior protocerebrum are the medial equatorial fascicle (MEF), lateral equatorial fascicle (LEF), and posterolateral fascicle (PLF; Fig. 5C, D and F). The LEF is subdivided into anteriorly- and posteriorly-directed tracts, LEFa and LEFp (Fig. 5A–C, F and C, D, F, respectively). Further ventral is the ventral longitudinal fascicle (loV). Anteriorly, this massive fiber system has three components: the medial, intermediate, and lateral loV (loVMa, loVIa, loVLa, respectively; Fig. 5A–C and F). All three components converge and form a conspicuous confluence of fibers in the middle of the ventral cerebrum (Fig. 5B and F, white and black arrowheads), the ventral fibrous center (VFC). Beyond this confluence, the ventromedial fascicle continues and passes postero-medially into the cervical connective (CCT) that joins the brain with the thoracic ganglia (Fig. 5D and F). A more laterally-located fascicle, the postero-lateral component of the loV (loVP), moves nearly straight posterior, ending near to the posterior neuropil surface (Fig. 5C, D and F).

The conspicuous fiber systems that connect ventral and dorsal regions of the brain are the medial antennal lobe tract (mALT), the median bundle (MBDL), and the central descending protocerebral tract (deCP). The mALT primarily carries ascending fibers from the antennal lobe, travels dorso-posteriorly along the central complex, and turns laterally towards the calyx and lateral horn (Fig. 5A–E). The MBDL contains numerous ascending and descending fibers connecting the superior medial protocerebrum (SMP) with the subesophageal ganglion (SEG) and tritocerebrum (Fig. 5A). The deCP arises in the superior protocerebrum, passes the peduncle medially, and aims for the ventro-medial cerebrum (VMC) and SEG (Fig. 5B and E).

Bundles of commissural fibers interconnecting the two brain hemispheres are grouped around the central complex. Dorsally, one can distinguish four main commissures, including (fromanterior to posterior; for nomenclature see Strausfeld, 1976) the anterior–dorsal commissure (ADC, dorsal of the medial lobe of the mushroom body; Fig. 5A); the fronto-dorsal commissure (in between the medial lobe and ellipsoid body; not shown); the supra-ellipsoid body commissure (SEC, dorsal of the ellipsoidbody; Fig. 5A and E); the superior arch commissure (SAC, dorsalof the fan-shaped body; Fig. 5B and E), and the superior commis-sure of the postero-lateral protocerebrum (sPLPC, dorso-posterior of the fan-shaped body; Fig. 5D and E). Commissures passing ventral of the central complex are (from anterior to posterior) the antennal lobe commissure (ALC, ventral of the medial lobe; Fig. 5A and F), the commissure of the lateral accessory lobe and sub- ellipsoid commissure (LALC and SuEC, ventral of the ellipsoid body; Fig. 5A and F), the great commissure (GC, ventral of the fan-shaped body; Fig. 5C and F), and the posterior commissure of thepostero-lateral protocerebrum (pPLPC; Fig. 5D and F).

Several shorter fiber bundles entering the center of neuropil compartments (rather than extending along compartment boundaries) can be distinguished. Used as points of reference in this and the accompanying paper (Wong et al., 2013) are the vertical tract of the superior lateral protocerebrum (vSLPT, penetrates the SLP from antero-dorsal; Fig. 5B), the vertical posterior tract (vP), projecting between the lateral horn and posterior lateral protocerebrum (not shown), the vertical tract of the ventro-lateral protocerebrum (vVLPT, enters the VLPa from ventral; Fig. 5B), and the horizontal tract of the ventrolateral protocerebrum (hVLPT, enters the VLPa from lateral; Fig. 5A).

Classification of lineages

In the previously published map of secondary lineages a nomenclature based on topology was introduced (Cardona et al., 2010a; Dumstrei et al., 2003a; Pereanu and Hartenstein, 2006). Using the easily identifiable mushroom body and antennal lobe as points of reference, twelve groups were defined, including the mushroom body (Fig. 6). Groups BA (basal anterior), DAL (dorsal anterior lateral), and DAM (dorsal anterior medial) have entry points at the anterior brain surface. BA lineages enter in close proximity to the antennal lobe (blue arrow in Fig. 6A; antennal lobe indicated by red "A" in Fig. 6B–G); the DAL lineage group enters anterior and lateral of the mushroom body vertical lobe (purple arrow in Fig. 6A; shown in shades of purple in Fig. 6B–G; tip of vertical lobe indicated by red "V" in Fig. 6B–G); and DAM lineages enter anterior and medial of the mushroom body vertical

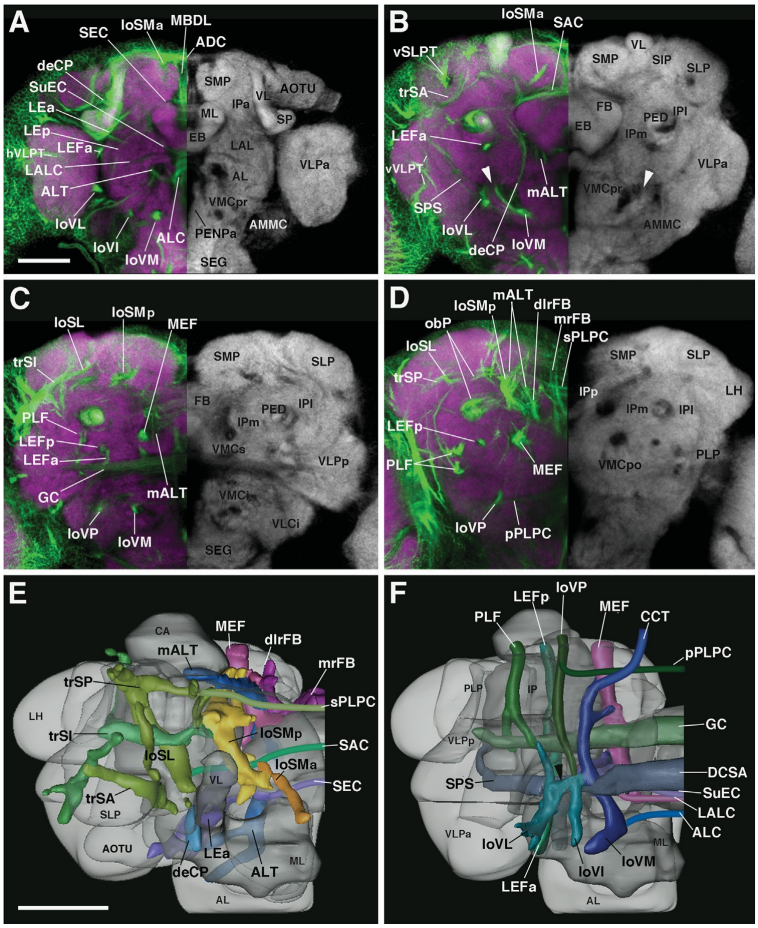

Fig. 5. Major fascicle systems of the adult ***Drosophila*** brain. ((A)–(D)) Z-projections of contiguous confocal sections of adult brains labeled with BP104 (green) and N-Cad (purple in right hemisphere; white in left hemisphere). Z-projections represent brain slices of 10–16 μm thickness at four different antero-posteror levels ((A), anterior optic tubercle AOTU and mushroom body lobes MB; (B) ellipsoid body EB; (C) fan-shaped body FB and great commissure GC; (D) lateral bend of antennal lobe tract, posterior to central complex mALT). The left hemisphere is a merged z-projection of BP104 (to label the major fascicles) and N-Cad (to label the neuropil compartments). The major fascicles are annotated on the left half of brain hemispheres containing the merged image. Neuropil compartments are annotated on the right brain hemisphere. For a complete list of abbreviations for compartments and fascicles, see Table 2 ((E)–(F)). Digital three-dimensional models of adult brain hemispheres viewed from dorsally (E) and ventrally (F), showing pattern of major fascicles (modified from Pereanu et al., 2010). Scale bar: 50 μm ((A)–(D); (E) and (F)).

lobe (yellow arrow in Fig. 6A; shown in shades of yellow in Fig. 6B–G). SAT entry-points of the groups DPL (dorsal posterior lateral) and DPM (dorsal posterior medial) are to be found at the dorsal brain surface. DPL is postero-lateral of the vertical lobe and antero-lateral of mushroom body calyx (DPL; turquoise arrow in Fig. 6A; shown in shades of cyan-turquoise in Fig. 6D–I; calyx indicated by red "C" in Fig. 6D–I); DPM is postero-medial of the vertical lobe and medial of the calyx (DPM; orange arrow in Fig. 6A; shown in shades of orange in 6D–I). The four lineages producing the mushroom body (MB), as well as CP (central posterior) and CM (central medial) lineages, enter at the posterior brain surface; CPs are located ventro-lateral of the mushroom body calyx (maroon arrow in Fig. 6A; maroon in Fig. 6H–I) and CMs ventro-medial of this structure (magenta arrow in Fig. 6A; magenta in Fig. 6H–I). Finally, the BL (basal–lateral) lineages converge on the lateral brain surface, surrounding the broad connection between the optic lobe and central brain (green arrows in 6A; shown in shades of green in 6B-I; optic lobe indicated by red "O" in Fig. 6B–I). BLA lineages enter from anterior (Fig. 6B–G), BLD lineages enter from dorsal (Fig. 6B–I), the BLP group enters from posterior (Fig. 6F–I), and BLV lineages enter from ventral (6D–I). Most of these main groups were further subdivided into smaller units of lineages entering the neuropil closely together, in the case of the BA lineage group, BAla, BAlp, or BAmas (Fig. 6B–G). As evident from Fig. 6, the position of SAT entry-points in relationship to each other and to the neuropil compartments is very similar in the larva and adult, if one takes into account the previously discussed growth of certain compartments, in particular the antennal lobe, optic lobe, and the superior protocerebrum, that occurs during metamorphosis.

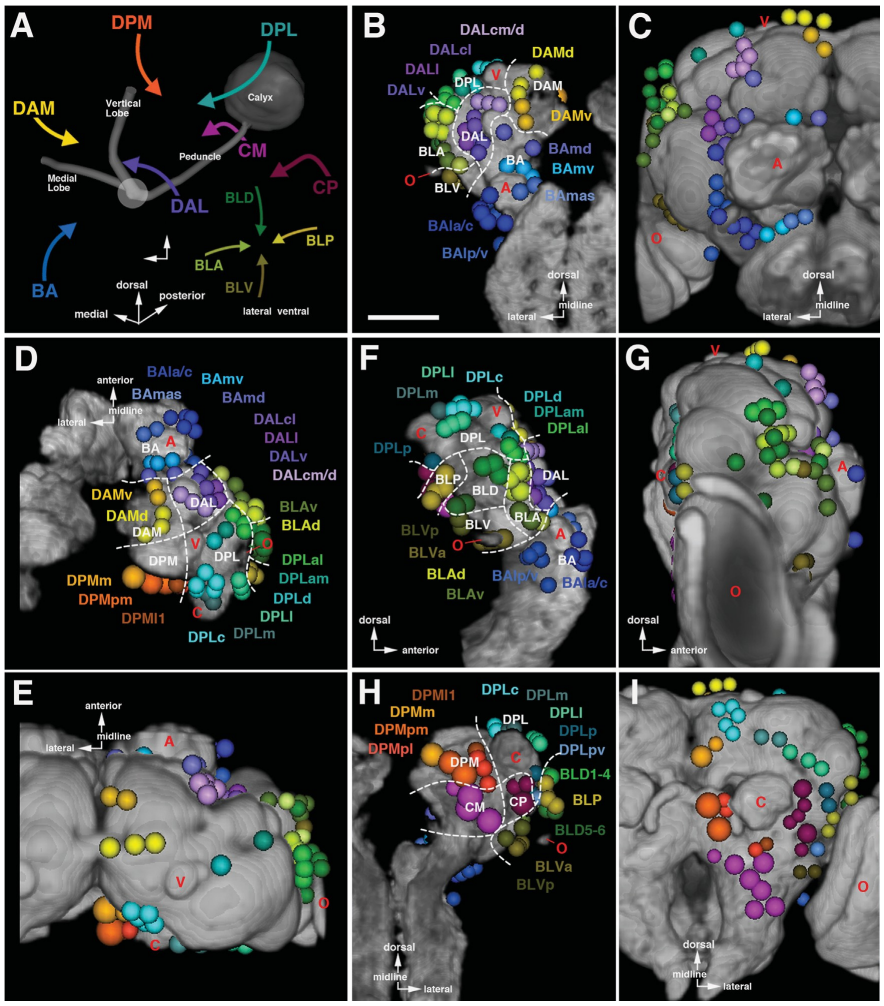

Fig. 6. Topological classification of secondary lineages. (A) Spatial relation between lineage groups and mushroom body. Arrows indicate neuropil entry points of lineages belonging to the group represented by acronyms (BA basal anterior; BLA basal lateral anterior; BLD basal lateral dorsal; BLP basal lateral posterior; BLV basal lateral ventral; CM central medial; CP central posterior; DAL dorsal anterior lateral; DAM dorsal anterior medial; DPL dorsal posterior lateral; DPM dorsal posterior medial). ((B)–(I)) Digital three-dimensional models of larval and adult brain hemispheres, showing position of neuropil entrypoints of lineages (colored spheres) in relationship to neuropil topography (gray). The neuropil surface model was generated by volume-rendering of a series of confocal sections of a brain hemisphere labeled with the synaptic marker nc82 or Brp (see Material and Methods). Four prominent elements of the neuropil surface are indicated in red lettering (A antennal lobe; C calyx; V tip of vertical lobe; O optic lobe). Panels are arranged in four pairs (B/C, D/E, F/G, H/I), with one member of each pair representing the larval brain (B, D, F, H), the other the adult brain (C, E, G, I). The pairs represent different view points (B/C: anterior; D/E: dorsal; F/G: lateral; H/I: posterior). White hatched lines on panels showing larval brains demarcate territories occupied by the different lineage groups that are annotated in white lettering (eg. BA, BLA). The affiliation of individual lineages with a group and subgroup is color-coded (BA blue; BLA yellow–green; BLD dark green; BLP light olive; BLV dark olive; CM magenta; CP maroon; DAL purple; DAM yellow; DPL turquoise; DPM orange). Lineage subgroups are annotated in colored lettering (eg. BAmd, BAmv) and set close to the corresponding colored spheres. Most subgroups are differentiated by different shades of color; in some cases where two subgroups are close to each other, they are represented by the same color, and the acronyms are contracted (e.g. BAla and BAlc is contracted as BAla/c). Neuropil growth between larval and adult stage causes entry points of lineages to move away from each other (see Figs. 2 and 3); entrypoints of lineages of the same subgroups typically stay together, and position of groups/subgroups relative to each other remains similar. For abbreviations of all lineages see Table 2. Scale bar: 50 μm ((A)–(I)).

In the remaining sections of this paper and in the accompanying paper (Wong et al., 2013), the above topological classification will be used to order the description of secondary lineages and their projections (Figs. 7–13). In the first set of figures, we describe the axonal projections of the adult secondary lineages, starting with lineages entering the anterior brain surface (BA: Fig. 7; DAL and DAM: Fig. 9), followed by those of the dorsal surface (DPL: Fig. 10), posterior surface (DPM, CM, CP: Fig. 12), and finally, lateral surface (BLA, DLD, BLP, BLV: Fig. 13). In each of these figures, the left column of panels show z-projections of frontal sections of left brain hemispheres, ordered from

posterior (top) to anterior (bottom). Each z-projection represents a brain slice of approximately 15–20 μm thickness in which segments of SATs, labeled by BP104, are visible. The panels on the right hand side of Figs. 7, 9, 10, 12, and 13 represent semi-schematic 3D maps of the group(s) of lineages shown in the corresponding figure. Lineages are represented as a sphere (location of SAT entry point into neuropil) and line (SAT trajectory in neuropil). In panels at the bottom, neuropil entry points are projected on a 3D volume rendering of the neuropil surface, which illustrates the position of the lineage in relation to prominent surface landmarks (e.g. antennal lobe, anterior optic tubercle, mushroom body). The large right panel at the top schematically shows the trajectories of SATs in the neuropil. A second set of figures (Figs. 8 and 11) document SATs of the eleven lineage groups at different developmental stages, including late larva (L3), pupa (P12, P24, P32, P48), and adult. Fig. 8 shows lineages located in the anterior part of the brain while Fig. 11 shows posterior lineages. To complement this paper as well as the accompanying paper (Wong et al., 2013), we have developed an online tutorial, the Drosophila Brain Lineage Atlas, which provides a three-dimensional description of adult secondary lineages (highlights neuropil entry points, SAT trajectories, and axonal projection patterns): https://www.mcdb.ucla.edu/Research/Hartenstein/dbla/.

The BA lineages (#1–17)

The BA group comprises lineages associated with the ventral brain compartments (antennal lobe, antenno-mechanosensory and motor center, ventro-medial cerebrum, ventro-lateral cere- brum, lateral accessory lobe). BA cell body clusters are grouped around the antennal lobe (AL). Four lineages, BAla1–4 (#1–4), form the antero-lateral BA subgroup whose SATs enter the neuropil in the niche formed between the ventral AL and antenno-mechanosensory and motor center (AMMC), the compartment receiving input from the auditory Johnston's organ and other mechanosensory bristles of the head (entry portal ptAL vl; Fig. 7A–C). BAlc (#5d/v; corresponding to the group of neurons called the lateral cluster in the literature, and labeled by the marker ***GH146-Gal4***; Lai et al., 2008) enters the lateral surface of the AL (ptAL l; Fig. 7A′, B and C). SATs of the postero-lateral BA group [BAlp1-4 (#6–9), BAlv (#10)] reach the neuropil further posteriorly, in the niche formed between the AL, ventro-lateral protocerebrum (VLP), and AMMC (pt VLP vm; Fig. 7A–C). The pair of medial ascending lineages, BAmas1 and 2 (#11–12), are located ventro-medially of the AL and project their SATs dorsally into the median bundle (ptAL vm; Fig. 7A–C). BAmd1 and 2 (#13–14; Fig. 7A–C) are located dorsally of the AL. The two separate hemilineage clusters of BAmd1 flank the mushroom body medial lobe; the dorsal HSAT (#13d) enters dorsally of the medial lobe (ptVL vm; Fig. 7A′ and B), the ventral HSAT (#13v) passes between the medial lobe and antennal lobe (ptALd; Fig. 7A′ and B). The SAT entry point of BAmd2 is obscured by the fibers of the median bundle and antennal nerve in the adult brain. BAmv1-3 (#15–17) form a compact group of SATs at the dorso-lateral surface of the AL in the larva. Whereas BAmv3 (whose entry point into the AL is also obscured by antennal nerve afferents) maintains this position (entry point ptAL d; Fig. 7B), the entry points of BAmv1 and BAmv2 come to lie at the ventral surface of the adult AL (ptAL v; Fig. 7A–C; see below).

Four BA lineages, BAla1 (#1, labeled by ***per-Gal4***; Spindler and Hartenstein, 2010; Spindler and Hartenstein, 2011), BAlc (#5d, dorsal hemilineage; labeled by ***GH146-Gal4***; Stocker et al., 1997), BAlp4 (#9), and BAmv3 (#17, labeled by ***GH146-Gal4***; Stocker et al., 1997) include all of the projection neurons connecting the AL and superior protocerebrum (calyx and lateral horn; Das et al., 2013; Lai et al., 2008) via the antennal lobe tracts (ALT; Fig. 7G; for a detailed description of the distinct entry portals of these lineages into the AL, see Das et al., 2013). The ventral HSAT of BAlc forms the intermediate bundle of the loV fascicle (loVI) that extends posteriorly into the inferior ventro-lateral cerebrum (VLCi; #5v in Fig. 7A, D and G). BAmas1 and 2 project dorsally through the median bundle towards the superior medial protocerebrum (SMP; #11–12 in Fig. 7A and G). BAmd1 and BAmd2 (#13–14) have commissural tracts. The dorsal HSAT of BAmd1 (#13d) projects medially directly behind the medial lobe and crosses in the fronto-dorsal commissure. Shortly after its entry point (#13d in Fig. 7A′), the trajectory of the HSAT becomes obscured by the dense labeling of the mushroom body medial lobe; the tract is visible until mid-pupal stages (Fig. 8F). The ventral HSAT of BAmd1 projects diagonally through the AL to cross in the antennal lobe commissure (#13v in Fig. 7A, D and G). BAmv1 (marked by ***per-Gal4***; Spindler and Hartenstein, 2010; Spindler and Hartenstein, 2011) and BAmv2 form the loVM that passes underneath the AL and extends posteriorly throughout the ventro-medial cerebrum (VMC; #15–16 in Fig. 7A, D, E and G). A major dorsal branch of BAmv1 (BAmv1d; #15d) curves dorsally towards the central complex, forming the posterior component of the lateral ellipsoid fascicle (LEp; Fig. 7D and G). Tracts of BAlp2 and BAlp3 form the lateral loV fascicle (loVL; #7–8 in Fig. 7A, D, E and G). The BAlp2 tract gives off a dorsal branch that extends along the lateral surface of the lateral accessory lobe (LAL; #7d in Fig. 7D).

Fig. 7. Trajectories of SATs formed by the BA lineage group. The left column of panels show z-projections of frontal sections of left brain hemispheres, ordered from posterior (top) to anterior (bottom). The right panels represent semi-schematic three-dimensional maps of the BA lineage group(s). Lineages are represented as a different colored spheres (location of SAT entry point into neuropil) and lines (SAT trajectory in neuropil). Fascicles are annotated in yellow letters and compartments in green ((A), (D)–(F)) or white ((B), (C) and (G)) letters; for abbreviations, see Table 2. Where one or more SATs associate with a specific fascicle, their numerical identifiers appear directly adjacent to the fascicle name. Bottom-right panels ((B) and (C)) show neuropil entry points of BA lineages projected on a three-dimensional volume rendering of the neuropil surface, illustrating the position of the lineage in relation to prominent surface landmarks, provided by specific compartments. Panel B presents an anterior view of both hemispheres. Prominent neuropil compartments shaping the surface topography are annotated in white lettering on the left side of panel B (e.g. AL antennal lobe; AOTU anterior optic tubercle; for complete list of abbreviations see Table 2); entry portals of specific lineages/lineage groups are shown by annotated hatched circles and arrows on the right side of panel B. Panel C shows antero-lateral view of right brain hemisphere; on this panel, names of lineage subgroups and their corresponding numbers are indicated. Hemilineages (represented by two separate spheres), are pointed out by single letters (d dorsal; v ventral) superimposed on spheres. (G) Schematics of trajectories of SATs of BA lineages at various levels overlaid on adult brain labeled with N-Cadherin (gray). Each level in G is represented by a corresponding frontal Z-projection (denoted by white arrows in (A), (D)–(F); see below). Z-projections are compressed (50%) along the *y*-axis, such as to give the set of these images the appearance of a cut-away diagram of the neuropil in antero-dorsal view. SATs entering the neuropil from anterior to associate with a specific fascicle are shown as opaque lines, converging on the signal-negative domain corresponding to that fascicle. Note, for example, the SATs of BAla1 (#1), BAlc d (#5d), BAlp4 (#9) and BAmv3 (#17), whose SATs form the antennal lobe tract (ALT). The colored lines representing these SATs target the signal-negative "hole" formed by the ALT in the posterior antennal lobe. After passing through that "hole" (and thereby disappearing "behind" the first z-projection), the lines representing the SATs are rendered semitransparent. Once they "reappear" in the space between the first (A) and second z-projection (D), the lines become opaque again. In cases where several SATs come close and cannot be separated (such as SATs which enter the ALT), lines of individual SATs are graphically "merged" by a thick, semitransparent line (blue in the case of the ALT). Hatching of (parts of) lines indicates that the corresponding segments of the SATs cannot be recognized in BP104-labeled adult brains, but are visible in larval/pupal stages, as well as MARCM clones of the corresponding lineages. ((A), (D)–(F)). Z-projections of frontal confocal sections adult brain left hemisphere labeled with N-Cadherin (purple) and Neuroglian (BP104, gray). Each z-projection represents a brain slice of approximately 15–20 μm thickness. Brain slices are ordered from anterior (A) to posterior (F) and correspond in antero-posterior location to those shown in Fig. 5A–D ((A) level of mushroom body lobes; (D) ellipsoid body; (E) fan-shaped body and great commissure; (F) lateral bend of the antennal lobe tract). Short segments of SATs and the fascicles they form in the neuropil, labeled by BP104, are visible. Only SATs and fascicles of BA group lineages are annotated. SATs are annotated by numbers, to save space; the correspondence of lineages and numbers is given in Table 1 and on panel C of this Fig. (e.g. #11–12 correspond to BAmas1-2). Scale bars: 25 μm ((A), (D)–(F)); 50 μm ((B) and (C)).

BAla3 (#3, Fig. 7A; marked by ***en-Gal4***; Kumar et al., 2009a), BAla4, BAlp1, and BAlv have single SATs that enter from a position lateral of the AL. BAla3, BAla4, and BAlp1 project medially towards the ventro-medial cerebrum (VMC), with BAlp1 crossing the loVM fascicle at its dorsal surface (#6 in Fig. 7D), and BAla3-4 crosses the medial loV (loVM) at its ventral surface (#3^{n} in Fig. 7D). BAlv has a short SAT that contacts the inferior ventro-lateral cerebrum from ventral (VLCi; #10 in Fig. 7D and G).

Of the BA lineages, nine (BAlc, BAlp1-4, BAlv, BAmd1, and BAmv1-2) can be individually followed from their point of entry deep into the neuropil throughout metamorphosis (Fig. 8; Fig. S1). Six BA lineages (BAla1-2, BAla3-4, BAmas1-2) form pairs whose

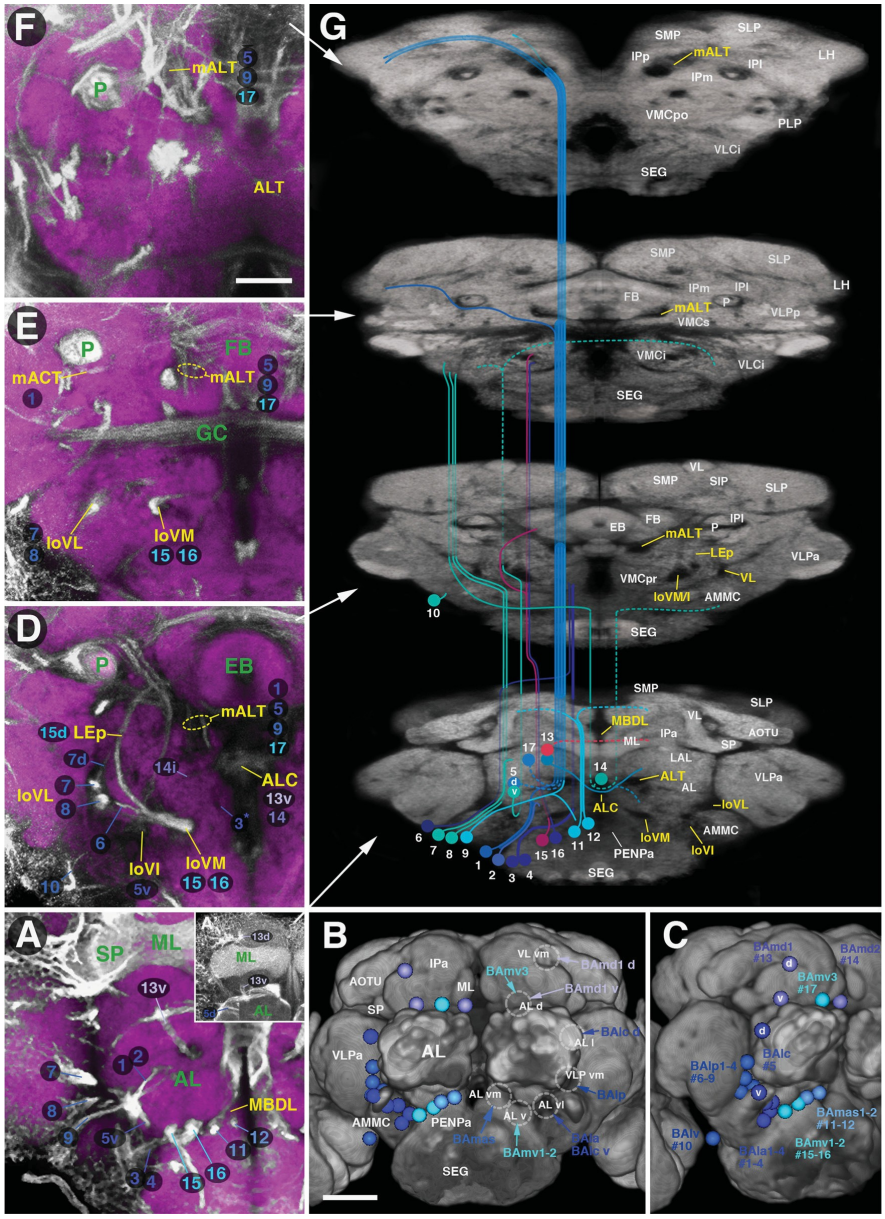

SATs are closely associated. The paired SATs of these lineages (indicated by the number corresponding to the first lineage of the pair followed by an asterisk; for example, "#3n" for the pair "BAla3-4"; Fig. 7D) can also be followed throughout metamorphosis (Fig. 8), but lineages within each pair are distinguishable only on the basis of clones or genetic markers. The points of entry of two BA lineages (BAmv3, #17; BAmd2, #14) become indistinct at later pupal stages because of strong surrounding labeling of antennal afferents (Fig. 8). BAmv3, marked by the ***GH146-Gal4*** driver (Stocker et al., 1997), enters the AL from dorsal (Fig. 7B–G, Fig. 8A′). BAmd2 (#14), clearly visible until P24, enters near the midline in between the two brain hemispheres (Fig. 8A′-B, C′-D and E′-F); the SAT joins the ventral HSAT of BAmd1, crossing in the antennal lobe commissure (ALC). In addition, BAmd2 has an ipsilateral branch that is fairly thin in the larva and early pupa, but increases in diameter and forms a visible tract in the late pupa and adult stages (#14i in Fig. 7D; Fig. 8J and L).

Changes in the position of BA lineages are mainly brought about by the general expansion of the anterior brain neuropil compartments, notably the AL, AMMC, and anterior ventrolateral protocerebrum (VLPa; see panels of left column of Fig. 8; Fig. 8A, C and E). The AMMC, formed around the mechanosensory component of the antennal nerve during metamorphosis, has no larval counterpart; it grows and expands in a region between the BAlp lineages (dorsolateral of the AMMC) and BAla lineages (ventro-medial of the AMMC) starting around P32 (Fig. 8G, I and K). Furthermore, the hemilineage clusters of BAlc (#5, Fig. S1C; white arrows) and BAmd1 (#13, Fig. S2C; white arrows) and their HSAT entry points move slightly apart. However, the relative positions of these and all other BA SAT entry points remain constant; with the notable exception of the BAmv1 and BAmv2 (#15–16) lineages which undergo an interesting switch in position relative to the AL (compare the yellow and orange spheres in the top two panels of Fig. S1A). In the larva, the SATs of BAmv1-2 enter dorsal of the AL (Fig. 8A, blue arrow); in the adult, they are ventral (Fig. 8K, blue arrow). This change comes about as a result of the metamorphic decay of the larval AL (AL_{Lar}) and the formation of the adult AL (AL_{Ad}). The AL_{Ad} primordium is visible in the late larva as a small domain of dense NCad-labeling at the dorsal edge of the AL_{Lar} (Fig. 8A). The AL_{Ad} domain expands throughout pupal development (Fig. 8C and E) and acquires a glomerular texture by P32 (Fig. 8G). At the same time, the glomerular composition of the AL_{Lar} decays and becomes invisible by P32. The neuropil entry point of BAmv1 and 2 in the larva is positioned dorsally of the AL_{Lar}, adjacent to the small AL_{Ad} primordium (Fig. 8A). As the AL_{Ad} primordium grows (P12, P24), it pushes the BAmv1/2 entry point ventro-medially (Fig. 8C and E, blue arrow). Note that at this transitional stage, the entry point is still dorsal of the decaying AL_{Lar} (Fig. 8C). Finally, by P48, the BAmv1/2 entry point is ventral of the AL_{Ad}.

DAL lineages (#18–32)

DAL lineages occupy a position dorsal of the BA group, surrounding the spur (SP) and lobes of the mushroom body (medial lobe ML; ventral lobe VL; see Table 2). Neurons of the first subgroup, DALcl1 and DALcl2 (#18–19), encircle the anterior optic tubercle (AOTU, a distinct compartment receiving input from the optic lobe via the anterior optic tract; Strausfeld, 1976; Fig. 9B and C). DALcl tracts enter the neuropil, at the junction between the mushroom body spur (SP) and vertical lobe (VL) (entry portals ptSP d and ptSP v; Fig. 9A and G). The second subgroup, DALcm1-2 and DALd (#20–22), is located dorso-medial of the DALcl lineages (Fig. 9A–C); its tracts enter the neuropil closely adjacent to the DALcl tracts, forming two entry portals that flank the base of the VL medially and laterally (ptVL vm and ptVL vl; Fig. 9C and G). Tracts of the third subgroup, DALv1-3 (#25–27), located ventrally of the ML, pass underneath the SP and ML (ptSP v; Fig. 9A–D and G). Further laterally, DALl1 and DALl2 (#23–24) enter the anterior surface of the ventro-lateral protocerebrum (VLP), laterally adjacent to the SP (ptVLP dm; Fig. 9A–D).

DALcl1 and DALcl2 each have two hemilineages whose diverging HSATs, in a "pincer-like" manner, enclose the SP (#18dn and #18vn; Fig. 9A, Fig. S2D and E). The ventral HSATs of DALcl1/2 pass underneath the SP and continue medially. Ventral DALcl1 (#18v) crosses the midline in the subellipsoid commissure (SuEC); ventral DALcl2 (#19v) joins the lateral ellipsoid fascicle (LE), along with DALv2 and DALv3 (see below), and projects to the central complex (#19v in Fig. 9A, D, E and G). The dorsal HSATs of both DALcl lineages curve over the dorsal surface of the SP and peduncle (P) and project towards the central complex, lateral accessory lobe (LAL), and superior medial protocerebrum (SMP; #18dn in Fig. 9A, D, E and G).

DALcm1 and DALcm2 have two hemilineages forming two paired HSATs. The medial HSAT passes behind the medial lobe into the fronto-medial commissure, following the dorsal HSAT of BAmd1 (FrMC; #20mn in Fig. 9A and G). As in the case of BAmd1d (#13d), the medial HSAT of DALcm that passes through the ML is clearly demarcated in the pupa, however it is indistinct in adult brains (Fig. 8C′ and F). The lateral HSATs of DALcm1-2 (#20ln), accompanied by the single SAT of DALd (#22), pass through the elbow formed by the VL and peduncle before turning ventrally (Fig. 9A, D–E, G; Fig. S2B). These tracts constitute the descending central protocerebral tract (deCP) that projects towards the ventral brain, including the VMC, VLCi, and SEG (Pereanu et al., 2010). DALv1 has a prominent SAT that projects straight posterior in between the ventro-lateral protocerebrum (VLP) and lateral accessory lobe (LAL) compartments (#25 in Fig. 9A, D and G), forming the anterior component of the lateral equatorial fascicle (LEFa; Pereanu et al., 2010). The LEFa bifurcates more posteriorly and enters the great commissure (GC; Fig. 9F and G; Fig. S5C and D). DALv2 (marked by ***EB1-Gal4*** and ***per-Gal4***; Spindler and Hartenstein, 2010, 2011) and DALv3 (marked by ***en-Gal4***; Kumar et al., 2009a) send their SAT dorso-medially, forming the anterior componenet of the lateral ellipsoid fascicle (LEa) that passes underneath the ML towards the central complex (#26n in Fig. 9A, D and G; Fig. S2D–E). DALv2 projects into the ellipsoid body, forming the R-neurons of this compartment; DALv3 is branched, crossing the ellipsoid body dorsally and ventrally in the supraellipsoid commissure (SEC; #27d) and subellipsoid commissure (SuEC; #27v, Fig. 9D; S2D-E), respectively.

DALl1 and DALl2 are located laterally of the SP. DALl2 projects a short SAT into the anterior part of the anterior ventro-lateral protocerebrum (VLPa; #24 in Fig. 9A and G); DALl1 has a long tract that passes posteriorly (#23 in Fig. 9D–G) and, after giving off a branch ventrally towards the posterior lateral protocerebrum (PLP), makes a 180 degree turn back towards anterior to reach the anterior optic tubercle (AOTU). The recurrent leg of the DALl1 SAT can be followed in the larva and early pupa (not shown), but is indistinct in the adult.

Changes in DAL lineage topology during metamorphosis occur when the emerging AOTU, which has no larval counterpart, pushes in between DALcl1-2 (#18–19, lateral) and DALcm1-2 (#20–21, medially; Fig. 8C–C′, E–E′ and G–G′). During this period, HSATs of these two pairs move slightly apart (arrows in Fig. S2C–D). These changes aside, all DAL lineages maintain their relative position. Most of the SATs or HSATs of the DAL group, including the ventral HSATs of DALcl1/2 and the SATs of DALd, DALl1, and DALv1 (#22, #23, #25), can be individually followed throughout development (Fig. 8). The dorsal HSATs of DALcl1/2 (#18dn), as well as both HSATs of DALcm1/2 (#20mn, 20ln) form pairs; DALv2 and DALv3 have tracts that are close together and cannot be separated (#26n). Furthermore, these paired tracts become fairly indistinct in BP104-labeled brains of late pupae (≥P48); as mentioned above, medial DALcm cannot be followed beyond its entry point into the neuropil of the adult brain.

DAM lineages (#28–32)

Clusters and SAT entry points of all five DAM lineages (#28–32) are located close to the brain midline, medial of the VL (entry portal ptVL dm; Fig. 9B–D). All DAM lineages have single SATs; tracts of DAMd2–3 (#29–30) and DAMv1-2 (#31–32) form pairs whose SATs cannot be separated from each other in the neuropil. DAM tracts can be clearly followed throughout pupal development (compare panels Fig. 8B, D, F, H, J and L; Fig. S2A–B). The DAMd1 SAT (#28) projects medially and crosses the midline in the anterior dorsal commissure (ADC, Fig. 9D and G). The paired DAMd2-3 tract (#29^{n}) projects posteriorly, forming the thick loSM fascicle (Fig. 9D–G). The DAMv1-2 pair (#31^{n}), located ventrally adjacent to DAMd2-3, forms a short tract that is directed dorso-posteriorly and terminates near the surface of the superior medial protocerebrum (SMP; Fig. 9D and G). The only developmental change affecting the DAM lineages is a dorsal shift in location, subsequent to the growth in volume of the ML and the surrounding anterior inferior protocerebrum (IPa)/SMP compartments (compare panels Fig. 8D, H).

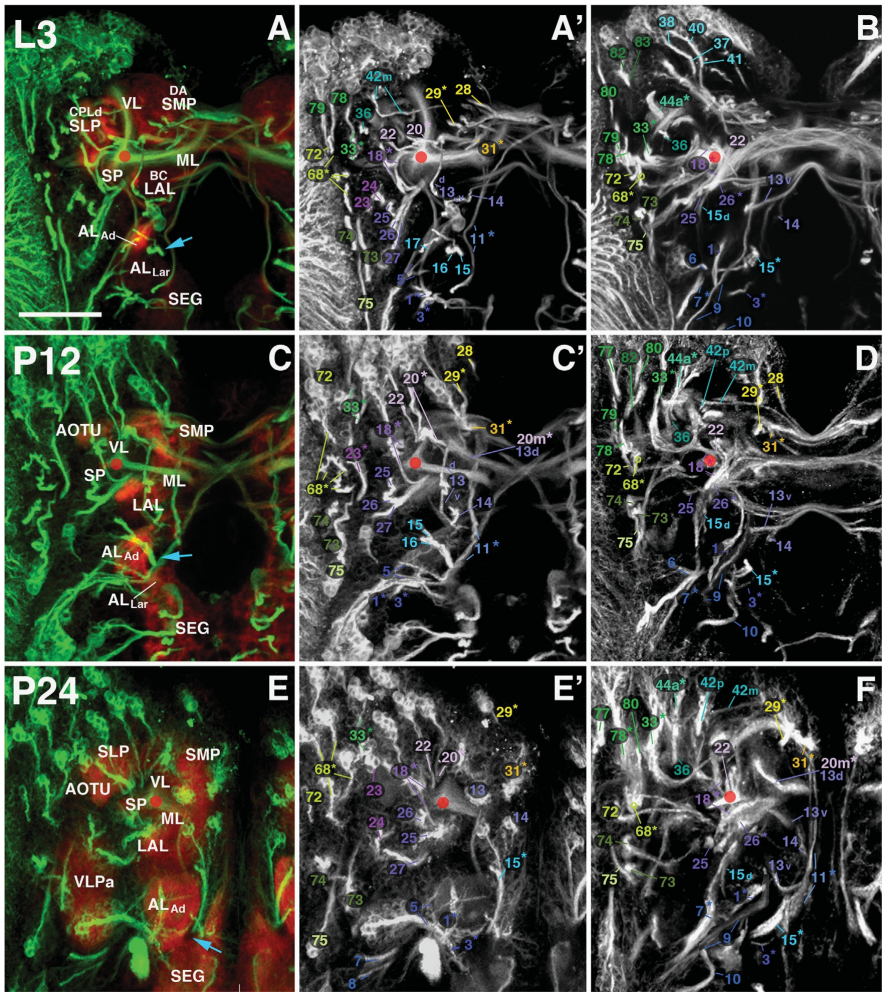

Fig. 8. Larval-to-adult development of lineages of the anterior brain. Panels of each side of this split figure are arranged in three rows and three columns. Each row represents one stage, indicated at the top-left corner (L3, A-B; P12, C-D; P24, E-F; P32, G-H; P48, I-J; Adult, K-L). All panels show z-projections of contiguous confocal sections of a brain hemisphere labeled with BP106 or BP104 and N-Cad, representing brain slices of 15–20 µm thickness. Z-projections of the first and second column (A/A′, C/C′, E/E′, G/G′, I/I′, K/K′) correspond to an anterior level (mushroom body lobes). Both BP104-labeling (secondary neurons, SATs and fascicles; green) and N-Cad labeling (neuropil; red) is shown in left panels; middle panels show BP104 labeling only (white; A′, C′, E′, G′, I′, K′). Panels of the right column (B, D, F, H, J, L) represent a "subanterior" level (ellipsoid body/primordium of ellipsoid body). Compartments visible at the anterior neuropil surface are annotated (white lettering, panels of left column; see Table 2 for complete listing of abbreviations). SATs and HSATs of individual lineages are annotated with a unique numerical identifier (see Table 1). Numbers followed by an asterisk indicate tracts formed by more than one SAT (typically two SATs) which cannot be followed separately. For example, "20*" stands for "20 and 21". Lower case letters ('a,' 'd,' 'i,' 'm,' 'p,' or 'v') indicate HSATs formed by individual hemilineages within a particular lineage. The red circle in each panel marks the location of the peduncle. The blue arrow in (A), (C), and (E) marks the entry point for the SATs of BAmv1/2. Scale bar: 50 µm.

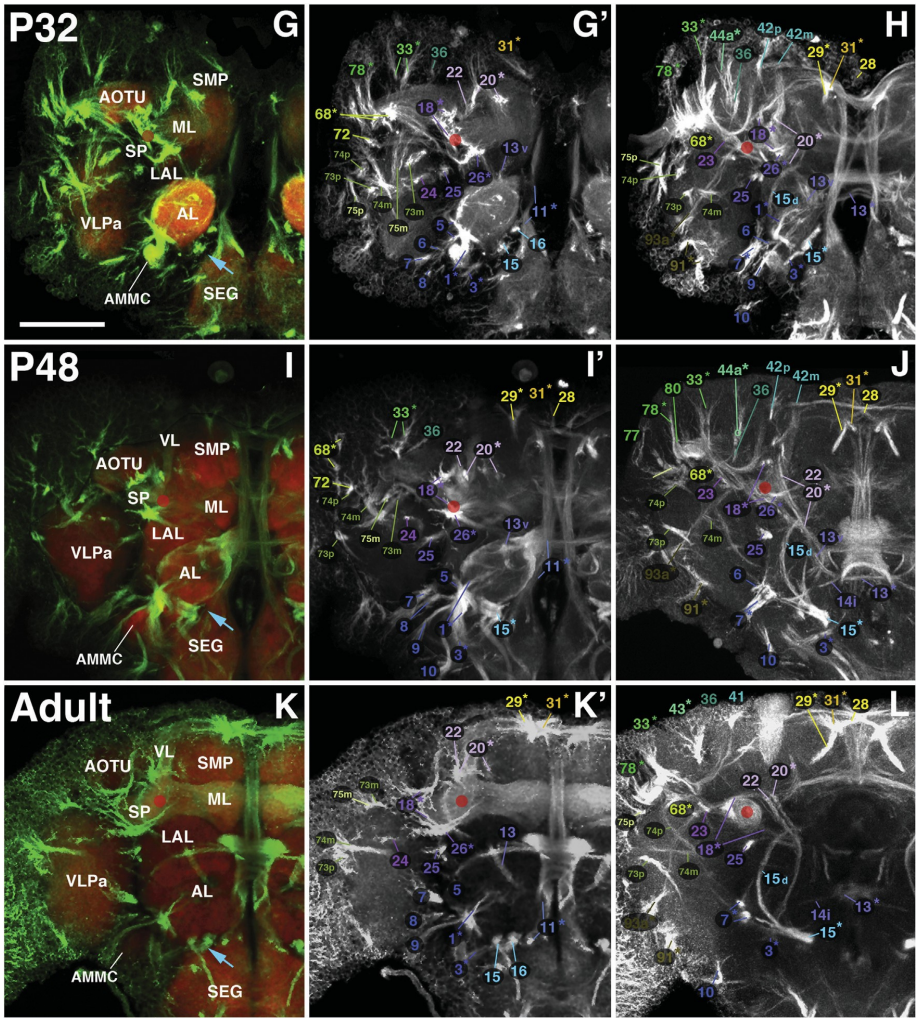

Fig. 8. (*continued*)

DPL lineages (#33–50)

DPL lineages are clustered over the dorso-lateral brain surface. The lineage subgroups DPLal1-3, DPLam, and DPLd are located anteriorly in the crevice between the anterior optic tubercle (AOTU) and superior lateral protocerebrum (SLP). All other DPL subgroups are located more posteriorly, surrounding the mushroom body calyx (CA): dorso-medially (DPLc1-5), dorsally (DPLm1-2), and dorso-laterally (DPLp1-2, DPLpv) (Fig. 10A–C and F). SATs of DPLal1-3 (#33–35) form a conspicuous, crescent shaped bundle that defines the anterior transverse superior fascicle (trSA). From the DPLal entry point, located at the lateral base of the SLP (ptSLP l; Fig. 10C–C″), this bundle curves ventro-medially, turns, and then continues dorso-medially to terminate superficially within the superior lateral protocerebrum compartment (SLP; Fig. 10A and G). A second, more ventral bundle curving around the peduncle at its ventral side branches off the trSA. According to the larval and adult clones of DPLal lineages (Wong et al., 2013), one of them (DPLal1, #33) is restricted to the trSA, whereas two (DPLal2-3) contribute to both the trSA and a ventral branch (#34d^{n} and #34v^{n} in Fig. 10A and G, Fig. S5A–B). DPLam (#36), marked by the ***en-Gal4*** driver (Kumar et al., 2009a), is located medially adjacent to the DPLal lineages (Fig. 10A–C″). The DPLam SAT enters between the AOTU and SLP (ptSLP a; Fig. 10C″), projects straight postero-ventrally, through the center of the hemi-circle formed by the trSA fascicle (Fig. 10A) and terminates in the inferior protocerebrum (purple line in Fig. 10G), laterally adjacent to the peduncle (Fig. 10D and G, Fig. S2C–D). We call this projection the vertical tract of the superior lateral protocerebrum (vSLPT; Fig. 10D). DPLd fibers (#42) enter laterally of the vertical lobe of the mushroom body (ptVL dl; Fig. 10A–C″). DPLd projects two HSATs: one is directed medially (#42m), curving around the anterior surface of the VL and entering the anterior dorsal commissure (ADC in Fig. 10A and G); the second one (#42p) projects postero-laterally, forming an anterior component of the loSL fascicle (Fig. 10A, D and G; Fig. S2D–E).

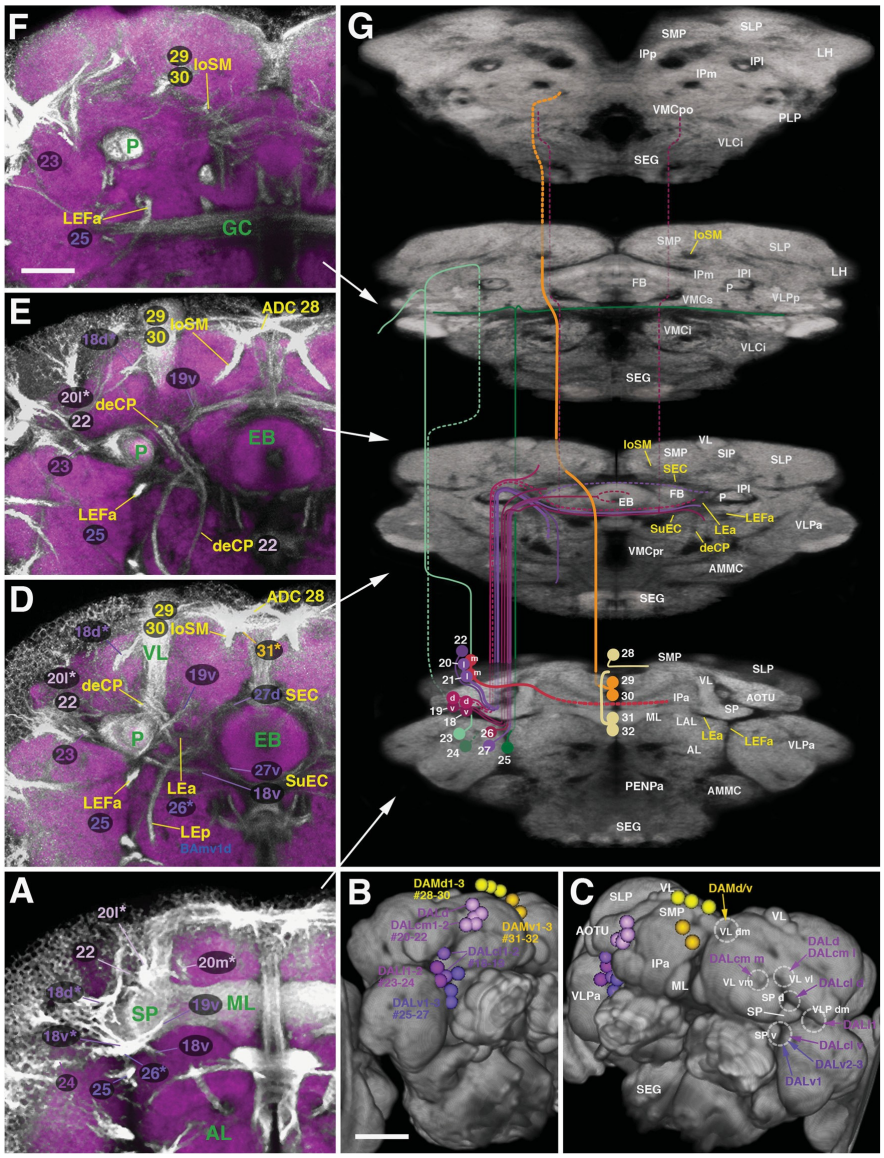

Fig. 9. Trajectories of SATs formed by the DAL and DAM lineage groups. The composition of this figure follows the same plan explained for Fig. 7, with sets of z-projections ((A), (D)–(F)) illustrating segments of the SATs and fascicles at different antero-posterior levels, neuropil surface views showing location of SAT entrypoints ((B) and (C)) and neuropil cut-away diagram depicting SAT trajectories (G). Note that some of the panels on the left ((E) and (F)) do not show the same z-projections as those depicted in Fig. 7 (e.g. E represents a level on slightly posterior to that shown in (D); (F) corresponds to the fan-shaped body/great commissure level, see white arrows pointing out antero-posterior levels of the z-projections). Panels B and C show antero-lateral view of right hemisphere (B) and dorsal antero-lateral view of both hemispheres (C). White lettering in C and G annotates neuropil compartments (left side of C) and SAT entry portals (right side of G); yellow lettering in G indicates fascicles (for alphabetical list of abbreviations, see Table 1). Scale bars: 25 μm ((A), (D)–(F)); 50 μm ((B) and (C)).

Among the posterior DPL lineages, the DPLc subgroup (#37–41) occupies the most medial position. DPLc lineages have short, ventro-medially directed SATs that enter through a common portal at the boundary between the lateral and medial superior protocerebrum compartments (ptSLP pm; Fig. 10C and G; yellow arrowhead at top of Fig. 10G). Tracts of DPLc1 (#37), c3 (#39), and c5

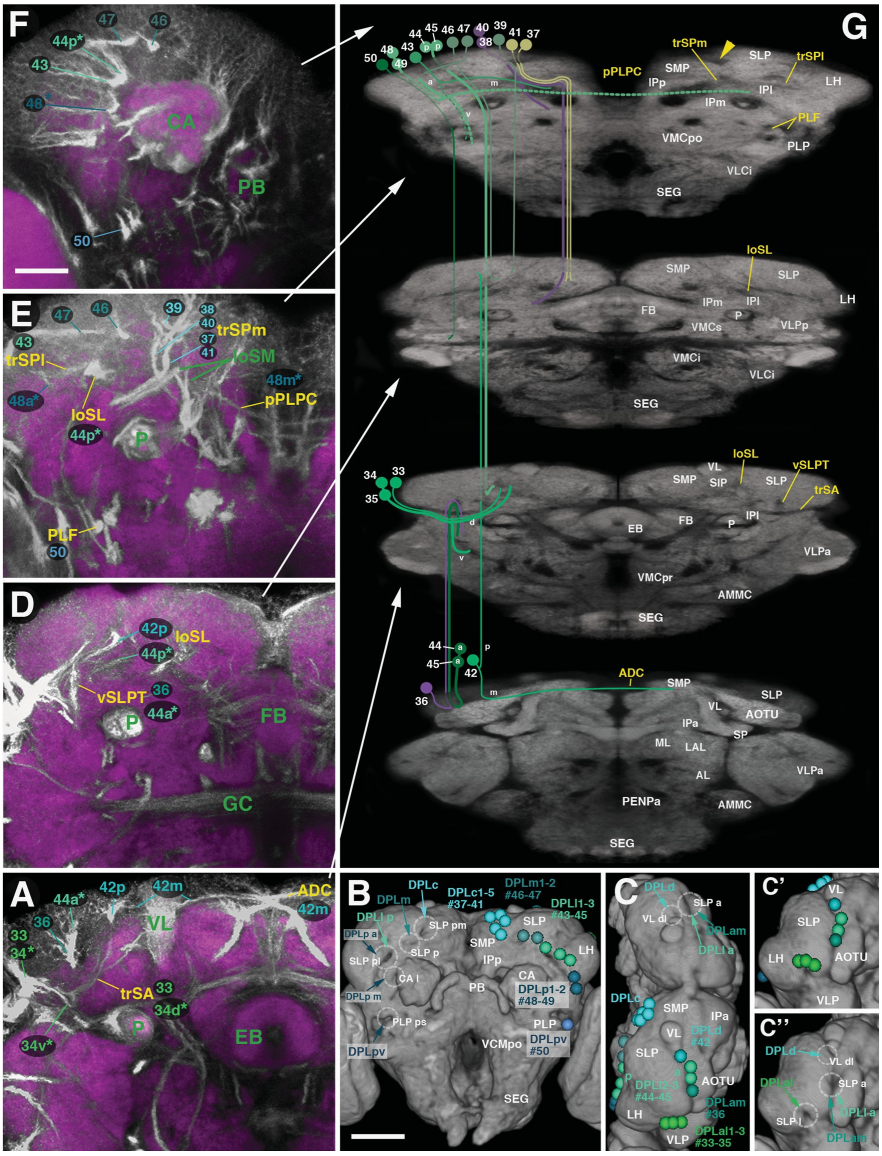

Fig. 10. Trajectories of SATs formed by the DPL lineage group. The composition of this figure follows the same plan explained for Fig. 7, with sets of z-projections ((A), (D)–(F)) illustrating segments of the SATs and fascicles at different antero-posterior levels, neuropil surface views showing location of SAT entrypoints ((B) and (C)) and neuropil cut-away diagram depicting SAT trajectories (G). Position of (A) and (D)–(F) along the antero-posterior axis is indicated by white arrows. Panels B and C show posterior view and dorsal view of both brain hemispheres, respectively. (C′) and (C″*) are antero-dorso-lateral views of right hemispheres. Neuropil compartments are annotated by white lettering on the right side of (B), the bottom half of (C), and in (C′). SAT entry portals (hatched circles) and annotation (small white letters) are shown on left side of (B), top half of (C), and in C″. Yellow lettering in G indicates fascicles (for alphabetical list of all abbreviations, see Table 2). Scale bars: 25 μm ((A), (D)–(F)); 50 μm ((B) and (C)).

(#41) converge upon a point directly lateral of the conspicuous loSM fiber system (green lettering in Fig. 10E), which at this level contains numerous bundles of the DPM and CM lineages (see below). From this point, DPLc1 and DPLc5 curve in a crescent shaped path underneath the loSM (medial component of the transverse posterior fascicle of the superior protocerebrum, trSPm; Fig. 10E and G, Fig. S3A and B). The SAT of DPLc3 (#39) projects straight anteriorly, rather than medially as with DPLc1 or DPLc5 (Fig. 10E and G, Fig. S3A and B). DPLc5 has a second HSAT (#41p in Fig. 11B and D; not distinguishable in BP106/BP104-labeled

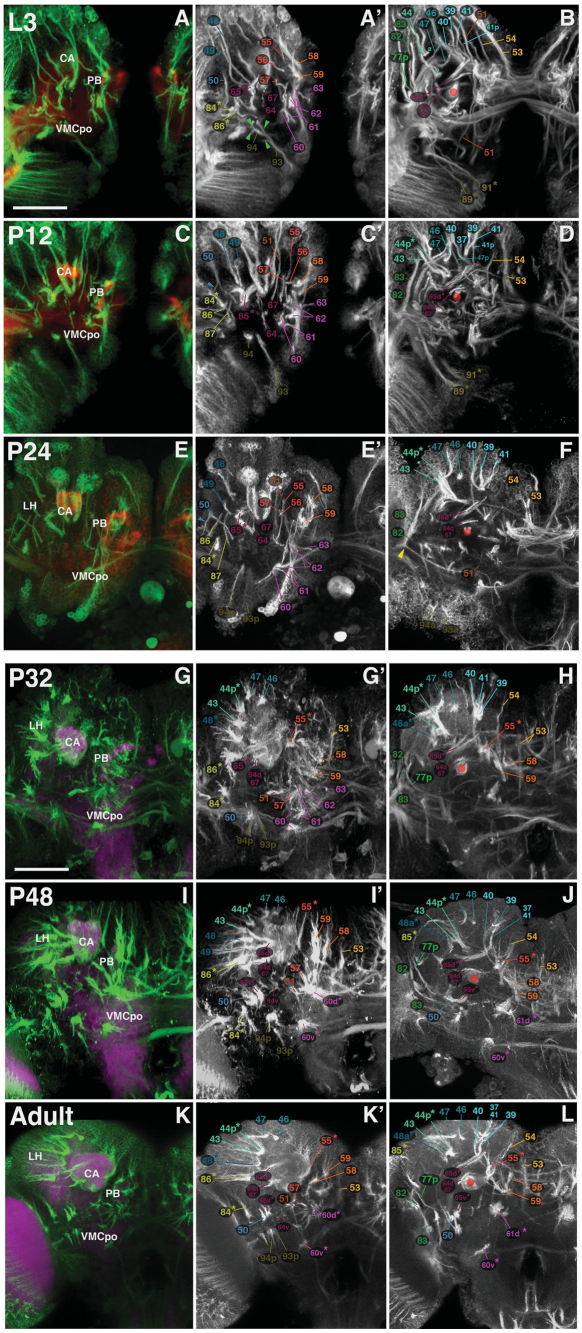

Fig. 11. Larval-to-adult development of lineages of the posterior brain. The composition of this figure follows the same plan explained for Fig. 8, with panels of each side of this split figure arranged in three rows and three columns. Rows represent stages, indicated by at upper-left corner of A, C, E, G, I, and K. Z-projections of the first and second column (A/A′, C/C′, E/E′, G/G′, I/I′, K/K′) correspond to a posterior level (mushroom body calyx; protocerebral bridge) where SATs approach the neuropil surface. Panels of the right column (B, D, F, H, J, L) represent a "subposterior" level (posterior surface of fan-shaped body/primordium of fan-shaped body). Compartments visible at the posterior neuropil surface are annotated (white lettering, panels of left column; see Table 2 for complete listing of abbreviations). SATs and HSAT′s of individual lineages are annotated with a numerical identifier (see Table 1). Scale bar: 50 μm.

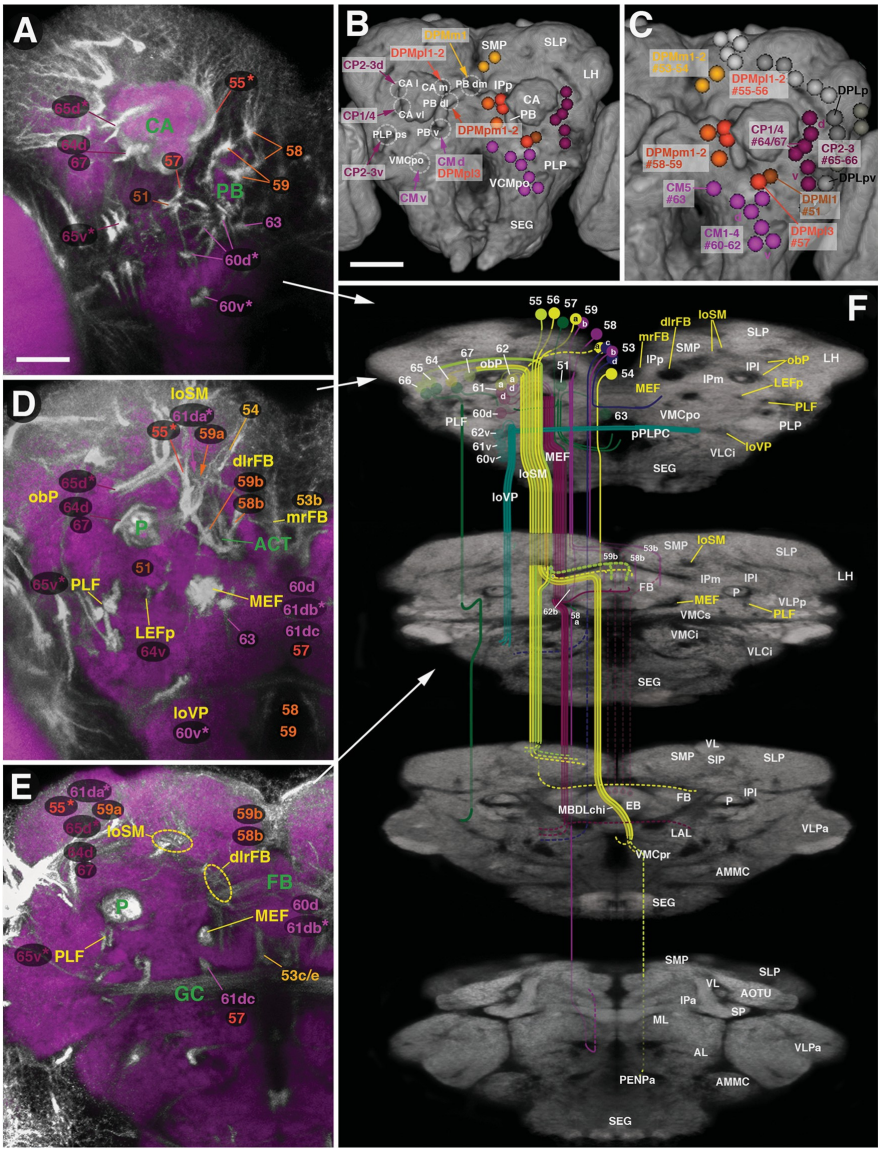

Fig. 12. Trajectories of SATs formed by the DPM, CM, and CP lineage groups. The composition of this figure follows the same plan explained for Fig. 7, with sets of z-projections (A, D, E) illustrating segments of the SATs and fascicles at different antero-posterior levels, neuropil surface views showing location of SAT entrypoints ((B) and (C)) and neuropil cut-away diagram depicting SAT trajectories (G). Position of A, D, and E along the antero-posterior axis is indicated by white arrows. Panel B shows posterior view of both brain hemispheres. C presents enlargement of posterior view of right hemisphere. White lettering on right side of B and G annotates neuropil compartments; hatched circles and white lettering on left side of B indicates SAT entry portals; yellow lettering in G indicates fascicles (for alphabetical list of abbreviations, see Table 2). Scale bars: 25 μm ((A), (D)–(F)); 50 μm ((B) and (C)).

preparations past P24), which enters at the posterior brain surface and projects anteriorly as part of the loSM system (see below). SATs of DPLc2 (#38) and DPLc4 (#40), located laterally adjacent to DPLc1/3/5 (#37, #39, #41), form a paired tract which extends ventrally and medially, curving around the loSM parallel to, but slightly more ventro-posteriorly than the crescent formed by DPLc1/5 (Fig. 10E and G, Fig. S3A–B).

DPLm1 (#46) and DPLm2 (#47) enter the posterior surface of the superior lateral protocerebrum, just dorsal of the calyx (ptSLP p; Fig. 10B and F). The SAT of DPLm1 projects anteriorly into the

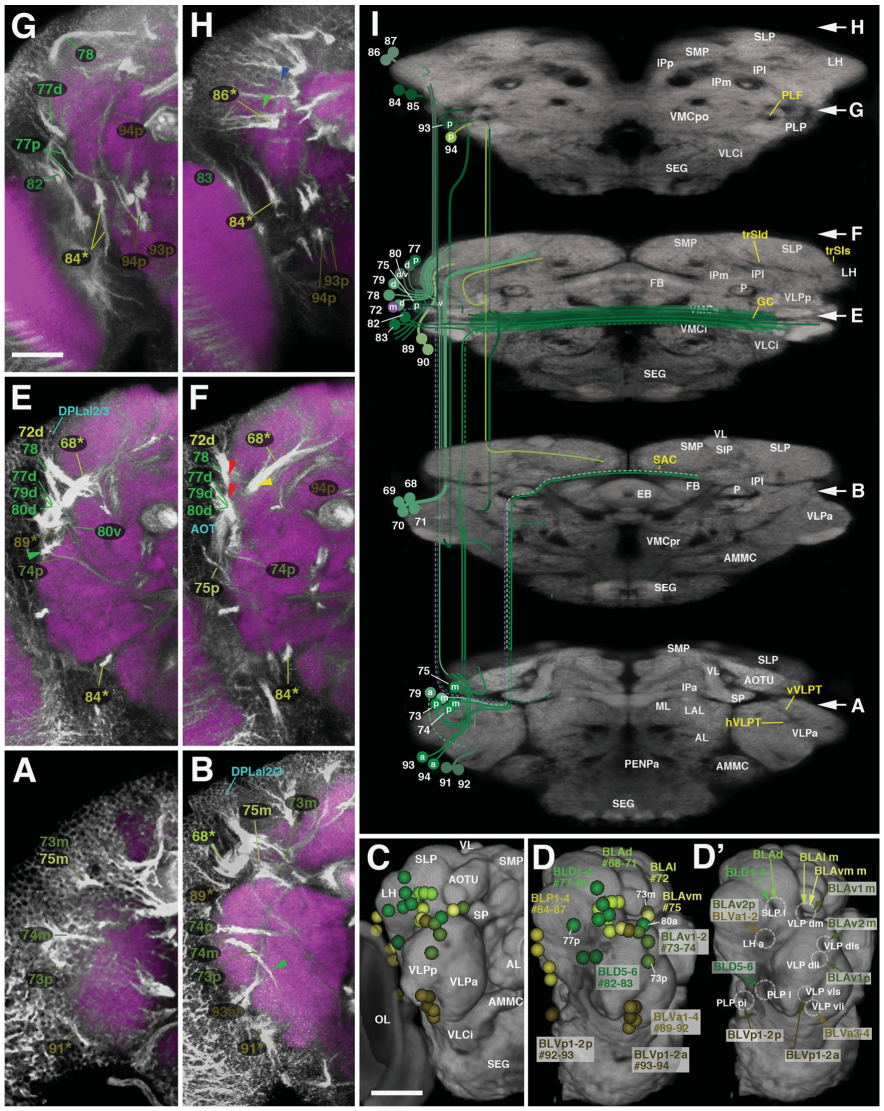

Fig. 13. Trajectories of SATs formed by the BLA, BLD, BLP, and BLV lineage groups. The composition of this figure follows the same plan explained for Fig. 7, with sets of z-projections (A, B, E-H) illustrating segments of the SATs and fascicles at different antero-posterior levels, neuropil surface views showing location of SAT entrypoints (C-D′) and neuropil cut-away diagram depicting SAT trajectories (I). Position of A, B, and E-H along the antero-posterior axis is indicated by white arrows at the right margin of panel I. Panels C-D′ all show antero-lateral view of right brain hemisphere. In D and D′, the optic lobe (OL) is removed from volume rendering of neuropil to gain clearer view of BLP and BLV lineage entry points. White lettering in C and I annotates neuropil compartments; hatched circles and white lettering in D′ indicates SAT entry portals; yellow lettering in I indicates fascicles (for alphabetical list of abbreviations, see Table 1). Scale bars: 25 μm ((A), (D)–(F)); 50 μm ((B) and (C)).

SLP; DPLm2 turns laterally towards the lateral horn (LH; Fig. 10E and G; Fig. S3A and B). DPLm2 has a second tract (#47p in Fig. 11D), no longer marked by BP104/BP106 after P12, which leaves the brain and projects to the ring gland.

SATs of DPL11-3 (#43–45) enter at the junction between the SLP and LH (ptSLP pl; Fig. 10B and F). DPL12 and DPL13 form a pair with two hemilineages each. The posterior HSATs of DPL12-3 (#44p^{n}) are directed anteriorly, forming a thick bundle that constitutes the loSL fascicle (Fig. 10D–G, Fig. S4A). The anterior DPL12-3 hemilineages (#44a^{n}) shift far anteriorly during metamorphosis (Fig. 8B, D, F, H, J and L); forming a paired HSAT that enters the SLP at its anterior surface close to DPLam (ptSLP a), and projecting parallel to DPLam ventrally into the inferior protocerebrum (Fig. 10A, B, D, and G; Fig. S4A). DPL11 (#43) enters next to the posterior HSATs of DPL12-3

(Fig. 10B), but extends medially, forming a thin fiber bundle, the trSPl, which converges upon the fiber tracts formed by the DPLc group (Fig. 10E–G; Fig. S3A).

The last DPL subgroup, DPLp (#48–50), includes clusters of neurons located at the posterior surface of the lateral horn, lateral of the calyx (LH, CA; Fig. 10B and F). DPLp1 and DPLp2 form a pair with two HSATs. One HSAT (#48m^{n}) enters via the entry portal ptCA l and projects medially, crossing over the peduncle and forming the most posterior of a dorsal set of commissures (pPLPC; Figs. 10B, E and G, Fig. S3C and D). The second HSAT (#48a^{n}) is a short, anteriorly directed tract that enters at the junction between the SLP and LH (ptSLP pl) and terminates in the LH (Fig. 10B, E and G; Fig. S3C and D). An additional fiber bundle (#48v^{n}) that branches off the anterior tract projects ventrally along the posterior vertical fascicle (Fig. 10G). DPLpv (#50) lies far more ventral, flanking the posterior surface of the posterior lateral protocerebrum (PLP; Fig. 10C and E–G). Its single SAT enters via the ptPLP ps portal and projects anteriorly as part of the fiber system called the posterior lateral fascicle (PLF; Fig. 10B, E and G; Fig. S3C and D). In the larva and early pupal stages, one can recognize a lateral branch of the DPLpv SAT that projects towards the optic lobe (blue arrowhead in Fig. 11A′, C′ and E′).

Of the 18 DPL lineages, nine (DPLam, DPLd, DPLc1, DPLc3, DPLc5, DPLm1-2, DPLl1, DPLpv) can be individually followed throughout pupal development (Figs. 8 and 11). DPLal1-3 form a triplet tract; DPLc2 and DPLc4, as well as DPLl2-3 and DPLp1-2 form paired tracts, all of which are clearly visible from larval to adult stages (Figs. 8 and 11). The cell body cluster location of DPL lineages is affected strongly by the expanding superior protocerebrum, which pushes many of the lineages far posterior. Thus, DPLc1-2 are fairly anterior in the larva (Fig. 8A′ and B), at the level of the VL and end up almost at the level of the CA in the adult (Fig. S3A and B). Cell bodies of DPLpv move from a postero-dorsal position in the larva to a postero-ventral one in the adult (#50; Fig. 11A′, C′, E′, G′, I′ and K′; Fig. S3C and D).

Four lineages, DPLc5, DPLm2, and DPLl2-3 deserve special mentioning because of the separation of hemilineage cell bodies and their HSATs. In the case of DPLc5, one HSAT follows the other DPLc tracts medially, whereas the other HSAT, clearly visible only in the larva and early pupa (#41p; Fig. 11B and D) first extends postero-ventrally; and then turns anteriorly into the loSM, following the general trajectory of DPM lineages (see below). For this reason, DPLc5 was previously named "DPMl3" (Pereanu and Hartenstein, 2006), but more aptly deserves the group designation DPLc, because it's anterior HSAT (and its clone geometry; see accompanying paper by Wong et al., 2013) shares more commonalities with DPLc lineages. The DPLc5 hemilineage generating the posterior HSAT separates from the anterior hemilineage, moving far posteriorly and ventrally (see accompanying paper). The paired DPLl2-3 also represent a case where hemilineage clusters become far removed from each other as discussed previously (see above). Finally, in the case of DPLm2, two hemilineages also seem to exist, one of which loses expression of the Neuroglian protein. Aside from the short, laterally-directed tract that is clearly visible in the larva, pupa, and adult, a second, thinner tract (#47p) is visible only in the larva and early pupa (compare #47 to #47p in Fig. 11D). The DPLm2 HSATp extends ventro-medially, exits the brain, and projects to the ring gland.

DPM lineages (#51–59)

Cell body clusters of the DPM group are situated at the dorso-medial surface of the brain, medially of the calyx. We distinguish a more dorso-anterior (DPMm1-2, #53–54), ventro-posterior (DPMpm1-2, #58–59), and lateral (DPMl1, #51; DPMpl1-3, #55–57) subgroups (Fig. 12A–C). DPMpl1-2 (#55–56) form a pair whose SATs enter the neuropil medially adjacent to the calyx (ptCA m) and continue antero-dorsally, following the loSM fascicle (Fig. 12A, B and D–F). DPMpl3 (#57), located further ventrally, forms an SAT that enters via the conspicuous ptPB v portal at the tip of the protocerebral bridge (PB) and projects along the MEF fascicle (Fig. 12A, B and D–F). DPMm1 (#53) and DPMpm1/2 (#58-59) represent three of the large and fast-cycling type II lineages that have been previously described to innervate the central complex (Bello et al., 2008; Boone and Doe, 2008; Izergina et al., 2009). Of the eight type II lineages, six of the dorso-posteriorly located type II lineages (CM1, CM3/4, DPMm1 and DPMpm1/2) are marked by expression of ***dll^{md23}-Gal4*** (Izergina et al., 2009) and ***earmuff (9D11-Gal4;*** Bayraktar et al., 2010). There are no known markers for the remaining two lineages (CP2/3). DPMm1, DPMpm1, and DPMpm2 include sub-lineages whose main SSATs, destined for the central complex (#53b, 58b, 59b), characteristically enter the neuropil in contact with the protocerebral bridge (entry portals ptPB dm and ptPB dl, respectively; Fig. 12B). As a result, the SSATs of the dorso-medial root and dorso-lateral roots of the fan-shaped body (mrFB, #53b-c; dlrFB, #58b/59b) project antero-posteriorly into the neuropil of the fan-shaped body (FB), respectively (Fig. 12D–F, Fig. S4B–C; Pereanu et al., 2010).

Additionally, DPMpm2 gives off an SSAT (#59a) projecting more dorsally, as part of the loSM (Fig. 12D–F); DPMpm1 has another SSAT (#58a) following the mALT antero-posteriorly (Fig. 12F). DPMm1 has multiple other SSATs; the four most prominent ones are a tract joining the loSM (#53a), one crossing the posterior brain surface towards the contralateral hemisphere (#53d), and two (#53c, e) extending ventrally and anteriorly along the ventro-medial surface of the fan-shaped body (Fig. 12E). #53c turns ventrally into the ventro-medial cerebrum (VMC; Fig. 12E and F); #53e continues anteriorly (not shown). DPMm2 (#54) is located laterally adjacent to DPMm1 and has a single SAT that enters the superior medial protocerebrum vertically via the ptPB dl portal (Fig. 12B, D). The distal SAT of DPMm2, which expresses BP106 only until P12 (Fig. 11D), turns anteriorly, extends over the roof of the central complex, and crosses to the contralateral hemisphere in the anterior chiasm that lies immediately posterior of the median bundle (MBDLchi in Fig. 12F). DPMl1 (#51), located next to DPMpl3 (#57) as it enters the MEF (Fig. 12A–C), has a long descending SAT that projects towards the subesophageal ganglion (SEG; Fig. 12F). The distal SAT is visible with BP106 only until stage P24 (Fig. 11B and D).

Cell body clusters and SATs of all DPM lineages perform a shift ventro-posteriorly as the superior medial protocerebrum and inferior protocerebrum expand during metamorphosis (Fig. 11B, D, F, H, J and L; Fig. S4B–C). Of the eight DPM lineages, four (DPMm1-2, DPMpm1-2) can be individually followed throughout metamorphosis (Fig. 11A–L). During the later stages of pupal development, axons formed by the three type II lineages (DPMm1, DPMpm1-2) break up into multiple thinner, parallel bundles that flank the protocerebral bridge (PB; #53, #58, #59 in Fig. 11G–L). The paired tract formed by DPMpl1-2 travels in the loSM fascicle and is also visible throughout development (#55^{n} in Fig. 11A–L). The distal DPMl1 and DPMpl3 lose expression of BP104 Neuroglian during later pupal stages and can only be identified in the adult brain on the basis of GFP-labeled MARCM clones. For all other DPM lineages, it is only possible to follow the SATs into the larger fascicle (e.g. loSM, MEF) to which they contribute; thus, a lineage trajectory can only followed when it is labeled by GFP (see accompanying paper by Wong et al., 2013).

CM lineages (#60–63)

CM lineages occupy the postero-medial brain cortex, ventro-medially of the calyx (CA; Fig. 12A–C). Three CM lineages (CM1,

CM3, CM4) are large type II lineages (called DM6, DM5 and DM4, respectively, in Bello et al., 2008). Each of these forms multiple sub-lineages, and possesses a complex array of sub-lineage tracts (SSATs). Only a subset of these, (the "main" SSATs), can be followed using global markers like BP106 or BP104. CM1 (#60) forms two main SSATs; CM4 (#62) possesses three; and CM3 (#61) has four (Fig. 12F). One SSAT of each of these three lineages enters at a ventral level into the ventro-medial cerebrum (ptVMCpo) and projects forward in the loVP fascicle (#60v^{n} in Fig. 12A, B, D and F). The other CM SSATs enter at the tip of the protocerebral bridge (ptPB v) and project straight anteriorly in the MEF (#60d^{n} in Fig. 12A, B and D–F). CM3 and CM4 form an additional SAT turning dorsally into the loSM (#61da^{n} in Fig. 12D and F). CM5 (#63), located close to the brain midline, projects a single SAT forward in the MEF (Fig. 12A–D and F). The CM5 SAT then leaves the MEF and turns ventro-posteriorly, exiting the brain towards the subesophageal ganglion (SEG; Fig. 12F; visible in MARCM labeled CM5 clone; see accompanying paper by Wong et al., 2013).

Whereas CM5 with its single SAT can be identified throughout metamorphosis (#63; Fig. 11A–L), the more complex CM1, CM3, and CM4 (#60–62) with their multiple SSATs present difficulties. In the larva, SSATs of each lineage still form one bundle. CM4 (#62) is situated furthest dorsally and its SSAT bundle enters right at the tip of the protocerebral bridge, where it splits to send one main SSAT dorsally into the loSM, one straight anteriorly into the MEF, and one ventrally into the loVp (PB; #62; Fig. 11A′). CM3 lies ventrally of CM4; its SSAT bundle projects dorsally, then splits into similar components as those of CM4 (#61; Fig. 11A′). CM1 lies medially adjacent to CM3 (#60; Fig. 11A′) and sends a dorsal SSAT into the MEF and a ventral one into the loVP. Already by P12, the cell body cluster of CM4 has split into two, one dorsal component connected to the SSATs that enters the loSM and MEF and one ventral component projecting as part of the loVP (Fig. 11C′). These separate clusters move further apart towards later stages of metamorphosis (Fig. 11E′, Fig. S4D and E). CM3 and CM1 undergo a similar change, but the dorsal and ventral components stay closer together than those of CM4 (Fig. S4C and D). From P32 onward, individual subcomponents are no longer clearly distinguishable: diffuse dorsal cell body groups with fibers coalesce into bundles joining the MEF and loSM with the ventral groups projecting into the loVp (Fig. 11G–L).

CP lineages (#64–67)

The CP group includes four lineages, CP1-4, located ventro-laterally of the calyx (CA; Fig. 12A–C). CP2 (#65) and CP3 (#66) form a paired lineage with joined tracts that cannot be distinguished from each other. CP1 (#64) and CP2/3 (#65–66) possess two hemilineages and form two HSATs each; CP4 (#67) has one. The dorsal HSATs of CP1-3 (#64d, 65d^{n}), joined by CP4 (#67), enter via the entry portals ptCA l and ptCA vl and project straight antero-medially, forming the oblique posterior fascicle (obP; Fig. 12A, B, D and F). The obP is a conspicuous landmark tract that crosses over the peduncle immediately in front of the CA and then turns anteriorly to merge with the loSM (Fig. 12D–F). Within the obP, the paired HSAT of CP2/3 is located further dorsally; tracts of CP1 (#64) and CP4 (#67), which are close and form a single bundle, are more ventral, nearly "touching" the peduncle (Fig. 12D). The ventral HSATs of CP2/3 (#65v^{n}) enter through the ptPLP ps portal and project forward as part of the posterior lateral fascicle (PLF), running ventro-laterally of the peduncle (Fig. 12A, B and D–F).The ventral HSAT of CP1 (#64v) joins the posterior component of the lateral equatorial fascicle (LEFp) that extends ventrally of and parallel to the peduncle (Fig. 12D).

All CP tracts can be followed throughout metamorphosis (Fig. 11A–L). As described above for the CM group, hemilineages of CP1-3 (#64–66) move apart from P24 onward (Fig. 11E′, G′ and I′; Fig. S3C and D). Dorsal tracts of CP2/3 (#65d/66d), and the merged CP1dorsal-CP4 tract (#64d/67), enter laterally of the CA. Entry points of the paired ventral CP2/3 HSAT (#65v/66v) and the ventral CP1 HSAT (#64v) move further ventrally. The three posterior lineages of the DPL group, DPLp1-2 (#48–49) and DPLpv (#50) are always closely associated with the CP group. The DPLp1-2 pair (#48–49), located laterally adjacent to the dorsal CP2/3 hemilineages (#65d/66d; Fig. 12C), joins them in the obP (Fig. S3C and D). DPLpv (#50) sits laterally adjacent to the ventral CP2/3 clusters and extends its SAT into the PLF (Fig. 12C, Fig. S3C and D).

BLA lineages (#68–75)

The BLA lineages fall into two subgroups, a dorsal one (BLAd1-4, BLAl) located laterally of the superior protocerebrum, and a ventral one (BLAv1-2, BLAvm) with cell bodies anteriorly and laterally of the anterior ventro-lateral protocerebrum (VLPa; Fig. 13A–F and I). BLAd1-4 (#68–71) and BLA1 (#72) are neighbors of the anterior DPLal lineages (#68^{n}, Fig. 13B). The SATs of the quartet BLAd1-4 (#68–71) coalesce into one thick bundle that passes medially underneath the anterior optic tract (AOT) and enters via the ptSLP l portal, then turns upward to form the trSl fascicle (yellow arrowhead in Fig. 13F) that extends into the superior lateral protocerebrum (Fig. 13B, D/D′, E, F and I). BLAl, ventrally adjacent to the BLAd cluster, has two hemilineages (#72). One HSAT (#72m; Fig. 13I) is directed antero-medially, extending over the dorso-anterior surface of the VLPa, parallel to the AOT; this SAT is distinguishable in BP106 labeled brains until P24 (Fig. 8B, D and F) and later becomes indistinct. The second, dorso-posteriorly directed HSAT (#72d; Fig. 13I) extends upward along the lateral surface of the SLP, joining the superficial component of the trSI fascicle formed by BLD1-4 (see below; Fig. 13E, F and I). The three ventral BLAs (BLAv1-2, #73–74; BLAvm, #75) have two hemilineages each with one of their HSATs directed medially, the other posteriorly. BLAv2 (#74), located furthest dorsally in the BLA group, projects its medial HSAT (#74m) through the ptVLP dls portal into the VLPa, where it forms the horizontal VLP tract (hVLPT; Fig. 13A, B, D/D′ and I). The posterior HSAT of BLAv2 (#74p) extends backward over the lateral surface of the VLPa and then turns medially through the ptLH a portal towards the great commissure (GC; Fig. 13E, F and I). BLAv1 (#73) forms a similar pattern, with one HSAT (#73m) projecting medially over the surface of the VLPa, close to the AOT and the BLAl towards the pt VLP dm portal (see above; Fig. 13A, B, D/D′ and I); and a second HSAT (#73p) extending posteriorly and then ventrally, through the pt VLP dli portal into the GC (Fig. 13A, B, D/D′ and I). BLAvm (#75), the ventral-most BLA lineage, sends one HSAT dorso-medially over the surface of the VLPa, and up into the anterior SLP (#75m; Fig. 13A, B and I); the posterior HSAT (#75p) projects along the lateral surface of the VLPa (Fig. 13F and I).

The tracts formed by all BLA lineages, with the exception of BLAl and the posterior HSAT of BLAvm, which are no longer visible after P32, can be followed throughout metamorphosis. Dorsal BLA clusters and SAT entry points maintain their position (Fig. 8A–L; Fig. S5). Ventral BLA clusters and their HSAT entry points move apart, following the enormous growth of the VLPa compartment (Figs. 6F, G; Fig. 8A–L; Fig. S5C, D). The hemilineage clusters of BLAv1 and BLAv2 become separated, with the medial cluster moving up towards the dorsal tip of the VLPa while the posterior hemilineage cluster moves laterally (Fig. 13D, Fig. S5C and D). The posterior HSATs of both BLAv1 and BLAv2 acquire an additional branch: one BLAv2 HSAT projects dorsally towards the lateral horn (LH; Fig. 13E, green arrowhead), while the BLAv1 HSAT projects ventrally, into the inferior ventro-lateral cerebrum (VLCi; Fig. 13B, green arrowhead; Fig. S5C and D).

BLD lineages (#77–83)

BLD lineages flank the lateral surface of the superior lateral protocerebrum and the lateral horn, posteriorly adjacent to the dorsal BLA lineages discussed above (SLP; LH; Fig. 13C and D). Four BLDs lineages, BLD1-4 (#77–80), have tracts that enter at the base of the superior lateral protocerebrum (ptSLP l), make a characteristic 180 degree turn, curving around the anterior optic tract (AOT) and backward, dorso-posteriorly along the surface of the SLP, forming the superficial component of the trSl fiber system (Fig. 13D/D′, E–I; Fig. S6A, B). This conspicuous fiber system (red arrowheads in Fig. 13F) lies posterior to and superficially of the similarly shaped tract carrying the BLAd SATs (see above; yellow arrowhead in Fig. 13F). It also contains the dorsal HSAT of BLAl (see above). BLD1 (#77), BLD3 (#79), and BLD4 (#80) consist of two hemilineages. Aside from the HSAT that joins the trSI (#77d, #79d, #80d; Fig. 13E, F and I), they have a ventrally directed HSAT. In the case of BLD4, located more anteriorly, this tract (#80v) grows ventrally into the anterior ventro-lateral protocerebrum (VLPa; Fig. 13E and I). The ventral HSAT of BLD1 (#77p), located further posteriorly, follows the surface of the posterior VLP (VLPp) compartment ventrally, then splits into a medial branch that enters the VLPp and a lateral one which extends towards the lobula of the optic lobe (Fig. 13G, I). BLD5 (#82) and BLD6 (#83) are located in the posterior brain, flanking the lateral horn ventro-posteriorly (LH; Fig. 13D, G and H). Best visible in the larva and early pupa (Fig. 11B, D and E), both BLD5 and BLD6 form characteristic L-shaped SATs that initially project ventrally along the surface of the posterior lateral protocerebrum (PLP) and then turn medially (Fig. 13G–I) to enter via the ptPLP l portal (Fig. 13D/D′, G and H). Both send a short lateral branch into the lobula at this medial turn (not shown). The SAT of BLD5 (#82, marked by expression of ***ato-Gal4***; Hassan et al., 2000; Spindler and Hartenstein, 2010, 2011) continues across the midline in the great commissure (GC); the short SAT of BLD6 (#83) terminates in the ventral VLPp (Fig. 13I, Fig. S6C and D).

Anterior BLD lineages (#77–83, BLD1-4) can be individually followed only throughout early stages of pupal development. Even at these early stages, it is difficult to separate the SATs in confocal sections taken in the (typical) frontal plane. However, BLD1-4 can be separated from each other by their characteristic additional branches (described above). This also makes it possible to assign MARCM clones to their proper lineages (see accompanying paper by Wong et al., 2013). Cell body clusters of the anterior BLD lineages maintain their antero-dorsal position (Fig. 6F and G; Fig. S6A and B). The analysis of GFP-labeled clones (see accompanying paper by Wong et al., 2013) indicates that the hemilineages of BLD1 (#77) and BLD3 (#79) move apart. In the case of BLD1, the hemilineage producing the ventral HSAT comes to lie posterior of the hemilineage projecting into the trSI; with BLD3, it is the other way around (Fig. S6B). Clusters and SATs of BLD5 and BLD6 are easy to follow throughout metamorphosis (Fig. 11B, D, F, H, J and L); clusters of these lineages also move posteriorly and ventrally, to end up in the niche between the posterior lateral protocerebrum (PLP) and the lobula (Fig. 13D).

BLP lineages (#84–87)

The BLP lineages form two pairs, BLP1-2 (#84/85) and BLP3-4 (#86/87), whose cell body clusters are located posteriorly of the lateral horn (LH) and posterior lateral protocerebrum (PLP; Fig. 13C, D, H and I). Each BLP lineage projects one SAT. The paired SAT of BLP1/2 (#84^{n}) enters via the pt PLP ps portal and extends antero-ventrally, following the lateral surface of the posterior lateral protocerebrum (PLP) and posterior ventro-lateral protocerebrum (VLPp), and projecting into the anterior ventro-lateral protocerebrum (VLPa; Fig. 13E–I). The paired BLP3/4 (#86^{n}) tract enters the neuropil at the boundary between the lateral inferior protocerebrum (IPl) and the LH and then turns dorso-laterally into the LH (ptLH p) where it ends (Fig. 13H, green arrowheads; Fig. 13I). The BLP3/4 (#86–87) tract is similar in entry and trajectory to the anterior HSAT pair formed by DPLp1/2 (#48–49), which lies medially of it (Fig. 13H, blue arrowhead; see above).

The two paired BLP tracts (#84/85 and #86/87) are clearly visible throughout metamorphosis (Fig. 11A′, C′, E′, G′, I′ and K′). The BLP3/4 cluster shifts upward and, in the P48 pupa and adult, comes to lie dorsally of BLP1/2 (Fig. 11I′/K′; Fig. S6C and D). Aside from BLP1-4, two other BLP lineages, BLP5 and BLP6, were described in the larval brain (Cardona et al., 2010a). Located ventrally of the other BLP lineages, the tracts of BLP5 and BLP6 extend anteriorly, passing ventrally of the transverse fiber systems connecting the lobula and the ventro-lateral protocerebrum (VLP). The BLP5-6 tracts are no longer distinguishable from P24 onward, and we recovered no MARCM clones (see accompanying paper by Wong et al., 2013). We speculate that these tracts, visible in the larva, belong to groups of neurons of the lobula.

BLV lineages (#89–94)

The BLV lineages form an anterior group (BLVa1-4, #89–92) and a posterior group (#93–94; BLVp1-2; Figs. 6F and G, 13D). BLVa1-4 (#89–92) are located ventro-laterally of the anterior ventro-lateral protocerebrum (VLPa) compartment; all of their SATs project dorsally. BLVa3 and 4 (#91, 92) have a short paired tract (#91^{n}) entering the ventro-lateral surface of the VLPa compartment (pt VLP vli; Fig. 13A, B, D/D′ and I). BLVa1-2 (#89, 90) forms another paired tract (marked by ***so-Gal4***; Chang et al., 2003; Fung et al., 2009; Spindler and Hartenstein, 2010). In the larva and early pupa (P12-24), BLVa1-2 are located ventrally, next to BLVa3-4 (Fig. 11B and D; Fig. S6A and B). The long BLVa1-2 tract extends vertically along the lateral surface of the VLP, entering at the base of the lateral horn (ptLH a; Fig. 13D/D′ and E) and terminating in the primordium of the lateral horn. At later pupal stages (P24, P32, P48), cell body clusters of BLVa1-2 perform a dramatic shift dorsally and in the adult come to lie at the dorsal surface of the VLPa, adjacent to the BLAd and anterior BLD clusters (Fig. 11F, G′, I′ and L′; Fig. S6A and B; see also accompanying paper by Wong et al., 2013).

BLVp1 (#93) and BLVp2 (#94; previously called BLVp3 in the larva; Cardona et al., 2010a) possess two hemilineages each which move away from each other during metamorphosis. In the larva and early pupa, BLVp1 and BLVp2 have a single cluster each, located at the ventro-posterior brain surface ventrally of the CM and CP lineages (Fig. 11A′ and C′). BLVp tracts are directed forward and split into a dorsal and a ventral HSAT (green arrowheads in Fig. 11A′). The dorsal HSATs enter the posterior lateral protocerebrum (ptPLP pi; Fig. 13D/D′, G and H) and form a component of the PLF fascicle. Dorsal BLVp1 (located medially of BLVp3) turns medially into the great commissure (GC); dorsal BLVp2 passes the GC and projects into the inferior protocerebrum (Fig. 13I). The ventral HSATs of BLVp1 and BLVp3 form a paired tract. In the larva and early pupa (P12), this tract projects anteriorly, passing the transverse fiber systems connecting the lobula and VLP ventrally, and reaching the VLPa. Starting around P24, the ventral hemilineages of BLVp1-3 move anteriorly and in the late pupa/adult come to lie at the ventro-lateral surface of VLPa, laterally adjacent to the BLVa3-4 clusters (#91a^{n} in Fig. 8H, J and L). The paired BLVp1-3 HSAT (#93a^{n}) enters the VLPa (pt VLP vls) and traverses the VLPa as the vertical VLP tract (vVLPT; Fig. 13D/D′ and I).

Discussion

SATs and neuropil fascicles can be followed throughout brain development

In the present work, we have assigned all lineage-related tracts of the ***Drosophila*** supraesophageal ganglion to fiber bundles that can be visualized by global markers, including antibodies directed against neuronal membrane proteins (BP104/6; resulting in positive labeling of bundles), as well as synaptic proteins (NCad/nc82; negative labeling of bundles). Lineage-related tracts arise in the larva when secondary neurons extend their axons, forming cohesive fiber tracts that we termed secondary axon tracts (Dumstrei et al., 2003b; Pereanu and Hartenstein, 2006). By the end of the larval stage, most secondary axon tracts of the supraesophageal ganglion have reached their full length. That is to say, tracts that in the mature (adult) brain will reach from the anterior neuropil (e.g. the antennal lobe) to the posterior neuropil (e.g. calyx or lateral horn) do so already in the larva. Based on the appearance of clones induced at later larval stages, it is evident that SATs of the late larva have not yet reached their full size in terms of number of axons: neurons born during late larval stages in many cases have only short axons or no axons (J.L., J. O., and V.H., unpublished). These late-born neurons then differentiate during early pupal stages and fasciculate with the earlier formed axons, leading to an increase in diameter of SATs. Furthermore, we show that only in a minority of lineages do axons that grow out in the pupa (presumably axons of late-born neurons) form novel branches that split off the pre-existing SAT (e.g. BAmv1).

SATs and the fascicles they form in the neuropil remain visible as conspicuous landmarks throughout metamorphosis and in the adult brain. Variations in the labeling properties of different SATs and fascicles arise around P24 when the differentiation of adult neurons is initiated. Some fascicles maintain a strong signal along their entire length; in other cases, labeling becomes fainter (e.g. lower signal-to-noise ratio, see Table 1). Typically, we observed that the most proximal segment of the tract remains strongly labeled, allowing one to follow its entry into the neuropil. More distally, however, the intensity of the labeling declines. Although the overall labeling of fascicles within the neuropil remains strong, it becomes very difficult to distinguish between individual SATs within a fascicle (formed by multiple lineages) by the late pupa (after P48).

Hemilineages and sub-lineages form separate tracts

In the majority of lineages (type I lineages), neuroblasts divide asymmetrically into next-generation neuroblasts and ganglion mother cells (GMCs). GMCs undergo one division, producing two neurons which typically follow two different fates (a and b). Recent work has shown that all neurons sharing the a fate or the b fate group together as a hemilineage. The two hemilineages formed by one neuroblast typically form two separate tracts (HSATs). In a good number of cases, one of the hemilineages undergoes cell death, leaving only one hemilineage and its HSAT (Truman et al., 2010). Other lineages maintain both hemilineages and HSATs. At the larval stage, HSATs of a lineage enter the neuropil very close to each other. This close proximity is maintained throughout metamorphosis in the majority of lineages possessing two hemilineages, including DALcl1/2, DALcm1/2, DPLal2/3, DPLd, and BLAv2. In a number of cases, hemilineages and their HSATs move slightly apart (BAlc, BAmd1, CP2/3, BLAl, BLAv1); in other cases (DPLc5, DPLl2/3, BLAl, BLAvm, BLD1, BLD3, BLVp1/2), the separation of hemilineages is more extreme, leading to HSAT entry portals being on opposite sides of the neuropil. In most of these cases (DPLl2/3, BLAvm, BLVp1/2), the gradual separation can be directly followed by analyzing the SAT patterns at successive, closely spaced pupal stages (P12, P18, P24, P32; see Fig. 3). In several other cases, notably concerning lineages located close to each other in the dorsolateral cortex (BLD1, BLD3, BLAl, DPLc5), the separation only became clear with the help of MARCM clones, where the two hemilineages were always labeled concurrently (see accompanying paper by Wong et al., 2013).

What is the mechanism behind the "movement" of hemilineages? We surmise that the SAT, or HSAT, is "anchored" in the neuropil where it interacts via a multitude of adhesion molecules with its neighboring cells, be they primary axons or glial cells. That would imply that the position of the entry portal of an SAT does not move relative to the neuropil. By contrast, the position of the cell bodies, distal to the entry portal, is more flexible. Large scale morphogenetic processes, like the unfolding of the optic lobe at the lateral surface of the brain, may lead to displacements of the cell bodies relative to their original position at the neuropil surface. In the case of two hemilineages whose cell body clusters are "pulled apart" we speculate that, although both HSATs initially contact the neuropil surface very close to each other, only one HSAT enters the neuropil. The other HSAT does not enter, but follows the neuropil surface tangentially, entering at a distant location through a separate, anterior portal. For both DPLl2/3 and BLVp1/2 this type of behavior can be observed. During metamorphosis, the cell body clusters of the anterior hemilineages move forward, reaching a position close to the anterior entry portals.

Neuroblasts of type II lineages follow a different pattern of proliferation from type I neuroblasts. Rather than forming ganglion mother cells, they produce more neuroblasts ("intermediate progenitors"; for review, see Brand and Livesey, 2011). An intermediate progenitor then behaves like regular (type I) neuroblast, giving rise to GMCs which divide into two neurons, thereby forming a sub-lineage. Even though more detailed work is required to establish the precise pattern of sub-lineages generated by DPMm1/DM1, DPMpm1/DM2, and the other type II lineages, it seems likely that at least some of the sub-lineages also generate their own axon bundles (SSAT). For example, the three type II lineages DPMm1, DPMpm1, and DPMpm2 each have a tract that passes on either side of the protocerebral bridge and then projects straight forward, forming the dorsomedial and dorsolateral roots of the fan-shaped body. These tracts most likely correspond to the X, Y, Z fiber systems which carry the columnar neurons of the central complex (Hanesch et al., 1989). Columnar neurons connect in a topographically ordered manner small segments of the protocerebral bridge with columns of the fan-shaped body and/or sectors of the ellipsoid body, but have no projections outside the central complex. We speculate that the columnar neurons form one, or several, sub-lineages of DPMm1, DPMpm1, and DPMpm2, while other neurons of these lineages, projecting outside the central complex via different tracts, represent other sub-lineages.

Comparison of protocols for visualizing fiber assembly and commissural nomenclature

In various invertebrate brains, such as the house fly ***Musca***, both tracts and fascicles have been defined, providing the most comprehensive treatment of gross anatomical fiber systems (Strausfeld, 1976). In this and other classical works on insect neuroanatomy, brain sections were stained with the reduced silver technique developed by Power and Chen (Chen and Chen, 1969; Power, 1943). This technique labels individual fibers and authors have noted that according to precise conditions, the labeling intensity varies according to cell type and depends strongly on parameters such as fiber diameter (Strausfeld, 1976). How can one compare the assemblies of fibers that have been defined as tracts/fascicles in previous studies of silver-stained fly brains with the

pattern of SATs/fascicles based on immunofluorescence of adhesion molecules and synaptic protein localization?

Thin axons, like those making up SATs in the larva and adult (~0.2 μm diameter; Cardona et al., 2010b), seem to show little if any labeling following silver impregnation. Fiber systems like the peduncle, or posterior roots of the fan-shaped body, appear mostly signal-negative (Strausfeld, 1976). On the other hand, many terminal axons, whose presynaptic sites are concentrated on thick "varicosities" or "boutons" (Cardona et al., 2010b; Prokop and Meinertzhagen, 2006; Watson and Schürmann, 2002) are labeled strongly (Strausfeld, 1976; Strausfeld and Li, 1999; Strausfeld et al., 2009). As a result, the pattern of fiber systems visible on sections using antibodies against neuronal molecules, such as Neurotactin (labeling axons) or Bruchpilot (labeling active zone at presynaptic sites), appears very different from what is visible on a silver-impregnated brain sections (e.g. the lightly stained SATs and SAT-based neuropil fascicles are barely visible on these sections, being overshadowed by the prominently labeled thick fibers). It is therefore difficult to reconcile the nomenclature of fascicles proposed on the basis of silver-impregnated sections of the ***Musca*** brain (Strausfeld, 1976) with the naming of fiber systems visible in brain confocal sections labeled with neuronal or synaptic antibodies.

A clear exception to this general rule are the commissures, most can be recognized in the silver-impregnated ***Musca*** brain and the immunofluorescently-labeled ***Drosophila*** brain. For these fiber systems, the original topology based nomenclature proposed by Strausfeld (1976) was taken over or modified slightly (Pereanu et al., 2010; Tanaka et al., 2012). For example, the "inferior interantennal connective" is now named the "antennal lobe commissure," the "subellipsoid connective" is called the "subellipsoid commissure," the "inferior ventral body connective" the "lateral accessory lobe commissure" (the prior names for the lateral accessory lobe of the dipteral brain was "ventral body"), the "arched connective of the ventral body" the "supraellipsoid commissure." In the posterior brain, the "superior arch commissure" and "great commissure" have maintained their name; the "commissure of the lateral horn" is renamed into the "dorsal commissure of the posterior lateral protocerebrum."

Among the longitudinal fascicles introduced for ***Drosophila***, only the antennal lobe tract (formerly "antenno-glomerular tract") and median bundle are easily recognizable in silver-stained and immunofluorescently-labeled sections. In addition, in the superior protocerebrum, the loSM defined here follows a similar trajectory as the "posterior division of the median fascicle" of Strausfeld (1976). More ventrally, the medial and lateral equatorial fascicles (MEF, LEF) are located at a position corresponding to the "equatorial horizontal fascicle" in ***Musca***. The oblique posterior fascicle (obP) may correspond to the "lateral horn-medial protocerebrum tract" of Strausfeld (1976). None of the transverse fiber systems formed by the SATs (trSA, trSI, trSP) appear as named entities in the ***Musca*** Atlas; although many tracts and fascicles defined for ***Musca*** have no obvious counterparts in the ***Drosophila*** brain using global markers like BP104 (anti-Neuroglian). One can hope that the great anatomical detail revealed by silver impregnation techniques in the ***Musca*** Atlas and in numerous previous studies can be eventually "translated" to confocal microscopy, using appropriate markers for individual neurons or subsets of neurons.

As previously discussed, we propose that the system of tracts and fascicles that is positively or negatively labeled by antibody labeling against neuronal proteins (e.g. Neurotactin, Neuroglian, N-Cadherin, and Bruchpilot) will provide a helpful anatomical framework for neurobiological studies dealing with specific neuronal subsets. These antibodies are readily available, and can be used in the background of specific neuronal markers (e.g. promoter or enhancer-driven Gal4 drivers combined with membrane-localized fluorescent reporters); thereby allowing the observer to directly relate the neuronal subset to SATs and neuropil fascicles. As shown in the accompanying paper (Wong et al., 2013), it is a straightforward task to determine the lineage identity of MARCM clones based on their characteristic fasciculation with specific SATs. Thus, this work serves as a foundation for assigning secondary neurons (visualized by stable GFP markers or as single-cell clones; Chiang et al., 2011; Jefferis et al., 2001; Lai et al., 2008; Lin et al., 2012) to a comprehensive map of well-defined SATs, taking us a step closer towards reconstructing the brain macrocircuit.

Tracts and fascicles across insect taxa

It has been generally assumed that, for the last several decades, the basic pattern of lineages is conserved among different insect groups (Boyan and Ball, 1993; Duman-Scheel and Patel, 1999; Jarvis et al., 2012; Thomas et al., 1984). This strong statement is based on the observation of conserved patterns of neuroblasts and various subsets of neurons. The map of neuroblasts of an individual segment of the ventral nerve cord in ***Drosophila*** (Broadus et al., 1995; Doe, 1992; Hartenstein and Campos-Ortega, 1984; Truman and Bate, 1988) and grasshopper (Bate, 1976; Doe and Goodman, 1985) contains the same number of columns (4) and rows (7) of neuroblasts. Lineages including specific subsets of neurons are found at identical positions within the ***Drosophila*** and grasshopper neuromere (Bossing et al., 1996; Schmid et al., 1999; Taghert et al., 1982; Udolph et al., 1993) where their neuroblast maps have also been constructed (Urbach et al., 2003; Urbach and Technau, 2003a, 2003b; Williams and Boyan, 2005; Younossi-Hartenstein et al., 1996; Zacharias et al., 1993), showing significant similarities in cell number and arrangement.

As lineages of the ***Drosophila*** brain form tracts and fascicles with characteristic trajectories, it is reasonable to assume that this will be the case for other insect brains as well. Thus, it follows that neuropil fascicles should adhere to a pattern that can be recognized in other insect groups as well, which, if true, would be a great advantage for comparative insect neuroanatomy. Specific antibodies for neuronal proteins have not been produced in many insects, but some of the antibodies raised against ***Drosophila*** (as well as vertebrate) proteins cross-react with epitopes in other taxa, and numerous groups use these as markers in their (confocal) study of various insect brains (e.g. Boyan et al., 2003; Dreyer et al., 2010; Huetteroth et al., 2010; Ignell et al., 2005; Mysore et al., 2011; Rybak et al., 2010). Several studies prepared recently (J.B. and V.H., pers. comm.; Larsen et al., 2009; Mysore et al., in prep.; Pereanu et al., 2010), including this work, strongly suggest that the pattern of neuropil fascicles labeled negatively when using antibodies cross-reacting with synaptic epitopes shows significant similarities to the ***Drosophila*** pattern described previously. In this work (Fig. S7), we compare the different neuropils, taken at corresponding antero-posterior levels (fan-shaped body), of four different insects, including ***Drosophila***, ***Aedes aegypti*** (Diptera), ***Tribolium castaneum*** (Coleoptera), and ***Cardiocondyla obscurior*** (Hymenoptera). Many fascicles, including the loSM and loSL of the superior protocerebrum, the MEF and LEF of the inferior protocerebrum, the loV separating ventro-lateral and ventro-medial cerebrum, the great commissure of the ventral cerebrum, and the dorsal and ventral commissure of the subesophageal ganglion can be tentatively identified on the basis of their entrypoints into the neuropil, and their positions relative to the surrounding compartments. It will be crucial to develop antibody markers that allow for the positive labeling of tracts and fascicles. Once that goal has been achieved, it will be possible to embark on a lineage-based, and thereby much more detailed comparative-evolutionary analysis of insect brain structure. It is likely, as proposed in previous studies (reviewed in Farris, 2005; Galizia and Rossler, 2010; Homberg, 2008; Strausfeld et al., 2009), that changes in brain anatomy of different insects (and animals in general) occurred by varying a basically conserved pattern of lineages. For

example, as suggested by the brain sections shown in Fig. S7, *Cardiocondyla*, and *Tribolium* have a much reduced lateral horn, which might be correlated to a similar reduction of the optic lobes in both species. One might speculate that the reduction in lateral horn volume is brought about by eliminating some of the lineages whose SATs (and terminal arborizations; see accompanying paper by Wong et al., 2013) enter this compartment. Once it is possible to positively label the SATs of lineages in different insect species, it will become possible to test this hypothesis.

Acknowledgements

We thank the members of the Hartenstein laboratory for critical discussions during the preparation of this manuscript. We are grateful to the Bloomington Stock Center and the Developmental Studies Hybridoma Bank for fly strains and antibodies. This work was supported by NIH grant (R01 NS29357-15). K.T.N. is supported by the NSF Graduate Research Fellowship Program (No. DGE-0707424). J.J.O. is supported by the Ruth L. Kirschstein National Research Service Award (No. GM007185).

Appendix A. Supporting information

Supplementary data associated with this article can be found in the online version at http://dx.doi.org/10.1016/j.ydbio.2013.07.008.

References

Ashburner, M., 1989. Drosophila. A Laboratory Manual. Cold Spring Harbor Laboratory Press, Cold Spring Harbor, NY, pp. 214–217.

Bate, C.M., 1976. Embryogenesis of an insect nervous system I. A map of thethoracic and abdominal neuroblasts in Locusta migratoria. J. Embryol. Exp. 35, 107–123.

Bausenwein, B., Dittrich, A.P., Fischbach, K.F., 1992. The optic lobe of ***Drosophila melanogaster***. II. Sorting of retinotopic pathways in the medulla. Cell Tissue Res. 267, 17–28.

Bayraktar, O.A., Boone, J.Q., Drummond, M.L., Doe, C.Q., 2010. Drosophila type II neuroblast lineages keep Prospero levels low to generate large clones that contribute to the adult brain central complex. Neural Dev. 5, 26.

Bello, B.C., Izergina, N., Caussinus, E., Reichert, H., 2008. Amplification of neural stem cell proliferation by intermediate progenitor cells in Drosophila brain development. Neural Dev. 3, 5.

Bieber, A.J., Snow, P.M., Hortsch, M., Patel, N.H., Jacobs, J.R., Traquina, Z.R., Schilling, J., Goodman, C.S., 1989. Drosophila neuroglian: a member of the immunoglobulin superfamily with extensive homology to the vertebrate neural adhesion molecule L1. Cell 59, 447–460.

Booker, R., Truman, J.W., 1987a. Postembryonic neurogenesis in the CNS of the tobacco hornworm, ***Manduca sexta***. I. Neuroblast arrays and the fate of their progeny during metamorphosis. Journal of Comparative Neurology 255, 548–559.

Boone, J.Q., Doe, C.Q., 2008. Identification of Drosophila type II neuroblast lineages containing transit amplifying ganglion mother cells. Dev. Neurobiol. 68, 1185–1195.

Bossing, T., Udolph, G., Doe, C.Q., Technau, G.M., 1996. The embryonic central nervous system lineages of ***Drosophila melanogaster***. I. Neuroblast lineages derived from the ventral half of the neuroectoderm. Dev. Biol. 179, 41–64.

Boyan, G., Reichert, H., Hirth, F., 2003. Commissure formation in the embryonic insect brain. Arthropod Struct. Dev. 32, 61–77.

Boyan, G.S., Ball, E.E., 1993. The grasshopper, Drosophila and neuronal homology (advantages of the insect nervous system for the neuroscientist). Prog. Neurobiol. 41, 657–682.

Brand, A.H., Perrimon, N., 1993. Targeted gene expression as a means of altering cell fates and generating dominant phenotypes. Development 118, 401–415.

Brand, A.H., Livesey, F.J., 2011. Neural stem cell biology in vertebrates and invertebrates: more alike than different? Neuron 70, 719–729.

Broadus, J., Skeath, J.B., Spana, E.P., Bossing, T., Technau, G., Doe, C.Q., 1995. New neuroblast markers and the origin of the aCC/pCC neurons in the Drosophila central nervous system. Mech. Dev. 53, 393–402.

Cardona, A., Saalfeld, S., Arganda, I., Pereanu, W., Schindelin, J., Hartenstein, V., 2010a. Identifying neuronal lineages of Drosophila by sequence analysis of axon tracts. J. Neurosci. 30, 7538–7553.

Cardona, A., Saalfeld, S., Preibisch, S., Schmid, B., Cheng, A., Pulokas, J., Tomancak, P., Hartenstein, V., 2010b. An integrated micro- and macroarchitectural analysis of the Drosophila brain by computer-assisted serial section electron microscopy. PLoS Biol. 8, e1000502.

Cardona, A., Saalfeld, S., Schindelin, J., Arganda-Carreras, I., Preibisch, S., Longair, M., Tomancak, P., Hartenstein, V., Douglas, R.J., 2012. TrakEM2 software for neural circuit reconstruction. PLoS One 7, e38011.

Chang, T., Younossi-Hartenstein, A., Hartenstein, V., 2003. Development of neural lineages derived from the sine oculis positive eye field of Drosophila. Arthropod Struct. Dev. 2003, 303–317.

Chen, J.S., Chen, M.G., 1969. Modification of the Bodian technique applied to insect nerves. Stain Technol. 44, 50–51.

Chiang, A.S., Lin, C.Y., Chuang, C.C., Chang, H.M., Hsieh, C.H., Yeh, C.W., Shih, C.T., Wu, J.J., Wang, G.T., Chen, Y.C., Wu, C.C., Chen, G.Y., Ching, Y.T., Lee, P.C., Lin, C.Y., Lin, H.H., Wu, C.C., Hsu, H.W., Huang, Y.A., Chen, J.Y., Chiang, H.J., Lu, C.F., Ni, R.F., Yeh, C.Y., Hwang, J.K., 2011. Three-dimensional reconstruction of brain-wide wiring networks in Drosophila at single-cell resolution. Curr. Biol. 21, 1–11.

Crittenden, J.R., Skoulakis, E.M., Han, K.A., Kalderon, D., Davis, R.L., 1998. Tripartite mushroom body architecture revealed by antigenic markers. Learn. Memory 5, 38–51.

Das, A., Sen, S., Lichtneckert, R., Okada, R., Ito, K., Rodrigues, V., Reichert, H., 2008. Drosophila olfactory local interneurons and projection neurons derive from a common neuroblast lineage specified by the empty spiracles gene. Neural Dev. 3, 33.

Das, A., Gupta, T., Davla, S., Prieto-Godino, L.L., Diegelmann, S., Reddy, O.V., Raghavan, K.V., Reichert, H., Lovick, J., Hartenstein, V., 2013. Neuroblast lineage-specific origin of the neurons of the Drosophila larval olfactory system. Dev. Biol. 373, 322–337.

de la Escalera, S., Bockamp, E.O., Moya, F., Piovant, M., Jiménez, F., 1990. Characterization and gene cloning of neurotactin, a Drosophila transmembrane protein related to cholinesterases. EMBO J. 9, 3593–3601.

Doe, C.Q., 1992. Molecular markers for identified neuroblasts and ganglion mother cells in the Drosophila central nervous system. Development 116, 855–863.

Doe, C.Q., Goodman, C.S., 1985. Early events in insect neurogenesis. I. Development and segmental differences in the pattern of neuronal precursor cells. Dev. Biol. 111, 193–205.

Dreyer, D., Vitt, H., Dippel, S., Goetz, B., El Jundi, B., Kollmann, M., Huetteroth, W., Schachtner, J., 2010. 3D standard brain of the red flour beetle Tribolium Castaneum: a tool to study metamorphic development and adult plasticity. Front. Syst. Neurosci. 4, 1–13.

Duman-Scheel, M., Patel, N.H., 1999. Analysis of molecular marker expression reveals neuronal homology in distantly related arthropods. Development 126, 2327–2334.

Dumstrei, K., Wang, F., Nassif, C., Hartenstein, V., 2003a. Early development of the Drosophila brain: V. Pattern of postembryonic neuronal lineages expressing DE-cadherin. J. Comp. Neurol. 455, 451–462.

Dumstrei, K., Wang, F., Hartenstein, V., 2003b. Role of DE-cadherin in neuroblast proliferation, neural morphogenesis, and axon tract formation in Drosophila larval brain development. J. Neurosci. 23, 3325–3335.

Farris, S.M., 2005. Evolution of insect mushroom bodies: old clues, new insights. Arthropod Struct. Dev. 34, 211–234.

Fischbach, K.F., Dittrich, A.P.M., 1989. The optic lobe of ***Drosophila melanogaster***. I. A Golgi analysis of wild-type structure. Cell Tissue Res. 258, 441–475.

Fung, S., Wang, F., Spindler, S.R., Hartenstein, V., 2009. Drosophila E-cadherin and its binding partner Armadillo/beta-catenin are required for axonal pathway choices in the developing larval brain. Dev. Biol. 332, 371–382.

Galizia, C.G., Rossler, W., 2010. Parallel olfactory systems in insects: anatomy and function. Annu. Rev. Entomol. 55, 399–420.

Hanesch, U., Fischbach, K.F., Heisenberg, M., 1989. Neuronal architecture of the central complex in Drosophila melanogaster. Cell Tissue Res. 257, 343–366.

Hartenstein, V., Campos-Ortega, J.A., 1984. Early neurogenesis in wild-type ***Drosophila melanogaster***. Roux's Arch. Dev. Biol. 193, 308–325.

Hartenstein, V., Spindler, S., Pereanu, W., Fung, S., 2008. The development of the Drosophila larval brain. Adv. Exp. Med. Biol. 628, 1–31.

Hassan, B.A., Bermingham, N.A., He, Y., Sun, Y., Jan, Y.N., Zoghbi, H.Y., Bellen, H.J., 2000. atonal regulates neurite arborization but does not act as a proneural gene in the Drosophila brain. Neuron 25, 549–561.

Helfrich-Förster, C., Shafer, O.T., Wülbeck, C., Grieshaber, E., Rieger, D., Taghert, P., 2007. Development and morphology of the clock-gene-expressing lateral neurons of ***Drosophila melanogaster***. J. Comp. Neurol. 500, 47–70.

Homberg, U., 2008. Evolution of the central complex in the arthropod brain with respect to the visual system. Arthropod Struct. Dev. 37, 347–362.

Hortsch, M., Patel, N.H., Bieber, A.J., Traquina, Z.R., Goodman, C.S., 1990. Drosophila neurotactin, a surface glycoprotein with homology to serine esterases is dynamically expressed during embryogenesis. Development 110, 1327–1340.

Huetteroth, W., El Jundi, B., El Jundi, S., Schachtner, J., 2010. 3D-reconstructions and virtual 4D-visualization to study metamorphic brain development in the sphinx moth ***Manduca sexta***. Front Syst. Neurosci. 4, 1–15.

Huser, A., Rohwedder, A., Apostolopoulou, A.A., Widmann, A., Pfitzenmaier, J.E., Maiolo, E.M., Selcho, M., Pauls, D., von Essen, A., Gupta, T., Sprecher, S.G., Birman, S., Riemensperger, T., Stocker, R.F., Thum, A.S., 2012. The serotonergic central nervous system of the Drosophila larva: anatomy and behavioral function. PLoS One 7, e47518.

Ignell, R., Dekker, T., Ghaninia, M., Hansson, B.S., 2005. Neuronal architecture of the mosquito deutocerebrum. J. Comp. Neurol. 493, 207–240.

Ito, K., Awano, W., Suzuki, K., Hiromi, Y., Yamamoto, D., 1997. The Drosophila mushroom body is a quadruple structure of clonal units each of which contains a virtually identical set of neurones and glial cells. Development 124, 761–771.

Ito, K., Awasaki, T., 2008. Clonal unit architecture of the adult fly brain. Adv. Exp. Med. Biol. 628, 137–158.
Ito, M., Masuda, N., Shinomiya, K., Endo, K., Ito, K., 2013. Systematic analysis of neural projections reveals clonal composition of the Drosophila brain. Curr. Biol. 23 (8), 644–655.
Iwai, Y., Usui, T., Hirano, S., Steward, R., Masatoshi, T., Uemura, T., 1997. Axon patterning requires D N-cadherin, a novel neuronal adhesion receptor, in the Drosophil aembryonic CNS. Neuron 19, 77–89.
Izergina, N., Balmer, J., Bello, B., Reichert, H., 2009. Postembryonic development of transit amplifying neuroblast lineages in the Drosophila brain. Neural. Dev. 4, 44.
Jarvis, E., Bruce, H.S., Patel, N.H., 2012. Evolving specialization of the arthropod nervous system. Proc. Nat. Acad. Sci. U.S.A. 109, 10634–10639.
Jefferis, G.S., Marin, E.C., Stocker, R.F., Luo, L., 2001. Target neuron prespecification in the olfactory map of Drosophila. Nature 414, 204–208.
Jefferis, G.S., Marin, E.C., Watts, R.J., Luo, L., 2002. Development of neuronal connectivity in Drosophila antennal lobes and mushroom bodies. Curr. Opin. Neurobiol. 12, 80–86.
Jiang, Y., Reichert, H., 2012. Programmed cell death in type II neuroblast lineages is required for central complex development in the Drosophila brain. Neural Dev. 7, 3.
Kumar, A., Fung, S., Lichtneckert, R., Reichert, H., Hartenstein, V., 2009a. Arborization pattern of engrailed-positive neural lineages reveal neuromere boundaries in the Drosophila brain neuropil. J. Comp. Neurol. 517, 87–104.
Kumar, A., Bello, B., Reichert, H., 2009b. Lineage-specific cell death in postembryonic brain development of Drosophila. Development 136, 3433–3442.
Kunz, T., Kraft, K.F., Technau, G.M., Urbach, R., 2012. Origin of Drosophila mushroom body neuroblasts and generation of divergent embryonic lineages. Development 139 (14), 2510–2522.
Lai, S.L., Awasaki, T., Ito, K., Lee, T., 2008. Clonal analysis of Drosophila antennal lobe neurons: diverse neuronal architectures in the lateral neuroblast lineage. Development 135, 2883–2893.
Larsen, C., Shy, D., Spindler, S.R., Fung, S., Pereanu, W., Younossi-Hartenstein, A., Hartenstein, V., 2009. Patterns of growth, axonal extension, and axonal arborization of neuronal lineages in the developing Drosophila brain. Dev. Biol. 335, 289–304.
Lee, T., Luo, L., 2001. Mosaic analysis with a repressible cell marker (MARCM) for Drosophila neural development. Trends Neurosci 24, 251–254.
Levine, R.B., 1984. Changes in neuronal circuits during insect metamorphosis. J. Exp. Biol. 112, 27–44.
Levine, R.B., Truman, J.W., 1985. Dendritic reorganization of abdominal motoneurons during metamorphosis of the moth, ***Manduca sexta***. J. Neurosci. 5, 2424–2431.
Libersat, F., Duch, C., 2002. Morphometric analysis of dendritic remodeling in an identified motoneuron during postembryonic development. J. Comp. Neurol. 450, 153–166.
Lichtneckert, R., Nobs, L., Reichert, H., 2008. Empty spiracles is required for the development of olfactory projection neuron circuitry in Drosophila. Development 135, 2415–2424.
Lin, S., Kao, C.F., Yu, H.H., Huang, Y., Lee, T., 2012. Lineage analysis of Drosophila lateral antennal lobe neurons reveals notch-dependent binary temporal fate decisions. PLoS Biol. 10, 1–17.
Mao, Z., Davis, R.L., 2009. Eight different types of dopaminergic neurons innervate the Drosophila mushroom body neuropil: anatomical and physiological heterogeneity. Front. Neural Circuits 3, 5.
Mysore, K., Flister, S., Muller, P., Rodrigues, V., Reichert, H., 2011. Brain development in the yellow fever mosquito ***Aedes aegypti***: a comparative immunocytochem- ical analysis using cross-reacting antibodies from ***Drosophila melanogaster***. Dev. Genes Evol. 221, 281–296.
Nordlander, R.H., Edwards, J.S., 1969. Postembryonic brain development in the monarch butterfly, Danaus plexippus plexippus, L. I. Cellular events during brain morphogenesis. Wilhelm Roux' Archiv. 162, 197–217.
Patel, N.H., Snow, P.M., Goodman, C.S., 1987. Characterization and cloning of fasciclin III: a glycoprotein expressed on a subset of neurons and axon pathways in Drosophila. Cell 48, 975–988.
Pereanu, W., Kumar, A., Jennett, A, Reichert, H., Hartenstein, V., 2010. Development-based compartmentalization of the Drosophila central brain. J. Comp. Neurol. 518, 2996–3023.
Pereanu, W., Hartenstein, V., 2006. Neural lineages of the Drosophila brain: a three-dimensional digital atlas of the pattern of lineage location and projection at the late larval stage. J. Neurosci. 26, 5534–5553.
Pfeiffer, B.D., Jenett, A., Hammonds, A.S., Ngo, T.T., Misra, S., Murphy, C., Scully, A., Carlson, J.W., Wan, K.H., Laverty, T.R., Mungall, C., Svirskas, R., Kadonaga, J.T., Doe, C.Q., Eisen, M.B., Celniker, S.E., Rubin, G.M., 2008. Tools for neuroanatomy and neurogenetics in Drosophila. Proc Natl Acad Sci USA. 105, 9715–9720.
Power, M.E., 1943. The brain of ***Drosophila melanogaster***. J. Morphol. 72, 517–559.
Power, M.E., 1952. A quantitative study of the growth of the central nervous system of a holometabolous insect, ***Drosophila melanogaster***. J. Morphol. 91, 389–411.
Prokop, A., Meinertzhagen, I.A., 2006. Development and structure of synaptic contacts in Drosophila. Semin. Cell Dev. Biol. 17, 20–30.
Rybak, J., Kuß, A., Lamecker, H., Zachow, S., Hege, H.C., Lienhard, M., Singer, J., Neubert, K., Menzel, R., 2010. The digital bee brain: integrating and managing neurons in a common 3D reference system. Front Syst. Neurosci. 4, 1–15.
Schindelin, J., Arganda-Carreras, I., Frise, E., Kaynig, V., Longair, M., Pietzsch, T., Preibisch, S., Rueden, C., Saalfeld, S., Schmid, B., Tinevez, J.Y., White, D.J., Hartenstein, V., Eliceiri, K., Tomancak, P., Cardona, A., 2012. FIJI: an open- source platform for biological-image analysis. Nat. Methods 9, 676–682.
Schmid, A., Chiba, A., Doe, C.Q., 1999. Clonal analysis of Drosophila embryonic neuroblasts: neural cell types, axon projections and muscle targets. Development 126, 4653–4689.
Schmidt, H., Rickert, C., Bossing, T., Vef, O., Urban, J., Technau, G.M., 1997. The embryonic central nervous system lineages of ***Drosophila melanogaster***, II. Neuroblast lineages derived from the dorsal part of the neuroectoderm. Dev. Biol. 189, 186–204.
Seibert, J., Urbach, R., 2010. Role of en and novel interactions between msh, ind, and vnd in dorsoventral patterning of the Drosophila brain and ventral nerve cord. Dev. Biol. 346, 332–345.
Shafer, O.T., Helfrich-Förster, C., Renn, S.C., Taghert, P.H., 2006. Reevaluation of ***Drosophila melanogaster's*** neuronal circadian pacemakers reveals new neuronal classes. J. Comp. Neurol. 498, 180–193.
Singh, K., Singh, R.N., 1999. Metamorphosis of the central nervous system of ***Drosophila melanogaster*** Meigen (Diptera: Drosophilidae) during pupation. J. Biosci. 24, 345–360.
Snow, P.M., Patel, N.H., Harrelson, A.L., Goodman, C.S., 1987. Neural-specific carbohydrate moiety shared by many surface glycoproteins in Drosophila and grasshopper embryos. J. Neurosci. 7, 4137–4144.
Spindler, S.R., Hartenstein, V., 2010. The Drosophila neural lineages: a model system to study brain development and circuitry. Dev. Genes Evol. 220, 1–10.
Spindler, S.R., Hartenstein, V., 2011. Bazooka mediates secondary axon morphology in Drosophila brain lineages. Neural Dev. 6, 16.
Sprecher, S.G., Cardona, A., Hartenstein, V., 2011. The Drosophila larval visual system: high-resolution analysis of a simple visual neuropil. Dev. Biol. 358, 33–43.
Stocker, R.F., Heimbeck, G., Gendre, N., de Belle, J.S., 1997. Neuroblast ablation in Drosophila P[Gal4] lines reveals origins of olfactory interneurons. J. Neurobiol. 32, 443–456.
Stocker, R.F., Lienhard, M.C., Borst, A., Fischbach, K.F., 1990. Neuronal architecture of the antennal lobe in ***Drosophila melanogaster***. Cell Tissue Res. 262, 9–34.
Strausfeld, N.J., 1976. Atlas of an Insect Brain. Springer-Verlag, Berlin, pp. 1–214.
Strausfeld, N.J., Li, Y., 1999. Representation of the calyces in the medial and vertical lobes of cockroach mushroom bodies. J. Comp. Neurol. 409, 626–646.
Strausfeld, N.J., Sinakevitch, I., Brown, S.M., Farris, S.M., 2009. Ground plan of the insect mushroom body: functional and evolutionary implications. J. Comp. Neurol. 513, 265–291.
Taghert, P.H., Bastiani, M.J., Ho, R.K, Goodman, C.S., 1982. Guidance of pioneer growth cones: filopodial contacts and coupling revealed with an antibody to Lucifer Yellow. Dev. Biol. 94, 391–399.
Tanaka, N.K., Endo, K., Ito, K., 2012. Organization of antennal lobe-associated neurons in adult ***Drosophila melanogaster*** Brain. J. Comp. Neurol. 520, 4067–4130.
Technau, G., Heisenberg, M., 1982. Neural reorganization during metamorphosis of the corpora pedunculata in ***Drosophila melanogaster***. Nature 295, 405–407.
Thomas, J.B., Bastiani, M.J., Bate, M., Goodman, C.S., 1984. From grasshopper to Drosophila: a common plan for neuronal development. Nature 310, 203–207.
Tissot, M., Stocker, R.F., 2000. Metamorphosis in Drosophila and other insects: the fate of neurons throughout the stages. Prog. Neurobiol. 62, 89–111.
Truman, J.W., Bate, M., 1988. Spatial and temporal patterns of neurogenesis in the central nervous system of ***Drosophila melanogaster***. Dev. Biol. 125, 145–157.
Truman, J.W., Booker, R., 1986. Adult-specific neurons in the nervous system of the moth, ***Manduca sexta***: selective chemical ablation using hydroxyurea. J. Neuro- biol. 17, 613–625.
Truman, J.W., Moats, W., Altman, J., Marin, E.C., Williams, D.W., 2010. Role of Notch signaling in establishing the hemilineages of secondary neurons in ***Drosophila melanogaster***. Development 137, 53–61.
Truman, J.W., Reiss, S.E., 1988. Hormonal regulation of the shape of identified motoneurons in the moth ***Manduca sexta***. J. Neurosci. 8, 765–775.
Truman, J.W., Schuppe, H., Shepherd, D., Williams, D.W., 2004. Developmental architecture of adult-specific lineages in the ventral CNS of Drosophila. Development 131, 5167–5184.
Udolph, G., Prokop, A., Bossing, T., Technau, G.M., 1993. A common precursor for glia and neurons in the embryonic CNS of Drosophila gives rise to segment- specific lineage variants. Development 118, 765–775.
Urbach, R., Schnabel, R., Technau, G.M., 2003. The pattern of neuroblast formation, mitotic domains and proneural gene expression during early brain develop- ment in Drosophila. Development 130, 3589–3606.
Urbach, R., Technau, G.M., 2003a. Segment polarity and DV patterning gene expression reveals segmental organization of the Drosophila brain. Develop-ment 130, 3607–3620.
Urbach, R., Technau, G.M., 2003b. Molecular markers for identified neuroblasts in the developing brain of Drosophila. Development 130, 3621–3637.
Wagh, D.A., Rasse, T.M., Asan, E., Hofbauer, A., Schwenkert, I., Dürrbeck, H., Buchner, S., Dabauvalle, M.C., Schmidt, M., Qin, G., Wichmann, C., Kittel, R., Sigrist, S.J., Buchner, E., 2006. Bruchpilot, a protein with homology to ELKS/CAST, is required for structural integrity and function of synaptic active zones in Drosophila. Neuron 49, 833–844.
Watson, A.H., Schürmann, F.W., 2002. Synaptic structure, distribution, and circuitry in the central nervous system of the locust and related insects. Microsc. Res. Tech. 56, 210–226.
Weeks, J.C., 2003. Thinking globally, acting locally: steroid hormone regulation of the dendritic architecture, synaptic connectivity and death of an individual neuron. Prog. Neurobiol. 70, 421–442.
Williams, J.L., Boyan, G.S., 2005. Building the central complex of the grasshopper Schistocerca gregaria: temporal topology organizes the neuroarchitecture of the w, xy, y, z tracts. Arthropod Struct. Dev. 34, 97–110.
Wong, D.C., Lovick J.K., Ngo, K.T., Omoto J.J., Bonsuthiratanna, W., Hartenstein, V. 2013. Postembryonic lineages of the Drosophila brain: II. Identification of lineage projection patterns based on MARCM clones. Dev. Biol. 2013, http://dx.doi.org/10.1016/j.ydbio.2013.07.009.
Younossi-Hartenstein, A., Nassif, C., Green, P., Hartenstein, V., 1996. Early neurogenesis of the Drosophila brain. J. Comp. Neurol. 370, 313-329.
Yu, H.H., Kao, C.F., He, Y., Ding, P., Kao, J.C., Lee, T., 2010. A complete developmental sequence of a Drosophila neuronal lineage as revealed by twin-spot MARCM. PLoS Biol. 8, e1000461.
Yu, H.H., Awasaki, T., Schroeder, M.D., Long, F., Yang, J.S., He, Y., Ding, P., Kao, J.C., Wu, G.Y., Peng, H., Myers, G., Lee, T., 2013. Clonal development and organization of the adult Drosophila cenetral brain. Curr. Biol. 23, 633-643.
Zacharias, D., Leslie, J., Williams, D., Meier, T., Reichert, H., 1993. Neurogenesis in the insect brain: cellular identification and molecular characterization of brain neuroblasts in the grasshopper embryo. Development. 118, 941-955.
Zecca, M., Basler, K., Struhl, G., 1996. Direct and long-range action of a wingless morphogen gradient. Cell. 87, 833-844.

Chapter 6

Postembryonic lineages of the *Drosophila* brain: II. Identification of lineage projection patterns based on MARCM clones

Postembryonic lineages of the *Drosophila* brain: II. Identification of lineage projection patterns based on MARCM clones

Darren C. Wong, Jennifer K. Lovick, Kathy T. Ngo, Wichanee Borisuthirattana, Jaison J. Omoto, Volker Hartenstein [n]

article info

Available online 18 July 2013

Keywords:
Brain
Development
Drosophila
Lineage
Mapping
SAT

abstract

The *Drosophila* central brain is largely composed of lineages, units of sibling neurons derived from a single progenitor cell or neuroblast. During the early embryonic period, neuroblasts generate the primary neurons that constitute the larval brain. Neuroblasts reactivate in the larva, adding to their lineages a large number of secondary neurons which, according to previous studies in which selected lineages were labeled by stably expressed markers, differentiate during metamorphosis, sending terminal axonal and dendritic branches into defined volumes of the brain neuropil. We call the overall projection pattern of neurons forming a given lineage the "projection envelope" of that lineage. By inducing MARCM clones at the early larval stage, we labeled the secondary progeny of each neuroblast. For the supraesophageal ganglion excluding mushroom body (the part of the brain investigated in the present work) we obtained 81 different types of clones. Based on the trajectory of their secondary axon tracts (described in the accompanying paper, Lovick et al., 2013), we assigned these clones to specific lineages defined in the larva. Since a labeled clone reveals all aspects (cell bodies, axon tracts, terminal arborization) of a lineage, we were able to describe projection envelopes for all secondary lineages of the supraesophageal ganglion. This work provides a framework by which the secondary neurons (forming the vast majority of adult brain neurons) can be assigned to genetically and developmentally defined groups. It also represents a step towards the goal to establish, for each lineage, the link between its mature anatomical and functional phenotype, and the genetic make-up of the neuroblast it descends from.

Introduction

In the field of developmental biology, the concepts of cell determination and cell lineage are fundamental to our understanding of the formation of complex tissues and organs. When talking about a cell lineage, we are referring to the genealogy (family tree) of groups of cells. The lineage produced by a progenitor cell is generally used synonymously with the progeny descending from this cell. During early stages of development, a progenitor cell initiates a genetic program that controls the later fate of this cell and its progeny. The genetic program of the progenitor is defined by the expression of cell fate determinants, typically transcription factors, that either remain active in the progeny or trigger the expression of a next tier of factors impacting the fate of the progeny (Guillemot, 2007; Shirasaki and Pfaff, 2002; Skeath and Thor, 2003). Thus, when embarking on the analysis of a complex organ, one of the assumptions that guides our research is that cells which possess a similar phenotype do so because they are part of a lineage produced by a common progenitor which, early on, expresses a set of transcription factors ("intrinsic determinants") controlling the fate of its lineage. Of course, this assumption has to always be tested against the alternative: extrinsic signals from the environment into which cells are placed trigger a genetic switch in these cells which controls their fate. In this scenario, the family tree of the cells is not important.

The fate of cell lineages in the *Drosophila* nervous system is heavily influenced by intrinsic determinants. A number of pioneering experiments in which neural progenitors (neuroblasts) were cultured in vitro revealed that, even when removed from their natural environment in the early embryo, neuroblasts are capable of dividing and producing progeny in the same number and cell type (assayed by expression of neurotransmitters) (Huff et al., 1989). Later studies identified many specific transcription factors expressed in neuroblasts (Doe, 1992; Urbach and Technau, 2003). Furthermore, it was shown that the timing of expression of a transcription factor is able to influence the fate of subsets of neurons ("sublineages") forming part of a lineage (Brody and

0012-1606/$ - see front matter
http://dx.doi.org/10.1016/j.ydbio.2013.07.009

Odenwald, 2000; Isshiki et al., 2001; Kambadur et al., 1998; Pearson and Doe, 2004). Thus, a neuroblast (N) divides asymmetrically, with one daughter cell (N') remaining in the state of a dividing neuroblast, whereas the other daughter cell (ganglion mother cell), after an additional round of division, becomes postmitotic and differentiates into two daughter cells (neurons or glia). The asymmetric division allows for a mechanism by which transcription factors are differentially inherited by daughter cells. The general model is that transcription factor (A), expressed during a specific time interval, will be inherited by one daughter cell or sublineage (α). Eventually, (A) is no longer expressed and a second one (B) turns on. All neurons born after (A) is turned off now inherit (B) and become a second sublineage (β). Several transcription factors were identified that are expressed in a sequential manner during neuroblast proliferation in the embryo and were shown, using molecular markers as a read-out, to influence the fate of embryonic-born (primary) neurons (Isshiki et al., 2001; Kambadur et al., 1998). However, it should be emphasized that many transcription factors are active in neuroblasts from before they are mitotically active through to a later developmental period, and that this window of expression varies for each transcription factor (Doe, 1992; Kumar et al., 2009a, 2009b; Lichtneckert et al., 2008; Urbach and Technau, 2003); these factors would be predicted to have an impact on the fate of an entire lineage.

Analyses of a few select lineages in the larval and/or adult brain support the idea that neuronal fate is controlled by factors inherited by entire lineages and by specific sublineages, which may manifest itself in a lineage's overall structure. Thus, lineages appear as "morphological units," with all axons forming one or two (in the case of hemilineages; Truman et al., 2010) bundles and terminal arborizations focusing on a discrete neuropil territory. For example, four lineages (MB1-4) form the mushroom body (Crittenden et al., 1998; Ito et al., 1997) and three lineages (vNB/BAla1, lNB/BAlc and dNB/BAmv3) include the majority of projection neurons connecting the antennal lobe with the protocerebrum (Lai et al., 2008). Endings of all secondary neurons of MB1-4 are confined to the calyx, peduncle, and lobes of the mushroom body; the antennal lobe-associated lineages innervate three compartments, namely the antennal lobe, calyx, and lateral horn (Das et al., 2013; Lai et al., 2008; Stocker et al., 1990). We will use the term "projection envelope" to describe the overall neuropil volume that is innervated by neurons of a lineage. Individual neurons in a lineage form restricted terminal arbors that target smaller volumes within the projection envelope. For example, the neurons produced by MB1-4 in the late embryo/early larva fill the γ-lobe; they are followed by neurons forming the α'/β' lobes, and finally by neurons of the α/β lobes (Ito et al., 1997; Kunz et al., 2012). In the case of dNB/BAmv3, most neurons innervate a single glomerulus of the antennal lobe and project to discrete regions within the calyx and lateral horn (Jefferis et al., 2001; Yu et al., 2010). It is reasonable to assume that the projection envelope of a lineage, which is shared by all neurons of that lineage, is determined to some extent by transcription factors expressed earlier in development and are common to the neuroblast of that lineage. In addition, other factors expressed later at defined temporal intervals, thereby only reaching neurons born during that interval, may be responsible for more specific structural and functional characteristics that set neurons of a lineage apart from each other.

Whereas both expression of molecular determinants of cell fate and the phenotypic elements of cell fate (e.g., shape of neuronal arbor, choice of pre and postsynaptic partners, physiological characteristics) can be studied in great detail, the complex cascade of molecular events linking the two levels has remained elusive. What mechanism acts on outgrowing axons and guides/restricts them to a specific compartment? How is this mechanism encoded in the cell fate determinants expressed in the neuroblast?

Drosophila offers a favorable system to address these questions: its nervous system is built by a relatively small number of lineages (previous descriptive maps yielded approximately 100 lineages per central brain hemisphere and 28 lineages per ventral nerve cord hemineuromere; Doe, 1992; Urbach and Technau, 2003; Younossi-Hartenstein et al., 1996). Lineages can be globally and/or individually labeled by antibodies for various neuronal proteins (e.g. mushroom body-specific antibodies: Crittenden et al., 1998; neuropeptide pigment-dispersing factor or PDF: Helfrich-Förster et al., 2007; neuropeptide IPNamide: Shafer et al., 2006) and reporter constructs (***LacZ*** and Gal4-based: e.g. ***en-Gal4***, Kumar et al., 2009b; ***Th-Gal4***, Mao and Davis, 2009; Gal4 lines expressed in ellipsoid body neurons, Renn et al., 1999). Maps of the expression of transcription factors in the neuroblasts, as well as the anatomical pattern of lineages at the larval stage, have been generated (Cardona et al., 2010; Pereanu and Hartenstein, 2006; Truman et al., 2004; Urbach and Technau, 2003; Urbach and Technau, 2004). In the accompanying paper (Lovick et al., 2013) we had mapped the association between lineages and neuropil fascicles and followed these fascicles throughout metamorphosis into the adult. In this paper, we have analyzed individual lineages at the adult stage by the MARCM technique (Lee and Luo, 2001), where a GFP reporter gene is activated by somatic recombination in neuroblasts shortly before they enter their larval phase of proliferation. In this manner, all secondary neurons produced by these neuroblasts (the "secondary lineages") are labeled as "clones." A clone includes the cluster of cell bodies derived from the larval neuroblast, as well as the axons and terminal arborizations of these cell bodies. Based on the trajectory of their axon bundles, we are able to assign clones to their respective lineages. We analyzed a total of 814 clones located in the supraesophageal ganglion, the largest part of the brain. Excluded from this study are clones in the optic lobes, whose modular (and probably not-lineage based) structure has been described previously (Bausenwein et al., 1992). Excluded are also clones representing the four well known lineages of the mushroom body (Crittenden et al., 1998; Ito et al., 1997; Kunz et al., 2012), and the lineages of the subesophageal ganglion, which will be analyzed in an upcoming study (Kuert et al., in preparation). Clones fell into 81 groups, where each group corresponded to a known lineage or lineage pair. We provide a brief description of the projection envelopes for all lineages. The complexity of these lineages clearly warrants a much finer level of analysis, taking into account aspects like overlap of terminal arborizations of different lineages, precise relationships between arborizations and compartment boundaries, and variations in the size and location of cell bodies. These investigations, which require that specimens with different clones are digitally registered to a "standard brain," will be presented in a series of upcoming studies. Note that numerous aspects of lineage analysis has been recently published in two large, independent studies where MARCM clones of secondary lineages were generated (Ito et al., 2013; Yu et al., 2013). The main purpose of the present work is to identify clones with defined lineages, contributing to the ultimate goal of linking the mature anatomical and functional phenotype of a lineage and its constituent neurons with the specific genetic make-up of the embryonic neuroblast that produces the lineage.

Material and methods

Fly stocks

Flies were grown at 25°C using standard fly media unless otherwise noted. Fly stocks used are the ones detailed in the "Clonal Analysis" section.

Immunohistochemistry

Samples were fixed in 4% paraformaldehyde in phosphate buffer saline (PBS, Fisher-Scientific, pH¼ 7.4; Cat No. #BP399-4). Tissues were permeabilized in PBT (phosphate buffer saline with 0.3% Triton X-100, pH¼ 7.4) and immunohistochemistry was performed using standard procedures (Ashburner, 1989). The following antibodies were provided by the Developmental Studies Hybridoma Bank (Iowa City, IA): mouse anti-Neurotactin (BP106, 1:10), rat anti-DN-cadherin (DN-EX #8, 1:20), mouse anti-Neuroglian (BP104, 1:30). Secondary antibodies, IgG (Jackson ImmunoResearch; Molecular Probes), were used at the following dilutions: Alexa 546-conjugated anti-mouse (1:500), DynaLight 649-conjugated anti-rat (1:400).

Clonal analysis

Clones were generated by Flp-mediated mitotic recombination at homologous FRT sites. Larval neuroblast clones were generated by MARCM (Lee and Luo, 2001; see below) or the Flp-out construct (Zecca et al., 1996; Ito et al., 1997).

Mitotic clone generation by Flp-out

To generate secondary lineages clones in the larva using the Flp-out technique; flies bearing the genotype:

(1) *hsflp, elav^{C155}-Gal4/+; UAS-FRT-rCD2, y+, stop-FRT-mCD8::GFP*
(2) *hsflp; Act5C-FRT-stop,y+-FRT-Gal4, UAS-tauLacZ/UAS-src::EGFP*

Briefly, early larva with either of the above genotype were heatshocked at 38 1C for 30–40 min. ***elav^{C155}-Gal4*** is expressed in neurons as well as secondary neuroblasts. Third instar larval and
adult brains were dissected and processed for immunohistochemistry (as described above).

Mitotic clone generation by MARCM

Mitotic clones were induced during the late first instar/early second instar stages by heat-shocking at 38 1C for 30 min to 1 h
(approximately 12–44 h ALH). GFP-labeled MARCM clones contain the following genotype:
Adult MARCM clones:

(1) *hsflp/+; FRTG13, UAS-mCD8GFP/FRTG13, tub-GAL80; tub-Gal4/+* or
(2) FRT19A GAL80, hsflp, UAS-mCD8GFP/ elav^{C155}-Gal4, FRT19A; UAS-CD8GFP/+

Larval MARCM clones:
hsflp, elav^{C155}-Gal4, FRTG13, UAS-mCD8GFP /Y or hsflp, elav^{C155}-Gal4, FRTG13, UAS-mCD8GFP /; FRT42D, tub-Gal80/FRT42D

Confocal microscopy

Staged ***Drosophila*** larval and adult brains labeled with suitable markers were viewed as whole-mounts by confocal microscopy [LSM 700 Imager M2 using Zen 2009 (Carl Zeiss Inc.); lenses: 40 ~ oil (numerical aperture 1.3)]. Complete series of optical sections were taken at 2-μm intervals. Captured images were processed by ImageJ or FIJI (National Institutes of Health, http://rsbweb.nih.gov/ij/ and http://fiji.sc/) and Adobe Photoshop.

2D registration of clones to standard brain

Brains with MARCM clones were labeled with DN-cad and BP104 to image the SAT and projection envelope relative to the BP104-positive fascicles and DN-cad-positive neuropil compartments. Fasciculation of the SAT of a clone with a fascicle allowed for its identification with a lineage, or lineage pair (see accompanying paper by Lovick et al., 2013). To generate the figure panels of this paper, *z*-projections of the individual MARCM clones were registered digitally with *z*-projections of a standard brain ("2D registration"). To this end, the standard brain was subdivided along the antero-posterior axis into six slices of approximately 20 mm thickness. These slices, each one characterized by one or more easily recognized landmark structures (antennal lobe, optic tubercle, ellipsoid body, fan-shaped body, lateral bend of antennal lobe tract, calyx), are introduced in Pereanu et al. (2010), and are depicted throughout the figures of this and the accompanying paper (Lovick et al., 2013). The process of 2D registration involved the following steps:

(1) The confocal stack depicting a given clone was imported into the FIJI program (National Institutes of Health, http://rsbweb.nih.gov/ij/ and http://fiji.sc/) and digitally oriented such that the peduncle was aligned with the *z*-axis of the stack.
(2) A *z*-projection of the entire clone (e.g., all sections of the green channel showing label) was generated.
(3) In the case of brains containing more than one clone, background fluorescence and/or fluorescence from other clones were digitally removed to allow visualization of a single clone.
(4) This *z*-projection was merged with a *z*-projection of the red channel (BP104 or DN-cad) derived from the confocal sections of one slice. The chosen slice is dependent upon the corresponding clone's SAT location. For example, consider the lineage BAlp4, whose SAT enters the antennal lobe posterolaterally. In terms of antero-posterior brain slices, this SAT forms part of the second slice ("level anterior optic tubercle").
(5) Both the anterior optic tubercle slice of the standard brain and the brain specimen containing the BAlp4 clone were imported as two layers into a file generated by the Adobe Photoshop program. Using few standard landmarks (location of the peduncle, tips of the MB vertical and medial lobe, vertical midline), the layer containing the clone (rendered temporarily semitransparent) was optimally fitted to the underlying layer representing the standard brain.
(6) The optimally-fitted layer containing the clone was re-opened in FIJI, and then merged with the red channel (BP104 or DN-cad) of the standard brain. For the panels of the figure set depicting clone SATs relative to BP104-positive fascicles (Figs. 4, 6, 9, 12, 15 and 17), the red channel (BP104) was rendered white in Adobe Photoshop. For the figure set depicting the projection envelopes of clones (Figs. 2, 3, 5, 7, 8, 10, 11, 13, 14 and 16), the red channel (DN-cad) was rendered magenta by duplicating it in the blue channel.

Results

MARCM clones reveal the projection envelope of secondary lineages

We analyzed a total of 814 secondary clones, distributed over 499 brains. About half of the brains had a single clone, the other half had two or more (up to five; brains containing in excess of five clones were discarded). Aside from clonal labeling of individual secondary lineages, most brains also contained labeled-endings of afferents from the optic lobe and/or antennal nerve. All clones could be assigned to a specific secondary lineage (or lineage pairs) based on the entry point and trajectory of the SAT, defined as the fiber bundle that directly emerges from the cell body cluster and enters the neuropil (Fig. 1A and B; BAlp4 clone assigned to BP104-labeled SAT). Given the number of clones analyzed, most secondary lineages were represented by more than one clone. We observed a wide range, with some lineages represented more than 20 times

and others less than five times (average: 10 clones per lineage; Table 2).

Based on our analysis of SAT development (see accompanying paper by Lovick et al., 2013), 56 lineages defined in the late larva have SATs that can be individually followed within the neuropil throughout development (Table 2). Within this group, we could identify clones in all cases except one, DALv3. The projection pattern of DALv3 has been characterized previously (Kumar et al., 2009a). A second group of 30 lineages (e.g., BAmas1/2; DALcm1/2) have SATs that form pairs or form a quartet (the four BLAd lineages). In these cases, it is not possible to predict whether the two lineages forming the pair (or quartet, in the case of BLAd1-4) will have projection envelopes that are identical or different. Within the group of 30 lineages, four pairs (BAmas1/2, DPMpl1/2, CP2/3, BLP1/2) were obtained that had clones with significantly different arborization patterns. This suggests that paired lineages with identical SATs form distinct arborization patterns (e.g. BAmas1/2; Fig. 4C11–12). In three pairs within this group (DPLl2/3, BLVa1/2, BLVa3/4) the patterns were very similar, but the trajectory of part of the SATs differed consistently (e.g. DPLl2/3 in Fig. 10B and F). In the case of the BLAd1-4 quartet we isolated three different classes of clones. In the eight remaining pairs (BAla3/4, DALcm1/2, DAMd2/3, DAMv1/2, DPLal2/3, DPLc2/4, DPLp1/2, BLP3/4) only one type of clone was recovered, suggesting that these lineages form identical arborization patterns. Alternatively, it is possible that we could recover clones for only one member of the pair, which is unlikely given the fact that an average of 10 clones per lineage was obtained for all other lineages.

A significant fraction of lineages form more than one SAT. In cases where these tracts separate from the very beginning where axon tracts enter the neuropil we tentatively assume that they represent two separate hemilineages (or sublineages, in case of type II lineages); ultimate proof for their status as "true" hemilineages would have to come from experimental studies such as those done for the thoracic lineages (Truman et al., 2010) or a small number of ***engrailed***-positive brain lineages (Kumar et al., 2009a). As described in the accompanying paper by Lovick et al. (2013), hemilineages move apart during metamorphosis in a number of cases. GFP labeled clones provided confirmation for this movement of hemilineages. All except one (BLAvm) of the lineages in question, notably BAlc, BAmd1, DPLl2/3, CP2/3, BLAl, BLAv1, BLVp1/2, were represented by more than five clones; for BLAvm we have three clones. In all cases, GFP labeling invariably marked both hemilineages simultaneously, whereas other independent lineages could be represent by a clone in some cases, but not in

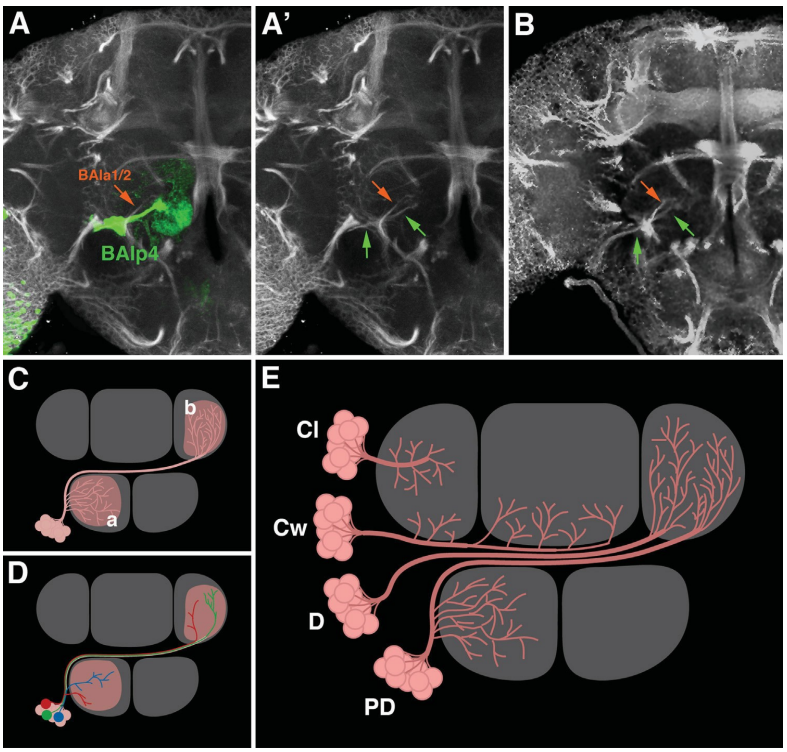

Fig. 1. Secondary lineages: SATs and projection envelope. (A–C) Assignment of clones to their respective secondary lineages is based on the entry point and trajectory of the SAT. Panel (A) shows a z-projection of an adult brain labeled with BP104 (white), containing a MARCM clone of the BAlp4 lineage (green). The SAT of BAla1/2 is shown in orange. Panel (A') shows BP104 channel of the same z-projection. Green arrows in (A'–B) point at the SAT of the BAlp4 clone; as visible by green arrows in (A'), the SAT follows one of the BP104-positive tracts that can be followed back through metamorphosis to lineage BAlp4. Panel (B) represents a z-projection of the standard brain used in this paper, at an antero-posterior level corresponding to the one used for (A/A'). Note invariant pattern of BP104-positive fiber bundles in (A/A') and (B) (green arrows: BAlptract; red arrow: BAla1/2 tract). (C–D) Relationship of individual neurons and projection envelope. Schematic representation of a lineage (pink) with a projection envelope including compartments "a" and "b". Individual neurons of the lineage could (all or in part) form arborizations throughout all compartments of the projection envelope [represented by red neuron in panel (D)], or could project to one or the other compartment [blue and green neuron in (D)]. (E) Classification of lineages based on the contour of projection envelope. Shown are four classes of lineages. In "PD" ("proximal distal") lineages, a long segment of the SAT connects proximal to distal arborizations. In "C" (continuous) lineages, branches emerge at more or less regular intervals along the entire length of the SAT. Two subtypes of continuous lineages, local ("Cl") and widefield ("Cw"), are illustrated. In "D" ("distal") lineages, terminal arborizations are delimited to the distal end of the SAT. Bar: 25 μm.

others. In cases of several lineages for which the movement of SATs and HSATs was difficult to follow (BLD1, BLD3, BLAl, DPLc5), the existence of two separating hemilineages was confirmed. In three cases, BAmd2, DPLm2, and DPMl1, the analysis of MARCM clones made it possible to identify the proper lineage in the adult brain. Thus, the SAT of BAmd2 cannot be followed beyond P24 because its entry and proximal SAT is masked by the arrays of antennal afferents surrounding it. A clone with the characteristic SAT entry point and crossing in the antennal lobe commissure confirmed BAmd2 for the adult brain. The same applied for DPMl1, whose characteristic descending SAT is not visible beyond P24. DPLm2 represents a unique case where the MARCM clone united two clusters of cells

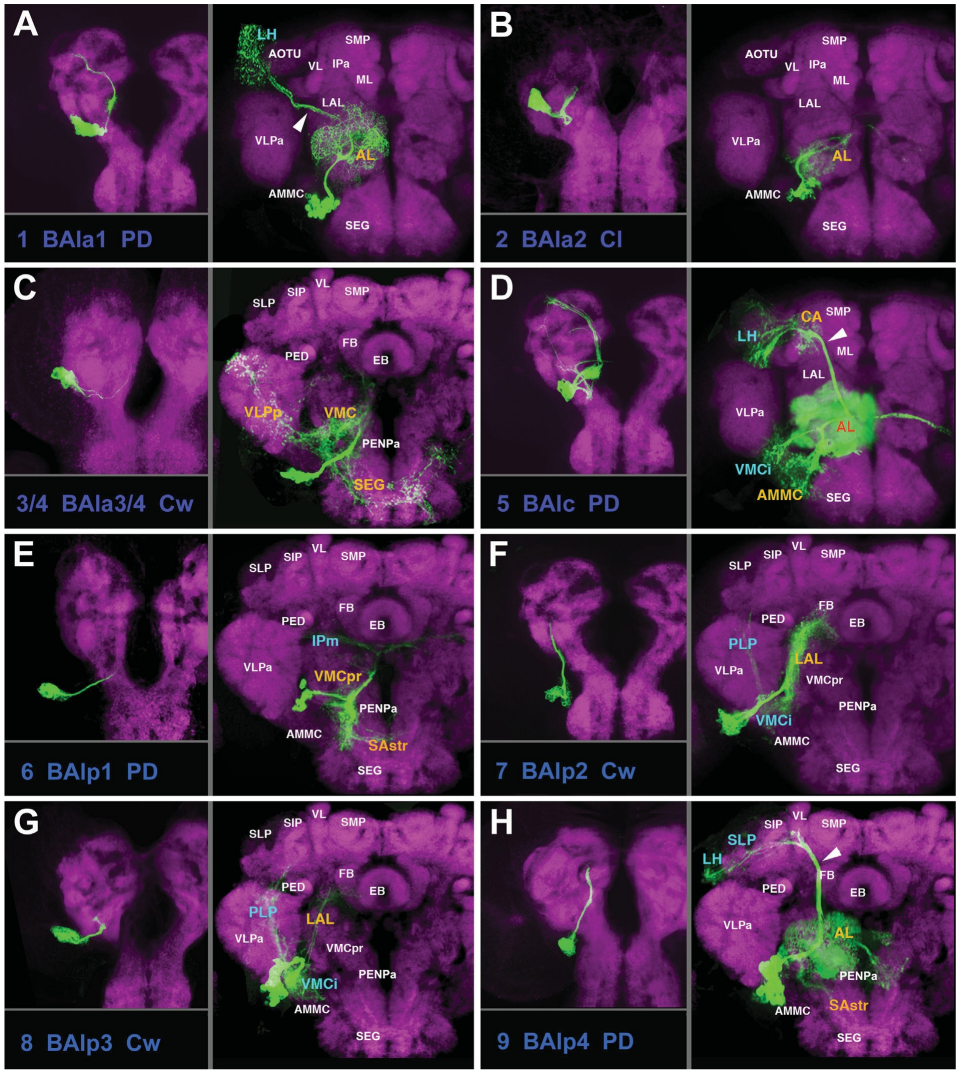

Fig. 2. (A–H) Clones representing lineages of the BA group (#1/BAla1–#9/BAlp4) in the larval and adult brain. This and the following Figs. 3, 5, 7, 8, 10, 11, 13, 14, 16 are designed in the same manner: Each lineage is represented by a panel showing z-projection of a larval brain hemisphere on the left, and of an adult hemisphere on the right. Number and abbreviation of the lineage is given at the bottom left of the panel. Next to the abbreviation, the type of lineage (C, P, PD) is indicated. Images were generated by registering full z-projection of clones (that is, a z-projection containing all sections of a stack showing GFP label) to a z-projection of a "slice" of the DN-cad-labeled standard brain, as described in the "Materials and methods" section. DN-cad visualizes neuropil compartments, annotated by white letters on part of panels showing adult brain. Compartments receiving major innervation by the lineage shown in a given panel are annotated by colored letters. Innervated compartments contained within the brain slice shown by DN-cad are in orange; compartments located significantly anterior or posterior to the slice shown appear in blue letters. For example, #1/BAla1 (A) is represented by a clone registered to an anterior brain slice [level optic tubercle (OTU)/mushroom body medial lobe (ML)]. Major compartments visible at that level are annotated by small white letters. Within this slice, only the antennal lobe is innervated by BAla1; it is annotated by orange letters. BAla1 projects postero-laterally towards the lateral horn, which is located in a slice posterior to the one shown. The lateral horn (LH) is therefore annotated by blue letters. For alphabetical list of all abbreviations see Table 1. Bar: 50 μm.

that had been previously considered to represent two separate lineages. Thus, in our larval analysis, DPM12 with a characteristic centrifugal axon bundle projecting to the ring gland was considered as a separate lineage (Pereanu and Hartenstein, 2006). MARCM clones showed that the ring gland associated axons form part of DPLm2 instead.

Classification of lineages based on the geometry of their projection envelope

The GFP-labeled clone, when superimposed on a backdrop of an adult brain labeled with a neuropil marker (anti-DN-cadherin; from here on called DN-cad) or axonal marker (anti-Neurotactin, from here on referred to as BP104), allows one to map the neurite arborizations of all neurons of a single lineage (the "projection envelope") with respect to brain neuropil compartments (Fig. 1C). Note that the relationship between the projection envelope of a lineage and the projection of an individual neuron forming part of a lineage is not simple (Fig. 1D). For example, when an envelope includes two neuropil compartments, a and b, there are two possibilities: (1) each individual neuron may also have arborizations in a and b (Fig. 1D, red neuron); or alternatively, a subset of neurons might only project to a or to b (Fig. 1D, green neuron and blue neuron, respectively). Nonetheless, documenting the projection envelope for each lineage represents a significant step towards describing brain circuitry. In this paper we will provide an overview of the projection envelopes for each lineage of the supraesophageal ganglion, following the same

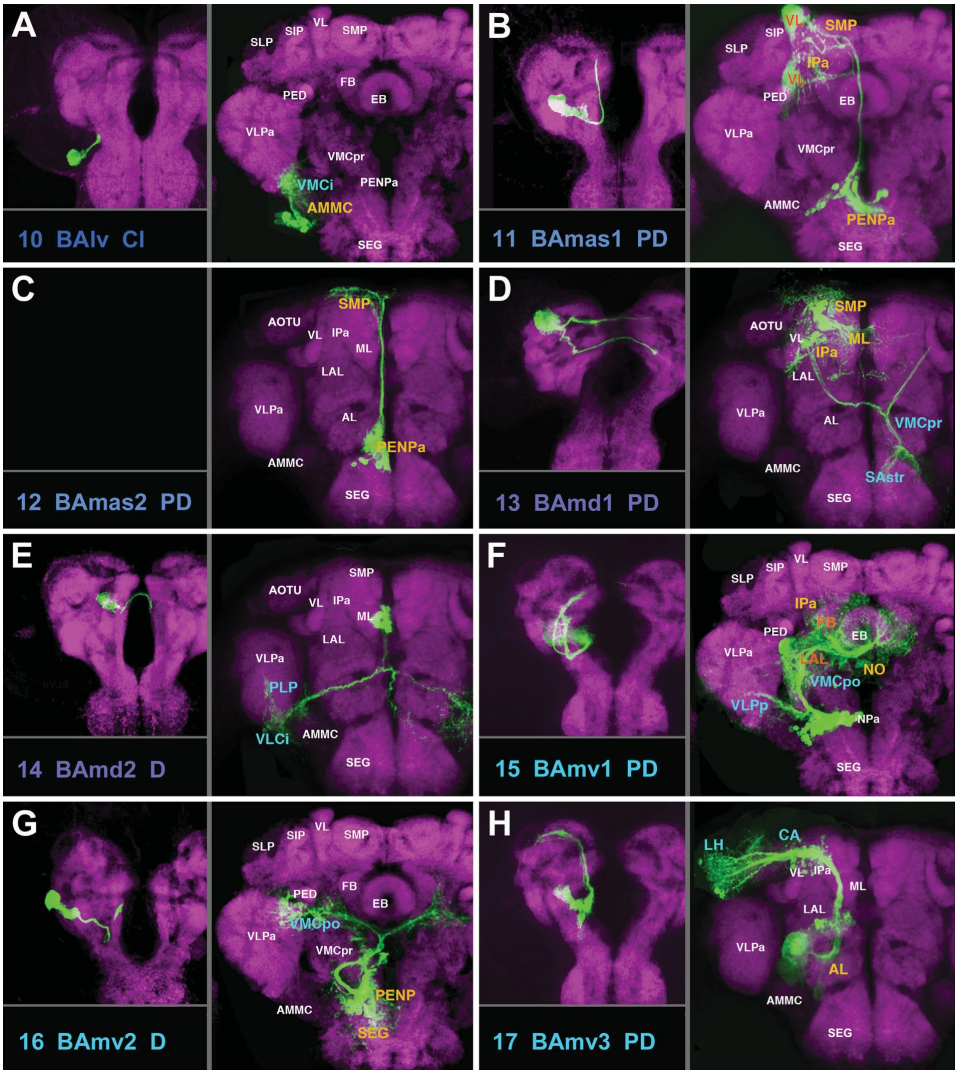

Fig. 3. (A–H) Clones representing lineages of the BA group (#10/BAlv–#17/BAmv3) in the larval and adult brain. For description of how panels are made and displayed, see legend of Fig. 2. Only one larval clone is shown for the pair BAmas1/2 (panels B and C). For alphabetical list of all abbreviations see Table 1. Bar: 50 μm.

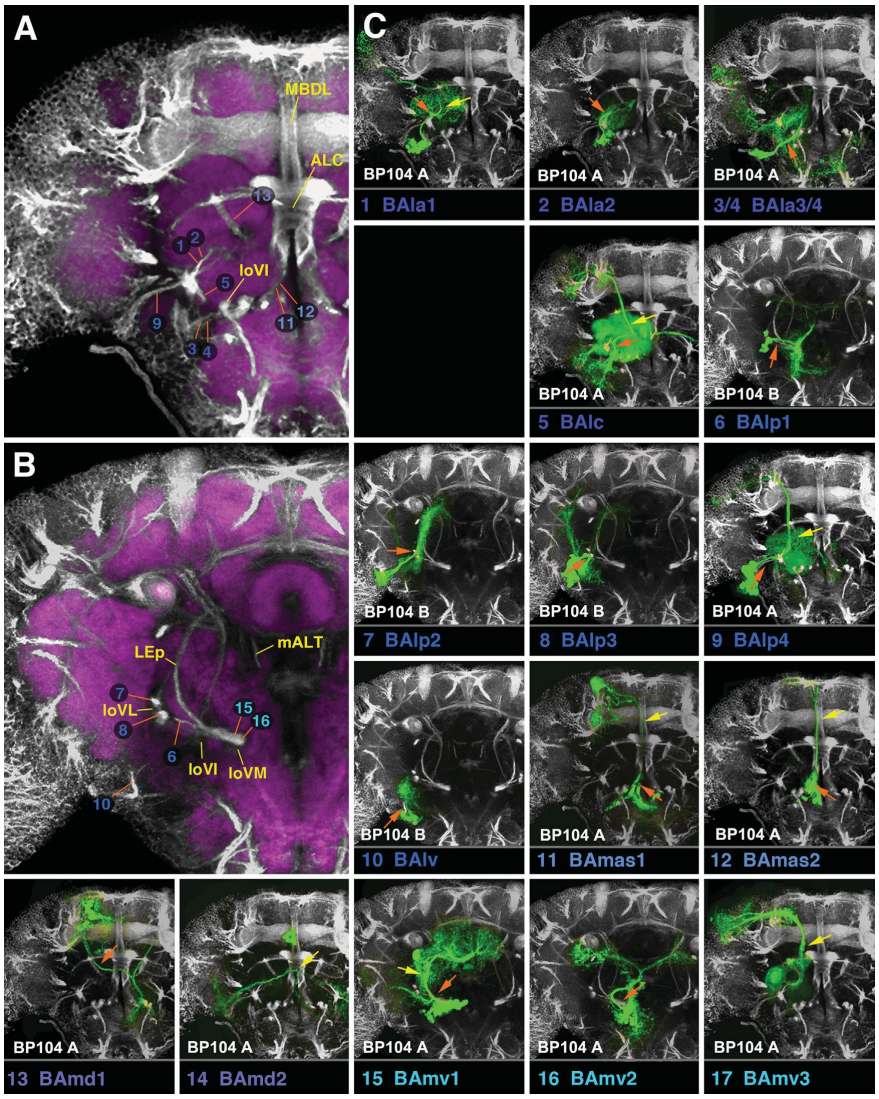

Fig. 4. Clones representing lineages of the BA group in the adult brain. This figure, as well as the following Figs. 6, 9, 12, 15, and 17, is all designed in the same manner. Large panels on the left (A, B in case of Fig. 4) show *z*-projections of frontal confocal sections of adult brain hemisphere labeled with BP104 (white, SATs and neuropil fascicles) and DN-cad (purple; neuropil compartments). Each *z*-projection represents a brain slice of approximately 15–20 mm thickness. Brain slices correspond to different levels along the antero-posterior ("*z*") axis. Panels A and B of this figure represent the two slices of the brain where BA lineage tracts enter the neuropil (A: level of optic tubercle and mushroom body lobes; B: posteriorly adjacent slice, marked by ellipsoid body). SATs of lineages are annotated by colored numbers; the same color key is used as in the accompanying paper by Lovick et al. (2013). In cases where two or more SATs or HSATs come very close and cannot be distinguished, the identifying numbers may be contracted into a single number followed by an asterisk; see, for example, the annotation of the HSATs of the DPLal2/3 lineages, #34/35, as "34v*" and "34d*", in Fig. 9A. Fascicles with which SATs are associated are annotated by yellow letters. (C) The small panels in section (C) of this figure show *z*-projections of clones representing lineages of the BA group. Panels were generated by registering *z*-projection of clones to a "slice" of the BP104-labeled standard brain, as described in the "Materials and methods" section. Each lineage is identified by a number and abbreviation (bottom of its panel), rendered in the same color as that used in panels A and B. For the BP104 channel (white), only slices shown in the left panels (A, B) are used and indicated at the bottom left of the panel ("BP104 A", "BP104 B"). For example, the first small panel depicts lineage #1/BAla1. The clone is registered to the anterior slice ("optic tubercle/mushroom body lobes"; shown at higher magnification in panel A), because the proximal SAT of BAla1 is contained within this slice. Panels with other lineages (e.g., #10/BAlv) use the more posterior slice (the one shown in panel B; ellipsoid body), because the SAT of BAlv is contained within that slice. In each small panel, the orange-colored arrow points at the proximal SATs by which the clone is identified. In terms of position and orientation, the arrow matches the orange line in panel on the left (A or B) which points at the corresponding BP104-labeled tract. Yellow arrows in the C-panels point at neuropil fascicles joined by the SAT. For example, the yellow arrow in the panel #1/BAla1 points at the beginning of the antennal lobe tract (ALT). For alphabetical list of abbreviations see Table 1. Bar: 25 μm.

topology-based ordering used in the accompanying paper (Lovick et al., 2013).

Representative clones and lineage restricted markers used in previous studies suggested that, aside from their topology (spatial relationship of a SAT entry point and projection relative to neuropil tracts and compartments), lineages can also be classified according to the "geometry", defined as the distribution of axonal/dendritic branches relative to the main SAT (Larsen et al., 2009). It should be noted that unlike vertebrate neurons, where dendritic branches connected to the cell body are separated from axonal branches, insect neurons have a neurite tree on which dendritic and axonal branches are frequently intermingled (Hartenstein et al., 2008; Watson and Schürmann, 2002). The degree of intermingling, nonetheless, varies for different neurons and presumably different lineages. For example, in the case of the well characterized lineages of antennal lobe (AL) projection neurons (e.g. BAmv3, BAlc, and BAla1), dendritic branches are concentrated along the proximal region of the SAT in the AL, whereas axonal branches are close to the distal tip of the SAT in the calyx (CA) and lateral horn (LH). The long segment of the SAT connecting proximal to distal, called the antennal lobe tract, is devoid of branches. Lineages with this geometry were classified as "PD" ("proximal distal") lineages (Larsen et al., 2009; Fig. 1E). In other lineages, branches emerged at more or less regular intervals along the entire length of the SAT ("continuous" or "C" lineages), or were all concentrated at its distal tip ("distal" or "D" lineages). Further

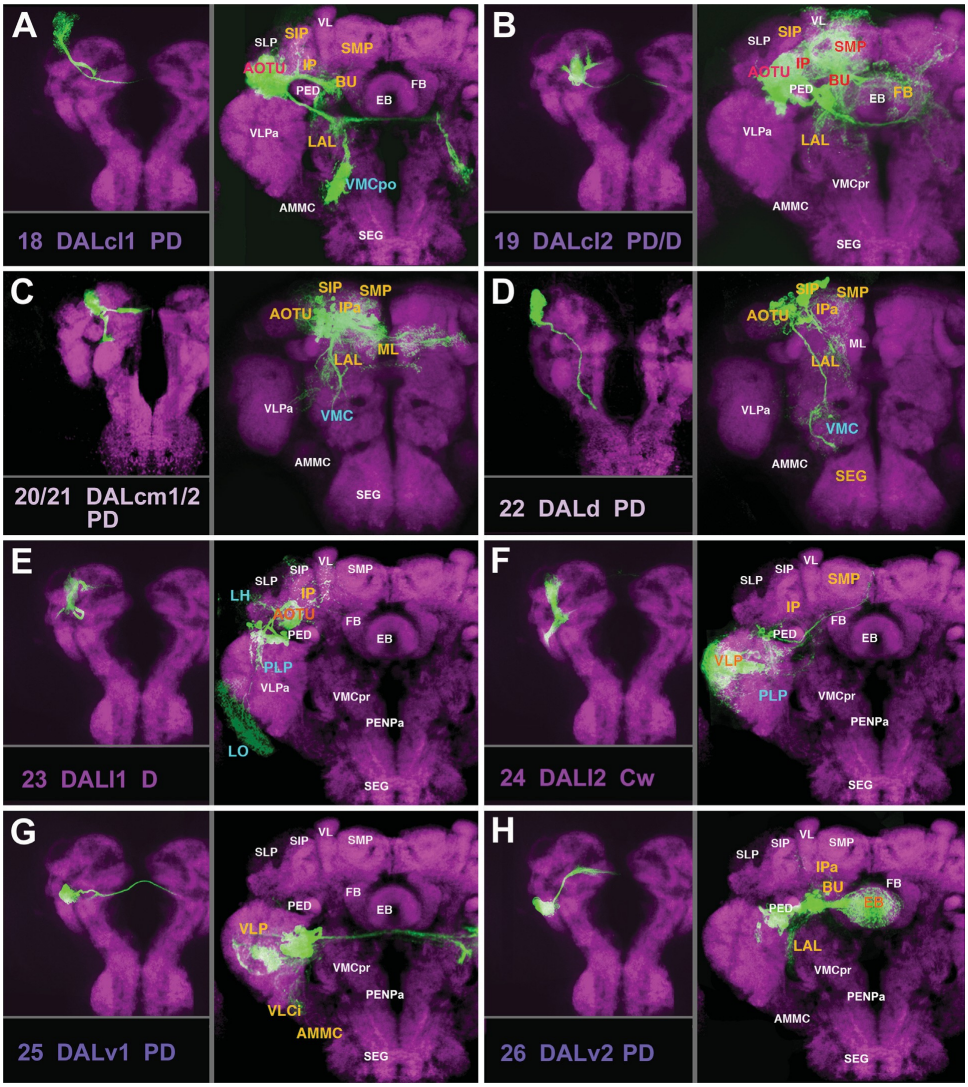

Fig. 5. (A–H) Clones representing lineages of the DAL group (#18/DALcl1–#26/DALv2) in the larval and adult brain. For description of how panels are made and displayed, see legend of Fig. 2. For alphabetical list of all abbreviations see Table 1. Bar: 50 μm.

analysis using fluorescent reporters differentially localized to either dendritic or axonal branches (e.g. UAS-ICAM5$^{\Delta ECD}$::mCherry and UAS-GFP-KDEL; Nicolai et al., 2010 and Okajima et al., 2005, respectively) can be used to compare their distribution in the C, D, and PD lineages.

In the following, clones representing individual lineages will be described in the order established for the lineage tracts in the accompanying paper (Lovick et al., 2013). Clones are documented in three sets of figures. In one set of figures, we show z-projections of clones with spatial respect to the BP104-labeled scaffold of neuropil fascicles, starting with lineages entering the anterior brain surface (BA: Fig. 4; DAL and DAM: Fig. 6), followed by those of the dorsal surface (DPL: Fig. 9), posterior surface (DPM, CM, CP: Fig. 12), and finally, lateral surface (BLA, BLD, BLP, BLV: Figs. 15 and 17). These figures illustrate the identification of clones with their corresponding lineages. The second set of figures show z-projections of clones registered to DN-cad-labeled brain slices, in the order as described above (BA: Figs. 2 and 3; DAL: Fig. 5; DAM: Fig. 7; DPL: Figs. 8 and 10; DPM: Fig. 11; CM and CP: Fig. 13; BLA and BLD: Fig. 14; BLP and BLV: Fig. 16), illustrating the projection envelopes of all lineages. In all panels of all these figures, the adult MARCM clone is paired with a larval clone (MARCM or Flp-out; see "Materials and methods" for more details) representing the corresponding lineage, documenting the similarity in SAT projection patterns between larval and adult stages. The third set of figures (supplementary Figs. S1–S5) show schematic renderings of SATs and main locations of terminal arborizations for all lineages. Lineages sharing important aspects of their projection are combined together, such that Fig. S1 shows lineages with SATs connecting ventral to dorsal compartments, Fig. S2 has lineages interconnecting ventral compartments, lineages in Fig.S3 are associated strongly with the central complex and mushroom body, Fig. S4 presents lineages of the superior protocerebrum projecting ventrally (including the subesophageal ganglion and

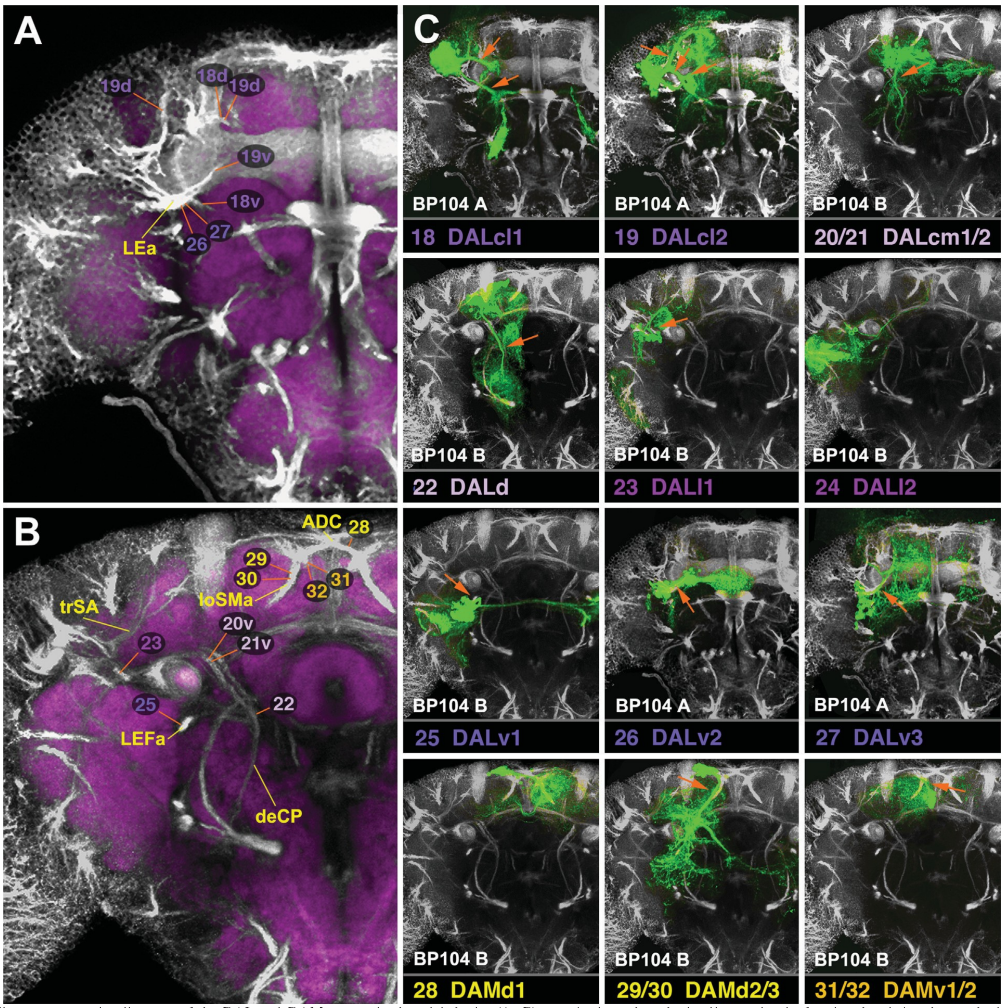

Fig. 6. Clones representing lineages of the DAL and DAM groups in the adult brain. (A, B) z-projections show brain slices at level of optic tubercle/mushroom body lobes (A) and ellipsoid body (B). (C) z-projections of clones representing lineages of the DAL and DAM group. For description of how panels are made and displayed, see legend of Fig. 4. For alphabetical list of all abbreviations see Table 1. Bar: 50 μm.

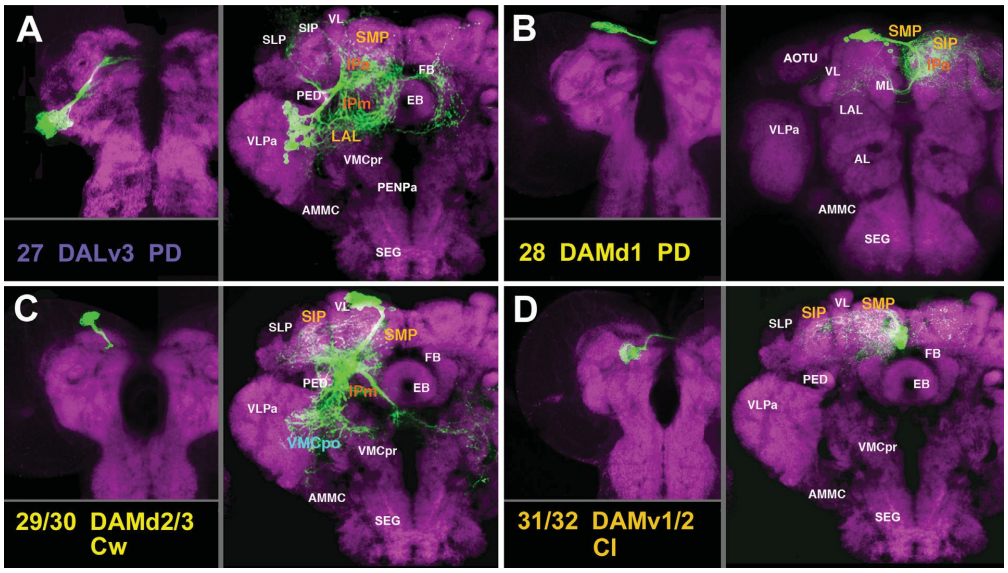

Fig. 7. (A–D) Clones representing lineages of the DAL group (#27/DALv3) and the DAM group in the larval and adult brain. For description of how panels are made and displayed, see legend of Fig. 2. For alphabetical list of all abbreviations see Table 1. Bar: 50 μm.

thoracico-abdominal ganglion), and Fig.S5 shows lineages interconnecting dorsal compartments of the brain.

BA lineages

The BA group comprises PD, C, and D lineages whose neurons are mostly associated with the ventral brain compartments (Figs. 2–4; Figs.S1, S2). Four PD lineages, BAla1 (#1; Fig. 2A), BAlc (#5; Fig. 2D; dorsal hemilineage), BAlp4 (#9; Fig. 2H), and BAmv3 (#17; Fig. 3H) include all of the projection neurons connecting the antennal lobe (AL) and superior protocerebrum. After forming proximal (dendritic) branches in the AL, neurites of all neurons of these lineages converge and exit the AL posteriorly as the common antennal lobe tract (ALT; yellow arrows in Fig. 4C1, C5, C9, C17). Axons of BAla1 soon leave this bundle and directly head for the lateral horn (LH) via the medial–lateral ALT (mlALT; Fig. 2A, white arrowhead; Fig. S1). The remaining three SATs (#5, 9, 17) stay together as the medial ALT (mALT) which continues dorso-posteriorly towards the calyx (CA), before bending laterally towards the LH (arrowheads in Figs.2D, H; 3H; Fig. S1). As published previously (Das et al., 2013), the lineage BAlp4 (#9) forms proximal branches that not only reach the AL, but also part of the ventrally adjacent subesophageal ganglion (abbreviated as SAstr in Fig. 2H; possibly a domain with gustatory input), and projects to the superior lateral protocerebrum (SLP), rather than the CA and LH (Figs. 2H; S1). The ventral hemilineage of BAlc (#5v) includes complex projection neurons which are mostly unrelated to the AL. They project ventro-posteriorly, forming the loVI fascicle (Figs. 4A, B; S2; see accompanying paper by Lovick et al., 2013). Proximal branches of the loVI arborize in the antenno-mechanosensory and motor center (AMMC; Fig. 2D). Distally, this tract forms a T-junction, with one branch projecting laterally into the inferior domain of the ventro-lateral cerebrum (VLCi) and the other branch crossing the midline via the great commissure to reach the contralateral inferior ventro-lateral cerebrum (VLCi; Figs. 2D; S2). In addition, a thin branch continues dorso-laterally towards the LH; this constitutes the lateral antennal lobe tract (not resolved in Figs. 2D; S1).

Two additional PD lineages, BAmas1 and BAmas2 (#11, #12; Fig. 3B, C), form a connection between the tritocerebrum and the superior medial protocerebrum (SMP) and mushroom body, respectively. Thus, proximal branches of BAmas1/2 form dense arborizations in the tritocerebrum. The tritocerebrum is also called, in a segment-neutral manner, anterior periesophageal neuropil (PENPa; Kumar et al., 2009b; Pereanu et al., 2010; Fig. 3B, C). The SATs of BAmas1/2 then project dorsally through the median bundle and reach the SMP (MBDL; Fig. 4C11, C12). Short distal terminal branches of BAmas2 end here; BAmas1 bends laterally and forms terminal arbors in the verticle lobe of the mushroom body (VL; Figs. 3B, C; S1).

BAmd1 (#13) and BAmd2 (#14) are complex lineages with commissural tracts. The dorsal HSAT of BAmd1 (#13d) projects medially directly behind the mushroom body medial lobe (ML) and crosses in the fronto-dorsal commissure; terminal branches innervate the medial lobe of both hemispheres, as well as the anterior inferior protocerebrum on the ipsilateral side (IPa; Figs. 3D; 4A, C13; S3). The ventral HSAT of BAmd1 (#13v) projects diagonally through the AL, crosses in the antennal lobe commissure (ALC), and then bifurcates into a dorsal branch directed towards the superior lateral protocerebrum (SLP) and a ventral branch with a large terminal domain in the lateral accessory lobe (LAL), ventro-medial cerebrum (VMC), and subesophageal ganglion (SEG) (Figs. 3D; 4C13; S4). BAmd2 (#14) enters near the midline, in between the antennal lobes of either side. The SAT bifurcates, with one branch crossing in the ALC (Figs. 4C14; S2). The ipsi- and contralateral branches project in a nearly symmetrical fashion postero-laterally, innervating the inferior ventro-lateral cerebrum (VLCi) and posterior lateral protocerebrum (PLP) (Figs. 3E; S2).

Another complex PD lineage, BAmv1 (#15), is marked by the *per-Gal4* driver line and has been documented previously (Spindler and Hartenstein, 2010; Spindler and Hartenstein, 2011). The large proximal SAT of BAmv1 (#15p) forms a major component of the loVM that passes underneath the AL into the ventro-medial cerebrum (VMC) (Fig. 4B, C15). The SAT splits into three

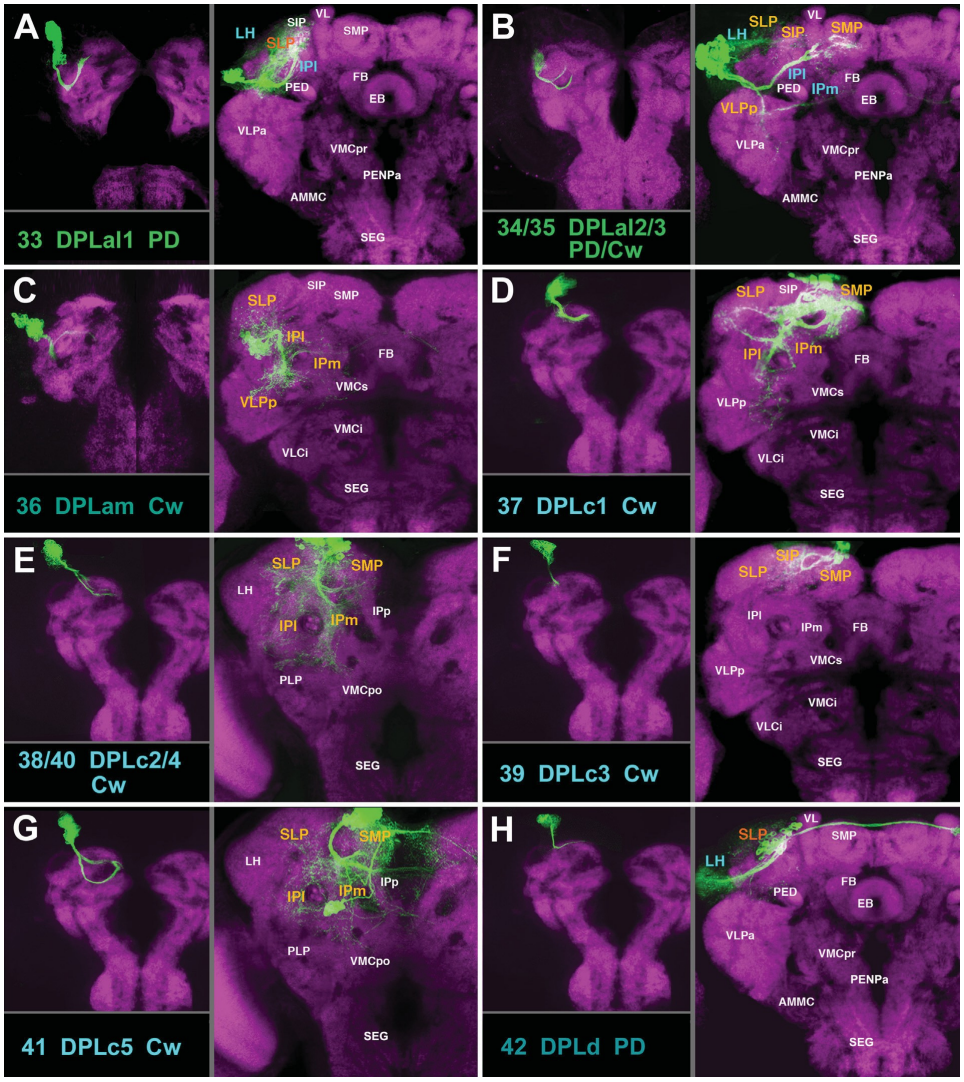

Fig. 8. (A–H) Clones representing lineages #33/DPLal1 to #42/DPLd of the DPL group in the larval and adult brain. For description of how panels are made and displayed, see legend of Fig. 2. For alphabetical list of all abbreviations see Table 1. Bar: 50 μm.

major branches: one curving dorsally and medially towards the central complex; the second continuing posteriorly into the VMC; the third one extending laterally towards the ventro-lateral protocerebrum (VLPa/p) (Fig. S2). Terminal branches innervate the lateral accessory lobe (LAL), the fan-shaped body (FB), the noduli (NO), the VMC, and the VLP (shown in orange letters in Figs. 3F; S2). BAmv2 (#16) has a distally branching (type D) single SAT that accompanies BAmv1 in the loVM fascicle (#15; Fig. 4B, C16). At the level of the great commissure (GC) the tract turns medially and dorsally and splits into an ipsilateral and contralateral component that innervate the VMC surrounding the great commissure (Figs. 3G; S2).

BAlp2 and BAlp3 (#7, #8) are lineages with long C-type SATs that contribute to the lateral component of the ventral longitudinal fascicle (loV; Fig. 4B, C7, C8). The BAlp2 tract splits into a dorsal branch with dense terminal fibers in the lateral part of the LAL compartment and a posterior branch that continues posteriorly (Fig. 2F), innervating the VLCi and PLP (Fig. S2). BAlp3 has a single tract that follows BAlp2 towards the VLCi and PLP (Figs. 2G; S2).

BAla3/4 (#3/4) and BAlv (#10) have C-type SATs, and BAlp1 (#6) has a PD-type SAT that enters from a position lateral of the AL (Fig. 4A, B, C). The first three of these lineages (#3/4, 6) project medially towards the ventro-medial cerebrum: BAlp1 crosses the loVM fascicle at its dorsal surface and BAla3/4 at its ventral surface (Fig. 4A, B, C3/4; C6). BAlp1 has terminal arborizations within the VMC compartment, with ventral branches reaching into the

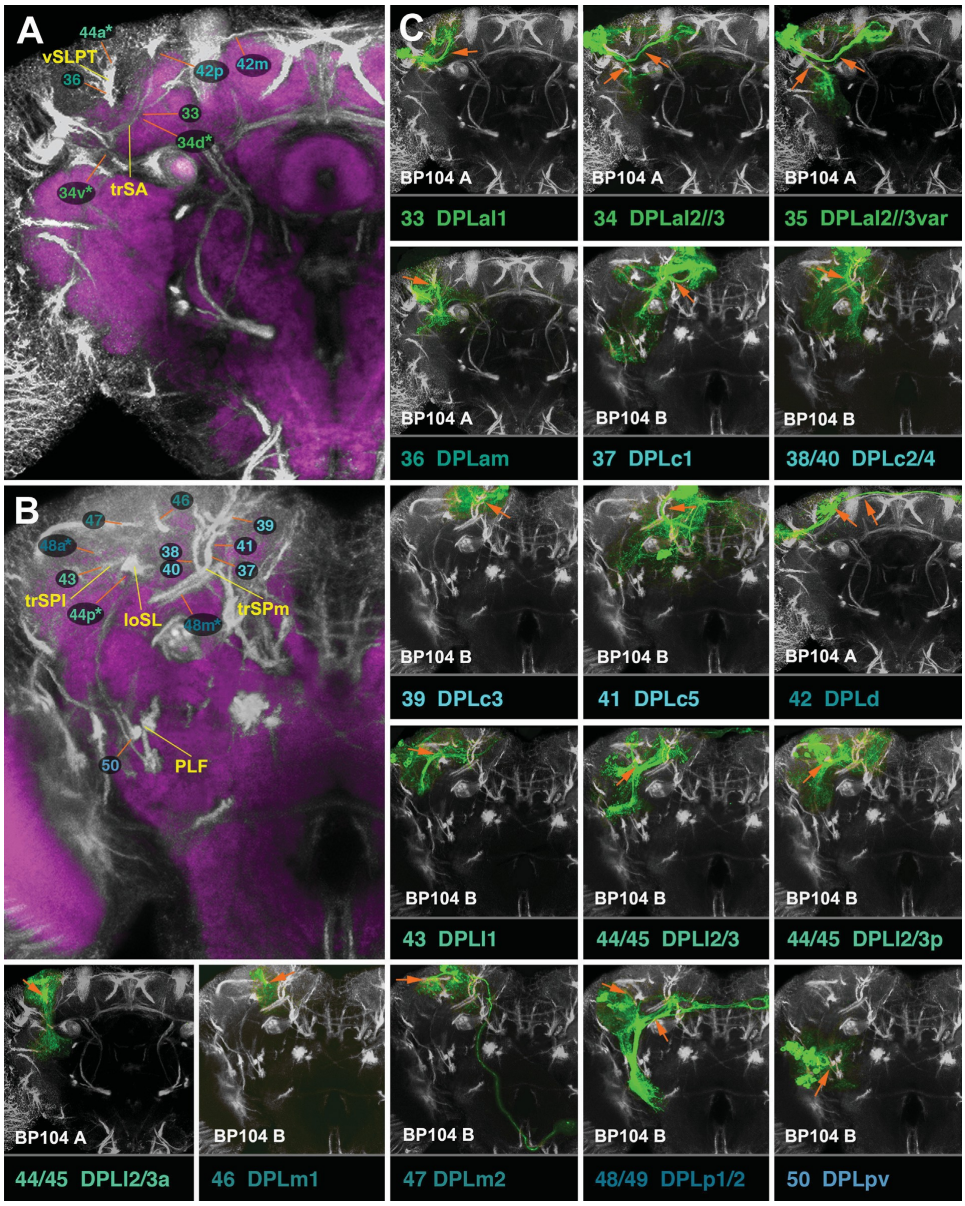

Fig. 9. Clones representing lineages of the DPL groups in the adult brain. (A, B) z-projections show brain slices at an anterior level (ellipsoid body; A) and posterior level (lateral bend of antennal lobe tract). (C) z-projections of clones representing lineages of the DPL group. For description of how panels are made and displayed, see legend of Fig. 4. The lineage pair DPLl2/3 is represented by three panels in C. The first two of these (C44 DPLl2, C45 DPLl3) shows the clone registered to the posterior brain slice, to show association of the posterior HSAT with the obP fascicle (orange arrows; compare to panel B). In the third panel (C 45/DPLl3a), z-projection of the anterior hemilineage of DPLl3 is registered with anterior brain slice, showing entrypoint of anterior HSAT into dorsal SLP (orange arrow). For alphabetical list of all abbreviations see Table 1. Bar: 50 μm.

SEG/PENPa (Figs. 2E; S2). BAla3, marked by the driver ***en-Gal4*** (Kumar et al., 2009b), has widespread terminals in the VMC (Fig. 2C; S2). BAla4 extends alongside BAla3; only a single type of clone was recovered for the BAla3/4 pair. BAlv (#10) contacts the inferior VLC (VLCi) from ventral (Fig. 4B, C10) and has terminal fibers confined to the VLCi and neighboring AMMC (Fig. 3A; Fig. S2).

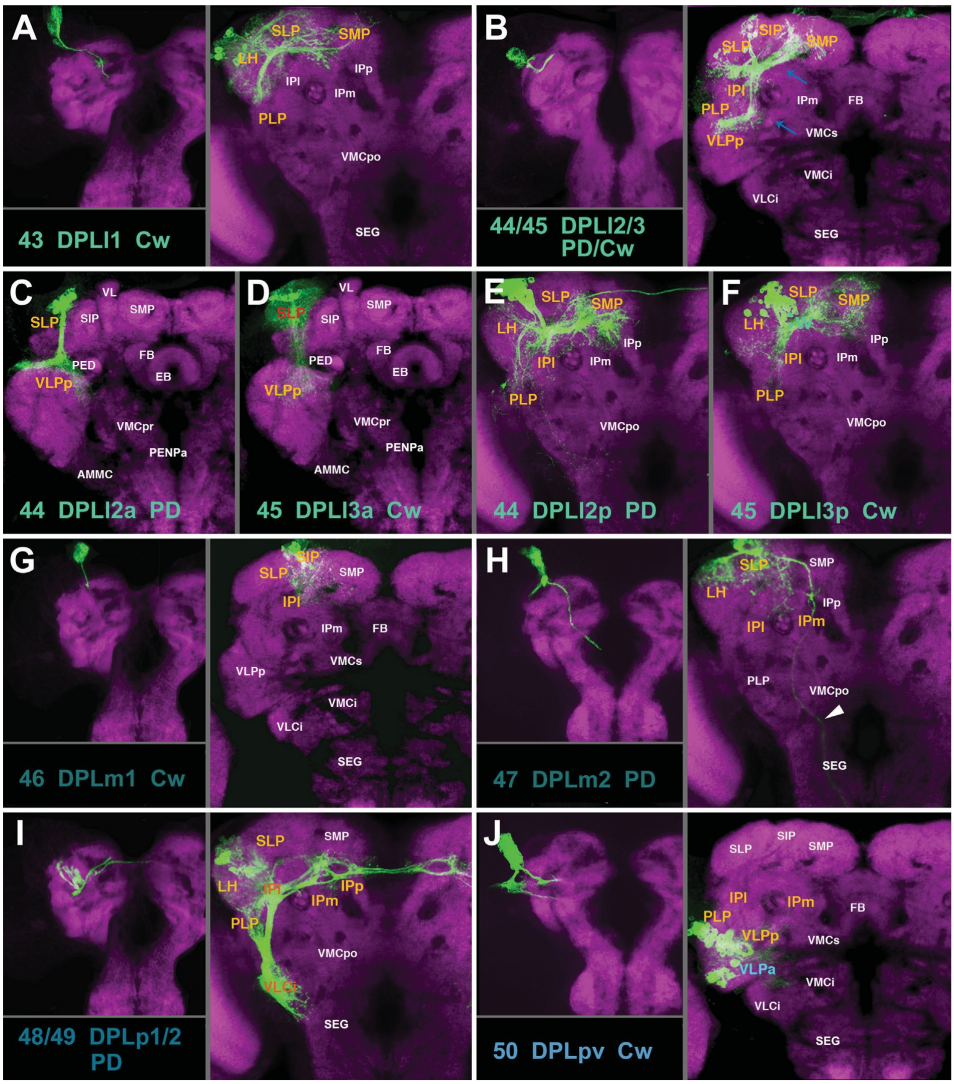

Fig. 10. (A–J) Clones representing lineages #43/DPLl1 to #50/DPLpv of the DPL group in the larval and adult brain. For description of how panels are made and displayed, see legend of Fig. 2. The lineage pair DPLl2/3 is represented by five modified panels. The first of these (B) shows z-projection of entire DPLl2 clone registered to a central slice of the brain (level of fan-shaped body). At the larval stage, only one type of clone, represented at the left of B, exists for the DPLl2/3 pair. Blue arrows point at anterior and posterior HSATs. Panels C and D show z-projections of the anterior hemilineages (#44 DPLl2a and #45/DPLl3a, respectively), registered to an anterior slice. Panels E and F show posterior hemilineages of DPLl2/3, registered to posterior brain slice. White arrows point at an anterior segment of the SAT which, in case of DPLl2, is dense and thin, and in case of DPLl3, wide and diffuse. For alphabetical list of all abbreviations see Table 1. Bar. 50 μm.

DAL lineages

Projections of the DAL lineages are predominantly associated with the medial and vertical lobes of the mushroom body (ML, VL), the central complex, and the adjacent protocerebral compartments (AOTU, SMP, IPa). Most of the DAL lineages, including the DALcl1/2, DALcm1/2, DALd, DALl1, and DALv1-3 are PD lineages with long tracts, many of which are commissural.

DALcl1 and DALcl2 (#18, #19; Figs. 5A, B; 6C18, C19), located laterally of the mushroom body vertical lobe (VL), form a pair of PD lineages associated with the anterior optic tubercle (AOTU), central complex, and adjoining compartments; each one consists of two hemilineages whose diverging HSATs in a "pincer-like" manner enclose the mushroom body spur (SP; Fig. 6A, C18, C19). Dense proximal branches of DALcl1 and DALcl2 innervate the AOTU (Figs. 5A, B; S3). The ventral hemilineage tract of DALcl1 (#18v) passes underneath the SP and continues medially, crossing the midline in the subellipsoid commissure (SuEC; Figs. 5A; S3). Terminal arborizations of this tract end bilaterally in the LAL. In addition, on each side, a posteriorly directed branch of DALcl1v

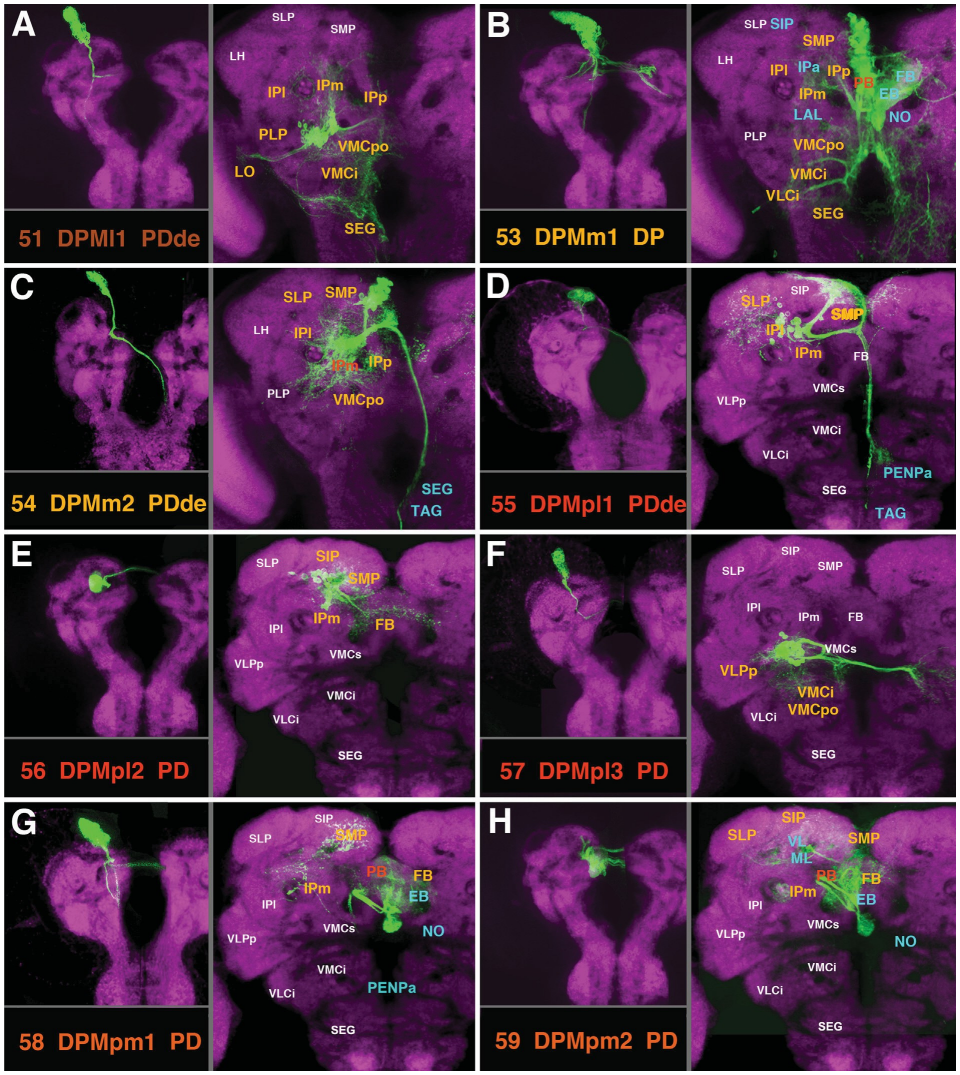

Fig. 11. (A–H) Clones representing lineages of the DPM group in the larval and adult brain. For description of how panels are made and displayed, see legend of Fig. 2. For alphabetical list of all abbreviations see Table 1. Bar: 50 μm.

projects along the MEF fascicle towards the posterior VMC compartment (VMCpo; Figs. 5 and 6A). The ventral DALcl2 hemilineage projects as part of the lateral ellipsoid fascicle (LEa) towards the central complex (Figs. 5B, 6A, C19; S3). Dorsal hemilineage tracts of DALcl1/2 (#18d/19d) curve over the dorsal surface of the spur (SP) and peduncle. DALcl1 projects in a fairly restricted manner to the bulb (BU, a small compartment relaying information towards the ellipsoid body, EB; Figs. 5A; S3); DALcl2 projects in a more widespread manner, including the BU, adjacent LAL, IP, and SMP (Figs. 5B and S3).

DALd (#22) and the DALcm1/2 pair (#20/21) are located medially of the mushroom body vertical lobe (VL; Figs. 5C, D; 6B, C20–22). DALd (#22) constitutes a PD lineage with dense proximal arborizations in the IPa and the superior intermediate protocerebrum (SIP), which surround the medial lobe and vertical lobe, respectively (Figs. 5D and S4). The SAT of DALd (#22) projects ventro-medially, crossing the peduncle, and continues as part of the central protocerebral descending fascicle (deCP; Fig. 6B, C22). Distal arborizations are found in the VMC and SEG (Figs. 5D and S4). The lineage pairs DALcm1/2 each have two PD hemilineages with very similar projection patterns in all recovered clones. This suggests that both lineage pairs possess the same projection envelope. The medial hemilineage tracts pass behind the medial lobe (ML) and enter the fronto-medial commissure (FrMC; Figs. 6C20–21 and S3). In terms of projection, arbors are found

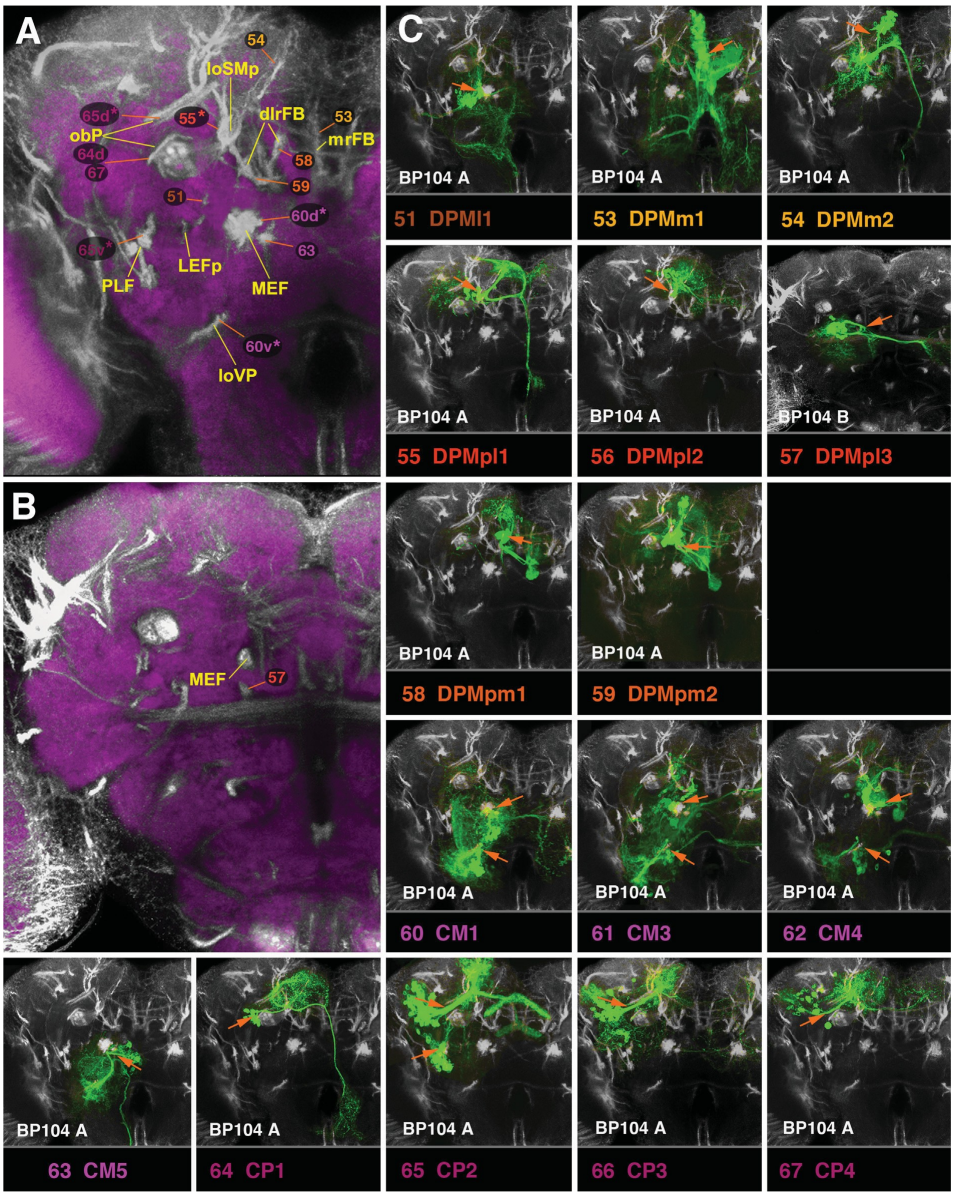

Fig. 12. Clones representing lineages of the DPM group in the adult brain. (A, B) z-projections show brain slices at a posterior level (lateral bend of antennal lobe tract; A) and central level (fan-shaped body, great commissure; B). (C) z-projections of clones representing lineages of the DPM group. For description of how panels are made and displayed, see legend of Fig. 4. For alphabetical list of all abbreviations see Table 1. Bar: 50 μm.

bilaterally in the ML and the surrounding IPa, AOTU, SIP, and SMP compartments (Figs. 5C and S3). The ventral hemilineage tracts of DALcm1/2 pass through the elbow formed by the VL and peduncle before turning ventrally (Figs. 5C and S4). This projection initially forms part of the deCP, but then separates from the fascicle, extending into the ventral brain as a separate, loose bundle. The proximal terminal branches are found throughout the anterior domain of the SMP, IP, and the distal branches in the VMC (Figs. 5C and S4).

Two DAL lineages, DALl1 and DALl2 (#23, #24), are located laterally of the DALcl group, flanking the anterior VLP compartment (VLPa; Figs. 5E, F and 6C23, C24). DALl1 (#23) is a PD lineage with a conspicuous recurrent projection. The SAT projects posteriorly, splits

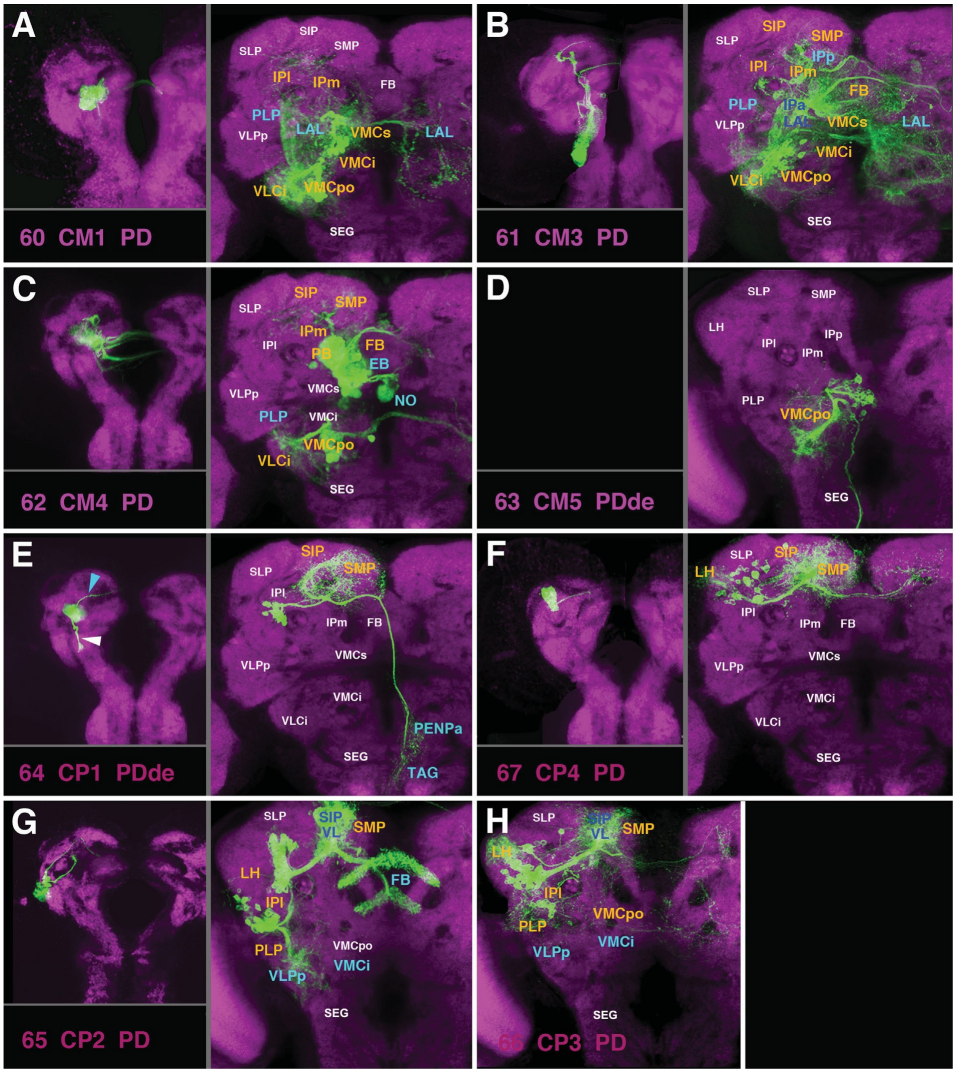

Fig. 13. (A–H) Clones representing lineages of the CM and CP group in the larval and adult brain. No larval clone for CM5 (D) was isolated. For the pair CP2/3 (G, H), only one larval clone (panel G, left) is shown. For description of how panels are made and displayed, see legend of Fig. 2. For alphabetical list of all abbreviations see Table 1. Bar: 50 μm.

into a ventral branch with arborizations in the PLP and adjacent lobula (LO), and a recurrent branch that turns dorsally and anteriorly forming arborizations in the anterior SLP, IP, and AOTU (Figs. 5E, 6B, and S5). DAL12 (#24; Fig. 5F) represents a C lineage. Its short SAT projects into the anterior VLPa where it splits into several groups of terminal arborizations filling much of the anterior and posterior VLP compartment (VLPa/p). A few "outlier" branches continue dorsomedially into the IP and SMP compartments (Fig. 5F).

The DALv group, comprising three PD lineages with commissural connections, is located ventral of the spur (SP). DALv1 (#25) has a long unbranched proximal SAT that forms the anterior component of the lateral equatorial fascicle (LEFa; Figs. 5G; 6B, C25) and then bifurcates into an ipsilateral and commissural branch that crosses in the great commissure. Terminal arborizations fill the ipsilateral and contralateral posterior VLP and neighboring VLCi compartments (Fig. 5G). Ipsilaterally, there is a projection to the posterior SEG (not shown). DALv2 (#26) and DALv3 (#27) are marked by the expression of ***per-Gal4*** and ***en-Gal4***, as described previously (Kumar et al., 2009b; Spindler and Hartenstein, 2010; Spindler and Hartenstein, 2011); proximal SATs form the lateral ellipsoid fascicle (LEa) (Figs. 5H; 6A, C26–27; 7A). The DALv2 (#26) lineage forms large proximal arborizations in the bulb (BU), as well as distal, ring-shaped branches of the ellipsoid body (EB; Figs. 5H; S3), that represent the ring (R)-neurons of the EB (Spindler and Hartenstein, 2011). Additional terminal arborizations of

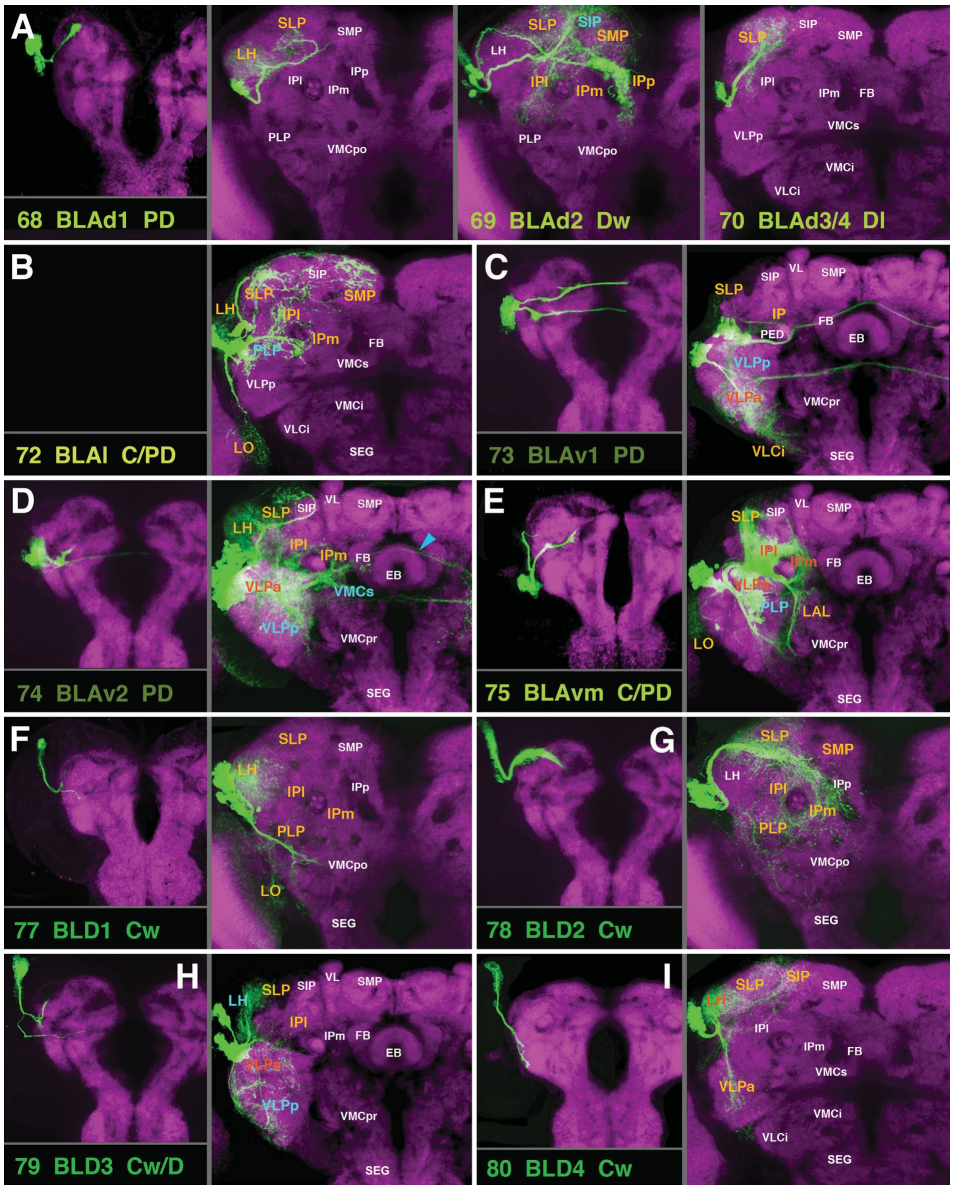

Fig. 14. (A–I) Clones representing lineages of the BLA group and lineages #77/BLD1-#80/BLD4 of the BLD group in the larval and adult brain. No larval clone for BLAl (B) was isolated. For the quartet BLAd1-4 (A) only one larval clone (panel A, left) is shown. For description of how panels are made and displayed, see legend of Fig. 2. For alphabetical list of all abbreviations see Table 1. Bar: 50 μm.

DALv2 are found in the adjacent LAL and IPa (Fig. 5H). DALv3 (#27), marked by the expression of ***en*** (Kumar et al., 2009b), projects alongside DALv2 in the LEa fascicle, which then splits into a dorsal and ventral commissural branch (Figs. 6A, C27; S3). DALv3 terminal arborizations are confined to the ipsilateral and contralateral inferior protocerebrum (IPa/m) and the SMP (Fig. 7A; see Kumar et al., 2009b for detail).

DAM lineages

The small group of DAM lineages is located in the anterior dorso-medial cortex and has arborizations predominantly associated with the SMP/SIP and adjacent IPm/IPa compartments. DAMd1 (#28), a PD lineage with a unique recurrent commissural projection, first crosses the midline in the anterior–dorsal

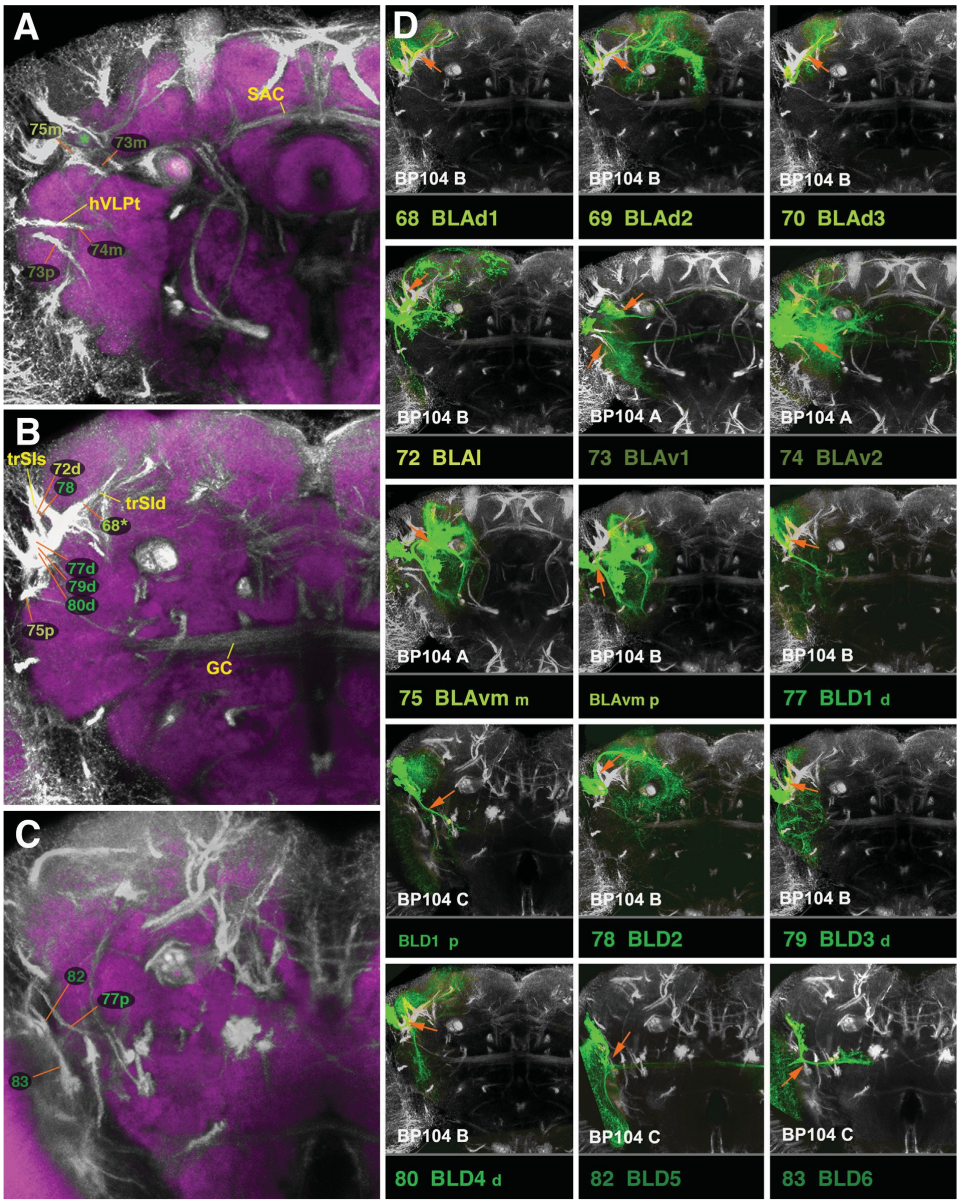

Fig. 15. Clones representing lineages of the BLA and BLD group in the adult brain. (A-C) z-projections show slices of the brain at an anterior level (A; level ellipsoid body), central level (B; fan-shaped body and great commissure) and posterior level (C; lateral bend of antennal lobe tract). (D) z-projections of clones representing lineages of the BLA and BLD group. For description of how panels are made and displayed, see legend of Fig. 4. The lineages BLAvm and BLD1 are represented by two panels each in D. The first of the BLAvm panels (D75 BLAvm m) shows the clone registered to the anterior brain slice, to show projection of the medial HSAT of BLAvm between VLPa and SLP (orange arrow). In the second BLAvm panel (BLAvm p) the posterior HSAT of BLAvm along the surface of the VLPp is indicated (orange arrow). Similarly, separate entry points of the dorsal and posterior HSATs of BLD1 are shown in panels D77 BLD1 d and BLD1 p, respectively. For alphabetical list of all abbreviations see Table 1. Bar: 50 µm.

commissure (ADC; Figs. 6B, C28; 7B). It forms profuse arborizations in the contralateral SMP, SIP, and IPa; and crosses back via the fronto-medial commissure (FrMC) to form distal arbors in the ipsilateral SMP and IPa (Figs. 6B, C28; 7B; S5). The DAMd2/3 pair (#29/30) comprises large C-type lineages (Figs. 6B, 7C). Among the clones recovered for this pair, only a single type of projection envelope could be observed. The DAMd2/3 tract forms the anterior longitudinal superior medial fascicle (loSMa), continuously giving

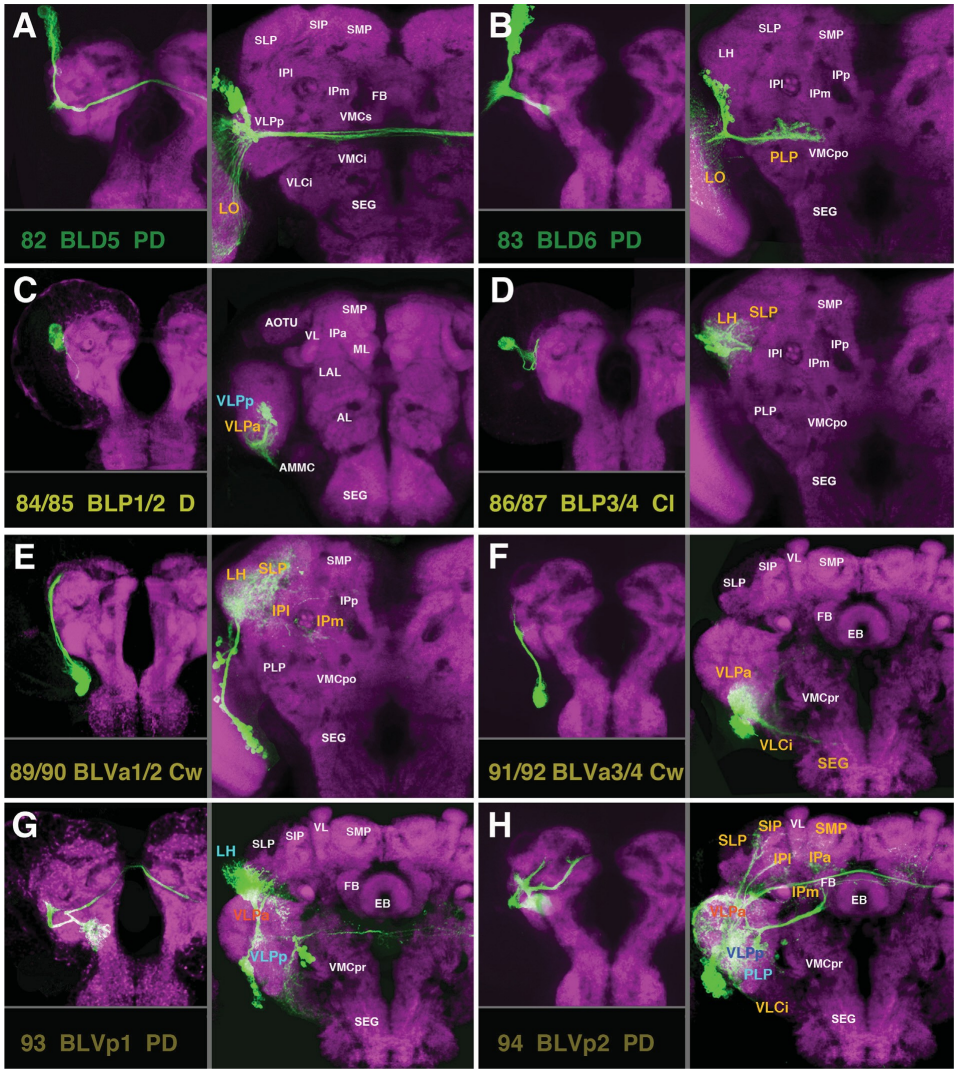

Fig. 16. (A–H) Clones representing lineages #82/BLD5-#83/BLD6 of the BLD group and lineages of the BLP and BLV group in the larval and adult brain. For description of how panels are made and displayed, see legend of Fig. 2. For alphabetical list of all abbreviations see Table 1. Bar: 50 µm.

off terminal arborizations throughout the SIP, SMP, and IPm compartments (Figs. 6B, C29–30; 7C; S5). Posteriorly, projections of DAMd2/3 extend ventrally to fill regions of the ipsilateral and contralateral VMCpo (Figs. 7C; S5). The DAMv1/2 (#31/32) paired lineages also possess an indistinguishable projection envelope. The short SAT enters the SMP from anterior (Fig. 6B, C31–32) and splays out into dense terminal arborizations, filling much of the SMP compartment (Figs. 7D; S5).

DPL lineages

DPL lineages predominantly innervate the lateral domains of the superior and inferior protocerebrum. Five lineages, DPLal1-3, DPLam, and DPLd represent the anterior subgroups, located dorso-laterally of the anterior optic tubercle (AOTU). DPLal1-3 (#33–35) are PD lineages recognizable by their crescent shaped SATs which form the anterior transverse fascicle of the superior protocerebrum (trSA; Figs. 8A, B; 9A, C33–35; S5). Proximal arborizations of DPLal1 (#33) fill the deep regions of the SLP, LH, and the adjacent lateral IP (IPl); distal arbors innervate the dorso-anterior SLP (Figs. 8A; S5). The DPLal2/3 (#34/35) pair has an indistinguishable projection envelope, each with two hemilineages (Figs. 8B; 9C34, C35). The dorsal hemilineage (#34/35d) resembles DPLal1 (#33), forming part of the trSA (Fig. 9A), but arborizing more widely than DPLal1 in the LH, SIP, SLP, SMP, and much of the IP (IPm/l, Fig. 8B). The ventral HSAT forms projections in the medial IP and the

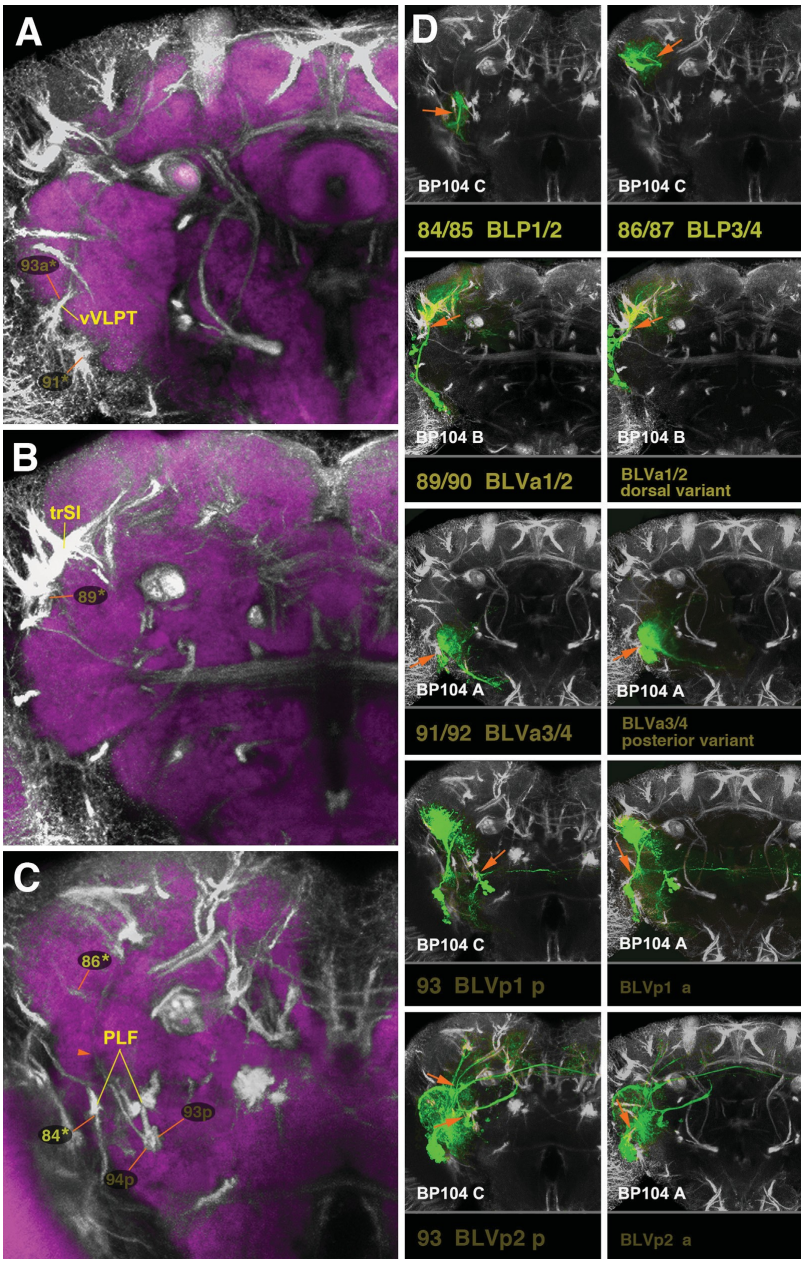

Fig. 17. Clones representing lineages of the BLP and BLV group in the adult brain. (A–C) z-projections show slices of the brain at an anterior level (A; level ellipsoid body), central level (B; fan-shaped body and great commissure) and posterior level (C; lateral bend of antennal lobe tract). (D) z-projections of clones representing lineages of the BLP and BLV group. The lineage pairs BLVa1/2 (#89/90) and BLVa3/4 (#93/94) each are represented by two panels which show differences in location of cell body clusters. Lineages BLVp1 (#93) and BLVp2 (#94) are shown in two panels each. The left panels (D93 BLVp1 p; D94 BLVp2 p) shows the clone registered to the posterior brain slice, to show projection of the posterior HSAT of BLVp1/2 along the PLF fascicle (orange arrows). In the right panels (BLVp1 a, BLVp2 a) the anterior HSATs of these lineages, penetrating the VLPa, are shown (orange arrow). For alphabetical list of all abbreviations see Table 1. Bar: 50 μm.

adjacent posterior VLP (VLPp) (Figs. 8B; S5). We recovered one clone where the two HSATs extended at a moderate distance from each other (Fig. 8C); this could represent a random variant, or indicate that DPLal2/DPLal3 do differ in regard to their exact HSAT pathfinding. DPLam (#36) is a C-type lineage marked by the expression of ***engrailed*** and has been described previously (Kumar et al., 2009b). Projecting its single SAT ventro-posteriorly via the vertical tract of the superior lateral protocerebrum (vSLPT; Figs. 8C, 9A, C36), DPLam arborizes widely in the anterior SLP and the central part of the IPl/m and the VLPp (Figs. 8C; S4). DPLd (#42) forms sparse proximal arborizations in the SIP and part of the adjacent SLP (Figs. 8H, 9C42). The lineage has two HSATs, a medial one crossing the midline in the anterior–dorsal commissure (ADC) and projecting to the contralateral SIP (#42 m; Figs. 8H and 9A), and a posterior one that extends posteriorly along the anterior part of the loSL fiber system, forming terminal arborizations in the LH and lateral SLP (#42p; Figs. 8H; 9C42; S5).

The remainder of the DPL group, including DPLc1-5, DPLl1-3, DPLm1-2, DPLp1-2, and DPLpv are located in the posterior brain cortex. DPLc1-5 (#37–41; Fig. 8D, G) enter through a common portal located at the junction between the SLP and SMP compartments (Fig. 9B; C37–41) and have arborizations focused on the superior and inferior protocerebrum. DPLc1 (#37) is a C lineage with a characteristic crescent-shaped tract that forms part of the medial trSP fiber system (trSPm, Figs. 8D; 9B, C37). Arborizations fill much of the SLP/SMP and the posterior part of the IPl/m (Figs. 8D; S5). DPLc2/4 (#38, #40) is a C-type lineage pair that also forms part of the trSP fascicle (Fig. 9B, C38–40). Unlike DPLc1, DPLc2/4 do not curve dorso-medially into the more anterior and dorsal part of the SMP; rather the pair remains close to the IPl/m, filling the compartment with widespread terminal arborizations and additional branches in the deep SLP/SMP compartments (Figs. 8E; S5). DPLc3 (#39), another C-type lineage, has a short, anteriorly-directed SAT and arborizes in the central parts of the SLP, SIP, and SMP (Figs. 8F; S5). DPLc5 (#41) possesses two hemilineages (#41a/p) which, in the adult are spaced relatively far apart from one another. The anterior hemilineage produces a curved SAT that enters alongside DPLc1-4 (Fig. 9B, C41), extending antero-medially into the anterior SMP and part of the SLP; its dense terminal arborizations fill this compartment and the adjacent domains of the IP (Figs. 8G; S5). The posterior DPLc5 hemilineage (#41p) is located at the ventro-posterior brain surface; the HSAT projects antero-dorsally, joining the loSM fascicle and crossing the midline in the ADC commissure (Fig. 9C41). Terminal arborizations overlap with those of the anterior hemilineage in the SMP and IPm (Fig. 8G).

DPLl1 (#43) and DPLl2/3p (#44/45p) enter the postero-lateral neuropil surface at the junction between the SLP and LH (Fig. 9C43–45). The DPLl2/3p pair projects anteriorly, forming the loSL fascicle (Fig. 9B). From the loSL fascicle, terminal branches sprout off and innervate the superior brain compartments (LH, SIP, SLP, and SMP) and ventrally directed branches also reach into the PLP, VLPp, and IPl (Figs. 10B, E, F; S4, S5). While the DPLl2/3p hemilineages innervate identical compartments, they have distinct fasciculation patterns. Only one of the hemilineages, DPLl2p (#44p), forms a tight tract; fibers of the other hemilineage (DPLl3p, #45p) are more loosely aggregated (Fig. 10E, F). This same characteristic holds true for the anterior hemilineages (#44/45a). As described in detail in the accompanying paper (Lovick et al., 2013), the anterior hemilineage tracts of DPLl2/3 (#44/45a) shift forward during metamorphosis and enter the anterior surface of the SLP (Fig. 9A, C44, C45); they project ventrally into the upper part of the VLPp compartment (Figs. 10C,D; S4). In contrast to DPLl2a (#44a), which forms a thin, compact tract with dense endings in a narrowly defined subdomain of VLPp (Fig. 10C), DPLl3a (#45a) axons form a loose tract and extend diffuse terminal arborizations along their entire trajectory from the SLP to the VLPp (Fig. 10D). DPLl1 (#43) enters the brain at the same point as DPLl2/3 (Fig. 9B, C43), but sends its tract medially via the trSP fascicle, arborizing in the posterior SLP/SMP; a lateral branch innervates the LH/PLP (Figs. 10A; S4, S5).

DPLm1 and DPLm2 (#46, #47; Fig. 10G, H) are located lateral of the DPLc cluster, dorsal of the mushroom body calyx. DPLm1 (#46) is a C-type lineage and projects anteriorly in the SLP (Fig. 9B, C46), producing branches in the SLP as well as the adjoining IPl/ SIP compartments (Figs. 10G; S5). DPLm2 (#47) also innervates the SLP and adjacent IP; in addition, it sends a short SAT laterally (Fig. 9B, C47) to form a terminal arbor in the lateral horn (LH; Figs. 10H; S5). A long, thin fiber bundle of DPLm2 leaves the brain and projects to the ring gland (Fig. 10H, arrowhead).

For the pair DPLp1/2 (#48/49), we were only able to isolate a single clonal type (Fig. 10I). The paired tract enters the postero-lateral neuropil surface at the base of the lateral horn (LH). A long, medial branch extends in the oblique posterior (obP) fascicle, across the peduncle and the brain midline, forming terminal arborizations along its trajectory in the posterior IP/SLP of both hemispheres (Figs. 9C48, C49; 10I; S4). The anteriorly-directed HSAT of DPLp1/2 penetrates into the LH and forms profuse terminal branches in this compartment (Figs. 9B; 11I; S4). A massive projection of DPLp1/2 is directed ventrally (#48v) along the vertical posterior tract (vP) into the PLP and posterior VLCi compartments (Figs. 10I; S4). The posterior-most of the DPL lineages, DPLpv (#50) enters the posterior neuropil surface ventro-laterally; its SAT follows the posterior lateral fascicle anteriorly (PLF; Fig. 9B, C50). Terminal branches appear along the entire length of the SAT and innervate the PLP/VLPp compartments and the adjacent IPl/m (Figs. 10J; S2).

DPM lineages

Located in the postero-medial brain, DPM lineages are primarily connected with the compartments of the central complex and the medial protocerebrum (SMP, SIP, IP). Three of the DPM lineages (DPMm1, DPMpm1, and DPMpm2) are type II lineages which have been recently described (Bayraktar et al., 2010; Bello et al., 2008; Boone and Doe; 2008; Ito and Awasaki, 2008; Izergina et al., 2009), where they were termed DM1 (DPMm1), DM2 (DPMpm1), and DM3 (DPMpm2), respectively. Expression of two genes, ***distalless*** (Izergina et al., 2009) and ***earmuff*** (Bayraktar et al., 2010), mark the type II lineages. Along with another type II lineage, CM4 (#62, see below; called DM4 in Bello et al., 2008), DPMm1, DPMpm1, and DPMpm2 (#53, #58, #59) include sub-lineages whose SATs characteristically enter through the dorso-lateral and medial roots of the fan-shaped body (dlrFB, mrFB; Fig. 12A, C53, C58, C59). They form the columnar neurons of the central complex, connecting specific small domains of the protocerebral bridge (PB) in a topographical manner with segments and sectors of the FB and EB, respectively (Ito and Awasaki, 2008; Yang et al., 2013; Figs. 11B, G, H; S3). In addition, these type II lineages have other sub-lineages with widespread terminal arborizations outside the central complex. The most prominent arborizations of DPMm1 (#53) are found in the (1) medial IP and deep layers of the adjacent SMP/SLP (via SSAT #53a following the loSM), (2) posterior VMC of both hemispheres (via SSAT #53d), (3) in the LAL, IPa, VLCi, VMCi, SEG (via the anterior and descending SSATs #53c; Figs. 11B; 12A, C53; S4; S5). DPMpm1, via its long forward-directed SSAT #58a, has terminal arborizations in the anterior SMP, IPm, and PENPa (tritocerebrum; Figs. 11G and S4). DPMpm2 (#59) arborizes more widely in the superior protocerebrum (SLP, SIP, SMP) and mushroom body lobes via its loSM-associated SSAT, #59a (Figs. 11H; S5).

Lineages DPMpl1 and 2 (#55, #56) enter the posterior neuropil as the most lateral component of the posterior loSM fascicle. The tract extends into the superior protocerebrum, with branches all along its length (SMP, SIP, SLP; Figs. 11D, E; 12A, C55, C56; S4; S5). DPMpl1 is one of the lineages with a long descending fiber bundle, which leaves the loSM, crosses in the chiasm of themedian bundle (MBDLchi), follows the median bundle ventrally, and forms terminal arborizations in the PENPa (tritocerebrum), SEG, and the thoracico-abdominal ganglion (TAG; Figs. 11D; 12A, C55; S4). The SAT formed by DPMpl2 (#56) has no descending projections, but, after leaving the loSM, it continues medially into the FB where it forms wide-field arborizations (Figs. 11E; S3). DPMpl3 (#57), whose cell bodies are initially located close to those of DPMpl1/2 (hence inclusion of this lineage in the same subgroup), but shift ventrally during metamorphosis, project along the MEF fascicle (Fig. 12B, C57) and innervate specific ventral compartments, including the VMCpo, VLPp, and VLCi. This lineage also has a strong commissural component, reaching, via the great commissure, the contralateral VLCi and VLPp (Figs. 11F; S2).

Two DPM lineages, DPMl1 (#51) and DPMm2 (#54), innervate the posterior brain compartments and send a descending tract towards the SEG and TAG (Figs. 11A, C; 12C51, C54; S4). DPMl1 (#51) arborizes more ventrally than DPMm2 (#54), including in the IP (IPl; IPm/p), VMCi, VMCpo, and SEG (Fig. 11A; S4). DPMm2 also branches in the posterior realm of the IP (IPl; IPm/p), as well as the adjoining SMP, SLP, and VMCpo (Figs. 11C; S4). DPMl1 also has a laterally-directed branch which reaches the lobula (LO).

CM lineages

Three of the four CM lineages (CM1, #60; CM3, #61; CM4, #62; labeled DM5, DM6, and DM4, respectively, in Izergina et al., 2009) are large type II lineages with multiple sub-lineages. Each of the three has one major ventral SSAT (the three ventral SSATs of CM1-4), forming the loVP fascicle (Lovick et al., 2013; #60v* in Fig. 12A), and arborize in the postero-ventral brain, including the VCMpo, VMCs, PLP, and VLCi compartments (Figs. 13A–C; S2). The ventral SSATs of CM3/4 have a commissural component crossing in the pPLPC commissure and reaching the postero-ventral compartments of the contralateral hemisphere (Figs. 13B, C; S2). The intermediate and dorsal SSATs of the lineages CM1-4 (#60d* in Fig. 12A) connect the postero-ventral brain to more anterior and dorsal regions of the neuropil. CM1 and CM3 each have one SSAT (#60d and 61d2) that travels with the MEF fascicle and arborizes posteriorly (VMCpo), as well as more anteriorly (VMCs, IPl/m, LAL; Figs. 12A; 13A, B; S2). CM1 (#60) has a conspicuous commissural component that interconnects the LAL compartments of either side (Figs. 13A; S2). CM3 (#61d1) also arborizes throughout the entire FB Figs. 13B; S3). As described in the previous section, CM4 (#62) is one of the four lineages (besides DPMm1, DPMpm1, and DPMpm2) which produces columnar neurons of the central complex: the CM4 SSAT (#62d) forming these arborizations is uncrossed and innervates the most lateral part of the PB and FB (Figs. 13C; S3). CM3 and CM4 have one other major SSAT (#61/62a) that projects dorsally along the loSM and interconnects dorsal protocerebral compartments along their antero-posterior axis (SIP/SMP; Figs. 13B, C; S5).

CM5 (#63), the most medial member of the CM group, has an SAT that enters the posterior neuropil medially of the MEF fascicle (Fig. 12A, C63). CM5 is the third lineage (besides DPMl1 and DPMm2) which has a long SAT descending posteriorly towards the thoracico-abdominal ganglion (TAG); its proximal arbors are focused on the VMCpo compartment (Figs. 13D; S4).

CP lineages

The four CP lineages (CP1-4) are located laterally adjacent to the CM group and form mostly projection neurons associated with the superior and inferior protocerebrum. The CP2/3 pair (#65/66) each produces a dorsal and ventral HSAT ($HSAT_d$, $HSAT_v$) that have a characteristic spatial relationship to the mushroom body peduncle (PED; Fig. 12A, C65, C66). Even though the two lineages innervate similar neuropil compartments, each shows distinctive differences. The lineage defined as CP2, with its dorsal HSAT (#65d), forms arborizations in the LH, SIP, and SMP and also projects to the mushroom body vertical lobe (VL) and fan-shaped body (FB) where it forms wide-field arborizations (Figs. 13G; S3; S5). The dorsal component of CP3 (#66d) has denser innervations in the LH, but misses the projection to the FB (Fig. 13H). The ventral HSATs of CP2/3 (#65/66v) project along the PLF fascicle that converges upon the peduncle from ventrally (Fig. 12A, C65, C66). They form terminal arbors along their axons in the ventrolateral and inferior protocerebrum (PLP, VLPp, IPm/l; Figs. 13G, H; S2).

CP1 and CP4 (#64, #67) have similar SATs to the $HSAT_d$s of CP2/3, crossing over the peduncle along the obP fascicle. Characteristically, the tracts of CP1 and 4 are closer to the peduncle than those of CP2/3 (compare Fig. 12C64/C67 to C65/C66). Both CP1 and CP4 have dense terminal arborizations in the LH, SIP, and SMP compartments (Fig. 13E, F). CP1 (#64), in the late larval brain, has a dorsal (blue arrowhead in Fig. 13E) and ventral hemilineage (white arrowhead in Fig. 13E): the $HSAT_v$ projects along the posterior LEF fascicle (LEFp). In the adult, the tract of the dorsal hemilineage (#64) can be followed along the loSM towards the MBDLchi, where it joins DPMm2 and DPMpl1 to descend towards the SEG/TAG (Figs. 12C64; S4). We identified a total of four clones in different brains for CP1. However, none of them had a ventral hemilineage component, even though a BP104-positive LEFp bundle could be clearly distinguished in the adult (Fig. 12A; see accompanying paper by Lovick et al., 2013). One possible explanation is that the ventral CP1 hemilineage undergoes apoptosis during metamorphosis. CP4 has only a dorsal component, both in the larva and adult (Figs. 13F; S5).

BLA lineages

BLA lineages are located at the antero-lateral neuropil surface. A subgroup of five dorsal BLAs, BLAd1-4 (#68–71) and BLA1 (#72), forms SATs that converge on one neuropil fascicle, the trSI (Figs. 14A, B; 15B, D68–72; S5), which primarily interconnects domains of the superior protocerebrum. For the four BLAds defined in the larva, three types of clones with different projection envelopes were recovered (Fig. 14A); these were assigned arbitrarily to the lineages BLAd1 (#68), BLAd2 (#69), and BLAd3/4 (#70/71). BLAd1 arborizes in the LH and SLP (Fig. 14A); BLAd2 is focused more on the SMP and SIP, but has an additional branch that follows the superficial trSI (trSIs), and innervates the posterior SLP, IPp, and IPm/l (Figs. 14A; S5); BLAd3/4 has restricted arborizations in the medial SLP (Figs. 14A; S5). The BLA1 lineage (#72) has two separate hemilineages. The dorsal hemilineage (#72d) projects along the trSIs (Figs. 14 and 15B; D72) and arborizes in the posterior regions of the LH, SLP, and SMP compartments (Figs. 14B; S5). The medial hemilineage tract (#72 m) follows the surface of the VLP, close to the anterior optic tract (green asterisk in Fig. 15A), and arborizes in the IPl/m and PLP, respectively (Figs. 14B; S2).

The three ventral BLA lineages, BLAv1 (#73), BLVa2 (#74), and BLAvm (#75), have two hemilineages each and interconnect ventrolateral compartments of both hemispheres, also forming projections to the superior protocerebrum (Fig. 14C, E). The medialhemilineage of BLAv1 (#73 m) projects over the anterior surface of

the VLPa compartment, following the anterior optic tract (Fig. 15A, D73); the tract then extends underneath the peduncle and crosses the midline in the superior arch commissure (SAC). Branches innervate (ipsi- and contralaterally) the VLPa/p and the anterior SLP/IP compartments (Figs. 14C; S1). The medial hemilineage of BLAv2 (#74 m) projects medially through the VLPa compartment along the hVLPT tract (Fig. 15A, D74). Although the $HSAT_m$ of the BLAv2 lineage arborizes in a similar ipsilateral territory as BLAv1m (IPl/m, Fig. 14D), the hemilineage lacks a strong commissural component across the SAC, but forms a bundle which crosses posteriorly of the central complex towards the contralateral IP (Fig. 14D, blue arrowhead). The posterior hemilineages of BLAv1/2 (#73/74p) are directed through the ventro-lateral protocerebrum (Fig. 15A) and across the great commissure, arborizing bilaterally in the VLPa/p (Figs. 14C, D; 15D73, C74; S2). The posterior hemilineage of BLAv2 (#74p) has a strong dorsally-directed branch towards the LH and SLP compartments (Figs. 14D; S1). The $HSAT_m$ of BLAvm (#75 m) is located at the antero-dorsal surface of the VLP, where it projects dorsally, passing the anterior optic tract (green asterisk in Fig. 15A, D75). The $HSAT_m$ of BLAvm has widespread terminal arborizations in the dorsal VLPa and dorso-posterior adjacent compartments: the SLP, IPl/m, and PLP (Figs. 14E; S1). The posterior hemilineage of BLAvm (#75p) is located at the lateral surface of the ventro-lateral protocerebrum. Its tract, similar to that of BLAl, follows the trajectory of the anterior optic tract (Fig. 15B, D75). Anteriorly, it sends arborizations into the LAL compartment (Fig. 14E); posteriorly, it innervates the PLP (Figs. 14E; S2).

BLD lineages

Six BLD lineages were defined in the larva. The anterior four of these, BLD1-4 (#77–80), lie posteriorly adjacent to the dorsal BLAs and, like those, mostly innervate the superior protocerebrum, with tracts forming the superficial component of the trSI (Figs. 14F–I; 15B, D77–80; S5). The terminal arborizations of BLD1 (#77) are fairly restricted to the LH (Figs. 14F; S5); BLD3 (#79) and BLD4 (#80) also innervate the LH, but have more widespread arborizations in adjacent areas of the superior protocerebrum (SLP, SMP, SIP; Figs. 14H, I; S5). Ventrally-directed branches of BLD3/4 arborize in the VLP compartment (Figs. 14H, I; S4). BLD2 (#78) follows the trSIs towards the posterior neuropil surface (Fig. 15B), arborizing in the posterior SLP/SMP, the IPp, IPl/m, and PLP (Figs. 14G; S5). BLD1 and BLD3 each has an additional hemilineage. In the case of BLD1, these neurons (#77p) are located further posteriorly and project into the PLP (Fig. 15C, D77). Terminal arborizations are to be found in the PLP, IP, and the lobula (Figs. 14F; S4). In the case of BLD3, one finds an anterior hemilineage (#79a) with projections to the ventral tip of the VLPa compartment (Fig. 14H).

Two additional BLD lineages, BLD5 and BLD6 (#82 and 83), are located at the postero-lateral neuropil surface and form connections with the lobula (LO) (Fig. 16A–B). BLD5, marked by the expression of the gene ***atonal*** (Hassan et al., 2000; Spindler and Hartenstein, 2010; Spindler and Hartenstein, 2011), has a characteristic straight commissural tract interconnecting the ipsi- and contralateral lobula (Figs. 15C, D82; 16A). BLD6 is located further ventro-posteriorly (Fig. 15C, D83); it has widespread arborizations in the LO, but innervates a restricted "focus" located in the posterior VLPp (Fig. 16B).

BLP lineages

BLP lineages form two pairs in the postero-lateral brain. BLP1/2 (#84/85) are located ventrally, projecting along the PLF fascicle that innervates ventral domains of the VLP compartments (Figs. 16C; 17C, D84, D85; S2). With the exception of a single clone (Fig. S7), all other clones assigned to the BLP1/2 pair have the same, fairly restricted projection envelope (Fig. 16C). The clone belonging to the exception (Fig. S7) possesses much more widespread arborizations in the PLP and posterior domains of the IP. This clone suggests that BLP1 and 2 possess different envelopes. BLP3/4 (#86/87) lineages are located dorsally; the pair sends a short dorso-anteriorly directed tract dorso-anteriorly, innervating the LH and the adjacent SLP compartment (Figs. 16D; 17C, D86, D87; S5).

BLV lineages

BLV lineages, similar to the BLA lineage group, innervate the ventro- and dorso-lateral protocerebrum. BLVa3/4 (#91/92) form a pair whose short SAT penetrates into the VLPa from ventrally; the lineage pair forms restricted terminal arborizations in the VLPa and the neighboring VLCi (Figs. 16F; 17A, D91, D92; S2). Even though the projection envelope of all clones recovered for this lineage is similar, it appears as if in some clones, the cell body cluster and SAT entry point are located more posteriorly than most other clones (Fig. 17D92/93, "posterior variant" of BLVa3/4"). BLVa1/2 (#89/90) form another pair with SATs that enter at the ventral side of the trSI fascicle (Fig. 17B) and terminates shortly thereafter (at the junction of the IP/SLP; Figs. 16E; 17D89/90; S5). Terminal arborizations of the BLVa1/2 pair are focused on the LH, SLP, and adjacent IPl/m compartments. Recovered clones for the BLVa1/2 pair had very similar projection envelopes but differed with respect to the location of the cell body clusters. In four out of 13 clones, the cluster was located dorso-anteriorly of the VLPa, at the level of the BLAd lineages ("dorsal variant" of BLVa1/2; Fig. 17D). The BLVa1/2 reporter, ***so-Gal4***, is expressed in the larval lineages (Chang et al., 2003) and remains on in the "dorsal variant" in the adult (VH, unpublished). In the remaining eight BLVa1/2 clones, the cell body clusters are spread out within an elongated volume of the cortex in the cleft between the optic lobe and VLP (Fig. 16E and left panel of Fig. 17D89/90). We speculate that these two variants (one with a dorsal position; the other with a ventral or spread-out dorsal-to-ventral position) represent the two lineages of the BLVa1/2 pair.

BLVp1/2 (#93, 94) each have two hemilineages that migrate apart during metamorphosis. The posterior hemilineages of BLVp1/2 (#93/94p; $HSAT_p$) project along the PLF (Fig. 17C, D93, 94). The BLVp1 $HSAT_p$ innervates the VLPp and VLCi compartments and, via a commissural tract crossing as part of the great commissure, innervates the contralateral VLPp (Figs. 16G; 17D94; S2). The $HSAT_p$ of the BLVp2 lineage has a different trajectory: two branches project dorsally to the superior protocerebrum (SLP, SIP, and SMP) and the anterior IP (IPa and IPl/m; Figs. 16H; S1). The anterior hemilineages of BLVp1/2 (#93a/94a) are located at the ventro-anterior brain surface and laterally adjacent to BLVa3/4 (Fig. 17A, D93, D94). Terminal arborizations branch in the VLP, SLP, and LH (Figs. 16G, H; S1). BLVp2 has a strong commissural component which crosses the SAC and projects to the contralateral VLP (Figs. 16H; S1).

Discussion

Identification of MARCM clones with secondary lineages

We show in this paper that MARCM clones induced in the early larva, labeling post-embryonically derived (e.g. secondary) neurons, can be assigned to specific lineages based on the stereotyped trajectory of their axonal tracts. These tracts are formed in the larva and, as documented in the accompanying paper, remain

visible as coherent, BP104-positive fiber bundles throughout metamorphosis (Lovick et al., 2013). Fifty-six lineages form tracts with unique properties; all but one of these 56 lineages (e.g. DALv3, marked by *en-Gal4*; Kumar et al., 2009b) has been represented in our collection of MARCM clones. All other lineages were represented at least twice, with many of them occurring at high frequencies ($n \geq 25$). We currently have no explanation for the existence of such "hot" and "cold" spots of clone induction. Given that the lineages begin to proliferate at slightly different time points at the first-to-second larval instar transition (Ito and Hotta, 1992; J.K.L and V.H., unpublished), we speculate that the exact timing of the heat pulse may play an important role for the large variations in the frequencies of clone generation.

Thirty lineages are paired (tracts of two adjacent clusters form one composite bundle) and eight form two "quartets" (four tracts coalesce into a single thick bundle). One of the "quartets" represents lineages of the mushroom body (MB), while the others are the four BLAd lineages (BLAd1-BLAd4). Based on the individually-labeled lineage MARCM clones, it is clear that within these composite bundles, axons of the different lineages do not intermingle. In brains labeled only with global markers (e.g. BP104), one cannot separate individual SATs within the pairs and quartets, and cannot predict how many clones with different projection envelopes to expect. All members of a pair/quartet could either form clones with identical projection envelopes or they could form two/four anatomically distinct clones. In nine cases, each member of the pair has a unique arborization pattern. For example, BAmas1/2, both of which project along the median bundle, appear to have distinct fields of arborization: proximal branches of BAmas1 project in the ventral PENPa (tritocerebrum) and the SEG, projecting towards the VL/SMP; while BAmas2 form proximal arborizations dorsally in the PENPa and distally and bilaterally in the SMP. Importantly, although these projection envelopes are clearly different, they include adjacent brain territories. This generally holds true for most lineages: lineages with neurons (and, at an earlier stage, neuroblasts) located close to each other also typically innervate adjacent neuropil territories (see schematic representations of projection envelopes in Figs. S1–S5). Another case in point is the quartet BLAd1-4, for which we could identify three different types of clones whose projection envelopes were all confined to the superior protocerebrum where they targeted contiguous territories (BLAd1: lateral horn; BLAd2: lateral SLP, SIP, SMP; BLAd3: medial SLP).

The fact that in case of the BLAd lineages we identified three, and not four, types of clones could mean that "the fourth" BLAd lineage has a projection envelope that is indistinguishable from one of the other three BLAd members; alternatively, we might have missed the clone, since that particular lineage (like DALv3 mentioned above) represents a cold spot of inducibility. The same reasoning applies to six pairs of lineages (see Table 2) for which also a single clone type was noted. It is unlikely that for all of these pairs one of the members was missed, given their good overall representation (e.g., 10 clones for the BAla3/4 pair, 11 for DALcm1/2, 14 for DAMd2/3, and 13 for DAMv1/2). In these cases, we favor the interpretation that a lineage might have been 'duplicated" to increase the overall number of neurons sharing the same projection envelope.

Lineage-based analysis of brain macrocircuitry

With respect to the overall shape of their projection envelopes, lineages fall into several classes. A more in depth discussion of these different classes will have to await the detailed analysis of projection envelopes relative to each other, and relative to the boundaries of neuropil compartments. To this end, clones are being registered to one "model brain," in which their spatial relationships can be established. We anticipate that this work (D.C.C.W. and V.H., unpublished) promises to yield further insight regarding the validity of compartment boundaries (Do projection envelopes of multiple lineages respect the boundaries defined on the basis of synapse density? Do projection envelopes reveal additional subdivisions of compartments?), as well as regarding brain macrocircuitry (How strongly are compartments connected on the basis of sharing in a certain number of projection envelopes?).

Some of these questions have been already addressed in two recent papers where, employing a MARCM-based approach, Ito et al., (2013) and Yu et al., (2013) have published a comprehensive atlas of secondary lineages for the adult *Drosophila* brain. They chose a terminology in which the term for a lineage was based upon one of the neuropil compartments heavily innervated by that lineage. Both studies concur with our conclusion that the pattern of projection and arborization of secondary lineages is highly invariant. Based on their characteristic SAT projection and projection envelope, most lineages depicted in Ito et al., (2013) and Yu et al., (2013) can be identified with the secondary lineages described here, even on the basis of *z*-projections alone. Note for example the close correspondence between the projection envelopes shown for the well documented type II DPM, CM, and CP lineages (DPMm1–DM1; DPMpm1–DM2; DPMpm2–DM3; CM4–DM4; CM3–DM6; CM1–DM5; CP2–DL1; CP3–DL2), but also other newly described lineages with long, characteristic SAT trajectories (e.g., BAmas1 – FLAa2; BAmas2 – FLAa3; BAmd2 – WEDd2; DALcl1 – AOTUv3; DALv1 – VLPa2; BLAv1 – VLPl&d1). However, given that clones described in Ito et al. (2013) and Yu et al., (2013) are presented in the absence of labeled fascicles, the unambiguous matching of their nomenclature with ours should await the careful comparison of confocal stacks. Nonetheless, three aspects concerning the overall coverage of lineages applying different driver lines to visualize clones deserve mentioning.

First, "cold spots," i.e., lineages, known to exist on the basis of independent data, which are not represented by MARCM clones are apparent in all three studies. Interestingly, DALv3 (independently documented by its expression of *engrailed*-Gal4; Kumar et al., 2009) seems to be a "universal cold spot," since it is not represented in our study, neither in that of Ito et al., (2013) or Yu et al., (2013). Other cold spots may depend on the driver line used; for example, the characteristic lineage of local antennal lobe interneurons, BAla2 (Das et al., 2013) is represented by multiple clones in our study, as well as in Yu et al., (2013), where it is called ALv2, but not in Ito et al., (2013). Similarly, BAmas1 (FLAa2) and BAmv2 (VESa2) are represented by clones in Yu et al., (2013), but not Ito et al., (2013).

Secondly, the mapping of lineages in our study is restricted to clones that could be clearly assigned to the BP104-positive fiber bundles corresponding to lineage associated axon tracts traceable from the larva into the adult. Following this approach, we could assign a type of clone to each lineage originally defined in the larva based on possessing a neuroblast and a unique SAT; the only exceptions were the DALv3 "cold spot," and the uncertainty concerning the six paired lineages for which we recovered only clone (see above). The study by Ito et al., (2013) lists a sizeable number of clones (e.g., the majority of their VPN clones), located in the lateral brain and including projections between optic lobe and central brain, that are most likely derived from neuroblasts that originate from the inner optic anlage. These lineages were not included in our larval catalog of central brain lineages (Pereanu and Hartenstein, 2006; Cardona et al., 2010), and are not considered in this paper, even though we also recovered frequent examples of VPN-type clones. The developmental definition of a boundary between central brain and optic lobe, in particular lobula, is complex, and will require further work.

Finally, the participation of secondary lineages in the production of glia also needs further clarifications. All classes of glia increase in number during the larval period, and part of this increase is due to the proliferation of dedicated glial progenitors (or glial cells themselves, which continue to divide), whereas another part results from the generation of glial cells from within secondary (neural) lineages (Pereanu et al., 2005). More recent studies have shown that several of the type II lineages are responsible for the generation of much of the ensheathing glia of the central complex (Viktorin et al., 2011), as well as some of the optic lobe associated glia (Viktorin et al., 2013). The use of *elav*-Gal4 as a driver precluded us from visualizing glial progeny among the clones described in this study. However, Yu et al., (2013), utilizing flip-out techniques (*actin5CP-FRT-stop-FRT-GAL4 and actin5CP-loxP-stop-loxP-lexA::p65*) and twin spot MARCM (*nSyb-GAL4*), describe a small number of lineages that included glia among their progeny. One of these, DM5 (CM1 in our nomenclature), produced both ensheathing glia and astrocyte like glia; another one, DL1 (CP2 in our nomenclature) generated a population of optic lobe-associated ensheathing glia that most likely corresponded to the set of glia described in Viktorin et al., (2013). However, none of the large number of central complex-associated ensheathing glia, derived from the type II DM lineages according to Viktorin et al., (2011) were labeled in Yu et al., (2013) or Ito et al., (2013). Aside from the possibility that this is due to a property of the driver line used, one may explain this discrepancy by the timing of clone induction. Thus, if the very first sublineages generated by the DM neuroblasts are dedicated glial progenitors, one might miss their progeny if clonal induction occurs at a slightly later time point.

A lineage-based approach to study mechanisms controlling Drosophila brain development

In previous studies, a number of secondary lineages marked by Gal4-reporters had been identified in the larval brain and linked to their adult counterparts. The best characterized lineages are the four lineages of the mushroom body (Ito et al., 1997; Ito and Awasaki, 2008; Lee et al., 1999; Zhu et al., 2003) and the five which form the projection and local interneurons of the antennal lobe (Das et al., 2013; Das et al., 2008; Komiyama et al., 2003; Lai et al., 2008; Yu et al., 2010). Additional lineages have been characterized based on the restricted expression pattern of transgenic reporters and protein markers (e.g., *en-Gal4*; *ato-Gal4*; *per-Gal4; empty spiracles*, *ems;* Hassan et al., 2000; Kumar et al., 2009b; Lichtneckert et al., 2008; Spindler and Hartenstein, 2010; Spindler and Hartenstein 2011; Srahna et al., 2006). The identification of projection envelopes of adult MARCM clones for all central brain lineages presented in this paper will aid in the identification of additional lineage-specific markers from among the numerous existing collections of *Gal4* enhancer-trap lines (Hayashi et al., 2002; Jenett et al., 2012; Pfeiffer et al., 2008).

Taking advantage of the fact that lineages form structural units whose individual neurons share a common trajectory and terminal arborization, a selected number of genes (encoding for members of developmentally-relevant molecular pathways or important cell-cell interactions, such as adhesion molecules) have been analyzed using a lineage-based approach. This type of approach was pioneered in a series of studies that revolve around the MB lineages. In these studies, the roles of many crucial players important for proliferation, cytoskeletal dynamics, and cell-to-cell adhesion were dissected through conditional loss- and gain-of-function experiments, using MB-specific drivers under Gal4/UAS control (Billuart et al., 2001; Lee et al., 2000a,b; Ng et al., 2002; Reuter et al., 2003; Scott et al., 2001). Additional lineage-specific (e.g. non-MB) Gal4 drivers have been identified and similar approaches (like the MB studies) have been taken to identify critical players for secondary lineage morphogenesis (through conditional knock-outs and gain-of-function, as described above; Bello et al., 2003; Kuert et al., 2012; Marin et al., 2012; Maurange et al., 2008; Spindler and Hartenstein, 2011; Zheng et al., 2006).

More recently, it has been demonstrated that neurons/lineages, which may express a common set of molecular factors, react very differently to the loss of these factors. This has been made possible by the identification and characterization of lineage-specific Gal4 lines and highlights the importance of utilizing a multi-lineage approach when studying neural development. One example is the role of the Par-complex proteins, Bazooka (Baz)/Par-3/Par-6, in determining the shape of secondary neurons (Spindler and Hartenstein, 2011). Outside the nervous system, the Par complex plays an essential role for epithelial cell polarity and migration (Cong et al., 2010; Ellenbroek et al., 2012; Hurd et al., 2003; Ohno, 2001; Wang et al., 2006; Wang et al., 2012). In some vertebrate neurons, Par appears to be required for the differentiation of nascent neuronal processes into axons and dendrites (Chen et al., 2006; Nishimura et al., 2004; Shi et al., 2004). In the *Drosophila* post-embryonic brain, Baz is expressed by neuronal progenitors and postmitotic neurons. A Gal4-inducible Baz::GFP fusion reporter (under the control of UAS enhancer sequences; Sánchez-Soriano et al., 2005) driven by *per-Gal4* (marking BAla1, BAmv1, DAlv2) and *ato-Gal4* (marking BLD5) revealed that the Baz protein accumulates at positions along the SATs where terminal branches will appear (Spindler and Hartenstein, 2011). For example, in the PD-type lineages BAla1 (using *per-Gal4*) and BLD5 (using *ato-Gal4*), Baz::GFP is both concentrated at the cortex—neuropil boundary and the distal ending of the SAT. Loss of function of Baz by MARCM results in ectopic terminal branches, either along the SAT (DALv2 and BAmv1) or at its distal tip (BLD5). In the case of BAla1, loss of *baz* results in aberrant pathway choices, forming additional SATs into the iALT (Spindler and Hartenstein, 2011). Interestingly, loss-of-function of another member of the Par family, *par6*, phenocopies *baz* loss-of-function clones in case of the DALv2 and BLD5 lineage, but not BAla1 and BAmv1, further supporting the notion that the requirement of different Par-complex members varies from one lineage to the next. A previous study, demonstrating that the Par complex is not required for the development of mushroom body lineages (Rolls and Doe, 2004), also supports this idea. Although the mushroom body lineages have been traditionally used as "test lineages" to understand gene function, it is clear that such an approach may not be sufficient. Since gene function (in the case of *baz* and *par6*) may be lineage-dependent, a "multi-lineage approach" is more favorable and will provide a clearer picture of gene function in developing neurons.

Dissecting lineages: hemilineages, sub-lineages, neurons

Many type I lineages consist of two hemilineages (Truman et al., 2010). To generate hemilineages, a neuroblast divides asymmetrically to produce an intermediate cell (ganglion mother cell, GMC). The GMC divides symmetrically to produce two post-mitotic sibling neurons. Typically, cell fate determinants (e.g. Numb, a repressor of Notch signaling) are asymmetrically segregated into the two neurons, such that one cell acquires an 'A' fate (inherits Numb and represses active Notch signaling) and the other acquires a 'B' fate (does not inherit Numb and has active Notch signaling; Lin et al., 2012; Truman et al., 2010). In some cases, one hemilineage is fated to undergo programmed cell death (Kumar et al., 2009a; Truman et al., 2010); in others, both hemilineages survive, but are morphologically and most likely, functionally unique. It was suggested that in cases where both hemilineages survive, two separate bundles or HSATs, emerge

Table 1
List of abbreviations of neuropil fascicles (left), compartments (center), and entry portals of lineage-associated tracts (right).

Fascicles	Abbr.	Compartments	Abbr.	Entry portals	Abbr.
Anterior–dorsal commissure	ADC	Antennal lobe	AL	Anterior entry portal of the ML	ptML a
Antennal lobe commissure	ALC	Antenno-mechanosensory and motor center	AMMC	Anterior portal of the lateral horn	ptLH a
Antennal lobe tract	ALT	Anterior optic tubercle	AOTU	Anterior superior lateral protocerebrum portal	ptSLP a
Inner antennal lobe tract	iALT	Anterior periesophageal neuropil	PENPa	Antero-dorsal entry portal of the VLP	ptVLP ad
Medial antennal lobe tract	mALT	Bulb	BU	Dorrso-lateral superior ventro-lateral protocerebrum portal	ptVLP dls
Outer antennal lobe tract	oALT	Ellipsoid body	EB	Dorsal antennal lobe portal	ptAL d
Anterior optic tract	AOT	Fan-shaped body	FB	Dorsal spur portal	ptSP d
Anterior superior transverse fascicle	trSA	Inferior protocerebrum	IP	Dorso-lateral entry portal of the ML	ptML dl
Central protocerebral descending fascicle	deCP	Anterior IP	IPa	Dorso-lateral inferior ventro-lateral protocerebrum portal	ptVLP dli
Cervical Connective	CCT	Lateral IP	IPl	Dorso-lateral portal of protocerebral bridge	ptPB dl
Commisure of the lateral accessory lobe	LALC	Medial IP	IPm	Dorso-lateral vertical lobe portal	ptVL dl
Dorsal commissure of anterior subesophageal ganglion	DCSA	Posterior IP	IPp	Dorso-medial entry portal of the ML	ptML dm
Dorsolateral root of the fan-shaped body	dlrFB	Lateral accessory lobe	LAL	Dorso-medial portal of protocerebral bridge	ptPB dm
Fronto-medial commissure	FrMC	Lateral horn	LH	Dorso-medial ventro-lateral protocerebrum portal	ptVLP dm
Great commissure	GC	Mushroom body	MB	Dorso-medial vertical lobe portal	ptVL dm
Horizontal ventrolateral protocerebral tract	hVLPT	Calyx	CA	Lateral antennal lobe portal	ptAL l
Intermediate superior transverse fascicle	trSI	Medial lobe	ML	Lateral portal of calyx	ptCA l
Deep bundle of irSI	trSI d	Peduncle	PED/P	Lateral portal of the posterior lateral protocerebrum	ptPLP l
Superficial component of trSI	trSI s	Spur	SP	Lateral portal of the superior lateral protocerebrum	ptSLP l
Lateral ellipsoid fascicle	LE	Vertical lobe	VL	Medial portal of calyx	ptCA m
Anterior LE	LEa	Noduli	NO	Posterior inferior portal of the posterior lateral protocerebrum	ptPLP pi
Posterior LE	LEp	Posterior lateral protocerebrum	PLP	Posterior portal of superior lateral protocerebrum	ptSLP p
Lateral equatorial fascicle	LEF	Protocerebral bridge	PB	Posterior portal of the lateral horn	ptLH p
Anterior LEF	LEFa	Subesophageal ganglion	SEG	Posterior superior portal of the posterior lateral protocerebrum	ptPLP ps
Posterior LEF	LEFp	Superior protocerebrum	SP	Posterior ventro-medial cerebrum portal	ptVMCpo
Medial equatorial fascicle	MEF	Superior intermediate protocerebrum	SIP	Postero-lateral portal of superior lateral protocerebrum	ptSLP pl
Medial root of the fan-shaped body	mrFB	Superior lateral protocerebrum	SLP	Postero-medial portal of superior lateral protocerebrum	ptSLP pm
Median bundle	MBDL	Anterior SLP	SLPa	Ventral antennal lobe portal	ptAL v
Oblique posterior fascicle	obP	Posterior SLP	SLPp	Ventral entry portal of the VLCi	ptVLCi v
Posterior commissure of the posterior lateral protocerebrum	pPLPC	Superior medial protocerebrum	SMP	Ventral portal of calyx	ptCA v
Posterior lateral fascicle	PLF	Ventro-lateral cerebrum	VLC	Ventral portal of protocerebral bridge	ptPB v
External component of PLF	PLFe	Anterior VLC	VLCa	Ventral spur portal	ptSP v
Dorsolateral component of PLF	PLFdl	Inferior VLC	VLCi	Ventro-lateral antennal lobe portal	ptAL vl
Dorsomedial component of PLF	PLFdm	Lateral VLC	VLCl	Ventro-lateral inferior ventro-lateral protocerebrum portal	ptVLP vli
Ventral component of PLF	PLFv	Ventro-medial cerebrum	VMC	Ventro-lateral portal ofcalyx	ptCA vl
Posterior superior transverse fascicle	trSP	Anterior VMC	VMCa	Ventro-lateral superior ventro-lateral protocerebrum portal	ptVLP vls
Lateral trSP	trSPl	Inferior VMC	VMCi	Ventro-lateral vertical lobe portal	ptVL vl
Medial trSP	trSPm	Post-commissural VMC	VMCpo	Ventro-medial antennal lobe portal	ptAL vm
Sub-ellipsoid commissure	SuEC	Pre-commissural VMC	VMCpr	Ventro-medial ventro-lateral protocerebrum portal	ptVLP vm
Subesophageal-protocerebral system	SPS	Superior VMC	VMCs	Ventro-medial vertical lobe portal	ptVL vm
Superior arch commissure	SAC	Ventro-lateral protocerebrum	VLP		
Superior commissure of the posterior lateral protocerebrum	sPLPC	Anterior VLP	VLPa		
Superior lateral longitudinal fascicle	loSL	Posterior VLP	VLPp		
Anterior loSL	loSLa				
Posterior loSL	loSLp				
Superior medial longitudinal fascicle	loSM				
Anterior loSM	loSMa				
Posterior loSM	loSMp				

Table 1 (*continued*)

Fascicles	Abbr.	Compartments	Abbr.	Entry portals	Abbr.
Supra-ellipsoid body commissure	SEC				
Ventral fibrous center	VFC				
Ventral longitudinal fascicle	loV				
Intermediate loV	loVIa				
Lateral loV	loVLa				
Medial loV	loVMa				
Posterior–lateral loV	loVP				
Vertical posterior fascicle	vP				
Vertical tract of the superior lateral protocerebrum	vSLPT				
Vertical tract of the ventro-lateral protocerebrum	vVLPT				

from the cell body cluster. Upon entering the neuropil, the two HSATs diverge and target different neuropil compartments. In this work and the accompanying paper (Lovick et al., 2013), we have identified 20 lineages possessing these properties (see Table 2). In the majority of cases, both the hemilineage cell body clusters and the neuropil entry points of their HSATs move apart to some extent during metamorphosis. This morphogenetic shift is extreme for several lineages (e.g. DPL12/3, DPLc5, BLAl, BLAv1, BLAvm, BLVp1/2). For eight of these lineages, although there is a single cell body cluster and SAT; the tract splits into two components with different trajectories (Table 2). In these cases, it remains unclear whether the existence of more than one tract suggests that there are two separate hemilineages; an in-depth analysis of individual neurons forming parts of these lineages may help answer this question.

Lineages and hemilineages are comprised of sequentially-born neurons, which may all share in the common projection envelope; however, they can be grouped into sub-classes which differ among each other in regards to their detailed phenotype (e.g. projection patterns). This has been investigated for the four lineages of the MB and for some of the lineages associated with the AL (Jefferis et al., 2001, 2004; Kunz et al., 2012; Lai et al., 2008; Lee et al., 1999; Yu et al., 2009, 2010; Zhu et al., 2003). The MB lineages undergo four sequential phases of proliferation, producing sub-lineageswith different properties (Lee et al., 1999; Zhu et al., 2003; Kunz et al., 2012). In the early embryo, MB neuroblasts give rise to a small set of non-intrinsic neurons (as opposed to the intrinsic neurons or Kenyon cells) that do not contribute to the neuropil of the mushroom body (Kunz et al., 2012). From mid-embryonic stages onward, the MB lineages switch to a mode that generates γ-neurons, followed by α′/β′ neurons (most of third instar larva), pioneer α/β neurons (at the start of metamorphosis), and α/β neurons (during mid-to-late phases of metamorphosis). Within these sub-lineages, neurons might form even smaller groupings, defined by the specific territory inside the calyx or MB lobes they innervate. For example, α/β neurons born at different times in the pupa appear to send terminal arbors to different domains of the calyx (Zhu et al., 2003).

The correlation between birth order and neuronal projection has been elucidated in great detail for the adNB/BAmv3 lineage. The projection envelope of this lineage includes the antennal lobe, calyx, and lateral horn (Lai et al., 2008). The antennal lobe is formed by over 50 specific glomeruli, each glomerulus characterized by the endings of olfactory neurons sharing a common olfactory receptor (Jefferis et al., 2001; Vosshall et al., 1999). Single-cell clonal analysis of the adNB/BAmv3 lineage (Yu et al., 2010) indicated that dendritic branches of neurons born at a certain time point always innervated a single, invariant glomerulus. In other words, dendrites innervate the antennal lobe in a largely non-overlapping, "tiled" manner. The same applies to axonal terminals which form an "odor map" in the calyx (Jefferis et al., 2001; Jefferis et al., 2004).

The projection envelopes shown for the central brain lineages will help to manage the large number of individual neurons that emerge in past and future studies of fly brain development and brain function. The shape of a large fraction of adult central brain neurons, imaged as single-cell clones, has recently become available (Chiang et al., 2011). Many of these neurons are readily identifiable as members of specific secondary lineages. A few examples are shown in Fig. S6. Panels A1–A5 show individual neurons that project along the median bundle, shared by lineages BAmas1 and BAmas2, and fall within the projection of BAmas2 (panel A; proximal arborization in dorsal PENPa compartment, distal arbors bilaterally in antero-dorsal SMP). Aside from this shared envelope, neurons shown in A1–A5 clearly differ in regard to the details of their distal arborization. For example, A1 has

Table 2
List of secondary lineages of the ***Drosophila*** brain.

A: Lineage name	B: Lineage SAT number	C: Number clones	D: Lineage type	E: Fascicle joined by lineage	F: Main ipsilateral compartments innervated by lineage	G: Commissure joined by lineage	H: Main contralateral compartments reached by lineage
BAla1	1	16	PD	mlALT	AL – LH		
BAla2	2	9	Cl	0	AL		
BAla3	3	10	Cw	0	VMC VLP SEG		
BAla4	4						
Balc	5 d	12	PD	mALT	AL-CA LH		
	5 v		PDco	loVI	AMMC – VLCi	GC	VLCi
BAlp1	6	9	PD	0	VMCpro SAsbtri Ipm		
BAlp2	7	6	Cw	loVL	LAL VLCi PLP		
BAlp3	8	9	Cw	loVL	LAL VLCi PLP IP l		
BAlp4	9	7	PD	mALT	AL SAsbtri – LHa SLPp SIP		
Balv	10	7	Cl	0	VLCi AMMCp		
BAmas1	11	7	PD	MBDL	PENPa SAsbtri-VL SMP SIP		
BAmas2	12	4	PD	MBDL	PENPad – SMPa		
BAmd1	13 d	12	PDco	0	SMP IP a ML	FrMC	ML
	13 v		PD	0	ML? IPa? –	ALC	VMCpr SAsbtri
BAmd2	14	9	Dl	0	0-VLCi PLP	ALC	VLCi PLP
BAmv1	15 d	16	PD	loVM LEp	LAL IPa SMPa – FB		
	15 p		Dw?	loVM	0?-VMCpo PLP		
	15 dn		Dw?		0?-VLPp		
BAmv2	16	12	Dw	loVM	0-VMCpo PENPa/p SAsbtri		
BAmv3	17	24	PD	mALT	AL – CA LH		
DALcl1	18 d	14	PD	0	AOTU SLP SIP – BU IP		
	18 v		PDco	0	0 – LAL	SuEC	LAL
	18 vn			MEF	LAL – VMCpo bilat		
DALcl2	19 d	9	PDco	0	AOTU SIP SMP – LAL	SuEC	SMP SIP LAL
	19 v		Dw	LEa	0 – FB SMP		
	19 dn		Cw	0	AOTU SIP SMP		
DALcm1	20/21 m		PDco	0	IPa LAL SIP SMP VL ML	FrMC	VL ML
DALcm2	20/21 v		PDde	deCP	AOTU SIP IP – VMC		
DALd	22	8	PDde	deCP	IPa AOTU LAL SIP SMP - VMC		
DALl1	23r	12	Dw	trSId	LH IP AOTU		
	23v			0	PLP Lo		
DALl2	24	7	Cw	0	VLPap PLP SMP IP		
DALv1	25	8	PDco	LEFa	VLP VLCi AMMC SEG	GC	VLP
DALv2	26	27	PD	LE a	BU IPa LAL – EB		
DALv3	27 d		PDco	LE a	SMP IPa/m/l	SEC	SMP IPa
	27 v		PDco	LE a	LAL IP	SuEC	LAL IP
DAMd1	28	2	PDco	ADC	SMP – SIP SMP IPa	FrMC	IPa SMP
DAMd2	29	14	Cw	loSMa	SMP SIP IPm VMCpo		
DAMd3	30						
DAMv1	31	13	Cw	0	SMP SIP		
DAMv2	32						
DPLal1	33	15	PD	trSA	SLPp LH IPl – SLPa		
DPLal2	34/35 d	16	PD	trSA	SLP LH IP – SIP SMP IP		
DPLal3	34/35 v		Cw	0	SLP IPm/l VLPp		
DPLam	36	12	Cw	vSLPT	SLP VLPp IPm/l		
DPLc1	37	10	Cw	trSPm	SLP IPm/l SMP		
DPLc2	38	9	Cw	trSPm	SLP LH IPm/l SMP		
DPLc4	40						
DPLc3	39	3	Cw	0	SLP SIP SMP		
DPLc5	41 a	14	Cw	trSPm	IPm/l SLP SMP		
	41 p		PDco	0	IP p/m SMP	ADC	SMP
DPLd	42 m	3	PDco	0	LH? SLP	ADC	SLP
	42 p		PD	trSId	SLP – LH		

Table 2 (*continued*)

A: Lineage name	B: Lineage SAT number	C: Number clones	D: Lineage type	E: Fascicle joined by lineage	F: Main ipsilateral compartments innervated by lineage	G: Commissure joined by lineage	H: Main contralateral compartments reached by lineage
DPLl1	43	2	Cw	trSPl	PLP SLP LH SMP		
DPLl2	44 p	21	PD	loSL	LH PLP IPl SLP (–) SIP SMP		
	44 a		PD	vSLP	SLP VLPp		
DPLl3	45 p	8	Cw	loSL	LH IP l SLP SIP SMP		
	45 a		Cw	vSLP	SLP? VLPp		
DPLm1	46	5	Cw	0	SLP SIP IP 1		
DPLm2	47	2	PD	0	IP m/l SLP (–) LH ncc		
DPLp1	48/49 m	23	PDco	obP	SLP LH – SMP	sPLPC	IPp/m/l PLP VLCi
DPLp2	48/49 v		Cw	(veP)	LH SLP IP l PLP VLCi		
	48/49 a		PD	0	LH (–) SLP		
DPLpv	50	7	Cw	PLF	PLP IPm/l VLPa/p		
DPMl1	51	4	PDde	DPPT	VMCpo/s PLP IP Lob-SEG		
DPMm1	53 a	20	Cw	loSMp	IPp IP m/l SMP SIP		
	53 b		PD	mrFB	PB – FB EB NO co		
	53 c		PD?de	mrFB	PB? – SEG VMCi PENPp VLCi IPa LAL		
	53 d		PDco	0	VMCpo	0	VMCpo
DPMm2	54	6	PDde	0	IP SLP SMP VMCpo VLPa (–) SMP	MBDLchi	SEG TAG
DPMpl1	55	4	PD co/de	loSMp	IP SLP SMPp – SMPa	MBDLchi	PENPa TAG
DPMpl2	56	3	PD	loSMp	SMP SIP IPp/m – FB		
DPMpl3	57	5	PDco	MEF	VMCpo (–) VLCi VLPp	GC	VMCpo VMCi VLPp
DPMpm1	58 a	24	PD?	mACT MBDL	PB? – SMP IP m PENPa		
	58 b		PD	dlrFB	PB – FB EB NO co		
DPMpm2	59 a	21	PDco	loSMp	SMP IPm SIP SLP VL ML	SAC	SMP SIP
	59 b		PD	dlrFB	PB – FB EB NO		
CM1	60 d	15	PD	MEF	VMCpo – IPm/l VMCs LAL	SuEC	LAL VMCi
	60 v		Cw	loVP	PLP VMCpo VMCi VLCi		
CM3	61 a	8	PDco	loSMp	SIP SMP IPm	SEC	SMP
	61 d1		PD?	MEF	VMCpo? IP? – FB		
	61 d2		PD?	MEF	VMCpo? IP? – LAL IPa		
	61 v		PDlco	loVP	PLP VMCpo – VLCi IPm/l/p	pPLPC	PLP
CM4	62 a	23	Cw	loSMp	SMP SIP		
	62 d		PD	MEF	PB – FB EB NO		
	62 v		PDco	loVP	PLP VMCpo VLCi	pPLPC	PLP
CM5	63	9	PDde	0	VMCpo – SEG TAG		
CP1	64 d	4	PDco/de	obP loSMp	SIP SMPp – SMPa	MBDL chi	PENPa TAG
	64 v		N				
CP2	65 d	13	PD	obP loSM OE	LH SIP SMP VL – FB		
	65 v		PD	PLF	PLP IPl – VLP VMC		
CP3	66 d	4	PDco	obP loSMp	LH PLP – SIP SMP VL	SEC	SMP SIP VL
	66 v		PD	PLF	PLP IPl – VMC VLP		
CP4	67	4	PDco	obP loSM	LH SLP – SIP VL SMP	SEC	SMP
BLAd1	68	15	PD	trSId	LH (–) SLP		
BLAd2	69 d	5	Dw	trSId	SIP SMP SLP IP		
	69 s		Dw	trSIs	SLP IP		
BLAd3	70	3	Dl	trSId	SLP		
BLAd4	71	0	N				
BLAl	72 d	6	Cw	trSIe	LH SLP SMP		
	72 m		PD	0	PLP – IP		
BLAv1	73 m	17	PDco	0	VLPa/p – SLP IPm/l	SAC	IPm/l VLPa
	73 p		PDco	0	VLPa/p	GC	VLPa/p
	73 pn		PD	0	VLPad (–) VLPav VLCi		
BLAv2	74 m	10	PD	0	VLPap SLPa IP m/l VMCs	pCCXc	IPm/l
	74 p		PDco	0	VLPp IPm/l	GC	IP VLP
	74 pn		Cl	0	LH		
BLAvm	75 m	3	Cw	0	VLPa SLP PLP IPm		

	75 p		PD	0	PLP – LAL PLP		
BLD1	77 d	5	Cw	trSIe	LH SLP		
	77 p		Cw	0	PLP IPm/l Lob		
BLD2	78	12	Cw	trSIe	SLP PLP SMP IPm/l		
BLD3	79 d	9	Cw	trSIe	SLP LH		
	79 vn		Cw	0	VLPp/a IPl		
	79 a		Dl	0	VLPa/p		
BLD4	80 d	10	Cw	trSIe	LH SLP SIP		
	80 v		Cl	0	VLPp		
BLD5	82	16	PDco	0	Lob	GC	Lob
BLD6	83	5	PD	0	Lob – PLP		
BLP1	84	1	Cw	PLF	PLP VLP IP Lob		
BLP2	85	13	Dl	PLF	VLPa VLPp		
BLP3	86	29	Cl	0	LH SLP		
BLP4	87						
BLVa1	89	4	Cw	0	LH SLP IPm/l		
BLVa2	90	9	Cw	0	LH SLP IPm/l		
BLVa3	91	8	Cw	0	VLPa VLCi SEG		
BLVa4	92	11	Cw	0	VLPa VLCi SEG		
BLVp1	93 p	10	PDco	PLFv	VLPp VLCi	GC	VLPp
	93 a		PDco	vVLPT	VLPa/po LH basal		
BLVp2	94 p	6	PDco	PLF	SIP SMP IPa	SEC	SIP
	94 a		PDco	vVLPT	VLPa SLPa IPm/l	SAC	VLPa

Column A: Lineage names.
Column B: Number identifying lineage-associated tracts (SATs). In lineages with multiple hemilineage tracts or sublineage tracts, these are individually listed (e.g., dorsal hemilineage tract of BAlc is identified as "5d", ventral hemilineage tract as "5v").
Column C: Number of MARCM clones isolated for lineage.
Column D: Main class of lineage based on contour of projection envelope. "PD": lineage with separate proximal and distal arborizations; "C": lineage with terminal arborizations emerging at more or less regular intervals along the entire length of the SAT; "D": lineages where arborizations are concentrated at distal tip of SAT. Lower case "l" ("local") stands for small volume filled by arborization; "w" ("wide") indicates large volume; "co" indicates commissural SAT; "de" signifies descending tract.
Column E: Neuropile fascicle joined by lineage-associated tract. For abbreviations of fascicle names, see Table 1. "0" indicates that tract does not form part of any designated fascicle.
Column F: Ipsilateral neuropile compartments receiving strong innervation by lineage. In cases of PD lineages where proximal and distal terminal arborizations can be distinguished based on labeled clone, a hyphen separates compartments receiving proximal arbors (left of hyphen) from those receiving distal arbors (right of hyphen). For abbreviations, see Table 1.
Column G: Commissure joined by lineage associated tract. For abbreviations, see Table 1.
Column H: Contralateral neuropile compartments receiving strong innervation by lineage. For abbreviations, see Table 1.

widespread, sparse endings bilaterally in the SMP; A2 projects only ipsilaterally; A3 has bilateral terminations which are denser and more restricted than those of A3. It is likely that these different projections, similar to those of adNB/BAmv3 neurons discussed above, are correlated to the birth dates of the corresponding neurons. Panels B1, C1, D1, and E1/E1' show single cell clones of neurons which follow the projection envelopes of lineages BLVa3/4 (B), DAMv1/2 (C), BLD2 (D), and vNB/BAla1(E), respectively.

An interesting case is presented in E2/E2': the neuron shown has proximal arborizations in the antennal lobe and follows the trajectory of the vNB/BAla1 SAT, passing underneath the peduncle towards laterally. However, distal arborizations are not in the lateral horn (as in the case of secondary vNB/BAla1 neurons), but in the ventrolateral protocerebrum. There are three other features that set the neuron shown in E2/E2' apart from secondary vNB/BAla1 neurons: the large cell body, located slightly more dorsally than secondary BAla1 cells, as well as the thick axon (compare E2 with E1). We propose that E2 shows a primary vNB/BAla1 neuron. A recent study (Das et al., 2013) indicated that many primary neurons of this lineage enter the antennal lobe through the same portal later used by the secondary's, form proximal terminal branches in the antennal lobe, and follow (in part) the medial antennal lobe tract. However, most of these primaries do not reach the larval counterpart of the lateral horn, but terminate in other (adjacent) territories (Das et al., 2013). These are all properties of the neuron shown in E2/E2'. We are currently preparing clones of brain lineages that include primary neurons (J.J.O. and V.H., unpublished), which will allow us to visualize the "primary projection envelope" of lineages, and thereby help to identify primary neurons. Ultimately, suitable Gal4 drivers have to be identified for all lineages, to then engage on a single-cell clonal analysis as the one pioneered for adNB/BAmv3.

Acknowledgments

We thank the members of the Hartenstein laboratory for critical discussions during the preparation of this manuscript. We thank S. Fung, F. Wang, J.D. Nguyen, and K. Wang for their involvement in generating larval and adult MARCM clones. We are grateful to the Bloomington Stock Center and the Developmental Studies Hybridoma Bank for fly strains and antibodies. This work was supported by the NIH Grant (R01 NS054814). K.T.N. is supported by the NSF Graduate Research Fellowship Program (No. DGE-0707424). J.J.O. is supported by the Ruth L. Kirschstein National Research Service Award (No. GM007185).

Appendix A. Supporting information

Supplementary data associated with this article can be found in the online version at http://dx.doi.org/10.1016/j.ydbio.2013.07.009.

References

Ashburner, M., 1989. Drosophila. A Laboratory Manual. Cold Spring Harbor Laboratory Press, Cold Spring Harbor, NY, pp. 214–217.
Bausenwein, B., Dittrich, A.P., Fischbach, K.F., 1992. The optic lobe of Drosophila melanogaster. II. Sorting of retinotopic pathways in the medulla. Cell Tissue Res. 267, 17–28.
Bayraktar, O.A., Boone, J.Q., Drummond, M.L., Doe, C.Q., 2010. Drosophila type II neuroblast lineages keep prospero levels low to generate large clones that contribute to the adult brain central complex. Neural Dev. 5, 26.
Bello, B.C., Hirth, F., Gould, A.P., 2003. A pulse of the Drosophila Hox protein abdominal – a schedules the end of neural proliferation via neuroblast apoptosis. Neuron 37, 209–219.
Bello, B.C., Izergina, N., Caussinus, E., Reichert, H., 2008. Amplification of neural stem cell proliferation by intermediate progenitor cells in Drosophila brain development. Neural Dev. 3, 5.
Billuart, P., Winter, C.G., Maresh, A., Zhao, X., Luo, L., 2001. Regulating axon branch stability: the role of p190 RhoGAP in repressing a retraction signaling pathway. Cell 107, 195–207.
Boone, J.Q., Doe, C.Q., 2008. Identification of Drosophila type II neuroblast lineages containing transit amplifying ganglion mother cells. Dev. Neurobiol. 68, 1185–1195.
Brody, T., Odenwald, W.F., 2000. Programmed transformations in neuroblast gene expression during Drosophila CNS lineage development. Dev. Biol. 226, 34–44.
Cardona, A., Saalfeld, S., Arganda, I., Pereanu, W., Schindelin, J., Hartenstein, V., 2010. Identifying neuronal lineages of Drosophila by sequence analysis of axon tracts. J. Neurosci. 30, 7538–7553.
Chang, T., Younossi-Hartenstein, A., Hartenstein, V., 2003. Development of neural lineages derived from the sine oculis positive eye field of Drosophila. Arthropod. Struct. Dev. 32, 303–317.
Chen, Y.M., Wang, Q.J., Hu, H.S., Yu, P.C., Zhu, J., Drewes, G., Piwnica-Worms, H., Luo, Z.G., 2006. Microtubule affinity-regulating kinase 2 functions downstream of the PAR-3/PAR-6/atypical PKC complex in regulating hippocampal neuronal polarity. Proc. Natl. Acad. Sci. USA 103, 8534–8539.
Chiang, A.S., Lin, C.Y., Chuang, C.C., Chang, H.M., Hsieh, C.H., et al., 2011. Three-dimensional reconstruction of brain-wide wiring networks in Drosophila at single-cell resolution. Curr. Biol. 21, 1–11.
Cong, W., Hirose, T., Harita, Y., Yamashita, A., Mizuno, K., Hirano, H., Ohno, S., 2010. ASPP2 regulates epithelial cell polarity through the PAR complex. Curr. Biol. 20, 1408–1414.
Crittenden, J.R., Skoulakis, E.M., Han, K.A., Kalderon, D., Davis, R.L., 1998. Tripartite mushroom body architecture revealed by antigenic markers. Learn. Mem. 5, 38–51.
Das, A., Gupta, T., Davla, S., Prieto-Godino, L.L., Diegelmann, S., Reddy, O.V., Raghavan, K.V., Reichert, H., Lovick, J., Hartenstein, V., 2013. Neuroblast lineage-specific origin of the neurons of the Drosophila larval olfactory system. Dev. Biol. 373, 322–337.
Das, A., Sen, S., Lichtneckert, R., Okada, R., Ito, K., Rodrigues, V., Reichert, H., 2008. Drosophila olfactory local interneurons and projection neurons derive from a common neuroblast lineage specified by the empty spiracles gene. Neural Dev. 3, 33.
Doe, C.Q., 1992. Molecular markers for identified neuroblasts and ganglion mother cells in the Drosophila central nervous system. Development 116, 855–863.
Ellenbroek, S.I., Iden, S., Collard, J.G., 2012. Cell polarity proteins and cancer. Semin. Cancer Biol. 22, 208–215.
Guillemot, F., 2007. Cell fate specification in the mammalian telencephalon. Prog. Neurobiol. 83, 37–52.
Hartenstein, V., Cardona, A., Pereanu, W., Younossi-Hartenstein, A., 2008. Modeling the developing Drosophila brain: rationale, technique and application. BioScience 58, 823–836.
Hassan, B.A., Bermingham, N.A., He, Y., Sun, Y., Jan, Y.N., Zoghbi, H.Y., Bellen, H.J., 2000. atonal regulates neurite arborization but does not act as a proneural gene in the Drosophila brain. Neuron 25, 549–561.
Hayashi, S., Ito, K., Sado, Y., Taniguchi, M., Akimoto, A., Takeuchi, H., Aigaki, T., Matsuzaki, F., Nakagoshi, H., Tanimura, T., Ueda, R., Uemura, T., Yoshihara, M., Goto, S., 2002. GETDB, a database compiling expression patterns and molecular locations of a collection of Gal4 enhancer traps. Genesis 34, 58–61.
Helfrich-Förster, C., Yoshii, T., Wülbeck, C., Grieshaber, E., Rieger, D., Bachleitner, W., Cusamano, P., Rouyer, F., 2007. The lateral and dorsal neurons of Drosophila melanogaster: new insights about their morphology and function. Cold Spring Harb Symp Quant Biol. 72, 517–525.
Huff, R., Furst, A., Mahowald, A.P., 1989. Drosophila embryonic neuroblasts in culture: autonomous differentiation of specific neurotransmitters. Dev. Biol. 134, 146–157.
Hurd, T.W., Fan, S., Liu, C.J., Kweon, H.K., Hakansoon, K., Margolis, B., 2003. Phosphorylation-dependent binding of 14-3-3 to the polarity protein Par3 regulates cell polarity in mammalian epithelia. Curr. Biol. 13, 2082–2090.
Isshiki, T., Pearson, B., Holbrook, S., Doe, C.Q., 2001. Drosophila neuroblasts sequentially express transcription factors which specify the temporal identity of their neuronal progeny. Cell 106, 511–521.
Ito, K., Awano, W., Suzuki, K., Hiromi, Y., Yamamoto, D., 1997. The Drosophila mushroom body is a quadruple structure of clonal units each of which contains a virtually identical set of neurones and glial cells. Development 124, 761–771.
Ito, K., Awasaki, T., 2008. Clonal unit architecture of the adult fly brain. Adv. Exp. Med. Biol. 628, 137–158.
Ito, K., Hotta, Y., 1992. Proliferation pattern of postembryonic neuroblasts in the brain of Drosophila melanogaster. Dev. Biol. 149, 134–148.
Ito, M., Masuda, N., Shinomiya, K., Endo, K., Ito, K., 2013. Systematic analysis of neural projections reveals clonal composition of the Drosophila brain. Curr. Biol. 23 (8), 644–655.
Izergina, N., Balmer, J., Bello, B., Reichert, H., 2009. Postembryonic development of transit amplifying neuroblast lineages in the Drosophila brain. Neural Dev. 4, 44.
Jefferis, G.S., Marin, E.C., Stocker, R.F., Luo, L., 2001. Target neuron prespecification in the olfactory map of Drosophila. Nature 414, 204–208.
Jefferis, G.S., Vyas, R.M., Berdnik, D., Ramaekers, A., Stocker, R.F., Tanaka, N.K., Ito, K., Luo, L., 2004. Developmental origin of wiring specificity in the olfactory system of *Drosophila*. Development 131, 117–130.

Jenett, A., Rubin, G.M., Ngo, T.B., Shepherd, D., Murphy, H., et al., 2012. A GAL4-driver line resource for Drosophila neurobiology. Cell Rep. 2, 991–1001.
Kambadur, R., Koizumi, K., Stivers, C., Nagle, J., Poole, S.J., Odenwald, W.F., 1998. Regulation of POU genes by castor and hunchback establishes layered compartments in the Drosophila CNS. Genes Dev. 12, 246–260.
Komiyama, T., Johnson, W.A., Luo, L., Jefferis, G.S., 2003. From lineage to wiring specificity: POU domain transcription factors control precise connections of Drosophila olfactory projection neurons. Cell 112, 157–167.
Kuert, P.A., Bello, B.C., Reichert, H., 2012. The labial gene is required to terminate proliferation of identified neuroblasts in post embryonic development of the Drosophila brain. Biol. Open 1, 1006–1015.
Kumar, A., Bello, B., Reichert, H., 2009a. Lineage-specific cell death in postembryonic brain development of Drosophila. Development 136, 3433–3442.
Kumar, A., Fung, S., Lichtneckert, R., Reichert, H., Hartenstein, V., 2009b. Arborization pattern of engrailed-positive neural lineages reveal neuromere boundaries in the Drosophila brain neuropil. J. Comp. Neurol. 517, 87–104.
Kunz, T., Kraft, K.F., Technau, G.M., Urbach, R., 2012. Origin of Drosophila mushroom body neuroblasts and generation of divergent embryonic lineages. Development 139, 2510–2522.
Lai, S.L., Awasaki, T., Ito, K., Lee, T., 2008. Clonal analysis of Drosophila antennal lobe neurons: diverse neuronal architectures in the lateral neuroblast lineage. Development 135, 2883–2893.
Larsen, C., Shy, D., Spindler, S.R., Fung, S., Pereanu, W., Younossi-Hartenstein, A., Hartenstein, V., 2009. Patterns of growth, axonal extension and axonal arborization of neuronal lineages in the developing Drosophila brain. Dev. Biol. 335, 289–304.
Lee, T., Lee, A., Luo, L., 1999. Development of the Drosophila mushroom bodies: sequential generation of three distinct types of neurons from a neuroblast. Development 126, 4065–4076.
Lee, T., Luo, L., 2001. Mosaic analysis with a repressible cell marker (MARCM) for Drosophila neural development. Trends Neurosci. 24, 251–254.
Lee, T., Marticke, S., Sung, C., Robinow, S., Luo, L., 2000a. Cell-autonomous requirement of the USP/EcR-B ecdysone receptor for mushroom body neuronal remodeling in Drosophila. Neuron 28, 807–818.
Lee, T., Winter, C., Marticke, S.S., Lee, A., Luo, L., 2000b. Essential roles of Drosophila RhoA in the regulation of neuroblast proliferation and dendritic but not axonal morphogenesis. Neuron 25, 307–316.
Lichtneckert, R., Nobs, L., Reichert, H., 2008. Empty spiracles is required for the development of olfactory projection neuron circuitry in Drosophila. Development 135, 2415–2424.
Lin, S., Kao, C.F., Yu, H.H., Huang, Y., Lee, T., 2012. Lineage analysis of ***Drosophila*** lateral antennal lobe neurons reveals notch-dependent binary temporal fate decisions. PLoS Biol. 10, E1001425.
Lovick, J.K., Ngo, K.T., Omoto, J., Wong, D.C., Nguyen, J.D., Hartenstein, V., Post-embryonic lineages of the Drosophila brain: I. Development of the lineage- associated fiber, Dev. Biol., 2013, http://dx.doi.org/10.1016/j.ydbio.2013.07.008. Mao, Z., Davis, R.L., 2009. Eight different types of dopaminergic neurons innervate the Drosophila mushroom body neuropil: anatomical and physiological heterogeneity. Front. Neural Circuits 3, 5.
Marin, E.C., Dry, K.E., Alaimo, D.R., Rudd, K.T., Cillo, A.R., Clenshaw, M.E., Negre, N., White, K.P., Truman, J.W., 2012. Ultrabithorax confers spatial identity in a context-specific manner in the Drosophila postembryonic ventral nervous system. Neural Dev. 7, 31.
Maurange, C., Cheng, L., Gould, A.P., 2008. Temporal transcription factors and their targets schedule the end of neural proliferation in Drosophila. Cell 133, 891–902.
Ng, J., Nardine, T., Harms, M., Tzu, J., Goldstein, A., Sun, Y., Dietzl, G., Dickson, B.J., Luo, L., 2002. Rac GTPases control axon growth, guidance and branching. Nature 416, 442–447.
Nicolai, L.J., Ramaekers, A., Raemaekers, T., Drozdzecki, A., Mauss, A.S., Yan, J., Landgraf, M., Annaert, W., Hassan, B.A., 2010. Genetically encoded dendritic marker sheds light on neuronal connectivity in Drosophila. PNAS 107, 20553–20558.
Nishimura, T., Kato, K., Yamaguchi, T., Fukata, Y., Ohno, S., Kaibuchi, K., 2004. Role of the PAR-3–KIF3 complex in the establishment of neuronal polarity. Nat. Cell Biol. 6, 328–334.
Ohno, S., 2001. Intercellular junctions and cellular polarity: the PAR-aPKC complex, a conserved core cassette playing fundamental roles in cell polarity. Curr. Opin. Cell Biol. 13, 641–648.
Okajima, T., Xu, A., Lei, L., Irvine, K.D., 2005. Chaperone activity of protein O-Fucosyltransferase 1 promotes Notch receptor folding. Science 307, 1599–1603.
Pearson, B.J., Doe, C.Q., 2004. Specification of temporal identity in the developing nervous system. Annu. Rev. Cell Dev. Biol. 20, 619–647.
Pereanu, W., Shy, D, Hartenstein, V., 2005. Morphogenesis and proliferation of the larval brain glia in Drosophila. Dev. Biol. 283, 191–203.
Pereanu, W., Hartenstein, V., 2006. Neural lineages of the Drosophila brain: a three-dimensional digital atlas of the pattern of lineage location and projection at the late larval stage. J. Neurosci. 26, 5534–5553.
Pereanu, W., Kumar, A., Jennett, A, Reichert, H., Hartenstein, V., 2010. Development-based compartmentalization of the Drosophila central brain. J. Comp. Neurol. 518, 2996–3023.
Pfeiffer, B.D., Jenett, A., Hammonds, A.S., Ngo, T.T., Misra, S., et al., 2008. Tools for neuroanatomy and neurogenetics in Drosophila. Proc. Natl. Acad. Sci. USA 105, 9715–9720.
Renn, S.C., Armstrong, J.D., Yang, M., Wang, Z., An, X., Kaiser, K., Taghert, P., 1999. Genetic analysis of the Drosophila ellipsoid body neuropil: organization and development of the central complex. J. Neurobiol. 41, 189–207.
Reuter, J.E., Nardine, T.M., Penton, A., Billuart, P., Scott, E.K., Usui, T., Uemura, T., Luo, L., 2003. A mosaic genetic screen for genes necessary for Drosophila mushroom body neuronal morphogenesis. Development 130, 1203–1213.
Rolls, M.M., Doe, C.Q., 2004. Baz, Par-6 and aPKC are not required for axon or dendrite specification in Drosophila. Nat. Neurosci. 7, 1293–1295.
Sánchez-Soriano, N., Bottenberg, W., Fiala, A., Haessler, U., Kerassoviti, A., Knust, E., Löhr, R., Prokop, A., 2005. Are dendrites in Drosophila homologous to vertebrate dendrites? Dev. Biol. 288, 126–138.
Scott, E.K., Lee, T., Luo, L., 2001. enok encodes a Drosophila putative histone acetyltransferase required for mushroom body neuroblast proliferation. Curr. Biol. 11, 99–104.
Shafer, O.T., Helfrich-Förster, C., Renn, S.C., Taghert, P.H., 2006. Reevaluation of Drosophila melanogaster's neuronal circadian pacemakers reveals new neuronal classes. J. Comp. Neurol. 498, 180–193.
Shi, S.H., Cheng, T., Jan, L.Y., Jan, Y.N., 2004. APC and GSK-3beta are involved in mPar3 targeting to the nascent axon and establishment of neuronal polarity. Curr. Biol. 14, 2025–2032.
Shirasaki, R., Pfaff, S.L., 2002. Transcriptional codes and the control of neuronal identity. Annu. Rev. Neurosci. 25, 251–281.
Skeath, J.B., Thor, S., 2003. Genetic control of Drosophila nerve cord development. Curr. Opin. Neurobiol. 13, 8–15.
Spindler, S.R., Hartenstein, V., 2010. The Drosophila neural lineages: a model system to study brain development and circuitry. Dev. Genes Evol. 220, 1–10.
Spindler, S.R., Hartenstein, V., 2011. Bazooka mediates secondary axon morphology in Drosophila brain lineages. Neural Dev. 6, 16.
Srahna, M., Leyssen, M., Choi, C.M., Fradkin, L.G., Noordermeer, J.N., Hassan, B.A., 2006. A signaling network for patterning of neuronal connectivity in the Drosophila brain. PLoS Biol. 4, E348.
Stocker, R.F., Lienhard, M.C., Borst, A., Fischbach, K.F., 1990. Neuronal architecture of the antennal lobe in Drosophila melanogaster. Cell Tissue Res. 262, 9–34.
Truman, J.W., Schuppe, H., Shepherd, D., Williams, D.W., 2004. Developmental architecture of adult-specific lineages in the ventral CNS of Drosophila. Development 131, 5167–5184.
Truman, J.W., Moats, W., Altman, J., Marin, E.C., Williams, D.W., 2010. Role of Notch signaling in establishing the hemilineages of secondary neurons in Drosophila melanogaster. Development 137, 53–61.
Urbach, R., Technau, G.M., 2003. Early steps in building the insect brain: neuroblast formation and segmental patterning in the developing brain of different insect species. Arthropod. Struct. Dev. 32, 103–123.
Urbach, R., Technau, G.M., 2004. Neuroblast formation and patterning during early brain development in Drosophila. Bioessays 26, 739–751.
Viktorin, G., Riebli, N., Popkova, A., Giangrande, A., Reichert, H., 2011. Multipotent neural stem cells generate glial cells of the central complex through transit amplifying intermediate progenitors in Drosophila brain development. Dev. Biol. 356, 553–565.
Viktorin, G., Riebli, N., Reichert, H., 2013. A multipotent transit-amplifying neuroblast lineage in the central brain gives rise to optic lobe glial cells in Drosophila. Dev. Biol. 379, 182–194.
Vosshall, L.B., Amrein, H., Morozov, P.S., Rzhetsky, A., Axel, R., 1999. A spatial map of olfactory receptor expression in the Drosophila antenna. Cell 96, 725–736.
Wang, Y., Du, D., Fang, L., Yang, G., Zhang, C., Zeng, R., Ullrich, A., Lottspeich, F., Chen, Z., 2006. Tyrosine phosphorylated Par3 regulates epithelial tight junction assembly promoted by EGFR signaling. EMBO J. 25, 5058–5070.
Wang, Y.C., Khan, Z., Kaschube, M., Wieschaus, E.F., 2012. Differential positioning of adherens junctions is associated with initiation of epithelial folding. Nature 484, 390–393.
Watson, A.H., Schürmann, F.W., 2002. Synaptic structure, distribution, and circuitry in the central nervous system of the locust and related insects. Microsc. Res. Tech. 56, 210–226.
Yang, J.S., Awasaki, T., Yu, H.H., He, Y., Ding, P., Kao, J.C, Lee, T, 2013. Diverse neuronal lineages make stereotyped contributions to the Drosophila locomotor control center, the central complex. J. Comp. Neurol. 521 (12), http://dx.doi.org/10.1002/cne.23366. (Spc1.).
Younossi-Hartenstein, A., Nassif, C., Green, P., Hartenstein, V., 1996. Early neurogenesis of the Drosophila brain. J. Comp. Neurol. 370, 313–329.
Yu, H.H., Awasaki, T., Schroeder, M.D., Long, F., Yang, J.S., He, Y., Ding, P., Kao, J.C., Wu, G.Y., Peng, H., Myers, G., Lee, T., 2013. Clonal development and organization of the adult Drosophila central brain. Curr. Biol. 23 (8), 633–643.
Yu, H.H., Chen, C.H., Shi, L., Huang, Y., Lee, T., 2009. Twin-spot MARCM to reveal the developmental origin and identity of neurons. Nat. Neurosci. 12, 947–953.
Yu, H.H., Kao, C.F., He, Y., Ding, P., Kao, J.C., Lee, T., 2010. A complete developmental sequence of a Drosophila neuronal lineage as revealed by twin-spot MARCM. PLoS Biol. 8, E1000461.
Zecca, M., Basler, K., Struhl, G., 1996. Direct and long-range action of a wingless morphogen gradient. Cell 87, 833–844.
Zheng, X., Zugates, C.T., Lu, Z., Shi, L., Bai, J.M., Lee, T., 2006. Baboon/dSmad2 TGF-beta signaling is required during late larval stage for development of adult-specific neurons. EMBO J. 25, 615–627.
Zhu, S., Chiang, A.S., Lee, T., 2003. Development of the Drosophila mushroom bodies: elaboration, remodeling and spatial organization of dendrites in the calyx. Development 130, 2603–2610.

Chapter 7

Patterns of Growth and Tract Formation During the Early Development of Secondary Lineages in the *Drosophila* Larval Brain

Discussion

The nervous system of *D. melanogaster* is a powerful model system for studying fundamental questions regarding development of classes of neurons and how they form the circuitry underlying behavior. This work adds to the growing literature regarding nervous system development and function.

The first chapter provides an introduction to the concept of neural lineages in the context of the central brain in *Drosophila melanogaster* and the neocortex of the vertebrate brain. We compare and contrast the structural and developmental nature of lineages, highlighting the importance of the lineage as a fundamental building block of neural circuitry and their possible correlation to function.

In the second chapter, we classify and describe the anatomy of embryonic-born (primary) neurons of lineages and their association with larval-born (secondary) neurons of the same lineages in the central brain (Hartenstein et al., 2015). In a previous study (Pereanu and Hartenstein, 2006) secondary neurons, which form coherent bundles in the late larval brain, were assigned to lineages based on location and projection pattern of secondary axon tracts (SATs) using a global marker (anti-Neurotactin/BP106). In chapter three of my thesis (Lovick et al., 2015), using BP106 and a second global marker (anti-Neuroglian/BP104), which label secondary and primary neuron axon tracts at different stages of development, we traced SATs to earlier stages of larval development and was able to associate primary lineage axon tracts (PATs) with the SATs and assign primary neurons to lineages following the same classification system introduced in Pereanu and Hartenstein (2006).

Because most primary lineages are described using global, rather than lineage-specific, markers, the resolution of the early larval brain map is insufficient as a resource for more detailed studies regarding larval function and behavior. Thus, a number of studies can and have been proposed to address this. One way is to identify additional lineage-specific GAL4 lines or generate neuroblast clones which also label entire lineages. Traditional methods of making clones has been unsuccessful, but newer genetic techniques (Birkholz et al., 2015; Hadjieconomou et al., 2011; Shimosako et al., 2014) may provide the answer to creating a primary neuron clone library much like the one described in chapter six of my thesis (Wong et al., 2013). A second approach, which is already underway, is to digitally reconstruct primary neurons at the late first larval instar stage. Using a web-based interface called CATMAID (Saalfeld et al., 2009), I, in collaboration with many other labs, are able to manually reconstruct individual neurons and their synapses in a serial TEM (transmission electron microscopy) stack. This will provide the highest resolution possible of neuron circuits and will serve as a tremendous resource for neuroscientists interested in understanding and modeling circuit function and the behaviors they are responsible for.

Additionally, it will be of great value to follow the development of primary neurons back to the time when they are born in the embryo using lineage-specific and global markers, in a manner similar to the approach used in the fourth chapter of my thesis to study the origin and early development of secondary lineages born in the larva (Lovick et al., 2015).

In the third chapter, we took advantage of the knowledge that the initiation of the secondary phase of neurogenesis which produces larval-born, adult-specific secondary

lineages occurs over an approximately 20-hour period (Ito and Hotta, 1992), to document when each secondary lineage is “born” during early larval development (Lovick and Hartenstein, 2015). Using the drug hydroxyurea (HU) which kills actively dividing cells, we systematically ablated neuroblasts (secondary neurons would not develop) in four hour windows covering this 20-hour period and observed at the late third larval instar stage the presence or absence of secondary lineages. This allowed us to construct a birth-date calendar for all central brain secondary lineages. Interestingly, loss of secondary lineages has little to no effect on the development of other lineages (remaining lineages maintain proper projection and arborization patterns). Furthermore, this technique enabled us to show that primary neurons which remodel and form part of adult brain circuitry do so with minimal dependence on secondary neurons (arborization not inhibited, but patterning of branches is), identify how secondary lineages contribute to adult brain compartments (e.g. the DALv2 lineage comprises the majority of neurons which form the ellipsoid body, a compartment which forms *de novo* during metamorphosis), and assess the requirement of connections between neurons of different lineages for proper branching morphogenesis.

It is especially interesting that ablation of secondary lineages does not greatly affect the development of others, strongly suggestive of the idea that neuroblasts and their progeny adhere to intrinsic developmental timers with little influence from neighboring secondary lineages. Further studies into the molecular mechanisms underlying this process would greatly add to the already existing literature on the intrinsic regulation of neuroblast proliferation. Another aspect that should be investigated in greater detail is the extrinsic mechanisms (from surrounding tissue or

from neurons which make direct contacts with) involved in orchestrating growth of collateral axons.

In the fourth chapter, using the global markers anti-Neurotactin/BP106 and *insc*-GAL4 (transgenic fly line that labels all secondary neuron cell bodies and axon tracts), we traced secondary lineages (based on SAT morphology and cell body location) from late larval development backwards in time to when they first appear at the late first instar larval stage (Lovick et al., 2015). We documented in detail the gross morphological changes that happen to central brain secondary lineages during larval development. Importantly, we saw that lineages extend axon tracts in the same order in which the lineages are born (compared to detailed birth-date calendar; Lovick and Hartenstein, 2015) and that hemilineages of a given lineage do not extend axon tracts at the same time; most secondary Type I lineages do not retain both hemilineages (shown by inhibiting apoptosis in secondary lineages by overexpression of p35); and that large morphogenetic movements of laterally located lineages is due in large part to the massive growth of the optic lobe during later stages of larval development (when the optic lobe primordium is ablated early in development by expression of a dominant negative form of EGFR, lateral lineages do not move much relative to their initial positions in the first instar larval brain). There are several interesting aspects which should be followed up on. Genetic studies addressing the temporal order in which axons grow (is this dependent upon when secondary neurogenesis is initiated in the larva?) and in the case of hemilineages, molecular mechanisms that dictate which hemilineage axon tract will extend first (possibly due to differential expression of Notch?). Also, it would be fascinating to explore how, as cell body clusters of lineages move around due

to the growing neuropil, maintain their axon tract within the neuropil. In particular, one could look at the mechanisms controlling how lineages are anchored at the point where they enter the neuropil.

In the fifth chapter, using the global markers anti-Neuroglian/BP104 and *insc*-GAL4, we followed and documented the development of larval-born central brain secondary lineages from the late third larval instar stage, through metamorphosis, into the adult (Lovick et al., 2013). Taking advantage of the classification system established in Pereanu and Hartenstein (2006), we were able to assign secondary lineages in the adult to the corresponding larval lineages based on the location of the cell body clusters and projection pattern within the neuropil. We also observed a number of interesting morphological changes which take place during metamorphosis including rearrangements of cell body clusters with little changes made to axon tracts and movement of hemilineages away from each other. In some cases, because global markers make it difficult to distinguish similar lineages which often contribute to the same axon tract, we were not able to determine exactly what happens to them during metamorphosis. This could easily be resolved with more specific labeling techniques (e.g. lineage-specific GAL4 lines or generation of neuroblast clones using the MARCM technique). Much like in the fourth chapter, it would be interesting to identify the mechanisms which anchor a lineage at the cortex-neuropil boundary. This is an important feature because the cell bodies of most lineages are pushed away from their original positions in the larva as the brain grows during metamorphosis. A second issue that should be followed up on is the complex anatomy of central complex lineages

(Type II lineages), which appear to have multiple axon tracts that may be representative of morphologically and presumably functionally distinct sublineages.

The sixth chapter is a follow up study to that presented in the fifth chapter. It takes advantage of the fact that the axon tracts of all lineages are now identifiable in the adult brain and adds to this by showing in detail the anatomy of entire lineages using a fluorescent marker. To this end, we used a genetic technique called MARCM (mosaic analysis with a repressible cell marker; Lee and Luo, 1999) to label individual neuroblasts and all of their progeny (one lineage; termed a clone) during the larval stage (Wong et al., 2013). We described the anatomy of each central brain secondary lineage in the adult and establish an atlas of neural circuitry at the level of the lineage. Each clone could be assigned to a lineage using the classification system of Pereanu and Hartenstein (2006) because of the study described present in chapter five of my thesis (Lovick et al., 2015). This information will be useful for experimental studies which focus on specific lineages (e.g. applying this anatomical knowledge to lineages in mutant conditions in order to assess a phenotype). Interestingly, all lineages and most, if not all, hemilineages have distinct branching patterns, even those that share similar projection patterns (axons projecting along the same tract). By comparing single-cell MARCM clones from the Fly Circuit database (Chiang et al., 2011) with our lineage clones, we noted that neurons of a given lineage exhibit distinct fields of arborization. Thus, it would be worthwhile to analyze the branching pattern diversity within a lineage and between lineages using single-cell clones (do they tile or overlap as for the antennal lobe projection neurons (Jefferis et al., 2001, 2004; Yu et al., 2010)? are these features that can be applied to an entire lineage?).

Future studies of adult central brain anatomy should focus on how the neurons within a lineage organize and interact with each other as well as neurons of other lineages to build neural circuitry. Several studies highlight the diversity of neuron projection patterns within a lineage, the most comprehensive are those of the mushroom body and antennal lobe lineages (Kunz et al., 2012; Lai et al., 2008; Lee et al., 1999; Yu et al., 2010; Zhu et al., 2003). As more genetic tools become available (e.g. the FlyLight GAL4 collection, Jenett et al., 2012), these types of analyses will be possible. Circuits which only consist of a few lineages, as observed by our MARCM clone library and others (Ito et al., 2013; Yu et al., 2013), are likely candidates for similar studies. One such example is the lineages which form the anterior visual input pathway (AVP) from the optic lobe via a small well-defined compartment called the anterior optic tubercle. Based on clones, we can conclude that only three secondary lineages interconnect this compartment with the ellipsoid body, a compartment known to be important for higher order processing of visually guided locomotion (Neuser et al., 2008; Seelig and Jayaraman, 2013, 2015). It will be exciting to understand not only how the neurons of these lineages organize to form this circuit, but also how they function to transmit and process visual input from the optic lobe. Furthermore, to get at how development of a lineage determines the function of its neuronal constituents, it would be exciting to elucidate at a molecular level how neurons within a lineage (those exhibiting similar but distinctive morphologies and presumably function) differ. Our lab is currently using RNA-seq technology to identify molecules differentially expressed between two sublineages of the ellipsoid body lineage DALv2. We are able to use FACs to separate the two sublineages, each of which can be uniquely labeled using

sublineage-specific GAL4 drivers with a nuclear fluorescent reporter. These sublineages differ such that they occupy similar but non-overlapping territories with respect to their axons and dendrites. We expect that we will identify slight differences in expression of structural genes (e.g. adhesion molecules) which will aid in our understanding of how these two sublineages develop and function with respect to one another as well as with other lineages in the AVP.

In Conclusion

This work encompasses many aspects regarding development of central brain lineages of *D. melanogaster*. It contributes to our understanding of neural development in many ways including providing, for the first time, a detailed description of the lineages which form the functional larval brain (primary neurons) as well as the development and morphogenesis of the larval-born secondary neurons which form the circuitry of the adult brain. In doing this, a number of fundamental developmental questions are addressed, but as to be expected, bring up many new questions.

Investigations into the diversity of neuronal phenotypes within a lineage (how neural subsets within a lineage organize in circuits) as well as understanding how neurons of different lineages make connections (through signaling mechanisms, guidance cues, adhesion molecules) would be of great interest. Of even greater import, and perhaps the long-term goal of many neurobiologists, would be to link neural circuits to animal behavior. It would be exciting to address this in the adult brain of *D. melanogaster* as the circuitry of the entire central brain has become much more well-

defined beyond the traditional systems (mushroom body and antennal lobe; centers for processing olfactory information) already being studied.

References

Birkholz O, Rickert C, Nowak J, Coban IC, Technau GM. 2015. Bridging the gap between postembryonic cell lineages and identified embryonic neuroblasts in the ventral nerve cord of Drosophila melanogaster. Biol Open. 4:420-434.

Chiang AS, Lin CY, Chuang CC, Chang HM, Hsieh CH, et al. Three-dimensional reconstruction of brain-wide wiring networks in Drosophila at single-cell resolution. Curr. Biol. 2011;21:1–11.

Hadjieconomou D, Rotkopf S, Alexandre C, Bell DM, Dickson BJ, Salecker I. 2011. Flybow: genetic multicolor cell labeling for neural circuit analysis in Drosophila melanogaster. Nat Methods. 8:260-266.

Ito K, Hotta Y. Proliferation pattern of postembryonic neuroblasts in the brain of Drosophila melanogaster. Dev. Biol. 1992;149:134–148.

Ito M, Masuda N, Shinomiya K, Endo K, Ito K. 2013. Systematic analysis of neural projections reveals clonal composition of the Drosophila brain. Curr Biol. 23:644-655.

Jefferis GS, Marin EC, Stocker RF, Luo L. Target neuron prespecification in the olfactory map of Drosophila. Nature. 2001;414:204–208.

Jefferis GS, Vyas RM, Berdnik D, Ramaekers A, Stocker RF, Tanaka NK, Ito K, Luo L. Developmental origin of wiring specificity in the olfactory system of Drosophila. Development.2004;131:117–130.

Jenett A, Rubin GM, Ngo TB, Shepherd D, Murphy H, et al. A GAL4-driver line resource for Drosophila neurobiology. Cell Rep. 2012;2:991–1001.

Kunz T, Kraft KF, Technau GM, Urbach R. Origin of Drosophila mushroom body neuroblasts and generation of divergent embryonic lineages. Developoment. 2012;139:2510-2522.

Lai SL, Awasaki T, Ito K, Lee T. Clonal analysis of Drosophila antennal lobe neurons: diverse neuronal architectures in the lateral neuroblast lineage. Development. 2008;135:2883–2893.

Lee T, Lee A, Luo L. Development of the Drosophila mushroom bodies: sequential generation of three distinct types of neurons from a neuroblast. Development. 1999;126:4065–4076.

Lee T, Luo L. Mosaic analysis with a repressible cell marker (MARCM) for Drosophila neural development. Trends Neurosci. 2001;24:251–254.

Lovick JK, Hartenstein V. 2015. Hydroxyurea-mediated neuroblast ablation establishes birth dates of secondary lineages and addresses neuronal interactions in the developing Drosophila brain. Dev Biol. 402:32-47.

Lovick JK, Kong A, Omoto JJ, Ngo KT, Younossi-Hartenstein A, Hartenstein V. 2015. Patterns of growth and tract formation during the early development of secondary lineages in the Drosophila larval brain. Dev Neurobiol. doi: 10.1002/dneu.22325.

Neuser K, Triphan T, Mronz M, Poeck B, Strauss R. 2008. Analysis of a spatial orientation memory in Drosophila. Nature. 453:1244-1247.

Pereanu W, Hartenstein V. Neural lineages of the Drosophila brain: a three-dimensional digital atlas of the pattern of lineage location and projection at the late larval stage. J. Neurosci. 2006;26:5534–5553.

Saalfeld S, Cardona A, Hartenstein V, Tomancak P. 2009. CATMAID: collaborative annotation toolkit for massive amounts of image data. Bioinformatics. 25:1984-1986.

Seelig JD, Jayaraman V. 2013. Feature detection and orientation tuning in the Drosophila central complex. Nature. 503:262-266.

Seelig JD, Jayaraman V. 2015. Neural dynamics for landmark orientation and angular path integration. Nature. 521:186-191.

Shimosako N, Hadjieconomou D, Salecker I. 2014. Flybow to dissect circuit assembly in the Drosophila brain. Methods Mol Biol. 1082:57-69.

Yu HH, Kao CF, He Y, Ding P, Kao JC, Lee T. A complete developmental sequence of a Drosophila neuronal lineage as revealed by twin-spot MARCM. PLoS Biol. 2010;8:E1000461.

Yu HH, Awasaki T, Schroeder MD, Long F, Yang JS, He Y, Ding P, Kao JC, Wu GY, Peng H, Myers G, Lee T. 2013. Clonal development and organization of the adult Drosophila central brain. Curr Biol. 23:633-643.

Zhu S, Chiang AS, Lee T. Development of the Drosophila mushroom bodies: elaboration, remodeling and spatial organization of dendrites in the calyx. Development. 2003;130:2603–2610.